Thermodynamic Properties of the Group IA Elements

Cite as: Journal of Physical and Chemical Reference Data **23**, 385 (1994); https://doi.org/10.1063/1.555945
Submitted: 09 December 1992 . Published Online: 15 October 2009

C. B. Alcock, M. W. Chase, and V. P. Itkin

Thermodynamic Properties of the Group IA Elements

C.B. Alcock

Department of Metallurgy and Materials Science, University of Toronto, Toronto, Canada M5S 1A4

M.W. Chase

Standard Reference Data Program, National Institute of Standards and Technology, Gaithersburg, MD 20899-0001

and

V. P. Itkin

Department of Metallurgy and Materials Science, University of Toronto, Toronto, Canada M5S 1A4

Received December 9, 1992; revised manuscript received February 14, 1994

This review describes thermodynamic properties of condensed phases of the alkali metals, excluding francium for which the amount of information is too limited. The properties considered are: heat capacities from 0 to 1600 K, temperatures and enthalpies of fusion and martensitic transformation in Li and Na; discussion of the Debye temperature and electronic heat capacity coefficient at absolute zero temperature is also included.

The paper is the second part of a series. Similar to our previous assessment of the IIA group [93ALC/CHA], this paper considers original studies, especially with respect to factors which influence the accuracy and reliability of results. Recommendations derived from such analyses are compared with most advanced previous reviews made at the Institute for High Temperatures (Moscow) [70SHP/YAK], [82GUR] and the National Institute of Standards and Technology (Washington) [85JAN]. The properties of individual elements of the group are compared and suggestions are made for experimental studies which should improve poorly measured quantities.

The review is supplemented by an IBM PC database which contains references, assessed data, brief description of studies and has facilities for fitting and plotting of data and for adding new information.

Key words: element; enthalpy; function; fusion; Gibbs energy; heat capacity; phase transition; thermodynamics.

Contents

List of Tables

List of Figures

1. Introduction

The thermodynamic properties of the alkali metals in the condensed state have been critically assessed several times in the last 20 years. Previous reviews [70SHP/YAK], [73HUL], [82GUR], [85JAN] contain extensive discussion of the experimental literature for all thermodynamic properties. A brief discussion is given in [89COX/WAG] which repeats the recommendation of [82GUR]. It should be emphasized however that such evaluations often are published several years after the date of the assessment. Reviews are made by teams of scientists over a period of several years and do not necessarily draw on data which are current at the date of publication; only [73HUL] and [85JAN] indicate the exact date of the evaluation.

Several assessments are concerned with only one or a few properties, or with a limited temperature range. As an example of this, [85OHS/BAB] estimated the temperature of fusion of the elements, and [85FIN/LEI] assessed only the heat capacity and enthalpy of the liquid metals. Several compilations embrace many elements and substances but recommend thermodynamic values without giving a discussion of the original data. The criteria used during the evaluation therefore remain unknown. Some of the values which are frequently quoted in the literature are copies of previous recommendations, for example, [73BAR/KNA], [77BAR/KNA], [89DIN]. Some compilations do not include the temperature-dependent data, giving only data at 298 K, and the temperatures and enthalpies of transformations and fusion, for example,

[76WAG/EVA], [77KEY], [81MED], [81WAG/EVA], [82NBS].

This assessment discusses principally measurements of the thermodynamic properties which have been published since 1930. Earlier data do not usually add to this review as samples tended to be less pure or defined, but there were some exceptions and several earlier publications of significant worth have been included. The discussion of the available data leads to recommendations which are compared with those in the published reviews mentioned above. The differences between the various recommendations are also discussed.

The properties reviewed in this assessment include: heat capacities from 0 K to 1600 K, the Debye temperatures and electronic heat capacity coefficients at 0 K, enthalpy difference and entropy at 298.15 K, temperatures and enthalpies of fusion, together with data related to the phase transformations in the alkali metals at ambient pressure.

The thermodynamic properties of these elements are well known as a general rule, but there are temperature regions where accurate information does not exist. The experimental difficulty in obtaining data for elevated temperatures stems from the high chemical reactivity of these elements. They can readily react with components of the surrounding atmosphere such as oxygen, nitrogen, carbon dioxide and water vapor. It is difficult to obtain materials of high purity, and it is easy to contaminate samples during measurements. This is especially true for the liquid alkali elements. The heat capacities of liquid Li, Na and K are known with less certainty than for the corresponding solids, and the data for liquid Rb and Cs have the highest uncertainty.

At low temperatures the thermodynamics of the β(bcc)=α(hcp) martensitic transformation in Li and Na is poorly known. The low-temperature crystalline modifications of Li and Na (Table 1–1) have been studied since the fifties. It was found that these phases are formed by a mechanism of displacive transformation which does not normally proceed to completion. A mixture of two phases therefore exists in most samples even at the lowest temperatures, and there is considerable confusion at the present time about the extent to which this transformation can be made to advance. Another problem appears near 0 K, where the heat capacity measurements are not very accurate.

The separate review for each element consists of a brief description of the relevant experimental studies with emphasis on the measured property, temperature range, the experimental technique, chemical analysis of the sample, the results and the accuracy of the data. Important information is often missing in the original studies. For example, the chemical analysis is not given or has been carried out for only some of the metallic impurities. Data are given sometimes in the form of small-scale graphs, fitted equations, smoothed values, and even values derived from the measured results (for example, the apparent temperature dependence of the Debye temperature); tables of original data are often omitted. It is difficult to assign an accuracy to the majority of studies, because details of analysis of the materials and the measurement technique are absent, which only serves to diminish the value of a review. The more reliable data are reproduced in the Appendices (Sec. 9 of each Chapter).

The selected heat capacity and enthalpy data are fitted to polynomials containing up to five-terms over limited temperature ranges. These equations are then used to calculate the entropy and enthalpy at different temperatures, and the results of these calculations are tabulated in Sec. 7 of each Chapter. The standard entropy, $S°(298.15\ K)$, and the enthalpy difference, $H°(298.15\ K)-H°(0)$, are also calculated. The standard entropy is rounded to 0.01 $J\cdot K^{-1}\cdot mol^{-1}$ and the enthalpy difference to $J\cdot mol^{-1}$ which is less than 5 % of the estimated uncertainty. Such a treatment makes the entropy and enthalpy values calculated below and above 298.15 K more consistent. The selected and calculated values are compared with the corresponding quantities which are quoted in other reviews [70SHP/YAK], [73HUL], [82GUR], [85JAN], [85BAB/OHS], [85FIN/LEI], [89COX/WAG]. The recommended values shown in Sec. 6 of each Chapter are sometimes very inaccurate due to lack of data. Those quantities which are considered to be poorly known are highlighted in each Chapter and listed in the concluding Chapter 7 to indicate the need for further investigation.

1.1. General Comments

1. Units. The units used throughout the text are temperature in K, enthalpy and Gibbs energy in $J\cdot mol^{-1}$, entropy and heat capacity, in $J\cdot K^{-1}\cdot mol^{-1}$.

2. Heat Capacity near 0 K. The heat capacity data below T – 5 K is normally represented by a two term equation:

$$C_p = \gamma T + 1943.78\ (T/\Theta_D)^3$$

where γ is the electronic contribution to the heat capacity and the term with Θ_D (the Debye temperature) represents the lattice contribution to the heat capacity. Values for γ and Θ_D are given for each study when appropriate. However, for K, Rb and Cs a two-term equation cannot describe accurately available data and a third term, δT^5, was added to the above equation.

3. Temperature Scale. The temperature scale used for the recommended values is ITS–90. Much of the reported data are given in terms of earlier temperature scales. Usually the scale used is not mentioned, so that we must guess as to the appropriate corrections to make. It should be noted that between 300 and 500 K, the corrections between all temperature scales are less than 0.04 K. These corrections are well within the uncertainty of the measured temperatures for the condensed phases. Nevertheless all experimental temperatures of fusion were corrected in Sec. 5 of each chapter to ITS–90 by adding or subtracting 0.01 to 0.04 K.

4. Atomic Masses. The relative atomic masses for the alkali metals have been reassessed through the years. The recommended thermodynamic values are based on the following relative atomic masses: Li 6.941, Na 22.989768, K 39.0983, Rb 85.4678, Cs 132.90543 (1991 data). Since the 1930's these values have changes by <0.007 for Li, Na and K, by +0.028 for Rb and +0.095 for Cs. The sensitivity of measurement techniques for the thermodynamic properties is beyond these changes.

TABLE 1.1. Crystal Structure and Lattice Parameters of the Elements of the IA Group from [85VIL/CAL]

Phase	Temperature interval of stability (K)	Structure	Lattice parameter (nm) at temperature (K)	
α-Li	<70[a]	hcp	a=0.3111 c=0.5093	(<70 K)
β-Li	70–453.65	bcc	a=0.35100	(at 298 K)
α-Na	<35[a]	hcp	a=0.3767 c=0.61541	(<35 K)
β-Na	35–370.95	bcc	a=0.4291	(at 298 K)
K	0 – 336.60	bcc	a=0.53298	(at 298 K)
Rb	0 – 312.45	bcc	a=0.5699	(at 298 K)
Cs	0 – 301.60	bcc	a=0.6465	(at 298 K)

[a]Note: Martensite start temperature M_s is given here.

1.2. References for the Introduction

70SHP/YAK E. E. Shpil'rain, K. A. Yakimovich, E. E. Totskii, D. L. Timrot, and V. A. Fomin, "Thermophysical Properties of Alkali Metals," V.A. Kirillin, ed., Izd. Standartov, Moscow (1970); Review.

73BAR/KNA I. Barin, and O. Knacke, "Thermochemical Properties of Inorganic Substances," Springer-Verlag, Berlin (1973); Review.

73HUL R. Hultgren, P. D. Desai, D. T. Hawkins, M. Gleiser, K. K. Kelley, and D. D. Wagman, "Selected Values of the Elements," Amer. Soc. Metals, Metals Park, Ohio 44073 (1973); Review.

76WAG/EVA D. D. Wagman, W. H. Evans, V. B. Parker, and R. H. Schumm, "Chemical Thermodynamic Properties of Compounds of Sodium, Potassium and Rubidium: An Interim Tabulation of Selected Values," National Bureau of Standards, Report NBSIR 76–1034 (1976); Review.

77BAR/KNA I. Barin, O. Knacke, and O. Kubaschewski, "Thermochemical Properties of Inorganic Substances," Supplement, Springer-Verlag, Berlin (1977); Review.

77KEY J. D. Cox, "CODATA Recommended Key Values for Thermodynamics, 1976," J. Chem. Thermodyn. **9**, 705–6 (1977); Report on CODATA Task Group on Key Values for Thermodynamics.

81MED V. A. Medvedev, G. A. Bergman, L.V. Gurvich, et al, V. P. Glushko, gen. ed., "Thermal Constants of Substances," **10**, VINITI, Moscow (1981); Review

81WAG/EVA D. D. Wagman, W. H. Evans, V. B. Parker, R. H. Schumm, and R. L. Nuttall, Technical Note 270–8, U.S. Government Printing Office, Wash., DC (1981); Review.

82GUR L. V. Gurvich, I. V. Veits, V. A. Medvedev, et al, V. P. Glushko, gen. ed., "Thermodynamic Properties of Individual Substances," Nauka, Moscow, **4**, (1982); Review.

82NBS D. D. Wagman, W. H. Evans, V. B. Parker, R. H. Schumm, I. Halow, S. M. Bailey, K. L. Churney, and R. L. Nuttall, "The NBS Tables of Chemical Thermodynamic Properties," J. Phys. Chem. Ref. Data, 11, Supplement No. **2**, 392 pp (1982); Review.

85FIN/LEI J. K. Fink and L. Leibowitz, "Handbook of Thermodynamic and Transport Properties of Alkali Metals," ed. Ohse, R.W., Blackwell Sci. Publ., Oxford, (1985) 411–434; Review.

85JAN M. W. Chase, Jr., C. A. Davis, J. R. Downey, Jr., D. J. Frurip, R. A. McDonald, and A. N. Syverud, "JANAF Thermochemical Tables, 3rd Edition," J. Phys. Chem. Ref. Data 14, Supplement No. **1**, (1985); Review.

85OHS/BAB R. W. Ohse, J.-F. Babelot, J. Magill, and M. Tetenbaum, Pure Appl. Chem. **57**, 1407–26 (1985); Review.

85VIL/CAL P. Villars and L. D. Calvert, "Pearson's Handbook of Crystallographic Data for Intermetallic Phases," **2** and **3**, Amer. Soc. for Metals, Metals Park, OH (1985); Crystal structures, Review.

89COX/WAG J. D. Cox, D. D. Wagman, and V. A. Medvedev, "CODATA Key Values for Thermodynamics," Hemisphere Publ. Corp., New York, 260 (1989); Review.

89DIN A. T. Dinsdale, "SGTE Data for Pure Elements," National Phys. Lab., U. K., Report DMA (A)195 (1989); Review.

93ALC/CHA C. B. Alcock, M. W. Chase, and V. P. Itkin, J. Phys. Chem. Ref. Data **22**(1), 1–85 (1993), Review..

2. Lithium

2.1. Introduction

At ambient pressure Li has two crystalline modifications: α-Li at low temperatures and β-Li at higher temperatures (Table 1.1). The α-β transition of Li is a typical martensitic transformation. The direct β→α transformation starts on cooling β-Li at about 70 K; it is not completed at the lowest attained temperatures. The degree of transformation (phase proportion) after cooling to different temperatures is known approximately. The reverse α→β transformation starts on heating at about 95 K and ends at about 165 K. After deformation below 80 K a metastable fcc phase can also appear.

Below 70 K the measured C_p values and calculated thermodynamic functions are not accurate, they depend on the degree of transformation. The C_p data for Li between 70 and 600 K are well known, but above 600 K the uncertainty in the enthalpy and heat capacity values of liquid Li increases, and the data are in poor agreement. It is not clear if a minimum exists in the heat capacity values for the liquid Li.

2.2. Heat Capacity and Enthalpy Measurements

2.2.1. Temperature below 298.15 K

[35SIM/SWA]

Simon and Swain measured the heat capacity of a commercial *Kahlbaum* Li from 15 K to room temperature in an adiabatic calorimeter (about 100 experimental points). [35SIM/SWA] tabulated only smooth values (see Table 2.11, Fig. 2.2 and 2.3). The Debye temperature at 15 K was estimated as 328 K. The authors plotted ΔC_p vs T and observed a broad peak with a maximum at about 100 K. [55DOU/EPS] examined the results of [35SIM/SWA] and compared the C_p values with those for a sapphire sample, measured by the authors of [35SIM/SWA] and those obtained in the National Bureau of Standards in 1953, the latter values being about 4 % higher. At 300 K the value for C_p of Li [35SIM/SWA] was lower than that of [55DOU/EPS] also by about 4 %, and the complete set of data of [35SIM/SWA] probably has a systematic error of about 4 %. The authors of [55DOU/EPS] introduced a 4 % correction to the data of [35SIM/SWA] and calculated acceptable values for the standard entropy $S°(298\ K) = 28.37\ J·K^{-1}·mol^{-1}$ and the enthalpy difference $H°(298\ K)-H°(0) = 4560\ J·mol^{-1}$.

[57ROB]

Roberts measured the heat capacity of Li between 1.5 and 20 K in a Nernst calorimeter. The sample (Matthey & Co. Ltd. with 0.3 to 0.5 wt.% Na and 0.05 wt.% K) contained some oxide impurities. Reproducible results were obtained between 2.4 and 13 K, and above 17 K; the data between 13 and 17 K were poor, and an anomaly was found in this region. Below 2.4 K the measured values tend to be high, less reliable and rather scattered. The 44 experimental points measured in the range 2.4 to 4.5 K are shown in a small-scale graph and from these data $\gamma = 1.75\ mJ·K^{-2}\ mol^{-1}$ and $\Theta_D = 369$ K were calculated. The smoothed values given by Roberts are listed in the Table 2.20 (point at 2.5 K was corrected) and shown in Fig. 2.1 and 2.2. Some degree of oxidation of samples and unstable results below 2.4 K and at about 15 K are definite shortcomings of this study.

[59MAR]

Martin and his colleagues measured the heat capacity of Li several times at different temperatures [59MAR], [60MAR], [61MAR], [62MAR], [63FIL/MAR]. In these studies three different samples were used: a *natural* Li, and the isotopes ^{7}Li and ^{6}Li; the samples are fully described in the next paragraph and briefly mentioned in separate studies.

a. The *natural* Li sample was a commercial *sodium-free* grade of Lithium Corporation of America; the stated purity was 99.95 wt.%, principal impurities in wt.% were: K and Na − 0.005, Fe − 0.001, N − 0.02; the isotopic ratio was 92.6 % ^{7}Li and 7.4 % ^{6}Li; the density was 6.945 ± 0.003 g/cm^3 which is very close to that of natural Li.

b. The isotope ^{6}Li sample contained 99.3 % ^{6}Li, and was prepared by the Union Carbide Company for the Oak Ridge National Laboratory, Tennessee. (impurities in wt.%: Mg, Ba and Sr 0.01 each, Na and Cu 0.02 each, Fe 0.05, Ca 0.025).

c. The isotope ^{7}Li sample contained 99.99 at.% ^{7}Li; it had less than 0.001 wt.% of Na, K, Rb, and Cs. The results obtained with different materials vary; illustrations to this chapter and Tables in the Appendix include mostly data for *natural* Li or ^{7}Li samples.

Martin measured in [59MAR] C_p of ^{6}Li and ^{7}Li samples at 20 to 300 K in an adiabatic calorimeter with an accuracy of ± 0.2 % above 80 K, and ± 2 % at about 20 K. Between 20 and 30 K the heat capacity of the isotope ^{6}Li was slightly lower than that for *natural* Li. The reverse martensitic transformation occurred in ^{6}Li similar to *natural* Li, but in samples cooled to 20 K the overall thermal effect in ^{6}Li, 190 $J·mol^{-1}$, was smaller than that in *natural* Li, 273 $J·mol^{-1}$. The measured data were shown in small-scale graphs at 21–30 K (50 points) and 90–180 K (70 points for all samples). The tabulated smoothed values at 25–300 K are reproduced in Table 2.21 and shown in Fig. 2.3 (for ^{7}Li).

[60MAR]

Martin measured the heat capacity of *natural* Li from 20 to 300 K in an adiabatic calorimeter using two samples and five different thermal treatments. In total, about 120 data points were tabulated (Table 2.23). As Li has a phase transformation at about 80 K, the heat capacity of samples cooled below 80 K depends on the phase proportion which was not determined. On heating, the reverse transformation was observed at 90 to 170 K from an increase in the *apparent* C_p values measured during reverse transformation; the *apparent* C_p values varied within 4 %. Martin assumed that a sample cooled to 4 K after annealing at 300 K consists mostly of an α phase, and these C_p values were adopted for the pure α-Li. The enthalpy of the transformation, 58.5 $J·mol^{-1}$, was estimated from the difference between the true and *apparent* heat capacities.

The C_p data listed in Table 2.23 are essentially the same as those given in [59MAR]; some of the data are shown in

Fig. 2.3. The standard entropy was calculated by the author as $S°(298\ K) = 29.08 \pm 0.17\ J·K^{-1}·mol^{-1}$.

The melting point of the sample was measured carefully by Martin with a Pt resistance thermometer as 453.65 ± 0.1 K, using low rates of fusion and crystallization.

[61MAR]

Martin also measured the heat capacity of the isotope ^6Li and *natural* Li samples from 0.4 to 1.5 K in an isothermal calorimeter. For each sample two series of 35 measurements were made. The results, shown in a small-scale graph, were fitted to two-term polynomials. The electronic specific heat coefficient of the *natural* Li was $\gamma = 1.63 \pm 0.03\ mJ·K^{-2}\ mol^{-1}$ and the Debye temperature $\Theta_D = 335 \pm 30$ K; for the isotope ^6Li Martin found $\gamma = 1.64 \pm 0.03\ mJ·K^{-2}\ mol^{-1}$ and $\Theta_D = 380 \pm 60$ K. Martin suggested that the value of γ is independent of isotopic composition. The values calculated using these parameters are given in Table 2.24 and shown in Fig. 2.1 for *natural* Li.

[62MAR]

The *natural* Li sample was studied from 100 to 300 K in a modified calorimeter and the smoothed results were tablulated in steps of 10 K. The deviation between the values of this study (Table 2.26) and those of [60MAR] reached 0.4 % below 140 K (Fig. 2.3). To avoid the martensitic transformation, care was taken not to cool the sample below 80 K.

[63FIL/MAR]

Filby and Martin measured the heat capacity of *natural* Li and isotopes ^6Li and ^7Li in the temperature range from 3 to 30 K in an adiabatic calorimeter. The accuracy of these measurements was about 1 %. About 400 data points are given in the form of the Debye temperature values calculated from the C_p values. The authors tabulated smoothed C_p values for each sample (Table 2.27, Fig. 2.2). No difference was observed between samples which were cooled to 20 and 4 K. An anomaly at 15 K found in [57ROB] was not confirmed. The Debye temperature at 0 K was estimated as 344.0 ± 2.5 K for *natural* Li, 367.0 ± 2.5 K for isotope ^6Li, and 337.0 ± 2.5 K for ^7Li. The authors assumed that their samples contained about 80 % α-Li and 20 % β-Li. Filby and Martin studied the isotope ^7Li also in the range 0.4 to 1.5 K. About 60 points were shown in a small-size graph. From these measurements the Debye temperature was determined as $\Theta_D = 356 \pm 60$ K and $\gamma = 1.65 \pm 0.02\ mJ·K^{-2}\ mol^{-1}$.

[64MAR/ZYC]

Martin and Zych remeasured the ^7Li sample in a calorimeter between 0.35 and 2 K. The results of these measurements, 40 points of heat capacity of the sample plus container, are shown in a small-scale graph. The heat capacity of the container was estimated and subtracted from the experimental data, and the difference, heat capacity values for the sample, was fitted to an equation corresponding to $\gamma = 1.71\ mJ·K^{-2}\ mol^{-1}$ and $\Theta_D = 260 \pm 10$ K (Fig. 2.1). The C_p values calculated using these γ and Θ_D (Table 2.28 and Fig. 2.1) disagree with previous investigations by the same authors and may be the result of errors in the measurements or estimation of heat capacity of the container.

2.2.2. Temperature above 298.15 K

[50CAB]

Cabbage measured the enthalpy of liquid Li from 780 to 1280 K in a drop calorimeter using a commercial 99 % Li material from Eimer and Amend; samples were analyzed before and after experiment and contained up to 0.37 wt.% Li_2O and 0.92 wt.% LiN. The original 30 points for liquid Li have a considerable scatter of ± 25 − 30 %; the average values are listed in Table 2.12 and shown in Fig. 2.5. The data were fitted to a two-term equation

$$H°(T,l) - H°(298\ K,cr) = 345.5 + 20.33T\ J·mol^{-1}.$$

Using literature data and his own measurements, Cabbage recommended two C_p expressions from the melting point to 773 K.

$$C_p° = 55.2 - 31.95\times10^{-3}T\ J·K^{-1}·mol^{-1};$$

and from the melting point to 1273 K

$$C_p° = 41.14 - 11.33\times10^{-3}T\ J·K^{-1}·mol^{-1}.$$

The values calculated by these equations disagree substantially with subsequent measurements. Solid Li was measured in the interval 378 to 424 K (11 points); Cabbage suggested that these data are even worse than those for liquid Li. The average C_p value between 298 K and the melting point was estimated as $16.6\ J·K^{-1}·mol^{-1}$. The results of this study are very inaccurate.

[50KUB]

Kubaschewski quoted a dissertation by 0. Huchler (Techn. Hochschule, Stuttgart, 1944) who determined the heat capacity of liquid Li from the melting point to 550 K as a constant value $C_p° = 29.3 \pm 1.2\ J·K^{-1}·mol^{-1}$.

[50YAG/UNT]

Yaggee and Untermeyer estimated the heat capacity of Li from rates of cooling. At 473 to 773 K four C_p values were obtained; they are given in Table 2.13. The rapid increase in C_p values with temperature observed in this study contradicts other data. The authors estimated their error as ± 10 %, but it is probably much higher.

[51BAT/SMI]

Bates and Smith measured the enthalpy of liquid Li from 773 to 1273 K in a Bunsen calorimeter. Fifteen experimental points are listed in Table 2.14 and shown in Fig. 2.5. They were described by the linear equation

$$H°(T,l) - H°(273\ K,cr) = -4113 + 27.94T\ J·mol^{-1}$$

Bates and Smith estimated their accuracy as 5 %.

[52RED/LON]

Redmon and Lones measured the enthalpy of Li, containing 0.036 wt.% metallic impurities (Na − 0.005, Ca − 0.02, K −

0.01, Fe − 0.001 %) and 0.06 wt.% nitrogen, in a drop calorimeter from 473 to 1373 K. The 69 experimental points showed a scatter within 5 %; they were combined in 16 average points given in Table 2.15 and shown in Fig. 2.5. The data were described by an equation

$$H°(T,l)-H°(273\ K,cr) = -5287 + 28.82T + 4.07\times10^{-4}T^2\ J\cdot mol^{-1}.$$

The derived C_p values are shown in Table 2.16 and Fig. 2.4. The levels of metallic impurities in these samples were checked after the experiment, and the total was found to have increased to 0.45 wt.% due to interaction with the stainless container.

[55DOU/EPS]

Douglas *et al.* measured the enthalpy of Li (Maywood Chemical Co., 0.2 wt.% metallic impurities, vacuum distilled) from 273 to 1173 K in an ice drop calorimeter. Two samples were used: sample 1 had 99.98 at.% Li, non−metallic impurities in ppm: 0 − 280, N − 30; metallic impurities in ppm: Fe − 36, Ni − 6, Ca − 290, Na − 160. Sample 2 had 99.99 at.% Li and metallic impurities: Fe − 6, Ni − 3, Ca − 10, Na − 30 ppm. No reliable values for oxygen and nitrogen were obtained for sample 2, but the authors assumed that these were less than half of the respective amount for sample 1. According to thermal analysis, sample 1 had a melting point 453.57 K, and sample 2, T_{fus} = 453.62 ± 0.001 K; the triple point was estimated as 453.69 ± 0.03 K based on the presence of 0.011 at.% of soluble and insoluble impurities in sample 2.

The enthalpy data are listed in Table 2.17 and shown in Fig. 2.5. The accuracy was estimated by the authors as ± 0.5 % up to 433 K, ± 0.3 % from 523 to 1073 K. The data were fitted to three equations: for solid Li at 298 − 453.69 K

$$H°(T,cr)-H°(273\ K,cr) = -8827 + 52.29T - 1.285\times10^{-1}T^2 + 2.45\times10^{-4}T^3 - 1.542\times10^{-7}T^4\ J\cdot mol^{-1},$$

for liquid Li at 453.69 − 693 K

$$H°(T,l)-H°(273\ K,cr) = -6599.1 + 33.036T - 2.909\times10^{-3}T^2\ J\cdot mol^{-1};$$

for liquid Li at 693 − 1173 K

$$H°(T,l)-H°(273\ K,cr) = -5315.4 + 29.342T - 2.509\times10^{-4}T^2\ J\cdot mol^{-1}.$$

C_p values derived from the above equations are given in Table 2.18 and shown in Fig. 2.3 and 2.4. The enthalpy of fusion was derived from the first and second equations as $\Delta_{fus}H$ = 3000 ± 15 J·mol^{-1} at 453.69 K. The study could be assessed as very careful.

[56SCH/HIL]

Schneider and Hilmer measured the enthalpy of Li (purity was not stated) in a mixing calorimeter from 398 to 553 K (Table 2.19, Fig. 2.5). The average heat capacity was determined for solid Li between 403 and 450 K as $C_p^°$ = 26.8 ± 0.4 J·K^{-1}·mol^{-1}, and for liquid Li between 493 and 553 K as $C_p^°$ = 25.9 ± 1.2 J·K^{-1}·mol^{-1} which is a very low value. The enthalpy of fusion was determined as 2950 ± 40 J·mol^{-1}.

[59NIK/KAL]

Nikol'skii *et al.* measured the heat capacity of Li (the purity was not stated) by stepped heating in a calorimeter with isothermic shield at 473 − 673 K. Four points are shown in the graph and five smooth values were tabulated; they are reproduced in Table 2.22. The accuracy of measurements is low. Contrary to other studies, C_p values increased with rising temperature.

[62ALA/PCH]

Aladyev and Pchelkin (quoted from [70SHP/YAK]) measured the heat capacity of commercial Li, containing 0.5 wt.% Na and 0.02 wt.% K, in an isothermal calorimeter at 473 to 1573 K. The scatter of these data was considerable, ± 8 %. The smoothed values, listed in Table 2.25 and shown in Fig. 2.4 are taken from [70SHP/YAK].

[65SHP/SOL], [70SHP/KOV]

Shpil'rain *et al.* measured the enthalpy of Li (99 wt.%) from 773 to 1573 K in a boiling-point calorimeter. The sample had impurities in wt.%: Na 0.26, K 0.001, Ca 0.003, N 0.0072, other impurities <0.015. The results (18 points) are tabulated and reproduced in Table 2.32 and shown in Fig. 2.5. Interaction between the samples and the niobium container and oxidation of Li was mentioned as sources of error. The results obtained were fitted to the equation, quoted in [65SHP/SOL]

$$H°(T,l)-H°(373\ K,cr) = -8085 + 29.06T - 1.502\times10^{5}/(T-273),\ J\cdot mol^{-1}.$$

The error was estimated by the authors as ± 2 %. Heat capacities calculated from the above equation are given in Table 2.33 and shown in Fig. 2.4.

[67ACH/FIS]

Achener and Fisher measured the enthalpy of Li from 367 to 1422 K by drop calorimetry. The 21 data points (Table 2.29, Fig. 2.5) are taken from a graph given in the review [85FIN/LEI].

[69NOV/GRU]

Novikov *et al.* measured the enthalpy of Li in an ice drop calorimeter from 459 to 921 K. The specimen had a composition in wt.%: 99.33 Li, 0.38 Na, 0.14 Mg, 0.01 K and Al, 0.001 Fe, 0.003 Ca, 0.005 heavy metals, and 0.012 N. According to the authors, the error in enthalpy measurements was about ± 0.3 %. The results of 13 measurements and the derived C_p values are given in Tables 2.30 and 2.31 and shown in Fig. 2.4 and 2.5. No experimental details are given; this makes estimation of the accuracy of this study difficult.

[83NOV/ROS]

Novikov *et al.* measured the enthalpy in the range 320 to 700 K using an ice drop calorimeter. The material had a

composition in wt.%: Li > 99.5, Na < 0.06, K < 0.005, Mg < 0.02, Ca < 0.03, Mn < 0.001, Fe < 0.005, Al < 0.003, SiO_2 < 0.01, N (nitrides) < 0.05. The sample was placed in a stainless steel container, and there was evidence that the container reacted with Li. The authors listed enthalpy values from 328 to 695 K (Table 2.34, Fig. 2.5). The results for solid and liquid Li were fitted to five-term equations which yield widely oscillating C_p° values. Therefore, the present authors fitted the data of [83NOV/ROS] to simpler polynomials for solid Li

$$H^\circ(T,\text{cr}) - H^\circ(273\text{ K,cr}) = -3347 + 5.0685T + 2.8296\times10^{-2}T^2\text{ J mol}^{-1};$$

and for liquid Li

$$H^\circ(T,\text{l}) - H^\circ(273\text{ K,cr}) = -5467 + 29.616T - 6.0553\times10^{-4}T^2\text{ J mol}^{-1}.$$

The heat capacities calculated by the above equations are shown in Figs. 2.3, 2.4, and listed in Table 2.35. The enthalpy of fusion was estimated as $\Delta_{fus}H = 3022 \pm 27$ J·mol^{-1} at $T_{fus} = 453.7$ K. The study has low accuracy.

2.3. Discussion of Heat Capacity and Enthalpy Data

2.3.1. β-Li below 298.15 K

Measurements near 0 K. Below 4 K the heat capacity was measured in [57ROB], [61MAR], [63FIL/MAR], [64MAR/ZYC]. The results are shown in a C_p/T vs T^2 graph (Fig. 2.1). The electronic contribution to the heat capacity (γ) and the Debye temperature (Θ_D), derived from these data, are listed below.

Table 2.1 and Fig. 2.1 show that the results disagree. Only studies [61MAR] and [63FIL/MAR] give consistent results; [64MAR/ZYC] probably has some errors because the Θ_D value is very low. The data of [57ROB] lead to higher values of γ and Θ_D. [61MAR] and [63FIL/MAR] compared isotopes ^{6}Li, ^{7}Li and *natural* Li and found that they have different Debye temperatures as shown in Table 2.1; however, the value of γ for different isotopic compositions was about the same, $\gamma = 1.63$ mJ·K^{-2} mol^{-1}.

[63FIL/MAR] recommended for *natural* Li $\Theta_D = 344 \pm 2.5$ K. These values were accepted here and used to derive the heat capacity equation for the temperature range from 0 to 4 K

$$C_p^\circ = 1.63T + 0.04775T^3\text{ mJ·K}^{-1}\text{·mol}^{-1}. \quad (1)$$

Measurements between 4 and 30 K. For this temperature range, the C_p measurements were made in [35SIM/SWA] (above 15 K), [57ROB] (1.5 − 20 K), [60MAR] (above 20 K), [63FIL/MAR] (3 − 30 K). The data agree within 3 % (Fig. 2.2). However, the presence of two phases, α-Li and β-Li, complicates the selection of the best values. [60MAR] listed various results for different samples and thermal treatments. To decrease the uncertainty, those thermal treatments were selected which showed a smaller degree of the reverse transformation (smaller fraction of α-Li in cooled specimens); then the data can be treated as applicable to β-Li. Values selected for the interval 4 − 30 K were taken from measurements made with a *natural* Li sample cooled to 4 K [63FIL/MAR]. They agree with the results of [60MAR] obtained with a sample cooled to 20 K. The selected values are listed in Table 2.2.

The above information was fitted to an equation for the temperature range 4 − 30 K:

$$C_p^\circ = 0.03632 - 6.37\times10^{-3}T - 0.21707T^{-2} + 6.1723\times10^{-4}T^2 + 2.914\times10^{-5}T^3\text{ J·K}^{-1}\text{·mol}^{-1}. \quad (2)$$

Measurements between 30 and 298 K. Above 30 K the data of [35SIM/SWA] (15–300 K), [59MAR], [60MAR] (20–300 K), [62MAR] (100–300 K) agree within 4 % (Fig. 2.3). The disadvantages of [35SIM/SWA] were discussed above. Good agreement is observed between the results of [59MAR], [60MAR], and [62MAR] obtained in two different calorimeters. The average results for specimens cooled to 20 K in [60MAR] were selected as the best between 30 and 85 K. The *apparent* heat capacity above 85 K increased due to the reverse martensitic transformation; therefore, some portion of α-Li was present in these specimens. For temperatures 90 and 95 K, the results for a single-phase specimen cooled to 85 K [60MAR] were selected. Between 100 and 300 K better values were obtained in [62MAR]. At 300 K there is a discrepancy between the values obtained by low-temperature calorimety [60MAR], [62MAR], 24.9 J·K^{-1}·mol^{-1}, and by drop calorimetry in [55DOU/EPS], 24.68 J·K^{-1}·mol^{-1}; the average of these two methods, C_p° (300 K) = 24.8 J·K^{-1}·mol^{-1} was adopted for the calculations. The values selected at different temperatures are listed below in Table 2.3.

The heat capacity values listed in Table 2.3 were fitted to two equations for the ranges from 30 to 110 K

$$C_p^\circ = -2.407 + 3.035\times10^{-2}T + 6.8415\times10^{2}T^{-2} + 2.54\times10^{-3}T^2 - 1.311\times10^{-5}T^3,\ \text{J·K}^{-1}\text{·mol}^{-1} \quad (3)$$

and from 110 to 298.15 K

$$C_p^\circ = 5.085 + 0.151T - 3.666\times10^{4}T^{-2} - 4.0596\times10^{-4}T^2 + 4.1985\times10^{-7}T^3\text{ J·K}^{-1}\text{·mol}^{-1}. \quad (4)$$

The Eqs 1 − 4 were used to calculate $C_p^\circ(T)$, $H^\circ(T) - H^\circ(0)$ and $S^\circ(T)$. The calculated values are shown in Table 2.9. The heat absorbed during heating of Li samples cooled to 55 K was on average 29 J·mol^{-1} [60MAR]; this amount of heat corresponds to about 55 % of β-Li transformed to α-Li. The entropy of transformation for samples cooled to 55 K was found from the area under the $\Delta C_p/T$ vs T curve as 0.23 J·K^{-1}·mol^{-1}. These values $\Delta H = 29$ J·mol^{-1} and $\Delta S = 0.23$ J·K^{-1}·mol^{-1} were added at 100 K to the calculated functions S°(100 K) and H°(100 K) − H°(0). At the standard temperature, the heat capacity, enthalpy and entropy were calculated as

C_p°(298.15 K)	= 24.822 J·K^{-1}·mol^{-1}
S°(298.15 K)	= 28.987 J·K^{-1}·mol^{-1}
H°(298.15 K) − H°(0)	= 4617.16 J·mol^{-1}

These values are compared with those recommended in different reviews in Table 2.4.

The values adopted in Table 2.4 are close to those selected in [85JAN]. The discrepancies between reviews, which are about 15 $J \cdot mol^{-1}$ for the enthalpy and 0.3 $J \cdot K^{-1} \cdot mol^{-1}$ for the entropy, originated mostly from different treatments of the same experimental information. The uncertainty of the adopted value of 30 $J \cdot mol^{-1}$ for $H°(298.15\ K) - H°(0)$ and 0.3 $J \cdot K^{-1} \cdot mol^{-1}$ for $S°(298.15\ K)$ reflects mostly the uncertainty in the phase composition below 85 K and an approximation made for the evaluation of the enthalpy and entropy of the reverse martensitic transformation. The calculated values differ from [82GUR]; although the discrepancy is small, it is worth mention, and new values based on the present calculations were adopted.

2.3.2. β-Li above 298.15 K.

Above 298.15 K the enthalpy and heat capacity of solid Li was measured in [55DOU/EPS], [56SCH/HIL], [83NOV/ROS]. The C_p data are scattered within 8 % (Fig. 2.3). The results of [55DOU/EPS] were used to derive the equation from 298 to 453 K.

$$C_p^\circ = -41.033 + 220.639\times10^{-3}T + 14.039\times10^{5}T^{-2} - 177.38\times10^{-6}T^{2}\ J \cdot K^{-1} \cdot mol^{-1} \quad (5)$$

Reviews [73HUL], [82GUR], [85JAN] quoted [55DOU/EPS] as a main source and the adopted C_p values almost coincide. [82GUR] recommended for solid Li a three-term equation

$$C_p^\circ = 1.309 + 0.056287T + 6.017\times10^{5}T^{-2},\ J \cdot K^{-1} \cdot mol^{-1}$$

2.3.3. Liquid Li

Several enthalpy and heat capacity measurements are described in [50CAB] (ΔH, 780 − 1280 K), [50KUB] (C_p° = 29.3 J $K^{-1}mol^{-1}$ at 453–550 K), [50YAG/UNT] (C_p, 473–773 K), [51BAT/SMI] (ΔH, 760–1269 K), [52RED/LON] (ΔH, 503–1361 K), [55DOU/EPS] (ΔH, 323–1168 K), [56SCH/HIL] (ΔH, 404–523 K), [59NIK/KAL] (C_p, 473–673 K), [62ALA/PCH] (C_p, 473–1573 K), [67ACH/FIS] (ΔH, 482–1423 K), [69NOV/GRU] (ΔH, 459–921 K), [70SHP/KOV] (ΔH, 788–1573 K), [83NOV/ROS] (ΔH 328–694 K). The results are shown in Fig. 2.4 for C_p and in Fig. 2.5 for the enthalpy.

The enthalpy data of [52RED/LON], [55DOU/EPS], [56SCH/HIL], [67ACH/FIS], [69NOV/GRU], [70SHP/KOV], [83NOV/ROS] agree satisfactorily and could be described by a common equation (Fig. 2.5), while those of [50CAB] and [51BAT/SMI] fell out of the general trend and contain some errors. The scatter of individual points in [52RED/LON], [69NOV/GRU], [70SHP/KOV], [83NOV/ROS] is considerable; the heat capacity values derived from these sources vary within 7% (Fig. 2.4).

Judging by the description of technique, materials, and procedure, [55DOU/EPS] seems to be the most carefully done. This study was assessed in [70SHP/YAK], [73HUL], [82GUR], [85JAN] as the most reliable. In this evaluation [55DOU/EPS] was selected as a basis for recommendations. According to this study, the heat capacity of liquid Li decreases with temperature; initially the decrease is rapid from 30.5 $J \cdot K^{-1} \cdot mol^{-1}$ at the melting point to 29 $J \cdot K^{-1} \cdot mol^{-1}$ at 700 K; then the decrease decelerates to about 0.1 $J \cdot K^{-1} \cdot mol^{-1}$ per 100 kelvins above 700 K. The heat capacity was described in [55DOU/EPS] by two linear equations: from the melting point to 700 K as

$$C_p^\circ = 33.035 - 5.818\times10^{-3}T,\ J \cdot K^{-1} \cdot mol^{-1} \quad (6)$$

and from 700 to 1200 K as

$$C_p^\circ = 29.342 - 0.5018\times10^{-3}T,\ J \cdot K^{-1} \cdot mol^{-1}. \quad (7)$$

Both equations were adopted in this assessment. The C_p values calculated by Eq. 6 and 7 do not show the minimum which was postulated in the reviews [70SHP/YAK], [82GUR] and [85FIN/LEI]. It could be suggested that the minimum was not reached in the temperature range of the measurements of [55DOU/EPS]. Minima in heat capacity values were observed in other liquid alkali metals, and one could be expected in Li. The only evidence of its existence at 1300 K was given in [62ALA/PCH], which is not considered to be a reliable study at this temperature.

Using the same input, previous reviewers recommended different values and equations. Below 1200 K [70SHP/YAK] used [55DOU/EPS] (Eq. 6 and 7); Shpil'rain *et al.* suggested a minimum at 1200 K and proposed a third C_p equation for 1200 − 2000 K on the basis of the data of [62ALA/PCH], [70SHP/KOV], [52RED/LON]

$$C_p^\circ = 26.87 + 1.536\times10^{-3}T\ J \cdot K^{-1} \cdot mol^{-1}.$$

[73HUL] also adopted values from [55DOU/EPS] below 1200 K; at higher temperatures Hultgren *et al.* assumed a constant

$$C_p^\circ = 28.7\ J \cdot K^{-1} \cdot mol^{-1}.$$

Gurvich *et al.* [82GUR] combined the results of seven studies: [51BAT/SMI], [52RED/LON], [55DOU/EPS], [62ALA/PCH], [67ACH/FIS], [69NOV/GRU], [70SHP/KOV], and fitted the combined data to one equation from the melting point to 3000 K:

$$C_p^\circ = 31.227 - 5.265\times10^{-3}T + 2.050\times10^{5}T^{-2} + 2.628\times10^{-6}T^{2}\ J \cdot K^{-1} \cdot mol^{-1}$$

According to this equation, the heat capacity decreases from 30.4 $J \cdot K^{-1} \cdot mol^{-1}$ at the melting point, to a minimum 28.8 $J \cdot K^{-1} \cdot mol^{-1}$ at 1000 K (Fig. 2.4), and then C_p increases again to 29.6 $J \cdot K^{-1} \cdot mol^{-1}$ at 1600 K.

Fink and Leibowitz [85FIN/LEI] used the enthalpy data of [51BAT/SMI], [52RED/LON], [55DOU/EPS], [67ACH/IS], [69NOV/GRU], [70SHP/KOV] to derive a cubic equation for the enthalpy which corresponds to the quadratic equation for C_p

$$C_p^\circ = 32.992 - 6.4199\times10^{-3}T + 2.0166\times 10^{-6}T^2 \text{ J}\cdot\text{K}^{-1}\cdot\text{mol}^{-1}.$$

This equation has a minimum at about 1600 K and corresponds to values which are close to [62ALA/PCH] (within 2 %, Fig. 2.4). However, the data of [62ALA/PCH] deviate from other sources above 800 K and are not considered reliable. Disagreement is observed between the values calculated by the above equation [85FIN/LEI] and heat capacities, derived from the enthalpy measurements of [55DOU/EPS], [69NOV/GRU], [70SHP/KOV] (Fig 2.4).

The C_p equations recommended in [82GUR] and in [85FIN/LEI] do not appear to be the best possible. To assess the correctness of treatments of the data, it should be remembered that the enthalpy data are less sensitive to changes than heat capacities. Small fluctuations in the enthalpy values may result in significant changes in the derived C_p values, and their analysis can signal the presence of problems in the experimental enthalpy data. Therefore it seems important to compare not only the measured enthalpies but the heat capacities derived from these measurements which should be combined with the directly measured C_p data.

Bringing together data of different quality in one statistical pool may result in emphasizing inaccurate data over better results, and errors can propagate in a fitted equation. Therefore the recommendations of [82GUR] and [85FIN/LEI] may be influenced by poor measurements, since they appear to be inaccurate at high temperatures.

[85JAN] used the results of [55DOU/EPS] and extrapolated them smoothly to 2000 K. Such a treatment seems to be simple and reasonable, and it was also adopted in this assessment. If Eq. 7 is extrapolated beyond the limit of measurements of 1173 K to the much higher temperature of 1600 K, it still describes the heat capacities with an acceptable accuracy, giving the values which, in the opinion of present authors, are better than those calculated by equations recommended in [70SHP/YAK], [82GUR] and [85FIN/LEI]. The present authors suggest that Eq. 7 can be safely used up to 1600 K. The existence and location of a probable minimum in the C_p values requires further investigation. The values of $C_p^\circ(T)$, $S^\circ(T)$ and $H^\circ(T)-H^\circ(298.15\text{ K})$ from 298.15 to 1600 K were calculated using Eqs 5, 6 and 7. They are listed in Table 2.10.

2.4. Phase Equilibrium Data

2.4.1. β-α Martensitic Transformation of Li

The β-α transformation of Li on cooling is a typical diffusionless martensitic transformation. It extends over a wide temperature range, and has a considerable thermal hysteresis between the direct process on cooling and the reverse process on heating. It begins on cooling below the so-called martensite start temperature designated as M_s. Initially the nuclei of α-Li grow very rapidly, and a portion of the high temperature β phase is transformed into the α phase. The growth region of the new phase generates new interface and strain energy in the surrounding material. As the surface and deformation Gibbs energies are always positive, they reduce the driving force of the transformation, and it stops. On lowering the temperature, the Gibbs energy of the phase transformation becomes more negative, more nuclei are able to grow, and another portion of the low-temperature phase will be formed. External forces can act similarly to supercooling, making the energy difference between two phases more negative and promoting the transformation. In the case of Li (and Na) even at the lowest attained temperature, the transformation was never completed. The degree of transformation depends on the rate of cooling, temperature, deformation, grain size, chemical composition, and thermal treatment history of samples.

On heating a partially transformed sample, the reverse α-Li→β-Li transformation begins at a temperature designated as A_s, and extends over a considerable temperature range ending at a temperature designated as A_f; a hysteresis is always observed between the direct and reverse transformations (see the scheme below).

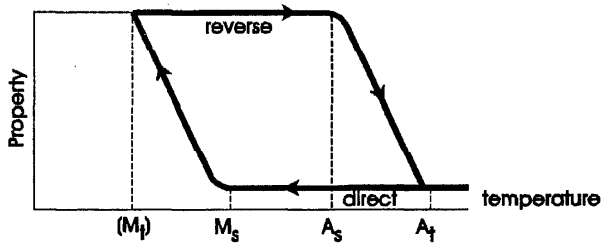

To describe the transformation the several characteristic temperatures should be given: M_s, A_s, A_f. Each of these temperatures can vary from sample to sample.

The thermal effect accompanying the reverse α-Li→β-Li transformation was measured in a calorimeter [60MAR]. It was found from the area under the C_p vs T curve, where ΔC_p is the heat capacity difference between the *true* heat capacity of a sample in which the transformation was suppressed or completed and the *apparent* heat capacity of a sample in which the reverse transformation occurs. On heating, the value of ΔC_p increases from zero at A_s to a maximum at some temperature, T_{max} (another characteristic temperature frequently used), where the rate of the reverse transformation is highest, and then gradually decreases to zero when the transformation is completed at A_f. The magnitude of ΔC_p depends mostly on the degree of the preceding direct transformation, i.e. on the amount of α-Li formed in a sample during cooling. However, the degree of transformation was not measured for specimens used for calorimetry. It was adopted from the literature, which gives a wide variety of values up to 90 % [60HUL/ROS]. Therefore, the total enthalpy of α-β transformation of Li was estimated only approximately. A similar procedure could be applied for the entropy by integrating the $\Delta C_p/T$ vs T curve.

[47BAR]

Barrett determined by X-ray analysis the transformation in a deformed commercial Li at 78 K. The high-temperature β modification with lattice parameter a = 0.35 nm was partially transformed to an fcc form with a = 0.441 nm, the transformation being accompanied with audible clicks. The fcc phase disappeared on heating above 156 K.

[48BAR/TRA]

Barrett and Trautz investigated, by X-ray diffraction, a commercial Li (99.45 wt.% Li; impurities according to spectrographic analysis: Si, Mg, Pb, Fe, Sn 0.01 wt.% each; Na and Cu 0.001 wt.%; Al 0.002 wt.%). A better sample from Battelle Memorial Institute (99.86 wt.% Li) was used to check the results obtained with the commercial material. After a sample had undergone 80 % plastic deformation in liquid nitrogen (78 K), it showed diffraction lines of an fcc phase with parameter a = 0.441 nm. The transformation was identified as martensitic. Without deformation quite different lines were observed, and they belonged to an α phase with lattice parameters a = 0.314, c = 0.470 nm. The phase composition of samples was estimated from the intensity of the strongest lines; the amount of low-temperature phase in all experiments was less than 60%. The transformation has a thermal hysteresis of 40 − 50 K. The β→α transformation started on cooling at about M_s = 71 K.

[56BAR]

Barrett remeasured the lattice parameters of the α phase a = 0.3111, c = 0.5093 nm and the β phase, a = 0.3491 nm at 78 K. Deformation at low temperatures produces a metastable fcc phase at the expense of the α and β phases. Without deformation only the β and α phases were observed.

[60HUL/ROS]

Hull and Rosenberg studied the transformation of 99.7 wt.% Li, (by X-ray analysis). On cooling, the transformation starts at M_s = 76 K, and the amount of the converted phase increases with decreasing temperature. However, below 20 K no additional α phase was found. The maximum amount of the α phase present in samples was estimated as about 90 %.

[60MAR]

Martin measured the heat capacity of *natural* Li (composition is given in Sec. 2.2.1.) after different heat treatments. α-Li formed on cooling was transformed to β-Li on heating in an adiabatic calorimeter; the process was accompanied by heat absorption, which was exhibited as an increase in the *apparent* heat capacity above the true value. The reverse transformation started at 90 − 100 K, reached its maximum rate at T_{max} = 100 − 110 K and ended at 160 − 170 K. The amount of heat absorbed depended on the thermal treatment and varied from 24 to 43.5 J·mol^{-1}. When samples were cooled to 55 K, about 29 J·mol^{-1} was absorbed; Martin used results of [56BAR] that such cooling forms about 50 % α phase and estimated the total enthalpy of the α-β transformation as 58 J·mol^{-1}.

[81TRI/SLO]

Trivisonno *et al.* measured the velocity and the attenuation of ultrasonic vibrations at the frequency 10 MHz in single crystals of lithium at 20 to 180 K. When the sample was slowly cooled from 130 K (0.25 K min^{-1}), a large increase in attenuation and decrease in velocity was observed at M_s = 64 K. The M_s point was not well defined; its range extended in different experiments from 61 to 70 K. On heating, the reverse transformation started at A_s = 90 − 95 K, and ended at about A_f − 130 K.

[88SAU/MIO]

Saunders *et al.* estimated the Gibbs energy of the β-α transformation of Li above 200 K as $\Delta_{trs}G$ = 154 − 2T J·mol^{-1}, which corresponds to $\Delta_{trs}H$ = 154 J·mol^{-1} and equilibrium temperature T_{trs} = 77 K. This estimation has high uncertainty which can be greater than 50 %.

2.4.2. Fusion of Li

The measurements of the temperature of fusion were mentioned above in studies [55DOU/EPS], [60MAR] and [83NOV/ROS] (Sec. 2.2). Additional information is given below.

[35LOS]

Losana obtained by thermal anlysis the melting point of Li containing 0.015 wt.% Na, T_{fus} = 453.35 ± 0.1 K.

[52KIL]

Kilner measured 99.5 wt.% Li in a mixing calorimeter, T_{fus} = 452.15 ± 1 K, and $\Delta_{fus}H$ = 2890 ± 300 J·mol^{-1}.

[56SAL/AHM]

Salmon and Ahmann studied the Li-Na system by thermal and chemical analysis. The commercial lithium sample of Maywood Chemical Co. contained 99.8 wt.% Li, with the major impurities in wt.% Na − 0.02, Ca − 0.06, Fe − 0.03, Si − 0.015, heavy metals − 0.09. The melting point of Li was determined as 452.55 ± 0.5 K.

[58KEL/KAN]

Keller *et al.* studied the Ba-Li system by thermal analysis. Lithium was purchased from the Foote Mineral Co., and according to the gravimetric analysis, the sample had 99.86 − 99.9 wt.% Li, and according to the spectrographic analysis less than 0.1 wt.% Na. Several determinations gave an average melting point of 453.65 ± 0.5 K.

[61PON]

Ponyatovskii studied melting of a commercial Li (99.8 wt.% Li) by thermal analysis under high pressure. The melting temperature increased from 455.15 ± 1.5 K at ambient pressure to 507 ± 1.5 K at 30,000 atm.

[63WEA/JOH]

Weatherford *et al.* (quoted from [85OHS/BAB]) determined by thermal analysis T_{fus} = 454.9 K.

[68LUE/KEN]

Luedemann *et al.* (quoted from [85OHS/BAB]) determined by differential thermal analysis T_{fus} = 453.69 ± 2.0 K.

[72CUN/JOH]

Cunningham *et al.* studied the Li-S system by differential thermal analysis. A high-purity reactor grade lithium (99.98 wt.%) was obtained from the Foote Mineral Co. An average of two determinations was 453.65 ± 1.0 K.

[76HUB/PUL]

Hubberstey *et al.* found by thermal analysis of distilled 99.99 wt.% Li that the melting point is 453.64 ± 0.02 K; this is an average of 15 determinations on six samples. Special attention was paid to the depression of melting point by nitrogen and hydrogen. According to the description given in [76HUB/PUL], the obtained value seems to be very accurate.

The enthalpy of fusion was measured in [55DOU/EPS], [56SCH/HIL], and [83NOV/ROS] described in Sec. 2.2.2. Two more studies are given below.

[37BIN]

Binayendra reported the enthalpy of fusion of Li determined in a calorimeter, $\Delta_{fus}H = 3$ kJ·mol^{-1}. No experimental details are given. The same value was obtained in [37BIN] from a theoretical estimation of physical properties.

[71MAL/GIG]

Malaspina *et al.* determined the enthalpy of fusion of Li (*Fluka and Koch Light Lab* 99.9+ wt.% Li) in a Calvet calorimeter. The calorimeter was slowly heated in the temperature range 643 to 733 K. The heat effect was determined from a thermogram, the average of four determinations $\Delta_{fus}H$ = 2970 ± 60 J·mol^{-1}. On the basis of the literature and their own data, the authors of [71MAL/GIG] recommended the value $\Delta_{fus}H$ = 2975 ± 60 J·mol^{-1}.

2.5. Discussion of Phase Equilibrium Data

2.5.1. β-α Martensitic Transformation of Li

The β-α transformation of Li is described by several characteristic temperatures:

a. M_s—martensite start temperature, of the direct β→α transformation,
b. A_s— start temperature of the reverse α→β transformation,
c. A_f— finish temperature of the reverse transformation,
d. T_{max} — temperature at which the heat absorption process reaches its maximum during the reverse transformation.

The measured temperatures are listed in Table 2.5.

The adopted temperatures are: M_s = 70 ± 5 K (average of all measurements), A_s = 95 ± 5 K [60MAR], [81TRI/SLO], A_f – 165 ± 10 K [60MAR]. In previous reviews only one of several characteristic temperatures was selected from study [60MAR] to describe the transformation: the average of M_s and A_s in [73HUL] and [82GUR], and T_{max} in [85JAN].

The enthalpy of transformation was determined by integration of ΔC_p (difference between *apparent* and *true* C_p) vs T [60MAR]. The measured effect is related to the degree of martensitic transformation during sample preparation; this degree was not measured in [60MAR]; it was estimated from other sources. Therefore, the uncertainty in the recommended molar enthalpy of transformation could be about ± 50 %.

The adopted enthalpy for the complete transformation 54 ± 25 J·mol^{-1} was estimated using the maximum effect measured in [60MAR] 43.5 J·mol^{-1} and a degree of transformation of 80 %, which was assumed in agreement with X-ray data of [60HUL/ROS] for similar conditions. The values adopted in [73HUL] and in [81MED] are different because of different treatment of the same data [60MAR]. It should be mentioned that recently Saunders *et al.* [88SAU/MIO] estimated the enthalpy of this transformation as 154 J·mol^{-1} and equilibrium temperature T_{trs} = 77 K from theoretical consideration. This drastic difference between two estimates of the enthalpy of the β-α transformation requires further investigation. Both methods have high uncertainties; however, the value derived from calorimetric experiment appears to be more accurate. The entropy of the complete transformation was estimated as $\Delta_{trs}S$ = 0.43 J·K^{-1}·mol^{-1} by integrating the $\Delta C_p/T$ vs T curve of [60MAR] and adopting the value at 80% transformation.

2.5.2. Fusion of Li

Table 2.7 lists suggested temperatures of fusion of Li. The measured temperatures were corrected to ITS–90. The adopted melting point T_{fus} = 453.65 ± 0.05 K was selected as an average of the three most accurate studies [55DOU/EPS], [60MAR], [76HUB/PUL]. It agrees, within the uncertainty limits, with the majority of recent data. The selected value almost coincides with the recommendation of [85OHS/BAB] and is very close to the previous assessments of [73HUL], [82GUR] and [85JAN].

The adopted enthalpy of fusion 3000 J·mol^{-1} coincides with previous recommendations [73HUL], [82GUR] and [85JAN]. It is based on the accurate measurements of [55DOU/EPS]. Measurements [37BIN], [56SCH/HIL], [83NOV/ROS] and [71MAL/GIG] give the same value within the error limits; however, each of them may have had some systematic errors. The uncertainty of the recommended value change was estimated to be about ± 30 J/mol.

2.6. Adopted Values

Electronic contribution to C_p: γ = 1.63 ± 0.04 mJ·K^{-2}·mol^{-1}
Debye temperature at 0 K: Θ_D = 344 ± 2.5 K.

Heat Capacity Equations

β-Li

(Below 70 K materials has a small portion of α-Li)

Temperature range 0 – 4 K:

$$C_p^\circ = 1.63\times10^{-3}T + 4.775\times10^{-5}T^3 \text{ J·K}^{-1}\text{·mol}^{-1}.$$

Temperature range 4 – 30 K:

$$C_p^\circ = 0.03632 - 6.37\times10^{-3}T - 0.21707T^{-2} + 6.1723\times10^{-4}T^2 + 2.914\times10^{-5}T^3 \text{ J·K}^{-1}\text{·mol}^{-1}.$$

Temperature range 30 – 110 K:

$$C_p^\circ = -2.407 + 3.035\times10^{-2}T + 6.8415\times10^{2}T^{-2} + 2.54\times10^{-3}T^2 - 1.311\times10^{-5}T^3 \text{ J·K}^{-1}\text{·mol}^{-1}.$$

Temperture range 110 – 298.15 K:

$$C_p^\circ = 5.085 + 0.151T - 3.666\times10^{4}T^{-2} - 4.0596\times10^{-4}T^2 + 4.1985\times10^{-7}T^3 \text{ J·K}^{-1}\text{·mol}^{-1}.$$

Temperature range 298.15 − 453.65 K:
$C_p^\circ = -41.033 + 220.639\times10^{-3}T + 14.039\times10^{5}T^{-2} - 177.38\times10^{-6}T^2$ J·K^{-1}·mol^{-1}.

Liquid Li
Temperature range 453.65 − 700 K:
$C_p^\circ = 33.035 - 5.818\times10^{-3}T$ J·K^{-1}·mol^{-1}.

Temperature range 700 − 1600 K:
$C_p^\circ = 29.342 - 0.502\times10^{-3}T$ J·K^{-1}·mol^{-1}.

Values at 298.15 K
C_p°(298.15 K) = 24.78 ± 0.1 J·K^{-1}·mol^{-1};
S°(298.15 K) = 28.99 ± 0.3 J·K^{-1}·mol^{-1};
H°(298.15 K)−H°(0) = 4617 ± 30 J·mol^{-1}.

Phase Equilibrium Data
Martensitic β-α Transformation
Start of the direct transformation: M_s = 70 ± 5 K;
Start of the reverse transformation: A_s = 95 ± 5 K;
End of the reverse transformation: A_f = 165 ± 10 K.
Enthalpy of transformation: $\Delta_{trs}H$ = 54 ± 25 J·mol^{-1}.
Entropy of transformation: $\Delta_{trs}S$ = 0.43 ± 0.2 J·K^{-1}·mol^{-1}.

Fusion
Temperature of fusion: T_{fus} = 453.65 ± 0.05 K.
Enthalpy of fusion: $\Delta_{fus}H$ = 3000 ± 30 J·mol^{-1}.

2.7. Calculated Thermodynamic Functions of Li

The thermodynamics functions presented in Tables 2–9 and 2–10 are calculated using the equations presented in the previous section. Values in brackets are calculated by using the equations for the next higher adjacent temperature intervals.

2.8. References for Li

35LOS L. Losana, Gazz. Chim. Ital. **65**, 851–64 (1935); T_{fus}.
35SIM/SWA F. Simon and R. C. Swain, Z. Physik. Chem. **B28**, 189–98 (1935); C_p (15–300 K).
37BIN N. S. Binayendra, Gazz. Chim. Ital. **67**, 714–5 (1937); $\Delta_{fus}H$.
47BAR C. S. Barrett, Phys. Rev. **72**, 245 (1947); M_s.
48BAR/TRA C. S. Barrett and O. R. Trautz, Trans. AIME **175**, 579–601 (1948); M_s.
50CAB A. M. Cabbage, USAEC Rept. AECD-3240 (1950); ΔH (378–1276 K).
50YAG/UNT F. L. Yaggee and S. Untermeyer, USAEC Rept. ANL-4458 (1950) Nucl. Sci. Abstr. 4, 902 (1950); C_p (473–773 K).
50KUB O. Kubaschewski, Z. Elektrochem. **54**, 275–288 (1950); C_p (454–550 K).
51BAT/SMI A. G. Bates and D. J. Smith, USAEC Rept. K-729 (1951); ΔH (773–1273 K).
52KIL S. B. Kilner, J. Amer. Chem. Soc. **74**, 5221–2 (1952); T_{fus}, $\Delta_{fus}H$.
52RED/LON R. F. Redmond and J. Lones, USAEC Rept. ORNL-1342 (1952); ΔH (503–1361 K).
55DOU/EPS T. B. Douglas, L. F. Epstein, J. L. Dever, and W. H. Howland, J. Amer. Chem. Soc. **77**, 2144–50 (1955); C_p (323–1169 K), T_{fus}, $\Delta_{fus}H$.
56BAR C. S. Barrett, Acta Cryst. **9**, 671–7 (1956); Lattice parameter of α-Li.
56SAL/AHM O. N. Salmon and D. H. Ahmann, J. Phys. Chem. **60**, 13–14 (1956); T_{fus}.
56SCH/HIL A. Schneider and O. Hilmer, Z. Anorg. Allgem. Chem. **286**, 97–117 (1956); ΔH (345–494 K), $\Delta_{fus}H$.
57ROB L. M. Roberts, Proc. Phys. Soc. **B70**, 744–52 (1957); C_p (1.5–20 K).
58KEL/KAN D. V. Keller, F. A. Kanda, and A. Z. King, J. Phys. Chem. **62**, 732–3 (1958); T_{fus}.
59MAR D. L. Martin, Physica **25**, 1193–99 (1959); C_p (20–300 K).
59NIK/KAL N. A. Nikol'skii, N. A. Kalakutskaya, I. M. Pchelkin, T. V. Klassen, and V. A. Vel'tischeva, "Problems of Heat Transfer," ed. M. A. Mikheev, Acad. Sci. USSR, Moskva (1959), translated in USAEC Report AEC-tr-4511, 1–38 (1962); C_p (473–673 K).
60HUL/ROS D. Hull and H. M. Rosenberg, Cryogenics **1**, 27–32 (1960); M_s, A_f.
60MAR D. L. Martin, Proc. Roy. Soc. (London) **A254**, 444–54 (1960); C_p (20–300 K), T_{fus}.
61MAR D. L. Martin, Proc. Roy. Soc. (London) **A263**, 378–86 (1961); C_p (0.4–1.5 K).
61PON E. G. Ponyatowskii, Phys. Met. Metall. **11** (3), 146–147 (1961); T_{fus}, High Pressure.
62ALA/PCH I. M. Pchelkin, Ph.D. Thesis (I. T. Aladyev, supervisor), Moscow, ENIN (1962) (Referred in [70SHP/YAK], 49); C_p (473–1573 K).
62MAR D. L. Martin, Can. J. Phys. **40**, 1166–73 (1962); C_p (100–300 K).
63FIL/MAR J. D. Filby and D. L. Martin, Proc. Roy. Soc. (London) **A276**, 187–203 (1963); C_p (3–30 K).
63WEA/JOH W. D. Weatherford, Jr., R. K. Johnston, M. L. Valtierra, and J. W. Rhoades, Aeronautical Systems Division, Wright-Patterson Air Force Base, Ohio, Report ASD-TDR-63-413 (1963); T_{fus}.
64MAR/ZYC D. L. Martin, D. A. Zych, and C. V. Heer, Phys. Rev. **A135**, 671–9 (1964); C_p (0.35–2.0 K).
65SHP/SOL E. E. Shpil'rain, Yu. A. Soldatenko, K. A. Yakimovich, V. A. Fomin, V. A. Sarchenko, A. M. Belova, D. N. Kagan, and I. F. Krainova, High Temp. **6**, 870–4 (1965); ΔH (773–1373 K).
67ACH/FIS P. Y. Achener and D. L. Fisher, U.S. Aerojet General Corp. Report AGN-8191, **6**, San Ramon, CA (1967); ΔH (367–1422 K).
68LUE/KEN H. D. Luedemann and G. C. Kennedy, J. Geophys. Res. **73**, 2795–2805 (1968); T_{fus}.
69NOV/GRU I. I. Novikov, V. A. Gruzdev, O. A. Kraev, A.A. Odintsov, and V. V. Roschupkin, High Temp. **7**, 65–8 (1969); ΔH, C_p (459–921 K).
70SHP/KOV E. E. Shpil'rain and B. N. Koverdyaev, (Referred in [70SHP/YAK], 51, 52); ΔH (773–1573 K).
70SHP/YAK E. E. Shpil'rain, K. A. Yakimovich, E. E. Totskyi, D. L. Timrot, and V. A. Fomin, "Thermophysical Properties of Alkali Metals," Izd-vo Standartov, Moscow (1970); Review.
71MAL/GIG L. Malaspina, R. Gigli, and V. Piacente, Gazz. Chim. Ital. **101**, 197–203 (1971); $\Delta_{fus}H$.
72CUN/JOH P. T. Cunningham, S. A. Johnson, and E. J. Cairns, J. Electrochem. Soc. **119**, 1448–50 (1972); T_{fus}.
73HUL R. Hultgren, P. D. Desai, D. T. Hawkins, M. Gleiser, K. K. Kelley, and D. D. Wagman, "Selected Values of the Thermodynamic Properties of the Elements," Amer. Soc. Metals, Metals Park, OH, 281–8 (1973); Review.
76HUB/PUL P. Hubberstey, R. J. Pulham, and A. E. Thunder, J. Chem. Soc., Far. Trans. I **72**, 431–5 (1976); T_{fus}.
81MED V. A. Medvedev, et al, "Thermal Constants of Substances," **10**, Glushko, V.P., editor, VINITI, Moscow (1981); Review.
81TRI/SLO J. Trivisonno, A. R. Slotwinski, and M. P. Johnson, J. Phys. (Paris) 42, C5, 983–8 (1981); M_s, A_s.
82GUR L. V. Gurvich, I. V. Veits, V. A. Medvedev, et al, V. P. Glushko, gen. ed., "Thermodynamic Properties of Individual Substances," Nauka, Moscow, **4** (1), 244–7 (1982); Review.
83NOV/ROS I. I. Novikov, V. V. Roschupkin, and L. C. Fordeyeva, Int. J. Thermophys. **4**, 227–33 (1973); ΔH (320–700K).

85FIN/LEI J. K. Fink and L. Leibowitz, in the book "Handbook of Thermodynamic and Transport Properties of Alkali Metals," ed. R. W. Ohse, Blackwell Sci. Publ., Oxford, (1985) 411–434; liquid Li, review.

85JAN M. W. Chase, Jr., C. A. Davis, J. R. Downey, Jr., D. J. Frurip, R. A. McDonald, and A. N. Syverud, "JANAF Thermochemical Tables," J. Phys., Chem. Ref. Data **14**, Supplement No. **1**, 1428–31 (1985); Review.

85OHS/BAB R. W. Ohse, J.-F. Babelot, J. Magill, and M. Tetenbaum, Pure Appl. Chem. **57**, 1407–1426 (1985); T_{fus},, Review.

88SAU/MIO N. Saunders, A. P. Miodownik, and A. T. Dinsdale, CALPHAD **12**, 351–74 (1988); $\Delta_{trs}G$, estimate.

89COX/WAG J. D. Cox, D. D. Wagman, and V. A. Medvedev, "CODATA Key Values for Thermodynamics," Hemisphere Publ. Corp., New York, 251 (1989); Review.

2.9. Appendix – Experimental Results of Li

Tables 2.11 to 2.35 present heat capacity or enthalpy data taken from the original articles. As a result, the numerical values listed in this Appendix are the actual experimental values, tabular smoothed values, values calculated from equations, or values extracted from a graph. Where necessary, values are converted to joules (from calories). In all cases, the table heading indicates the type of data listed.

The enthalpy data for Li are given mostly as $\Delta H = H°(T) - H°(T_{ref})$, where T_{ref} is usually equal to 273 or 298 K. When temperature $T > T_{fus}$, then the values of ΔH include the enthalpies of fusion (Tables 2.12, 14, 15, 17, 19, 29, 30, 32, 34).

For plotting the enthalpy data the correction $H°(298.15\ K) - H°(273\ K)$ was estimated as 614 $J \cdot mol^{-1}$; and that of $H°(373\ K) - H°(298.15\ K)$ as 1918 $J \cdot mol^{-1}$.

TABLE 2.1. Electronic contribution to heat capacity and the Debye temperature of Li

Reference	γ, $mJ \cdot K^{-2} \cdot mol^{-1}$	Θ_D, K	Temp. range, K
Original studies			
57ROB	1.75	369	2.4– 4.5
61MAR (natural Li)	1.63 ± 0.03	335 ± 30	0.4– 1.5
61MAR (^{6}Li)	1.64 ± 0.03	380 ± 60	0.4– 1.5
63FIL/MAR (natural Li)		344 ± 2.5	estimate
63FIL/MAR (^{6}Li)		367.5 ± 2.5	estimate
63FIL/MAR (^{7}Li)		337 ± 2.5	estimate
63FIL/MAR (^{7}Li)	1.65 ± 0.02	356 ± 60	0.4– 1.5
64MAR/ZYC	1.71 ± 0.02	260 ± 10	0.4– 2.0
Review			
73HUL	1.67 ± 0.04		
Adopted			
MAR, 61MAR	1.63 ± 0.0	344 ± 2.5	63FIL/

TABLE 2.2. Values of [63FIL/MAR] selected to derive heat capacity equation for β-Li below 30 K

T/K	$C_p°$, $J \cdot K^{-1} \cdot mol^{-1}$	T/K	$C_p°$, $J \cdot K^{-1} \cdot mol^{-1}$
		14	0.147
4	0.00958	16	0.210
5	0.0140	18	0.290
6	0.0200	20	0.387
7	0.0274	22	0.505
8	0.0365	24	0.644
9	0.0481	26	0.799
10	0.0619	28	0.981
12	0.0984	30	1.187

TABLE 2.3. Values of [60MAR] and [62MAR] selected to derive heat capacity equations for β-Li at 30– 298.15 K

T/K	C_p°, J·K^{-1}·mol^{-1}	T/K	C_p°, J·K-1·mol^{-1}
30	1.19	140	17.58
35	1.785	150	18.41
40	2.475	160	19.15
45	3.255	170	19.84
50	4.075	180	20.46
55	4.985	190	21.02
60	5.925	200	21.52
65	6.885	210	21.98
70	7.820	220	22.40
75	8.770	230	22.79
80	9.695	240	23.16
85	10.59	250	23.46
90	11.52	260	23.77
95	12.28	270	24.05
100	12.92	280	24.33
110	14.33	290	24.62
120	15.55	300	24.80
130	16.63		

TABLE 2.4. Comparison of the heat capacity, enthalpy and entropy values for β-Li at 298.15 K

Reference	C_p°(298.15 K) J·K^{-1}·mol^{-1}	S°(298.15 K) J·K^{-1}·mol^{-1}	H°(298.15 K)-H°(0) J·mol^{-1}
73HUL	24.761	29.28 ± 2.0	4628
82GUR	24.860	29.12 ± 0.2	4632 ± 40
85JAN	24.623	29.085	4622
89COX/WAG	24.860	29.12 ± 0.2	4632 ± 40
Adopted	24.82 ± 0.1	28.99 ± 0.3	4617 ± 30

TABLE 2.5. Characteristic temperatures of martensitic transformation of Li

Reference	Temperature, K				Comments
	M_s	A_s	A_f	T_{max}	
Original studies					
47BAR			156		X-ray analysis
48BAR/TRA	71				X-ray analysis
60MAR	70	90–100	160–170	100–110	C_p Measurements
60HUL/ROS	76				X-ray analysis
81TRI/SLO	61-70	90-95		130	
Ultrasonic					technique
Reviews					
73HUL	80 ± 10 (average Ms & As)				Based on 60MAR
82GUR	80				Based on 60MAR
85JAN				107.25	Based on 60MAR
Adopted	70 ± 5	95 ± 5		165 ± 10	Based on 60MAR, 81TRI/SLO

Table 2.6. Enthalpy of martensitic transformation of Li.

Reference	$\Delta_{trs}H$, J·mol^{-1}	Comments
Originial studies		
60MAR	58	Estimated from C_p measurements
88SAU/MIO	154	Estimated
Reviews		
73HUL	46 ± 2	Based on 60MAR
81MED	43 ± 4	Based on 60MAR
Adopted		
60HUL/ROS	54 ± 25	Based on 60MAR,

TABLE 2.7. Temperature of fusion of Li

Reference	T_{fus}, K	Comments
Original studies		
35LOS	453.35 ± 0.1	Thermal analysis
52KIL	452.15 ± 1	Enthalpy measurements
55DOU/EPS	453.69 ± 0.03	Enthalpy measurements
56SAL/AHM	452.55 ± 0.5	Thermal analysis
58KEL/KAN	453.65 ± 0.5	Thermal analysis
60MAR	453.65 ± 0.1	Thermal analysis
61PON	455.15 ± 1.5	Thermal analysis
63WEA/JOH	454.9	Thermal analysis
68LUE/KEN	453.65 ± 2.0	Thermal analysis
72CUN/JON	453.61 ± 1.0	Thermal analysis
76HUB/PUL	453.60 ± 0.02	Thermal analysis
83NOV/ROS	453.66	Enthalpy measurements
Reviews		
73HUL	453.7 ± 0.5	Based on 35LOS, 55DOU/EPS, 58KEL/KAN
82GUR	453.69 ± 0.03	Based on 55DOU/EPS, 60MAR
85JAN	453.69	Based on 55DOU/EPS
85OHS/BAB	453.7 ± 0.1	Based on several studies
Adopted		
60MAR,	453.65 ± 0.05	Based on 55DOU/EPS, 76HUB/PUL

TABLE 2.8. Enthalpy of fusion of Li

Reference	$\Delta_{fus}H$, J·mol^{-1}	Comments
	Original studies	
37BIN	3000	Calorimeter
52KIL	2890 ± 300	Enthalpy measurements
55DOU/EPS	3000 ± 15	Enthalpy measurements
56SCH/HIL	2950 ± 40	Enthalpy measurements
71MAL/GIG	2970 ± 60	Calvet calorimeter
83NOV/ROS	3022 ± 27	Enthalpy measurements
	Reviews	
73HUL	3000 ± 40	Based on 52KIL, 55DOU/EPS
82GUR	3000 ± 20	Based on 55DOU/EPS
85JAN	3000 ± 15	Based on 55DOU/EPS
	Adopted	
	3000 ± 30	Based on 55DOU/EPS

TABLE 2.9. Thermodynamic functions of Li below 298.15 K

T/K	C_p° J·K^{-1}·mol^{-1}	$H^\circ(T)$-$H^\circ(0)$ J·mol^{-1}	$S^\circ(T)$ J·K^{-1}·mol^{-1}
5	0.0149	0.0281	0.0102
10	0.0613	0.1975	0.0319
15	0.1770	0.7583	0.0758
20	0.3884	2.1273	0.1532
25	0.7178	4.8390	0.2728
30	1.1873 (1.196)	9.5387	0.4429
35	1.763	16.871	0.6678
40	2.460	27.384	0.9475
45	3.245	41.615	1.2819
50	4.095	59.944	1.6673
60	5.916	109.902	2.5731
70	7.806	178.499	3.6268
80	9.672	265.946	4.7917
90	11.426	371.560	6.0336
100	12.986	522.816	7.5503
110	14.273 (14.328)	659.374	8.8508
120	15.557	808.949	10.152
130	16.627	969.984	11.440
140	17.571	1141.068	12.707
150	18.411	1321.056	13.949
160	19.164	1508.999	15.162
170	19.842	1704.090	16.344
180	20.456	1905.633	17.496
190	21.013	2113.020	18.617
200	21.519	2325.717	19.708
210	21.981	2543.249	20.769
220	22.403	2765.197	21.802
230	22.790	2991.185	22.806
240	23.145	3120.883	23.784
250	23.474	3453.999	24.735
260	23.778	3690.276	25.662
270	24.062	3929.492	26.565
280	24.329	4171.459	27.445
290	24.581	4416.018	28.303
298.15	24.822 (24.776)	4617.162	28.987

TABLE 2.10. Thermodynamic functions of Li above 298.15 K

T/K	C_p° J·K^{-1}·mol^{-1}	$H^\circ(T)$-H°(298.15 K) J·mol^{-1}	$S^\circ(T)$ J·K^{-1}·mol^{-1}
298.15	24.78	0.00	28.99
300.00	24.79	45.85	29.14
400.00	27.62	2647.15	36.61
453.65 (sol)	29.38	4177.26	40.19
453.65 (liq)	30.40	7177.26	46.81
500.00	30.13	8579.85	49.75
600.00	29.54	11563.36	55.19
700.00	28.99	14488.69	59.70
800.00	28.94	17385.24	63.57
900.00	28.89	20276.77	66.98
1000.00	28.84	23163.28	70.02
1100.00	28.79	26044.77	72.76
1200.00	28.74	28921.24	75.27
1300.00	28.69	31792.69	77.57
1400.00	28.64	34659.12	79.69
1500.00	28.59	37520.53	81.66
1600.00	28.54	40376.92	83.51

TABLE 2.11. SMOOTHED heat capacity of Li [35SIM/SWA]

T/K	C_p°, J·K^{-1}·mol^{-1}	T/K	C_p°, J·K^{-1}·mol^{-1}
15	0.188	120	15.23
20	0.397	130	16.19
25	0.707	140	17.07
30	1.142	150	17.82
35	1.728	160	18.54
40	2.397	180	19.58
45	3.222	200	20.59
50	4.167	220	21.55
60	5.983	240	22.09
70	7.866	260	22.76
80	9.707	280	23.26
90	11.25	300	23.68
100	12.76		
110	14.06		

TABLE 2.12. EXPERIMENTAL enthalpy values [$H^\circ(T)$-H°(298 K)] of Li [50CAB]

T/K	ΔH, J·mol^{-1}	T/K	ΔH, J·mol^{-1}
773	16130	1074	22855
879	17620	1273	27860
1015	21510		

TABLE 2.13. EXPERIMENTAL heat capacity of Li [50YAG/UNT]

T/K	C_p°, J·K^{-1}·mol^{-1}	T/K	C_p°, J·K^{-1}·mol^{-1}
473	23.2	673	32.2
573	29.9	773	33.1

TABLE 2.14. EXPERIMENTAL enthalpy values [$H°(T)$-$H°(273\ K)$] of Li [51BAT/SMI]

T/K	ΔH, J·mol^{-1}	T/K	ΔH, J·mol^{-1}
760	17050	1083	6340
764	17630	1126	7680
773	17050	1153	27440
918	21345	1173	28630
923	21520	1254	31130
942	22420	1255	31570
1077	26540	1269	30460
1079	25760		

TABLE 2.15. EXPERIMENTAL enthalpy values [$H°(T)$-$H°(273\ K)$] of Li [52RED/LON]

T/K	ΔH, J·mol^{-1}	T/K	ΔH, J·mol^{-1}
503	9645	955	22790
547	9960	1013	24350
581.5	12110	1035.5	25300
643	13430	1077.5	26650
682	14520	1142.5	27810
766	16340	1216	30550
833	19350	1291	31890
887	20410	1361	35140

TABLE 2.16. SMOOTHED heat capacity of Li [52RED/LON]

T/K	$C_p°$, J·K^{-1}·mol^{-1}	T/K	$C_p°$, J·K^{-1}·mol^{-1}
500	29.23	1000	29.63
600	29.31	1100	29.72
700	29.39	1200	29.80
800	29.47	1300	29.88
900	29.55		

TABLE 2.17. EXPERIMENTAL enthalpy values [$H°(T)$-$H°(273\ K)$] of Li [55DOU/EPS]

T/K	ΔH, J·mol^{-1}	T/K	ΔH, J·mol^{-1}
323	1235	673	14320
373	2529	773	17220
413	3624	773	17215
443	4482	873	20110
458	7928	972	22965
473	8379	1069	25758
573	11380	1168	28630

TABLE 2.18. SMOOTHED heat capacity of Li [55DOU/EPS]

T/K	C_p°, $J \cdot K^{-1} \cdot mol^{-1}$	T/K	C_p°, $J \cdot K^{-1} \cdot mol^{-1}$
298.15	24.65	580	29.66
300	24.68	600	29.54
320	25.10	620	29.43
340	25.63	640	29.31
360	26.25	660	29.19
380	26.92	680	29.07
400	27.61	700	28.99
420	28.30	750	28.96
440	28.96	800	28.94
453.70(sol)	29.38	850	28.91
453.70(liq)	30.39	900	28.89
460	30.35	950	28.86
480	30.24	1000	28.84
500	30.12	1050	28.81
520	30.01	1100	28.79
540	29.89	1150	28.76
560	29.77	1200	28.74

TABLE 2.19. EXPERIMENTAL enthalpy values [$H^\circ(T)$-H°(293 K)] of Li [56SCH/HIL]

T/K Solid Li	ΔH, $J \cdot mol^{-1}$	T/K Liquid Li	ΔH, $J \cdot mol^{-1}$
404	2770	455	7080
418	3260	456	7200
433	3660	458	7140
441	3820	461	7260
448	4060	467	7380
451	4100	477	7810
		492	8280
		507	8650
		523	9110

TABLE 2.20. SMOOTHED heat capacity of Li [57ROB]

T/K	C_p°, $J \cdot K^{-1} \cdot mol^{-1}$	T/K	C_p°, $J \cdot K^{-1} \cdot mol^{-1}$
1.5	0.00276	8	0.038
2.0	0.00381	9	0.0498
2.5	0.00498	10	0.0636
3.0	0.00628	12	0.0996
3.5	0.00778	14	—
4.0	0.00950	16	—
5.0	0.01402	18	0.302
6.0	0.02054	20	0.399
7.0	0.0286		

TABLE 2.21. SMOOTHED heat capacity of Li [59MAR]

Temp., K	99.3 % ^{6}Li Cooled to 20 K C_p°, J·K^{-1}·mol^{-1}	99.3 % ^{6}Li Cooled to 85 K C_p°, J·K^{-1}·mol^{-1}	100 % ^{7}Li C_p°, J·K^{-1}·mol^{-1}
25	0.619	—	0.732
30	1.025	—	1.21
35	1.53	—	1.81
40	2.13	—	2.51
45	2.79	—	3.30
50	3.51	—	4.14
55	4.31	—	5.02
60	5.13	—	6.00
65	5.99	—	6.96
70	6.84	—	7.90
75	7.69	—	8.85
80	8.55	—	9.78
85	9.41	—	10.69
90	10.28	10.27	11.58
95	11.16	11.00	12.35
100	12.38	11.69	13.06
110	14.19	13.03	14.38
120	14.67	14.20	15.59
130	15.50	15.31	16.69
140	16.44	16.31	17.61
150	17.29	17.19	18.49
160	18.10	17.98	19.28
170	18.80	18.72	19.96
180	19.35	19.35	20.56
190	19.91	19.91	21.15
200	20.39	20.39	21.64
210	20.87	20.87	22.05
220	21.35	21.35	22.46
230	21.81	21.81	22.84
240	22.23	22.23	23.20
250	22.60	22.60	23.51
260	22.92	22.92	23.81
270	23.23	23.23	24.12
273.15	23.33	23.33	24.21
280	23.53	23.53	24.38
290	23.80	23.80	24.68
298.15	24.01	24.01	24.90
300	24.05	24.05	24.95

TABLE 2.22. SMOOTHED heat capacity of Li [59NIK/KAL]

T/K	C_p°, J·K^{-1}·mol^{-1}	T/K	C_p°, J·K^{-1}·mol^{-1}
473	28.75	623	29.71
523	29.07	673	30.03
573	29.38		

TABLE 2.23. SMOOTHED heat capacity of Li [60MAR]

	Heat capacity after 7 different thermal treatments[a]						
	No. 1	No. 2	No. 3	No. 4	No. 5	No. 6	No. 7
T/K	C_p°, $J \cdot K^{-1} \cdot mol^{-1}$,						
22	0.490	0.500	—	—	—	0.510	—
25	0.695	0.715	—	—	—	0.724	—
30	1.15	1.18	—	—	—	1.20	—
35	1.75	1.78	—	—	—	1.79	—
40	2.44	2.46	—	—	—	2.49	—
45	3.22	3.25	—	—	—	3.26	—
50	4.05	4.06	—	—	—	4.09	—
55	4.96	4.97	—	—	—	5.00	—
60	5.86	5.92	—	6.02	—	5.93	—
65	6.85	6.88	—	6.97	—	6.89	—
70	7.77	7.82	—	7.89	—	7.82	—
75	8.72	8.77	—	8.80	—	8.77	—
80	9.65	9.70	—	9.72	—	9.69	—
85	10.56	10.59	—	10.62	—	10.59	—
90	11.47	11.47	—	11.47	11.52	11.49	11.49
95	12.36	12.33	13.36	12.30	12.28	12.34	11.25
100	13.35	13.35	13.37	13.27	12.97	13.36	12.96
105	15.34	15.24	15.85	14.92	13.64	—	—
110	16.03	16.18	15.64	15.49	14.27	16.21	14.28
115	15.99	16.06	15.38	15.63	14.90	—	—
120	16.19	16.22	15.70	15.90	15.48	16.09	15.49
125	16.52	16.49	16.14	16.31	16.04	—	—
130	16.92	16.84	16.62	16.78	16.56	16.84	16.59
135	17.38	17.29	17.08	17.27	17.06	—	—
140	17.87	17.75	—	17.74	17.53	17.70	17.52
145	18.33	18.16	—	18.16	17.97	—	—
150	18.72	18.55	—	18.59	18.38	18.55	18.40
155	19.06	18.95	—	18.95	18.76	—	—
160	19.38	19.33	—	19.33	19.15	19.28	19.18
165	19.77	19.73	—	19.73	19.53	—	—
170	—	—	—	—	19.88	—	19.87
175	—	—	—	—	20.19	—	—
180	—	—	—	—	20.49	—	20.47
190	—	—	—	—	21.05	—	21.05
200	—	—	—	—	21.55	—	21.54
210	—	—	—	—	21.98	—	21.96
220	—	—	—	—	22.38	—	22.38
230	—	—	—	—	22.74	—	22.77
240	—	—	—	—	23.10	—	23.12
250	—	—	—	—	23.43	—	23.44
260	—	—	—	—	23.76	—	23.74
270	—	—	—	—	24.06	—	24.05
273.15	—	—	—	—	24.16	—	24.15
280	—	—	—	—	24.36	—	24.32
290	—	—	—	—	24.64	—	24.61
298.15	—	—	—	—	24.86	—	24.84
300	—	—	—	—	24.90	—	24.88

[a]Note: Treatment Scheme
No.1 = cooling from room temperature to 4 K (1st specimen);
No.2 = cooling from room temperature to 20 K (1st specimen);
No.3 = cooling from 170 K to 55 K, no anneal (1st specimen);
No.4 = cooling from room temperature to 55 K, anneal at 300 K (1st specimen);
No.5 = cooling from room temperature to 85 K (1st specimen);
No.6 = cooling from room temperature to 20 K (2nd specimen);
No.7 = cooling from room temperature to 85 K (2nd specimen).

TABLE 2.24. SMOOTHED heat capacity of Li [61MAR]

T/K	C_p°, mJ·K^{-1}·mol^{-1} ^{6}Li	C_p°, m J·K^{-1}·mol^{-1} *natural* Li
0.5	0.82	0.82
1.0	1.64	1.68
1.5	2.46	2.62

TABLE 2.25. SMOOTHED heat capacity of Li [62ALA/PCH]

T/K	C_p°, J·K^{-1}·mol^{-1}	T/K	C_p°, J·K^{-1}·mol^{-1}
473	30.49	1073	28.02
573	29.77	1173	27.73
673	29.19	1273	27.59
773	28.90	1373	27.59
873	28.46	1473	27.73
973	28.17	1573	28.02

TABLE 2.26. SMOOTHED heat capacity of Li [62MAR]

T/K	C_p°, J·K^{-1}·mol^{-1}	T/K	C_p°, J·K^{-1}·mol^{-1}
100	12.92	200	21.52
110	14.33	210	21.98
120	15.55	220	22.40
130	16.63	230	22.79
140	17.58	240	23.16
150	18.41	250	23.46
160	19.15	260	23.77
170	19.84	270	24.05
180	20.46	280	24.33
190	21.02	290	24.62
		300	24.90

TABLE 2.27. SMOOTHED heat capacity of Li [63FIL/MAR]

T/K	99.9 % ^{7}Li C_p°, J·K^{-1}·mol^{-1}	92.7 % ^{7}Li C_p°, J·K^{-1}·mol^{-1}	99.3 % ^{6}Li C_p°, J·K^{-1}·mol^{-1}
3	0.00628	0.00628	0.00594
4	0.00979	0.00958	0.00900
5	0.0144	0.01400	0.0130
6	0.0208	0.0200	0.0183
7	0.0285	0.0274	0.0243
8	0.0382	0.0365	0.0323
9	0.0502	0.0481	0.0418
10	0.0650	0.0619	0.0538
12	0.101	0.0984	0.0837
14	0.151	0.147	0.124
16	0.215	0.210	0.176
18	0.296	0.290	0.241
20	0.395	0.387	0.320
22	0.514	0.505	0.415
24	0.654	0.644	0.532
26	0.812	0.799	0.662
28	0.992	0.981	0.813
30	1.201	1.187	0.990

TABLE 2.28. SMOOTHED heat capacity of Li [64MAR/ZYC]

T/K	C_p°, mJ·K^{-1}·mol^{-1}	T/K	C_p°, m J·K^{-1}·mol^{-1}
0.5	0.87	1.5	2.95
1.0	1.82	2.0	4.33

TABLE 2.29. EXPERIMENTAL enthalpy values [$H°(T)$-$H°$(273 K)] of Li [67ACH/FIS]

T/K	ΔH, J·mol^{-1}	T/K	ΔH, J·mol^{-1}
482	7500	980	22400
511	8600	1033	24200
532	9400	1090	25600
560	10200	1144	27200
589	10700	1201	28800
642	12400	1259	30400
700	14300	1316	31500
753	15700	1316	31700
811	17700	1370	33600
860	19200	1423	35400
922	20400		

TABLE 2.30. EXPERIMENTAL enthalpy values [$H°(T)$-$H°$(298 K)] of Li [69NOV/GRU]

T/K	ΔH, J·mol^{-1}	T/K	ΔH, J·mol^{-1}
459	7852	893.4	20706
487	8817	701.5	15156
560	11009	729.7	15951
630.3	13038	765.9	16960
799	17950	901.8	20979
858.2	19676	920.9	21555
867	19979		

TABLE 2.31. SMOOTHED heat capacity of Li [69NOV/GRU]

T/K	C_p°, J·K^{-1}·mol^{-1}	T/K	C_p°, J·K^{-1}·mol^{-1}
473	30.72	723	29.04
523	30.20	773	28.98
573	29.62	823	28.95
623	29.47	873	28.92
673	29.33	923	28.89

TABLE 2.32. EXPERIMENTAL enthalpy values [$H°(T)$-$H°$(373 K)] of Li [70SHP/KOV]

T/K	ΔH, J·mol^{-1}	T/K	ΔH, J·mol^{-1}
788	14582	1202	27182
788	14512	1204	26875
973	19312	1274	29331
995	21400	1305	29439
995	21467	1373	31806
1073	23262	1374	31539
1075	21824	1409	32189
1173	25260	1472	35401
1173	26100	1573	37114

TABLE 2.33. SMOOTHED heat capacity of Li [70SHP/KOV]

T/K	C_p°, $J \cdot K^{-1} \cdot mol^{-1}$	T/K	C_p°, $J \cdot K^{-1} \cdot mol^{-1}$
773	29.66	1273	29.21
873	29.48	1373	29.18
973	29.37	1473	29.16
1073	29.29	1573	29.15
1173	29.24		

TABLE 2.34. EXPERIMENTAL enthalpy values [$H^\circ(T)$-H°(273 K)] of Li [83NOV/ROS]

T/K	ΔH, $J \cdot mol^{-1}$	T/K	ΔH, $J \cdot mol^{-1}$
328.00	1333	447.25	4595
333.15	1484	448.95	4616
343.15	1742	449.35	4656
345.05	1762	450.55	4702
349.45	1895	451.75	4708
382.45	2763	452.45	4751
395.75	3094	457.35	7932
407.75	3389	462.25	8095
416.85	3678	476.45	8509
427.35	3966	487.75	8872
427.95	4008	532.45	10131
433.95	4199	535.35	10154
434.35	4166	540.15	10395
436.15	4251	596.25	11985
441.15	4393	598.25	11998
442.45	4441	631.95	13028
442.75	4447	660.05	13835
444.05	4458	694.25	14818
444.15	4486		

TABLE 2.35. SMOOTHED heat capacity of Li [83NOV/ROS]

T/K	C_p°, $J \cdot K^{-1} \cdot mol^{-1}$	T/K $J \cdot K^{-1} \cdot mol^{-1}$	C_p°
350	24.88	453.65(liq)	29.06
375	26.29	500	29.01
400	27.70	550	28.95
425	29.12	600	28.89
450	30.53	650	28.83
453.65(sol)	30.74	700	28.77

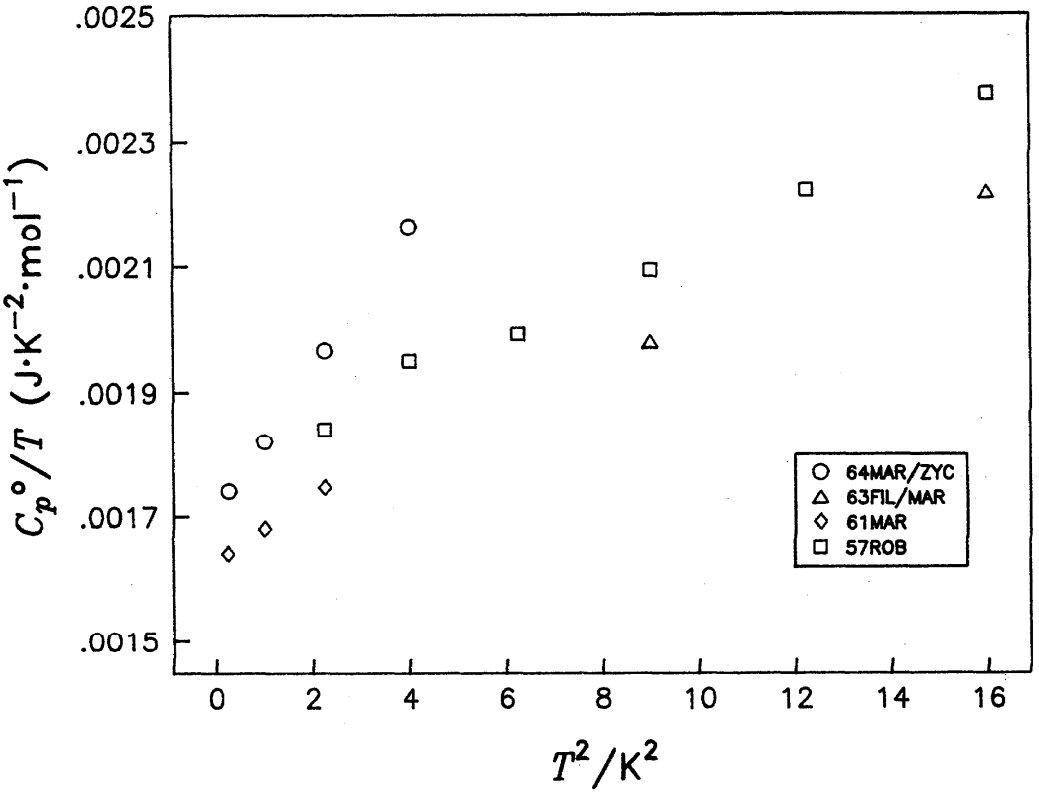

FIGURE 2.1. C_p/T versus T^2 for Li below 4 K

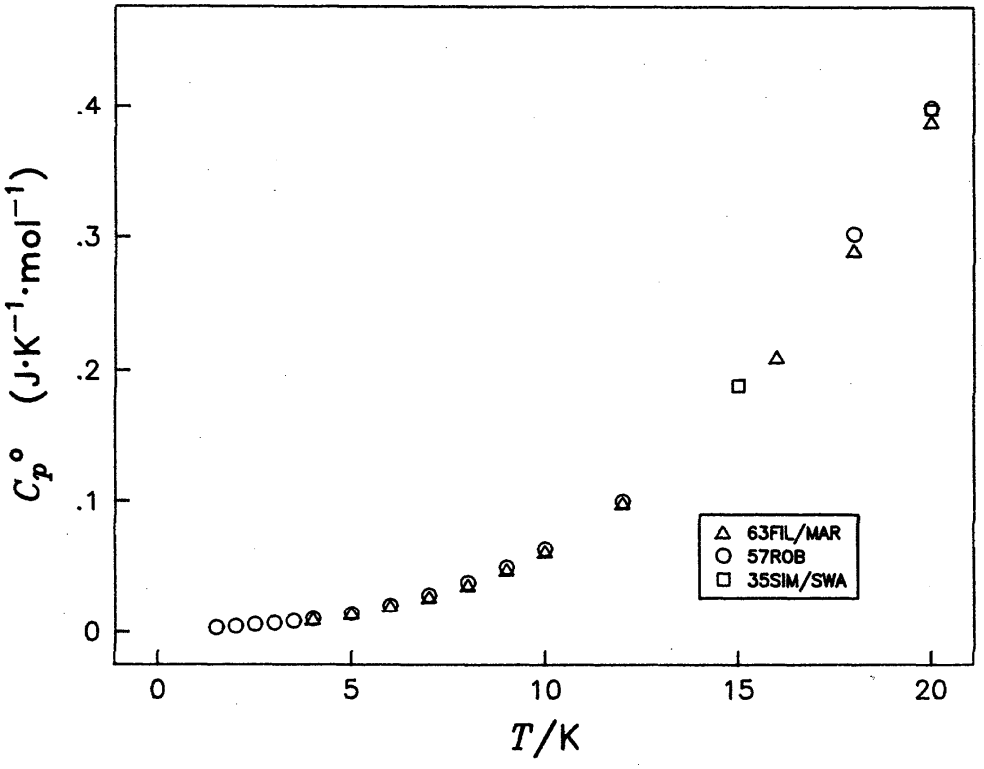

FIGURE 2.2. Heat Capacity of Li below 20 K

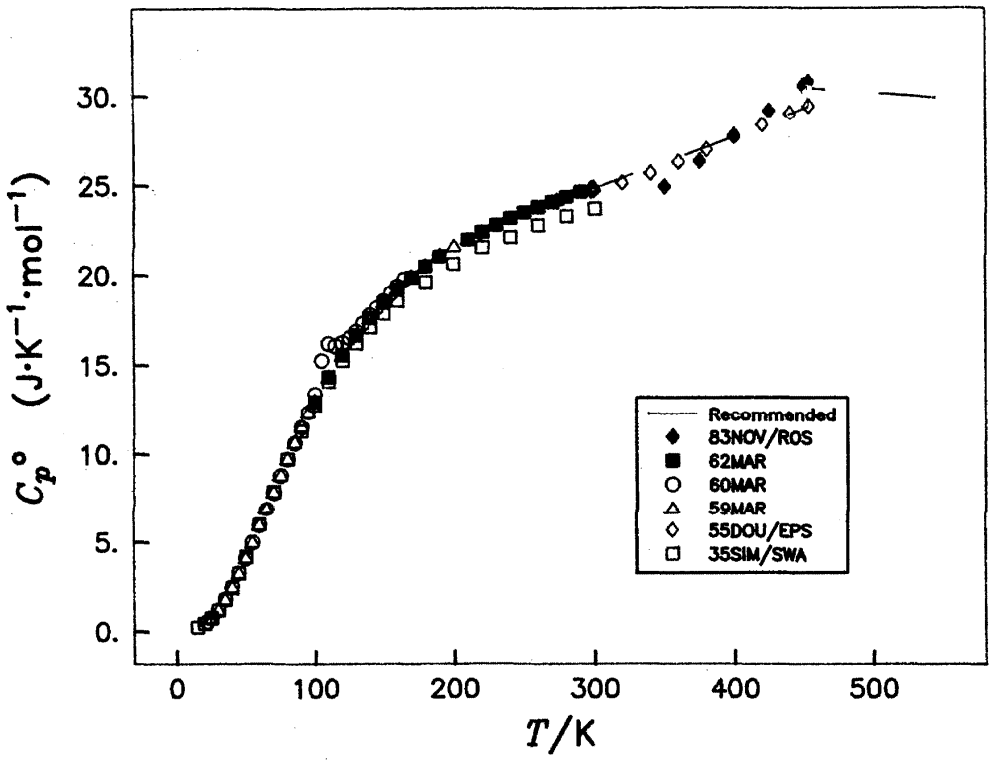

FIGURE 2.3. Heat Capacity of Solid Li

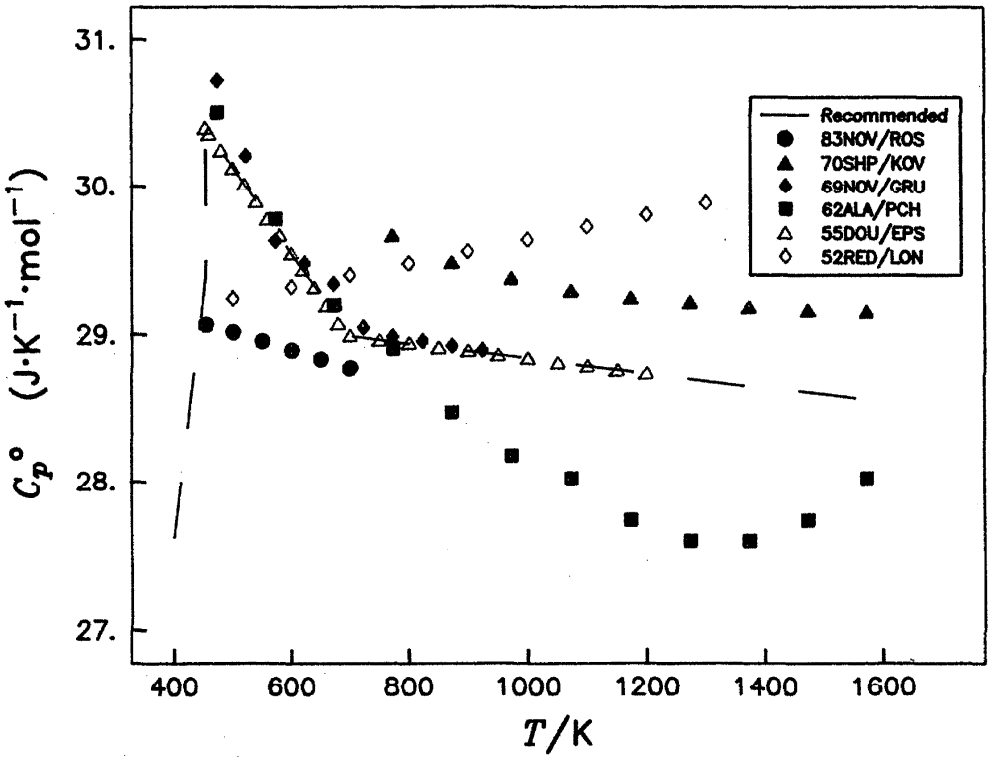

FIGURE 2.4. Heat Capacity of Liquid Li

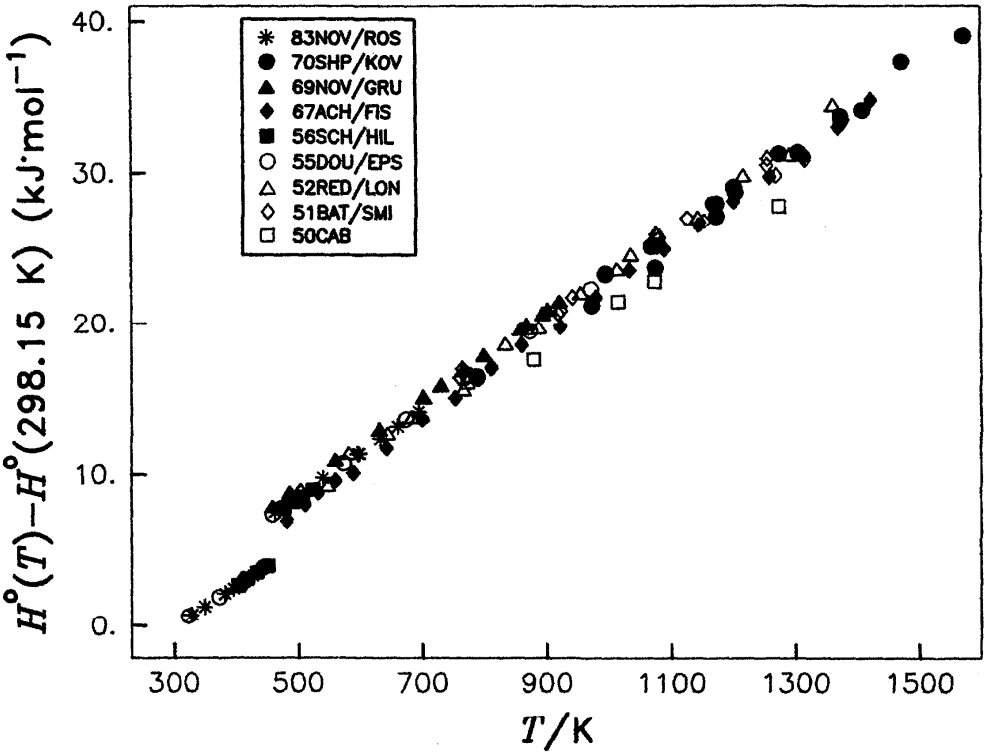

FIGURE 2.5. $H°(T)-H°(298.15\ K)$ of Li

3. Sodium

3.1. Introduction

At ambient pressure sodium has two crystalline modifications α (α-Na) and β (β-Na) (Table 1.1). Similar to Li, the martensitic β-α transformation in Na, which starts at about 35 K on cooling, distorts the heat capacity data at low temperatures. Samples cooled below 35 K consist of a mixture of two phases, β-Na and α-Na, with different heat capacities. The phase proportion in such samples is usually known only crudely. On cooling to helium temperature, the transformation only proceeds to less than 50 % completion. On heating partially transformed samples above 45 K, a reverse transformation starts, accompanied by heat absorption, and the process is spread over 30 degrees. This phenomenon must be taken into consideration for selecting experimental data.

The heat capacity data were measured accurately between 50 and 1200 K. The uncertainty in the heat capacity values of liquid Na increases above 1200 K.

3.2. Heat Capacity and Enthalpy Measurements

3.2.1. Temperature below 298.15 K

[18EAS/ROD]

Eastman and Rodebush measured C_p of a commercial *Kahlbaum* Na in an adiabatic calorimeter. According to the authors the error of these measurements did not exceed ± 1 %. Thirteen measured points between 64.6 and 293.5 K are given in Table 3.12 and shown in Fig. 3.3. These data agree satisfactorily with modern results.

[26SIM/ZEI]

Simon and Zeidler measured heat capacity of a commercial *Kahlbaum* sodium from 17 to 118 K (10 points, see Table 3.13 and Fig. 3.3) in an adiabatic calorimeter. The Debye temperature was estimated from the low-temperature portion of the data as 159 K. On the basis of their own and literature data, the authors estimated heat capacity between 10 K and the melting point. The results of this study agree satisfactorily with modern data.

[48PIC/SIM]

Pickard and Simon measured heat capacity of Na between 2 and 25 K. The sample was described only as *pure* and *hydrogen-free*. The experimental heat capacity values (31 points) were presented in a small-scale graph; the rounded values were tabulated and are reproduced in Table 3.15 and shown in Fig. 3.2. Two unusual features were observed: an anomaly at about 7 K, and a low value of the Debye temperature at 0 K Θ_D = 88 K which increased rapidly with the temperature of the observations. The discrepancy may be caused by errors in the measurements. The low-temperature portion of the measurements was not considered in this assessment as inaccurate.

[54RAY]

Rayne measured heat capacity of a commercial sample containing 99.9 % Na (principal impurity 0.02 wt.% K) between 0.2 and 1 K by a low-temperature calorimeter. The results showed a reproducible cusp-shaped anomaly around 0.87 K which Rayne explained as a martensitic transformation in the sample. However, the reverse martensitic transformation usually becomes visible at much higher temperatures; this effect was not confirmed in other studies; it could therefore be a result of error in these measurements. The data of [54RAY] were omitted from further consideration in the present work.

[54DAU/MCD]

Dauphinee *et al.* measured heat capacity of Na between 55 and 315 K in a semi-automatic adiabatic calorimeter. The sample was described as having a residual electrical resistance $\rho_{273K}/\rho_{4.2K}$ = 500 − 1000. The accuracy of measurements was estimated as ± 0.1 %. Between 150 and 250 K a small *hump* of about 0.5 % appeared on the heat capacity curve; the scatter within this region is greater than outside of it; an effect due to thermal treatment was observed in this region. These irregularities were explained by Dauphinee *et al.* as also being due to a phase transformation, but the temperature range lies above the end of the reverse martensitic transformation. This effect was probably caused by a malfunction of the equipment. The heat capacity values are shown in a small-scale graph (120 points) together with a smoothed line. Readings were taken from this line in steps of 20 or 10 kelvins. They are listed in Table 3.18 and shown in Fig. 3.3.

[55PAR/QUA]

Parkinson and Quarrington measured heat capacity of Na from 1.4 to 20 K. They used *pure* redistilled Na provided by the Pure Metals Committee of the Department of Scientific and Industrial Research of UK (no analysis is given). The authors did not notice any anomaly. The data are given in a graphic form (27 points), from which rounded values were tabulated. They are reproduced in Table 3.19 and shown in Fig. 3.1 and 3.2. From these data the authors calculated γ = 1.8 ± 0.2 $mJ \cdot K^{-2} mol^{-1}$ and Θ_D = 158 K.

[57ROB]

Roberts measured the heat capacity of Na between 1.3 and 20 K. The sample was provided by the Atomic Energy Research Establishment, Harwell; the material had 99.995 % Na; no information on impurities is given. The preparation, handling and measurements were made in a He atmosphere. The heat capacity values (31 points) are shown in a small-scale graph below 5.5 K. Rounded values were tabulated from 1.5 to 20 K; they are reproduced in Table 3.21 and shown in Fig. 3.1 and 3.2. From the data in the temperature range 2.5 to 4 K (16 points), β and Θ_D were calculated as γ = 1.37 ± 0.04 $mJ \cdot K^{-2} mol^{-1}$ and Θ_D = 158.2 K. Below 2.5 K the measured values are more scattered. When 15 additional points in the interval 1.3 − 2.5 K were included, the results became less accurate γ = 1.45 $mJ \cdot K^{-2} mol^{-1}$ and Θ_D = 159 K.

[60GAU/HEE]

Gaumer and Heer measured heat capacity in a magnetic refrigerator calorimeter from 0.4 to 2 K using a distilled sample of commercial A.C.S. grade Na with a stated purity of 99.99 %. Forty data points were shown in a small-scale graph,

with $\gamma = 1.32$ mJ·K^{-2}mol^{-1} and $\Theta_D = 158$ K. The heat capacity values calculated from these parameters are given in Table 3.23 and shown in Fig. 3.1.

[60LIE/PHI]

Lien and Phillips measured the heat capacity of a 99.99 wt.% Na sample from 0.15 to 1.4 K. The sample was cast into a calorimetric container in an inert atmosphere. About 50 data points were shown in a small-scale graph. The anomaly reported in [54RAY] was not observed. The measured data yielded $\Theta_D = 156$ K and $\gamma = 1.45$ mJ·K^{-2}·mol^{-1}. These parameters are used to calculate heat capacity given in Table 3.24 and shown in Fig. 3.1.

[60MAR]

Martin measured heat capacity from 20 to 300 K in an adiabatic calorimeter (Fig. 3.3). Two samples were used: a *cast* sample which was provided by Phillips, Eindhoven, with residual resistance $\rho_{273K}/\rho_{4K} = 5000$, and a *free* sample by the Atomic Energy Research Establishment, Harwell, with residual resistance 3000; no chemical analysis was provided in [60MAR] for either sample. The accuracy of the measurements was ± 0.2 % above 80 K, decreasing to + 2 % at 20 K. Martin tabulated measured heat capacity values after five different thermal treatments, and the results for the *cast* specimen are given in Table 3.25. There was no significant difference between the *cast* and *free* samples. Martin denied the existence of an anomaly around 200 K which was observed in [54DAU/MCD]. On heating two-phase samples prepared by cooling below 35 K, the reverse martensitic transformation was observed from 40 to 80 K. The shape of the heat capacity curve and the magnitude of this effect depends on the history and thermal treatment of the samples. The measured heat varied from 6 to 19 J·mol^{-1} and the maximum rate of this process was observed at $T_{max} = 45$ to 55 K. Assuming that about 45 % of β-Na was transformed into α-Na, Martin estimated the total effect of the β-α transformation in Na as about 42 J·mol^{-1}. The Debye temperature was estimated as 160 K for α-Na and 153 K for β-Na, the standard entropy of β-Na was calculated as $S°(298.15\ K) = 51.21 \pm 0.50$ J·K^{-1}·mol^{-1}.

[61MAR]

Martin measured heat capacity of Na from 0.4 to 1.5 K in an isothermal calorimeter. Two samples from Phillips, Eindhoven, had residual resistivity $\rho_{273K}/\rho_{4K} = 1600$ and 5000. The 3 small-scale graphs with a total of 120 points are shown in the paper. The values of γ and Θ_D are given for each sample; their averages are $\beta = 1.381 \pm 0.020$ mJ·K^{-2}·mol^{-1} and $\Theta_D = 156.5 \pm 2$ K. According to these parameters the heat capacity values were calculated and shown in Table 3.26 and Fig. 3.1. Martin assumed that the value of β of the β-Na is higher than that of α-Na by 20 %, and the Debye temperature of β-Na is lower than that of α-Na by 9 K.

[63FIL/MAR]

Filby and Martin measured the heat capacity of a sample, supplied by L. Light, Colnbrook, England, in an adiabatic calorimeter in the temperature range 3 to 30 K (Fig. 3.2). Spectrographic analysis showed Ca 0.1 − 0.01 wt.%; Ba and Fe 0.01–0.001 wt.%; Ag, Al and Cu 0.001 to 0.0001 wt.%. The specimen was melted inside the container under vacuum. The accuracy of measurements was about 1 %. An unexpected evolution of heat was observed between 4 and 16 K, the total amount being about 0.2 J·mol^{-1}. The effect was explained by the annealing of defects created by the martensitic transformation, but this is questionable since nobody else observed a similar effect in this temperature range in Na. To vary the degree of the martensitic transformation, the sample was submitted to 7 different thermal treatments (Table 3.28 and Fig. 3.2). The authors assumed that after cooling from room temperature to 3 K, 50 % of β-Na transforms into α-Na, whereas cooling to 20 K transforms only 25 % of β-Na. By thermal cycling between 90 K and 3 K, the martensitic transformation was partially depressed, and separate heat capacity values were estimated for β-Na and α-Na; they are reproduced in Table 3.29. The results correspond to the Debye temperature of β-Na $\Theta_D = 152.5$ K and α-Na $\Theta_D = 159$ K.

3.2.2. Temperature above 298.15 K

[13REN], [14REN]

Rengade measured the heat capacity of a commercial Na in a Bunsen ice calorimeter, which was additionally distilled in vacuum at 673 K (analysis was not given). The melting point of this material was determined as 371.05 K, and the enthalpy of fusion as 2619 J·mol^{-1}. The 11 results for solid Na are given in a graph in [14REN]; they were described by an equation for solid N_a

$$C_p^\circ = 14.83 + 0.0448T \text{ J·K}^{-1}\text{·mol}^{-1}.$$

The values calculated are given in Table 3.11 and shown in Fig. 3.3. The heat capacity of liquid Na near the melting point was determined as 32.14 J·K^{-1}·mol^{-1}. The obtained heat capacity data have low accuracy; however, the values of T_{fus} and $\Delta_{fus}H$ agree well with modern data and were included in Tables 3.7 and 3.8.

[27DIX/ROD]

Dixon and Rodebush measured heat capacity of a commercial sample of electrolytic Na, purified by vacuum melting. The method was based on measuring the adiabatic temperature-pressure coefficient (dT/dP), and was subject to experimental difficulties due to the high thermal conductivity of sodium. Two values obtained at 394 K and at 451 K and are shown in Table 3.14 and Fig. 3.4. They agree with modern data.

[50GIN/DOU]

Ginnings *et al.* measured heat capacity of Na between 304 and 1170 K in an ice drop calorimeter. The distilled Na sample was analyzed spectrochemically after the experiment; Ca and Li 0.0001 − 0.001 wt.%, K 0.001 − 0.01 wt.%; the samples contained about 0.01 wt.% of Na_2O and 0.006 wt.% hydrogen. The measured 65 points were reduced to 14 average values given in Table 3.16 and are shown in Fig. 3.5. For solid Na the results are described by equation

$$H°(T,cr)-H°(273\ K,cr) = -8612 + 41.536T - 0.0586T^2 + 80.69\times10^{-6}T^3\ J\cdot mol^{-1};$$

for liquid Na between melting point and 1170 K:

$$H°(T,l)-H°(273\ K,cr) = -7239 + 36.674T - 66.7265\times10^{-4}T^2 + 552000\exp(-13600/T),\ J\cdot mol^{-1}.$$

The derived heat capacity values are reproduced in Table 3.17 and shown in Fig. 3.3 and 3.4. Later [52DOU/BAL] changed the heat capacity equation for liquid Na to

$$C_p° = 37.466 - 19.148\times10^{-3}T + 10.628\times10^{-6}T^2\ J\cdot mol^{-1}.$$

The accuracy in the enthalpy measurements was estimated as 0.2 %; this corresponds to an uncertainty of 0.4 % in heat capacity values. The authors did not notice any effect due to thermal treatment. Ginnings *et al.* also determined accurately the melting point as T_{fus} = 370.96 ± 0.03 K. This value was found from 20 cycling experiments in which Na was partially melted; the enthalpy of fusion was found as $\Delta_{fus}H$ = 2602 ± 9 J·mol^{-1}.

[56SCH/HIL]

Schneider and Hilmer measured the enthalpy of Na (Merck) from 323 to 523 K in a mixing calorimeter. The 7 points for solid Na and 10 for liquid Na are taken from a graph and reproduced in Table 3.20 and Fig. 3.5. At 343 – 368 K the average heat capacity for solid Na was 30.75 ± 0.6 J·K^{-1}·mol^{-1}, and for liquid Na 29.71 ± 0.4 J·K^{-1}·mol^{-1} at 463 – 503 K. The enthalpy of fusion was determined as $\Delta_{fus}H$ = 2640 ± 40 J·mol^{-1}.

[59MIT]

Mit'kina measured heat capacity of commercial Na by a method based on the measurement of the temperature increase of a wire anode-sample bombarded by electrons. From 423 to 673 K the heat capacity values (7 points) remained constant 30.8 J·K^{-1}·mol^{-1}. The accuracy of the study is low.

[59NIK/KAL]

Nikol'skii *et al.* measured heat capacity of Na (purity was not given) at 373 to 1073 K by direct heating at constant temperature. The 18 experimental values are given in a graph and 13 smoothed values were tabulated (Table 3.22 and Fig. 3.4). The accuracy of these measurements is about 5 %.

[62ALA/PCH]

Aladyev and Pchelkin (quoted from [70SHP/YAK], p. 68) measured heat capacity of liquid Na (stated impurities 0.04 % K, 0.01 % Li) in an isothermal calorimeter at 373 to 1573 K. The smoothed results (13 points) are listed in Table 3.27, and shown in Fig. 3.4; the original data have scatter of about 8 %.

[63GRU/ROS], [69NOV/GRU]

In two studies Gruzdev, Roschupkin *et al.* obtained the enthalpy of a commercial Na measured in an ice drop calorimeter from 373 to 1353 K. The specimen had 99.8 wt.% Na and 0.0005 wt.% Fe. The error in these measurements was estimated by the authors as ± 0.3 %; however, it is probably underestimated by at least 5 times. The 45 data points shown in graph in [63GRU/ROS] and listed in [69NOV/GRU] are reproduced in Table 3.35 and shown in Fig. 3.5. The authors fitted the data to two equations quoted in [70SHP/YAK]: for the interval 373 – 773 K

$$H°(T,l)-H°(373\ K,l) = -13226 + 39.1595T - 1.1489\times10^{-2}T^2 + 4.1955\times10^{-6}T^3,\ J\cdot mol^{-1};$$

and for the interval 773 – 1273 K

$$H°(T,l)-H°(373\ K,l) = -9638 + 25.339T + 1.342\times10^{-3}T^2 + 1900\log((T-273)/100),\ J\cdot mol^{-1}.$$

The smoothed C_p values given in [63GRU/ROS] and [69NOV/GRU] are reproduced in Table 3.36 and shown in Fig. 3.4.

[63EWI/STO]

Ewing *et al.* measured the enthalpy of Na (analysis showed 100 ppm K, 10 ppm O) at 428 to 1385 K in a copper drop calorimeter, using containers of two different constructions. Two series of experiments were performed in the interval 428–925 K (6 points) and for 552 – 1385 K (7 points); only the derived heat capacities are given in the study. Above 1000 K they are scattered within 3 %. The two sets of data differ by about 6 %, and they are given in Table 3.30 and shown in Fig. 3.4. The accuracy of measurements is considered to be low.

[65SHP/SOL]

Shpil'rain *et al.* measured the enthalpy of liquid Na from 573 to 1273 K in a boiling water calorimeter. The sample contained 99.8 wt.% Na, 0.008 wt.% Ca, and 0.007 wt.% of other impurities. The data (12 points, see Table 3.31 and Fig. 3.5) were fitted to an equation

$$H°(T,l)-H°(373\ K,l) = -12124 + 33.913T - 4.1066\times10^{-3}T^2 + 8.9421\times10^{-7}T^3\ J\cdot mol^{-1}.$$

The heat capacity values calculated by this equation are given in Table 3.32 and shown in Fig. 3.4. The experimental error was estimated as ± 1 %.

[67ACH/FIS]

Achener and Fisher (quoted from [85FIN/LEI]) measured the enthalpy of Na by drop calorimetry at 394 – 1451 K; 40 points are reproduced in Table 3.33 and shown in Fig. 3.5.

[67MAR]

Martin measured the heat capacity of Na from 300 to 475 K in an adiabatic calorimeter. The material from the Koch-Light, England, had impurities: Ca < 5 ppm, K <100 ppm, Mg < 20 ppm, Fe 5 ppm. The accuracy of the measurements was about 0.2 %. The results for solid Na were fitted to a seven-term equation and for liquid Na to a four-term equation; the calculated smoothed results are given in Table 3.34 and shown in Fig. 3.3 and 3.4. The melting point was determined

as 371.01 ± 0.005 K, and the enthalpy of fusion as $\Delta_{fus}H$ = 2598 ± 1 J·mol^{-1}.

[74FRE/CHA]

Fredrickson and Chasanov measured the enthalpy of Na from 554 to 1505 K, using a high-precision drop calorimeter. The material was reactor-grade Na containing 200 ppm K, <20 ppm 0, <10 ppm C, <8 ppm Ca, <25 ppm H. The sample was placed in a tantalum container in a dry box. The authors listed 16 enthalpy values (see Table 3.37). The data are shown in Fig. 3.5 after correcting to 273 K. The agreement with [50GIN/DOU], [65SHP/SOL] and [69NOV/GRU] is good. The enthalpy data obtained were fitted to the equation with a standard deviation of 0.52 %.

$$H°(T,l) - H°(298.15\ K,cr) = 3062.4 + 19.348T + 3.53315\times10^{-3}T^2 - 2.47879\times10^{6}T^{-1},\ J\cdot mol^{-1}.$$

The smoothed heat capacities are also given this study; they are listed in Table 3.38 and shown in Fig. 3.4.

3.3. Discussion of Heat Capacity and Enthalpy Data

3.3.1. β-Na below 298.15 K

Measurements below 4 K. Below 4 K the heat capacity was measured in [55PAR/QUA], [57ROB], [60LIE/PHI], [60GAU/HEE], [61MAR], [63FIL/MAR]. The results of these studies in form of γ and Θ_D values are listed in Table 3.1, and heat capacity values are shown in Fig. 3.1. It should be remembered that these results represent two-phase samples containing some amount of α-Na. Table 3.1 also includes the results of resonant frequency measurements [64BHA/STE] which have lower accuracy than calorimetric data.

The Θ_D data of [57ROB], [60GAU/HEE], [60LIE/PHI], [61MAR] vary from 156 to 158 K; the average value 157 ± 2 K was adopted here. The γ data vary from 1.32 to 1.44 mJ·K^{-2}·mol^{-1}, an average of three reliable concordant results [57ROB], [60GAU/HEE], [61MAR] gives γ = 1.36 ± 0.04 mJ·K^{-2}·mol^{-1} which was adopted here; almost the same value was recommended in [73HUL]. It should be pointed out that the adopted value of γ is close to the results obtained in non-calorimetric measurements [64BHA/STE].

The selected values of γ and Θ_D were combined in the heat capacity equation for the range from 0 to 4 K

$$C_p° = 1.36T + 0.502T^3\ mJ\cdot K^{-1}\cdot mol^{-1}. \quad (1)$$

Measurements between 4 and 30 K. The heat capacity measurements for this range were made in [26SIM/ZEI] (above 17 K), [48PIC/SIM] (2 − 25 K), [55PAR/QUA] (1.4 − 20 K), [57ROB] (1.5 − 20 K), [60MAR] (above 20 K), [63FIL/MAR] (3 − 30 K); the data agree within 3 % (Fig. 3.2 and 3-3).

Below 35 K samples consist of two phases, β-Na and α-Na, and the measured heat capacities depend on the proportion of these phases which is not usually known accurately. Little attention was paid to the thermal treatment of samples in earlier studies [26SIM/ZEI], [48PIC/SIM], [55PAR/QUA], [57ROB]. Martin *et al.* used seven treatment procedures in [63FIL/MAR] and five in [60MAR]. For low temperatures Martin preferred measurements made for a sample cooled down from room temperature to 2–3 K. This treatment should produce a sizeable fraction of α-Na. From measurements made on two-phase samples, Filby and Martin estimated the heat capacity of separate α-Na and β-Na. The partition was based on the questionable assumption that samples cooled to 3 K contain 50 % of α-Na while those cooled to 20 K have only 25 % (Table 3.29). Lacking structural measurements, the data of [60MAR] and [63FIL/MAR] cannot provide reliable heat capacity values for the separate phases. To decrease the error arising from an unknown phase composition, the present authors selected a treatment, which leads to a smaller percentage of α-Na, fast cooling from 293 to 20 K and slow from 20 to 3 K (No. 7 in Table 3.28). Similar results were obtained after fast cooling from 293 to 3 K, followed by heating to 30 K and a second cooling to 3 K (No. 2 in Table 3.28) [63FIL/MAR]. The results obtained after treatment No. 7 at 4 to 28 K are reproduced in Table 3.2. It was assumed that the tabulated values represent a two-phase specimen with a high concentration of β-Na. The tabulated values were used to derive equations for the temperature ranges 4 − 20 K (Eq. 2) and 20 − 50 K (Eq. 3):

$$C_p° = 0.8892 - 0.24962T - 3.8045T^{-2} + 0.02492T^2 - 2.604\times10^{-4}T^3\ J\cdot K^{-1}\cdot mol^{-1} \quad (2)$$

Measurements between 30 and 298.15 K. Above 30 K the data of [26SIM/ZEI] (17 − 118 K), [54DAU/MCD] (55 − 315 K), and [60MAR] (20 − 300 K) agree within 3 % (Fig. 3.3). A better agreement is observed between [54DAU/MCD] and [60MAR] which were performed in the same laboratory. However, the data of [54DAU/MCD] had irregularities between 150 and 250 K, and preference was given to the more consistent study [60MAR]. The heat capacity value measured at 30 K in [63FIL/MAR] 8.347 J·K^{-1}·mol^{-1} agrees with 8.32 J·K^{-1}·mol^{-1} obtained for a *free* sample in [60MAR] which was cooled from room temperature to 20 K. For 30 K the average 8.33 J·K^{-1}·mol^{-1} was selected (Table 3.3); for 35 K the value 10.52 J·K^{-1}·mol^{-1} was taken from [60MAR]. Above 35 K the adopted heat capacity values were taken from measurements made on a *free* specimen cooled to 35 K from room temperature. This treatment should provide a single-phase sample of β-Na. The selected values are listed below. The value at 300 K measured in [60MAR] 28.37 J·K^{-1}·mol^{-1} does not coincide with other measurements above 298 K, and was replaced by 28.16 J·K^{-1}·mol^{-1} obtained in [50GIN/DOU] and [67MAR]. The heat capacity values listed in Tables 3.2 and 3.3 were fitted to three equations for the ranges: from 20 to 50 K

$$C_p° = -17.3956 + 1.1205T + 1198.6T^{-2} - 0.01132T^2 + 3.66\times10^{-5}T^3\ J\cdot K^{-1}\cdot mol^{-1}, \quad (3)$$

from 50 to 150 K

$$C_p° = 3.193 + 0.4154T - 5570.2T^{-2} - 0.00291T^2 + 7.403\times10^{-6}T^3\ J\cdot K^{-1}\cdot mol^{-1}, \quad (4)$$

and from 150 to 298.15 K

$$C_p^\circ = 33.999 - 0.07412T - 7.4865\times104T^{-2} + 2.6801\times10^{-4}T^2 - 2.536\times10^{-7}T^3 \text{ J·K}^{-1}\text{·mol}^{-1}. \quad (5)$$

Eqs 1 – 5 were used to calculate $C_p^\circ(T)$, $H^\circ(T)-H^\circ(0)$ and $S^\circ(T)$. The calculations are shown in Table 3.9. The enthalpy of transformation of a sample cooled to 35 K was determined as about 8.4 J·mol^{-1} from the area of ΔC_p over a twenty-degree interval [60MAR]. The corresponding entropy changes were estimated as 0.14 J·K^{-1}·mol^{-1} from the area under the $\Delta C_p/T$ vs T curve. The reverse transformation reaches a maximum rate at 45 – 55 K. Therefore, the above values of the enthalpy and entropy of transformation were attributed to the temperature of 50 K in Table 3.9.

At the standard temperature the heat capacity, enthalpy and entropy were calculated as

$$C_p^\circ(298.15\text{ K}) = 28.161 \text{ J·K}^{-1}\text{·mol}^{-1}$$
$$S^\circ(298.15\text{ K}) = 51.103 \text{ J·K}^{-1}\text{·mol}^{-1}$$
$$H^\circ(298.15\text{ K}) - H^\circ(0) = 6432.02 \text{ J·mol}^{-1}$$

These values are compared with those recommended in other reviews (Table 3.4).

The calculated values are close to the recommendations of [73HUL]. The difference between the values listed above is mostly due to the various treatments of the same information. The maximum discrepancy for the enthalpy is about 30 J·mol^{-1} and for the entropy 0.35 J·K^{-1}·mol^{-1}. The difference between the calculated values and the recommendation of [82GUR] is noticeable. The present authors consider that the influence of the martensitic transformation on the thermodynamic functions was taken into account here more carefully than before, and this may be the reason for the deviation of the adopted values from previous recommendations. The uncertainties were increased to 30 J·mol^{-1} for $H^\circ(298.15\text{ K})-H^\circ(0)$ and 0.3 J·K^{-1}·mol^{-1} for $S^\circ(298.15\text{ K})$. They include the uncertainty in the phase composition below 40 K and in the enthalpy and entropy of the phase transformation.

3.3.2. β-Na above 298.15 K

Above 298.15 K the enthalpy or heat capacity of solid Na was measured in [13REN], [14REN] (ΔH), [50GIN/DOU] (ΔH), [56SCH/HIL] (ΔH), [67MAR] (C_p); the data agree satisfactorily within 4 %, and heat capacity values are shown Fig. 3.3. The best measurements [50GIN/DOU] and [67MAR] differ by less than 0.5 % below 360 K, but near the melting point the deviation increases to 2 %. Similar to the method used in [85JAN], the values of [67MAR] and [50GIN/DOU] were joined smoothly. The heat capacity values were fitted to an equation from 298 to 371 K

$$C_p^\circ = 53.941 - 194.429\times10^{-3}\,T + 361.905\times10^{-6}T^2 \text{ J·K}^{-1}\text{·mol}^{-1}. \quad (6)$$

Reviews [73HUL], [82GUR], [85JAN] used the same sources; their recommendations differ by less than 1 %. Present values almost coincide with [85JAN]. [82GUR] recommended for solid Na the equation

$$C_p^\circ = -23.346 + 120.736\times10^{-3}T + 13.848\times10^{5}T^{-2} \text{ J·K}^{-1}\text{·mol}^{-1}.$$

3.3.3. Liquid Na

The enthalpy and heat capacity of liquid Na were measured in a number of studies: [27DIX/ROD] (C_p, T = 394 and 451 K), [50GIN/DOU] (ΔH, 373–1170 K), [56SCH/HIL] (ΔH, 372–494 K), [59MIT] (C_p° = 30.8 J·K^{-1}mol^{-1}, 423–673), [59NIK/KAL] (C_p, 373–973 K), [62ALA/PCH] (C_p, 373–1573 K), [63EWI/STO] (ΔH, 589–926 K), [65SHP/SOL] (ΔH, 573–1273 K), [67ACH/FIS] (ΔH, 420–1475 K), [67MAR] (C_p, 371–475 K) [69NOV/GRU]] (ΔH, 376–1359 K), [74FRE/CHA] (ΔH, 554–1505 K). The enthalpy data (Fig. 3.5) agree well, except scattered values of [67ACH/FIS]. The heat capacity data (Fig. 3.4) are scattered within 7 %. Initially the C_p values decrease with increasing temperature from about 31.5–32 J·K^{-1}·mol^{-1} at the melting point to a minimum below 29 J·K^{-1}·mol^{-1} at 900–1000 K; at higher temperatures the heat capacity increases again reaching 30.6 J·K^{-1}·mol^{-1} at 1373 K [69NOV/GRU], and 31.6 J·K^{-1}·mol^{-1} at 1600 K [74FRE/CHA].

Using the same data, previous assessments recommended different values and equations. Shpil'rain *et al.* [70SHP/YAK] used the data of [50GIN/DOU], [62ALA/PCH], [69NOV/GRU], [65SHP/SOL] and adopted the slightly rounded equation of [50GIN/DOU] for the range 371 – 1100 K

$$C_p^\circ = 37.45 - 19.15\times10^{-3}T + 10.62\times10^{-6}T^2 \text{ J·K}^{-1}\text{·mol}^{-1}.$$

An equation proposed for 1100–1800 K was consistent with the data of [50GIN/DOU]

$$C_p^\circ = 24.60 + 4.23\times10^{-3}T \text{ J·K}^{-1}\text{·mol}^{-1}.$$

This equation agrees satisfactorily with the data of [50GIN/DOU], [62ALA/PCH], [69NOV/GRU], [65SHP/SOL], but disagrees with [63EWI/STO] and [74FRE/CHA] (Fig. 3.4).

[73HUL] used data from [50GIN/DOU], [65SHP/SOL], [67MAR]; below 1300 K the recommended values are close to those described by equation of [50GIN/DOU]. Above 1300 K Hultgren *et al.* assumed a constant heat capacity value of 30.12 J·K^{-1}·mol^{-1}.

[82GUR] combined the results of several studies: [50GIN/DOU], [62ALA/PCH], [65SHP/SOL], [67MAR], [69NOV/GRU], [74FRE/CHA] and recommended one equation for the range from the melting point to 2300 K (Fig. 3.4).

$$C_p^\circ = 38.121 - 19.493\times10^{-3}T - 0.688\times10^{5}T^{-2} + 10.240\times10^{-6}T^2 \text{ J·K}^{-1}\text{·mol}^{-1}$$

[85JAN] adopted heat capacities from [50GIN/DOU] and extrapolated them smoothly to 1600 K.

Fink and Leibowitz [85FIN/LEI] used the enthalpy data of [50GIN/DOU], [65SHP/SOL], [69NOV/GRU], [74FRE/CHA] and derived an equation

$$C_p^\circ = 40.656 - 26.41\times10^{-3}T + 14.363\times10^{-6}T^2 \ \mathrm{J\cdot K^{-1}\cdot mol^{-1}}.$$

This equation was compared with the heat capacity data of [27DIX/ROD], [59NIK/KAL], [62ALA/PCH], [63EWI/STO], [67MAR]. Between 600 and 1200 K, the heat capacity data agree with the equation satisfactorily within ± 2 %. However, outside this interval, the disagreement increases. The experimental heat capacity data show a more shallow temperature dependence. Since most measurements are not accurate, the discrepancy between recommended and experimental heat capacity values could be ascribed to inaccurate measurements. However, the study [67MAR] seems to be reliable, and its experimental values are lower by about 3 % than those calculated by the equation of [85FIN/LEI]. The statement of [85FIN/LEI] that the enthalpy data of [50GIN/DOU], [65SHP/SOL], [74FRE/CHA] agree well is correct (Fig. 3.5); however, the heat capacities derived from the enthalpy data are very sensitive to small enthalpy changes. It seems important to compare heat capacities derived from individual enthalpy measurements with those of heat capacity measured directly; this was not done in [85FIN/LEI], and it led to an inaccurate equation. It should be pointed out that the equation recommended by [82GUR] describes the data below 1100 K better than the equation of [85FIN/LEI].

According to the description of the method, material, and procedure, the study [50GIN/DOU] is accurate. It was selected here as the best below 1200 K and as a basis for comparison with other studies; [65SHP/SOL], [69NOV/GRU], [74FRE/CHA] confirmed the measurements of [50GIN/DOU] (Fig. 3.5). The heat capacity values obtained in [67MAR] are in excellent agreement with [50GIN/DOU]. The heat capacity equation recommended in [50GIN/DOU] was adopted here for the description of liquid Na between melting point and 1200 K (Fig. 3.4).

$$C_p^\circ = 37.466 - 19.148\times10^{-3}T + 10.628\times10^{-6}T^2 \ \mathrm{J\cdot K^{-1}\cdot mol^{-1}} \quad (7)$$

Equation 7 was extrapolated to 1600 K and compared with the measurements made at 1200 − 1600 K. It describes the available data with an acceptable accuracy, giving values which seem to be better than those recommended by Fink and Leibowitz (Fig. 3.4). Therefore, Eq. 7 can be safely used up to 1600 K. It should be remembered that a similar recommendation was made in [85JAN].

The values of $C_p^\circ(T)$, $S^\circ(T)$ and $H^\circ(T)-H^\circ(298.15\ \mathrm{K})$ were calculated up to 1600 K using Eq. 6 and 7. They are listed in Table 3.10.

3.4. Phase Equilibrium Data

3.4.1. β-α Martensitic Transformation of Na

The martensitic transformation, as explained briefly in the Introduction, cannot be described by one temperature and requires for complete definition a set of characteristic temperatures:

- M_s start temperature for the direct β→α transformation (or M_d − the highest temperature at which plastic deformation can promote the transformation, $M_d > M_s$);
- A_s start temperatures of the reverse α→β transformation;
- A_f finish temperatures of the reverse transformation.

Each of these temperatures can vary from sample to sample depending on the purity and thermal treatment history. The degree of the direct transformation, which never reaches 100 %, influences measured properties. This degree is difficult to quantify. Therefore, the literature gives for Na a wide spectrum of values from 1 to 50 %, and the enthalpy of the complete β-α martensitic transformation of Na is known very approximately. The studies described below were concerned with investigations of the different characteristics of this transformation.

[48BAR]

The existence of a low-temperature transformation in Na was first mentioned in this study. After cold working at 20 K of a C.P. grade sodium, a small diffraction peak appeared in addition to the β pattern at 78 K. The peak was interpreted as evidence of a fcc phase with a lattice parameter a = 0.5339 nm.

[55BAR]

Barrett showed by optical microscopy that a martensite-type transformation occurs at 36.2 ± 2 K in an unstrained sample consisting of grains of vacuum-distilled Na (Merck, 99.94 % pure). Samples with smaller unoxidized grains began transforming at about 31 K, and those with oxidized surfaces even at lower temperatures. The transformation was detected after cooling to 30.9 K in pure Na with large grains (oxygen < 0.001 %, K < 0.00001 %).

[56BAR]

Barrett investigated by X-ray analysis two materials: a commercial Na (Merck, impurities in wt.%: K 0.05, Al 0.001 − 0.002, Mg < 0.001, Cu < 0.001; Fe < 0.001 − 0.01; Si < 0.003; Ca < 0.001); and high-purity Na supplied by the Naval Research Laboratory, Washington, D.C. (<0.001 wt.% O and Ag). The low-temperature phase had an α structure with parameters a = 0.3767 nm and c = 0.6154 nm at 5 K. The transformation never proceeded to more than 50 % completion. The transformation started on cooling below M_s = 36 K and progressed with lowering temperature. Deformation below M_d = 51 K promoted the transformation while, above M_d, it suppressed it. The reverse process in an unreformed sample started at A_s = 45 K; the process proceeded until A_f = 87 K. A high-purity sample annealed at 175 K was 7 % transformed on cooling to 5 K. Deformation increased the amount of α-Na to 30 %.

[58MAR]

Martin investigated the reverse transformation in a calorimeter (details of procedure and materials are described

in [60MAR] in Sec. 3.2.1.). After cooling to 20 and 2 K, the reverse transformation started on heating at about $A_s = 45$ K. The measured effect was 4 $J \cdot mol^{-1}$ after cooling to 20 K and 16 $J \cdot mol^{-1}$ after cooling to 2 K. The amount of transformed phase was not determined.

[60DUG/GUG]

Dugdale and Gugan measured the electrical resistivity of Na from 4 to 300 K. High-purity samples from Phillips, Eindhoven, had a residual resistance ratio $\rho_{273K}/\rho_{4.2K} = 2500 \div 5000$; the low-temperature phase had a smaller resistivity. On cooling, the transformation began at $M_s = 30$ K; the amount of the α phase was estimated as 40 ± 10 % at the lowest temperature. On heating, the reverse transformation started at $A_s = 40$ K and ended at $A_f = 70$ K.

[60HUL/ROS]

Hull and Rosenberg studied the β-α transformation of a 99.998 wt.% Na sample by X-ray technique. The transformation started at about $M_s = 31$ K; the amount of α-Na increased with cooling; 40 − 50 % transformed β-Na was observed at 20 K. Further cooling to 6 K did not change essentially the amount of the new phase. The reverse cycle was practically completed at $A_f = 65$ K. Cycling (repeated cooling and heating) reduced the degree of transformation.

[64BHA/STE]

Bhattacharya and Stern measured from 20 to 70 K the resonant frequency of longitudinal vibrations (related to Young's modules) of two high-purity Na samples, with residual resistance ratio $\rho_{273K}/\rho_{4.2K} \approx 11000$ and 7000. On cooling, the transformation was observed at about 35 K. The electronic specific heat coefficient for the cast and thermally-cycled (heated above the reverse transformation) samples was 1.38 ± 0.1 and 1.4 ± 0.1 $mJ \cdot K^{-2} \cdot mol^{-1}$, and the Debye temperatures 155.5 ± 2 and 154 ± 2 K, respectively. The cycled sample consisted mostly of β-Na and the cast sample contained considerable amount of α-Na.

[76STE]

Stedman measured neutron scattering by large Na single crystals (diameter − 5 cm, length − 10–12 cm, analysis not provided). Cycling through the martensitic transformation at $M_s = 35.7$ K showed that the extent of transformation was small. Reflections of α-Na indicated that this phase was poorly developed.

[84BLA/KRE]

Blaschko and Krexner studied neutron scattering of Na single crystals (diameter − 1 cm, length − 1 cm). No measurable changes in the mosaic width and Bragg intensities were observed when passing through 36 K. This indicates that only a small amount of β-Na (<1 %) was transformed. The diffuse scattering increased steeply below 36 K and showed a pronounced hysteresis. The effect was explained by formation of an intermediate defect structure.

[88SZE/TRI]

Szente and Trivisonno measured the ultrasonic velocity and attenuation of a single crystal in the vicinity of M_s. The specimen was 5 mm thick, 16 mm in diameter, and had a resistance ratio $\rho_{273K}/\rho_{4.2K} = 2000$. On cooling, changes were noticed between 40 and 43 K. Making an allowance for a poor thermal contact, the authors of [88SZE/TRI] estimated $M_s = 35$ K. The reverse transformation started at about $A_s = 55$ K and ended at about $A_f = 80$ K. The reported temperatures were reduced by the present authors by 5 K as a correction for poor thermal conductivity. During the reverse process the crystals underwent a structural reorientation. The amount of transformed phase was described qualitatively as "less than a few percent", which could be as little as 1 %.

[88SAU/MIO]

Saunders *et al.* estimated the Gibbs energy of transformation in Na as $\Delta_{trs}G(\beta \rightarrow \alpha, T > 200\ K) = -104 + 2.0T\ J \cdot mol^{-1}$. This corresponds to an equilibrium temperature $T_{trs} = 52$ K. The estimation is crude and the relative uncertainty could be >50 % in the enthalpy and entropy of transformation.

3.4.2. Fusion of Na

The temperature of fusion of Na was measured in [13REN], [14REN], [50GIN/DOU], [67MAR] described in Sec. 3.2. Some additional information is given below.

[27EDM/EGE]

Edmondson and Egerton used a distilled commercial sodium (<0.2 wt.% K). The melting point was determined by thermal analysis as 370.85 ± 0.05 K.

[30LAD/THI]

Ladenburg and Thiele obtained by thermal analysis the melting point of *Kahlbaum* Na as 370.95 ± 0.1 K.

[35LOS]

Losana measured by thermal analysis melting point of *Kahlbaum* Na $T_{fus} = 370.85 \pm 0.1$ K.

[56DOU]

Douglas measured the equilibrium temperatures at various stages of melting of Na and Na-U mixtures. Na was purified by distillation and contained about 0.02 wt.% Na_2O as a major impurity. At constant temperature energy was supplied in small quantities melting the samples gradually. The melting point of Na, 370.97 ± 0.02 K, was determined using the experimental dependence of the equilibrium fusion temperature vs. the amount of melted material. The T_{fus} obtained by Douglas seems to be very reliable.

[56BRA/PEA]

Bradshaw and Pearson measured the resistivity of Na near the melting point. The sample from the Atomic Energy Research Establishment, Harwell, was distilled in stainless steel. The principal impurities were K − 25 ppm and O − 5 ppm. The sample was heated slowly, and the resistance was measured at 0.025 K intervals. Melting caused a sharp increase in the resistivity. The melting point was determined from cooling and heating experiments as 370.96 ± 0.04 K. This work is one of the best determinations of T_{fus}.

[61PON]

Ponyatovskii studied the influence of pressure on the melting point of Na. The temperature of fusion of a commercial Na sample (99.9 wt.%) was determined by thermal analysis on cooling and heating with an accuracy ± 1.5 K. The melting point of Na increased from 370.65 K at ambient pressure to 521 K at 30000 atm. The uncertainty of this study is high.

[69SCH/FRI]

Schmid *et al.* measured the atomic volume of Na near the melting point. The sample was 99.99 % pure and contained K < 100 ppm, Mg < 20 ppm, Fe < 5 ppm and Ca < 5 ppm according to a mass-spectrometric analysis. The melting point was determined as T_{fus} = 370.92 ± 0.005 K from a slope of the $\Delta V/V$ vs T dependence. The value obtained seems to be reliable, but the stated accuracy was overestimated and should be no better than ± 0.01 K. The study is considered to be reliable.

[69OTT/GOA]

Ott, Goates *et al.* investigated in series of studies [69OTT/GOA], [70GOA/OTT], [71OTT/GOA] several sodium binary phase diagrams. The material was a reactor grade Na with <200 ppm K, <100 ppm O. Another sample was obtained from J.T. Baker Reagent Grade sodium with < 10 ppm K, total stated impurities 0.004 wt.%. The melting point was determined by thermal analysis T_{fus} = 371.05 ± 0.2 K. This temperature was quoted in several studies, but was determined probably only once or twice. The obtained value is reliable, but not very precise.

[74ADL/FRI]

Adlhart *et al.* measured precisely changes in the lattice parameter ($\Delta a/a < 10^{-6}$) of high purity (99.99 % Na) single crystals in the vicinity of the melting point. Immediately below the melting point a decrease in the lattice parameter was observed. The melting point was detected from the temperature gradient between a sample and its mounting; during slow fusion the temperature of the crystal remained constant whereas the temperature of the mounting rose continuously. The melting point was determined as T_{fus} = 370.98 ± 0.02 K. The study is one of the best determinations of the melting point.

[76MIR/KEN]

Mirwald and Kennedy determined the influence of pressure on the melting temperature of 99.9 % Na by thermal analysis. At standard pressure T_{fus} = 370.75 K, at 6 GPa the temperature increased to 592 K, and the initial slope was about 86 K GPa^{-1}. The stated uncertainty ± 0.1 K was underestimated and should be ± 0.2 K.

[83KAM]

Kamioka measured the velocity of sound in 99.9 % Na (material from Furuuchi Kagaku K.K.) by the ultrasonic pulse transmission method. On melting, the sound velocity decreased by about 20 %. From heating and cooling experiments, the melting point was determined as T_{fus} = 370.95 ± 0.1 K. This value is quite reliable.

The enthalpy of melting was determined in [13REN], [14REN], [50GIN/DOU], [56SCH/HIL], [67MAR] described in Sec. 3.2.; some additional information is given below.

[37BIN]

Binayendra determined the enthalpy of fusion in a calorimeter 2.63 $kJ \cdot mol^{-1}$, but no experimental details are given. The same value was derived from a theoretical estimation of other physical parameters. It is difficult to judge the accuracy of [37BIN] from the reported information.

[71MAL/GIG]

Malaspina *et al.* determined the enthalpy of fusion of Na in a Calvet calorimeter. The material was *Fluka and Koch Light Lab* with 99.9+ wt.% Na. The calorimeter was heated slowly 0.6 − 1.1 K h^{-1} over the range 643 to 733 K. The heat of melting was determined from the area on the thermogram. The average of four determinations was $\Delta_{fus}H$ = 2644 ± 17 $J \cdot mol^{-1}$. Using the available literature and their own data, the authors of [71MAL/GIG] recommended the value $\Delta_{fus}H$ = 2623 ± 20 $J \cdot mol^{-1}$. Since the authors of [71MAL/GIG] did not recommend their own value, but a smaller one, they may not have been confident in their results; the reported accuracy was probably underestimated and should be about ± 40 $J \cdot mol^{-1}$.

3.5. Discussion of Phase Equilibrium Data

3.5.1. β-α Martensitic Transformation of Na

The martensitic transformation in Na is similar to transformation in Li discussed in Sec. 2.5.1. It is described by a set of characteristic temperatures: M_s − start temperature of the direct transformation and M_d − start temperature after plastic deformation; A_s − start temperature of the reverse transformation, A_f − finish temperature; T_{max} − temperature at which the rate of reverse reaction is highest. The measured and adopted characteristic temperatures for Na are listed in Table 3.5. The adopted characteristic temperatures are

M_s = 35 ± 3 K [55BAR], [56BAR], [60MAR], [64BHA/STE], [76STE], [84BLA/KRE], [88SZE/TRI],
A_s = 45 ± 5 K [56BAR], [58MAR], [60MAR], [88SZE/TRI],
A_f = 75 ± 10 K [60DUG/GUG], [60MAR], [88SZE/TRI].

The selected values are based on measurements made by different methods. In previous reviews only one temperature was usually given to describe the β-α transformation: A_s = 40 ± 5 K in [73HUL], M_d = 51 ± 5 K in [82GUR], T_{max} = 55 K in [85JAN].

Table 3.6 lists the total enthalpy of the β-α transformation of Na. The heat absorbed during the reverse transformation was determined in calorimetric experiment [60MAR]. The thermal effect varied depending on the thermal treatment of specimens, i.e., on the amount of α-Na formed on cooling.The total effect of the completed β-α transformation was estimated from the data [60MAR] assuming a certain degree of transformation (% of α-Na). Since the magnitude of thermal effects and the degree of transformation varied, the enthalpy

iof the β-α transformation is known only roughly; it has a high uncertainty of about 50 %. The adopted value was estimated using a mean value of three measurements made in [60MAR] for specimens cooled from room temperature to 2 K (the absorbed heat was 18.8, 15.1, 17.1 $J \cdot mol^{-1}$). The mean value 17 $J \cdot mol^{-1}$ was divided by 0.4, assuming 40 % conversion of β-Na into α-Na according to [60DUG/GUG]. The adopted enthalpy of transformation 42 $J \cdot mol^{-1}$ coincides with the recommendation of [60MAR] obtained using a different assumption. The exact percentage of α-Na in two-phase samples is difficult to determine; it could be less than 40 % [84BLA/KRE], [88SZE/TRE]. [88SAU/MIO] estimated the enthalpy of transformation as 104 $J \cdot mol^{-1}$ from theoretical consideration. This value differs substantially from that adopted here. The present authors consider that the value derived from calorimetric experiment is probably more correct. Additional combined heat capacity and structural study could clarify the problem.

The values reported in previous reviews [81MED] and [73HUL] were based on the same source [60MAR], but less attention was paid to the degree of transformation. The entropy of transformation was estimated in a manner similar to the enthalpy from C_p/T vs T dependence as $\Delta_{trs}S$ = 0.7 $J \cdot K^{-1} \cdot mol^{-1}$.

3.5.2. Fusion of Na

The experimental temperatures of fusion of Na are listed in Table 3.7. The measured temperatures were converted to ITS-90. The adopted melting point T_{fus} = 370.95 ± 0.05 K was selected as the rounded average of the seven most reliable studies [50GIN/DOU], [56DOU], [56BRA/PEA], [67MAR], [69SCH/FRI], [74ADL/FRI], [83KAM]. It agrees within the uncertainty limit with the majority of the recent data quoted above and with previous evaluations [73HUL], [82GUR], [85JAN], and [85OHS/BAB].

Table 3.8 lists the experimental values of the enthalpy of fusion of Na. The adopted enthalpy 2600 $J \cdot mol^{-1}$ is based on the most accurate measurements of [50GIN/DOU], [67MAR]. Studies of [56SCH/HIL] and [71MAL/GIG] agree with the selection, but have larger and less certain values. The uncertainty was estimated as about ± 25 $J \cdot mol^{-1}$. The selected value almost coincides with the recommendations of [73HUL], [82GUR] and [85JAN].

3.6. Adopted Values

Electronic contribution to C_p: γ = 1.36 ± 0.04 $mJ \cdot K^{-2} \cdot mol^{-1}$.

Debye temperature at 0 K: Θ_D = 157 ± 2.0 K.

Heat Capacity Equations

β-Na

(Below 50 K β-Na contains a small portion of α-Na)

Temperature range 0 − 4 K.

$C_p^\circ = 1.36\times10^{-3}T + 5.02\times10^{-4}T^3$ $J \cdot K^{-1} \cdot mol^{-1}$

Temperature range 4 − 20 K:

$C_p^\circ = 0.8892 - 0.24962T - 3.8045T^{-2} + 2.492\times10^{-2}T^2 - 2.604\times10^{-4}T^3$ $J \cdot K^{-1} \cdot mol^{-1}$

Temperature range 20 − 50 K:

$C_p^\circ = -17.3956 + 1.1205T + 1.1986\times10^{3}T^{-2} - 1.132\times10^{-2}T^2 + 3.66\times10^{-5}T^3$ $J \cdot K^{-1} mol^{-1}$

Temperature range 50−150 K:

$C_p^\circ = 3.193 + 0.4154T - 5.5702\times10^{3}T^{-2} - 2.91\times10^{-3}T^2 + 7.403\times10^{-6}T^3$ $J \cdot K^{-1} \cdot mol^{-1}$

Temperature range 150 − 298.15 K:

$C_p^\circ = 33.999 - 7.412\times10^{-2}T - 7.4865\times10^{4}T^{-2} + 2.6801\times10^{-4}T^2 - 2.536\times10^{-7}T^3$ $J \cdot K^{-1} \cdot mol^{-1}$.

Temperature range 298.15 − 370.95 K:

$C_p^\circ = 53.941 - 194.429\times10^{-3}T + 361.905\times10^{-6}T^2$ $J \cdot K^{-1} \cdot mol^{-1}$

Liquid Na

Temperature range 370.95 − 1600 K:

$C_p^\circ = 37.466 - 19.148\times10^{-3}T + 10.628\times10^{-6}T^2$ $J \cdot K^{-1} \cdot mol^{-1}$.

Values at 298.15 K

C_p°(298.15 K) = 28.16 ± 0.1 $J \cdot K^{-1} \cdot mol^{-1}$;

S°(298.15 K) = 51.10 ± 0.3 $J \cdot K^{-1} \cdot mol^{-1}$;

$H^\circ(298.15\ K) - H^\circ(0)$ = 6432 ± 30 $J \cdot mol^{-1}$.

Phase Equilibrium Data

Martensitic β-α Transformation

Start of the direct transformation: M_s = 35 ± 3 K;

Start of the reverse transformation: A_s = 45 ± 5 K;

End of the reverse transformation: A_f = 75 ± 10 K.

Enthalpy of transformation: $\Delta_{trs}H$ = 42 ± 20 $J \cdot mol^{-1}$.

Entropy of transformation: $\Delta_{trs}S$ = 0.70 ± 0.35, $J \cdot mol^{-1}$.

Fusion

Temperature of fusion: T_{fus} = 370.95 ± 0.05 K.

Enthalpy of fusion: $\Delta_{fus}H$ = 2600 ± 25 $J \cdot mol^{-1}$.

3.7. Calculated Thermodynamic Functions of Na

The thermodynamics functions presented in Tables 3.9 and 3.10 are calculated using the equations presented in the previous section. Values in brackets are calculated by using the equations for the next higher adjacent temperature intervals.

3.8. References for Na

13REN E. Renegade, Compt. Rend. Acad. Sci. **156**, 1897–9 (1913); T_{fus}, $\Delta_{fus}H$, C_p (288–373 K).

14REN E. Rengade, Bull. Soc. Chim. France **75**, 130–47 (1914); T_{fus}, $\Delta_{fus}H$, C_p (288–373 K).

18EAS/ROD E. D. Eastman and W. H. Rodebush, J. Amer. Chem. Soc. **40**, 489–500 (1918); C_p (65–294 K).

26SIM/ZEI F. Simon and W. Zeidler, Z. Phys. Chem. Leipzig **123**, 383–404 (1926); C_p (17–118 K).

27DIX/ROD A. L. Dixon and W. H. Rodebush, J. Amer. Chem. Soc. **49**, 1162–74 (1927); C_p (394, 451 K).

27EDM/EGE W. Edmondson and A. Egerton, Proc. Roy. Soc. (London) **A113**, 520–533 (1927); T_{fus}.

30LAD/THI R. Ladenburg and E. Thiele, Z. Phys. Chem. **B7**, 161–87 (1930); T_{fus}.

35LOS L. Losana, Gazz. Chim. Ital. **65**, 851–64 (1935); T_{fus}.

37BIN N. S. Binayendra, Gazz. Chim. Ital. **67**, 714–5 (1937); $\Delta_{fus}H$.

48BAR C. S. Barrett, Amer. Min. **33**, 749 (1948); M_s.

48PIC/SIM G. L. Pickard and F. E. Simon, Proc. Phys. Soc. (London) **A61**, 1–9 (1948); C_p (2–25 K).

50GIN/DOU D. C. Ginnings, T. B. Douglas, and A. F. Ball, J. Res. Nat. Bur. Std. **45**, 23–33 (1950); ΔH, (273.15–367 K, 423–1170 K), T_{fus}, $\Delta_{fus}H$.

52DOU/BAL T. B. Douglas, A. F. Ball, D. C. Ginnings, and W. D. Davis, J. Am. Chem. Soc. **74**, 2472–8 (1952); C_p (300–1170 K).

54DAU/MCD T. M. Dauphinee, D. K. C. McDonald, and H. Preston-Thomas, Proc. Roy. Soc. (London) **A221**, 267–275 (1954); C_p (55–315 K).

54RAY J. A. Rayne, Phys. Rev. **95**, 1428–34 (1954); C_p (0.2–1 K).

55BAR C. S. Barrett, J. Inst. Metals **84**, 43–44 (1955); M_s.

55PAR/QUA D. H. Parkinson and J. F. Quarrington, Proc. Phys. Soc. **A68**, 762–3 (1955); C_p (1.5–20 K).

56BAR C. S. Barrett, Acta Cryst. **9**, 671–7 (1956); M_s, A_s, A_f.

56BRA/PEA F. F. Bradshaw and S. Pearson, Proc. Phys. Soc. **B69**, 441–8 (1956); T_{fus}.

56DOU T. B. Douglas, J. Res. Nation. Bureau Stand. **52**(5), 223–6 (1954); T_{fus}.

56SCH/HIL A. Schneider and O. Hilmer, Z. Anorg. Allgem. Chem. **286**, 97–117 (1956); ΔH (345–494 K), $\Delta_{fus}H$.

57ROB L. M. Roberts, Proc. Phys. Soc. **B70**, 744–52 (1957); C_p (1.5–20 K).

58MAR D. L. Martin, Phys. Rev. Letters **1**, 4–5 (1958); C_p (40–100 K), $\Delta_{trs}H$.

59MIT E. A. Mit'kina, Atomic Energy (USSR) **7**, 163–65 (1959); C_p (423–573 K).

59NIK/KAL N. A. Nikol'skii, N. A. Kalakutskaya, I. M. Pchelkin, T. V. Klassen, and V. A. Vel'tischeva, "Problems of Heat Transfer," ed. M. A. Mikheev, Acad. Sci. USSR, Moskva (1959), translated in USAEC Report AEC-tr-4511, p. 1–39 (1962); C_p (473–673 K).

60DUG/GUG J. S. Dugdale and D. Gugan, Proc. Roy. Soc. **A254**, 184–204 (1960); M_s, A_s, A_f.

60GAU/HEE R. E. Gaumer and C. V. Heer, Phys. Rev. **118**, 955–7 (1960); C_p (0.4–2 K).

60HUL/ROS D. Hull and H. M. Rosenberg, Cryogenics **1**, 27–32 (1960); M_s, A_f.

60LIE/PHI W. H. Lien and N. E. Phillips, Phys. Rev. **118**, 958 (1960); C_p (0.14–1.4 K).

60MAR D. L. Martin, Proc. Roy. Soc. (London) **A254**, 433–43 (1960); C_p (20–300 K).

61MAR D. L. Martin, Phys. Rev. **124**, 438–41 (1961); C_p (0.4–1.5 K).

61PON E. G. Ponyatovskii, Phys. Met. Metall. **11**(3), 146–147 (1961); T_{fus}, High Pressure.

62ALA/PCH I. M. Pchelkin, Ph.D. Thesis (supervisor I.T. Aladyev), Moscow, ENIN (1962) (Referred in [70SHP/YAK], p. 68); C_p (473–1573 K).

63GRU/ROS V. A. Gruzdev and V. V. Roschupkin, in "Zhidkie Metally," eds. V.M. Borishanskii *et al*. Gosatomizdat, Moscow 248–255 (1963); ΔH (375–1359 K).

63EWI/STO C. T. Ewing, J. P. Stone, J. R. Spann, T. A. Kovacina, and R. R. Miller, U.S. Naval Res. Lab. Rept. NRL-5964 (1963); ΔH (373–1543 K).

63FIL/MAR J. D. Filby and D. L. Martin, Proc. Roy. Soc. (London) **A276**, 187–203 (1963); C_p (3–30 K).

64BHA/STE D. L. Bhattacharya and E. A. Stern, Proc. Low Temp. Phys., Intern. Conf. **LT9**, 1210–4 (1964); M_s, β, Θ_D.

65SHP/SOL E. E. Spil'rain, Yu. A. Soldatenko, V. A. Yakimovich, V. A. Fomin, V. A. Savchenko, V. A. Belova, D. N. Kagan, and I. F. Krainova, High Temp. **3**, 870–4 (1965); ΔH (573–1273 K).

67ACH/FIS P. Y. Achener and D. L. Fisher, USAEC Rept. AGN-8191, Vol. **6** (1967); ΔH (420–1475 K).

67MAR D. L. Martin, Phys. Rev. ***154***, 571–5 (1967); C_p (300–475 K), T_{fus}, $\Delta_{fus}H$.

69NOV/GRU I. I. Novikov, V. A. Gruzdev, O. A. Kraev, A. A. Odintsova, and V. V. Roschupkin, High Temp. **7**, 65–8, (1969); ΔH (375–1359 K).

69OTT/GOA J. B. Ott, J. R. Goates, D. R. Anderson, and H. T. Hall, Trans. Faraday Soc. **65**, 2870–8 (1969); T_{fus}.

69SCH/FRI E. Schmid, G. Fritsch, and E. Luescher, Z. Angew. Phys. **27**, 35–9 (1969); T_{fus}.

70GOA/OTT J. R. Goates, J. B. Ott, and C. C. Hsu, Trans. Faraday Soc. **66**, 25–9 (1970); T_{fus}.

70SHP/YAK E. E. Shpil'rain, K. A. Yakimovich, E. E. Totskyi, D. L. Timrot, and V. A. Fomin, "Thermophysical Properties of Alkali Metals," Izd-vo Standartov, Moscow (1970), Review.

71MAL/GIG L. Malaspina, R. Gigli, and V. Piacente, Gazz. Chim. Ital. **101**, 197–203 (1971); $\Delta_{fus}H$.

71OTT/GOA J. B. Ott, J. R. Goates, and D. E. Oyler, Trans. Faraday Soc. **67**, 31–4 (1971); T_{fus}.

73HUL R. Hultgren, P. D. Desai, D. T. Hawkins, M. Gleiser, K. K. Kelley, and D. D. Wagman, "Selected Values of the Thermodynamic Properties of the Elements," Amer. Soc. Metals, Metals Park, OH 44073, 325–35 (1973); Review.

74ADL/FRI W. Adlhart, G. Fritsch, and E. Luscher, Phys. Lett. **A48**, 239–40 (1974); T_{fus}.

74FRE/CHA D. R. Frederickson and M. G. Chasanov, J. Chem. Thermodyn. **6**, 629–33 (1974); ΔH (554–1505 K).

76MIR/KEN P. W. Mirwald and G. C. Kennedy, J. Phys. Chem. Solids **37**, 795–7 (1976); T_{fus}.

76STE R. Stedman, J. Phys. F: Metal Phys. **12**(6), 2239–46 (1976); M_s.

81MED V. A. Medvedev, *et al*.., "Thermal Constants of Substances," **10**, V. P. Glushko, editor, VINITI, Moscow (1981); Review.

82GUR L. V. Gurvich, I. V. Veits, V. A. Medvedev, et al, V. P. Glushko, gen. ed., "Thermodynamic Properties of Individual Substances," Nauka, Moscow, **4**(1), 309–12 (1982); Review.

83KAM H. Kamioka, J. Phys. Soc. Japan **52**, 2433–9 (1983); T_{fus}.

84BLA/KRE O. Blaschko and G. Krexner, Phys. Rev. *B* **30**(4), 1667–70 (1984); M_s.

85FIN/LEI J. K. Fink and L. Leibowitz, "Handbook of Thermodynamic and Transport Properties of Alkali Metals," ed. R. W. Ohse, Blackwell Sci. Publ., Oxford, (1985) 411–434; Liquid Na, Review.

85JAN M. W. Chase, Jr., C. A. Davis, J. R. Downey, Jr., D. J. Frurip, R. A. McDonald, and A. N. Syverud, "JANAF Thermochemical Tables," J. Phys. Chem. Ref. Data 14, Supplement No. **1**, 1565–8 (1985); Review.

85OHS/BAB R. W. Ohse, J.-F. Babelot, J. Magill, and M. Tetenbaum, Pure Appl. Chem. **57**, 1407–26 (1985); T_{fus}, Review.

88SAU/MIO N. Saunders, A. P. Miodownik, and A. T. Dinsdale, CALPHAD **12**, 351–374 (1988); $\Delta_{trs}G$, Estimate.

88SZE/TRI J. Szente and J. Trivisonno, Phys. Rev. B, Cond. Matter. **37**, 8447–50 (1988); M_s, A_s, A_f.

89COX/WAG J. D. Cox, D. D. Wagman, and V. A. Medvedev, "CODATA Key Values for Thermodynamics," Hemisphere Publ. Corp., New York (1989); Review.

3.9. Appendix – Experimental Results of Na

Tables 3.11 to 3.38 present heat capacity or enthalpy data as they were presented in the original article. As a result, the numerical values listed in this Appendix are the actual experimental values, tabular smoothed values, values calculated from equations, or values extracted from a graph. Where necessary, values are converted to joules (from calories). In all cases, the table heading indicates the type of data listed.

The enthalpy data for Na are given mostly as $\Delta H = H°(T) - H°(T_{ref})$, where T_{ref} is usually equal to 273 or 298 K. When temperature $T > T_{fus}$ and $T_{ref} < T_{fus}$, then the values of ΔH include the enthalpies of fusion (Tables 3.16, 20, 31, 33, 35, 37). The correction $H°(258.15\ K) - H°(273\ K)$ was estimated as 701 $J \cdot mol^{-1}$; the value $H°(373\ K) - H°(298.15\ K)$ was calculated as 4821 $J \cdot mol^{-1}$.

TABLE 3.1. Electronic contribution to heat capacity and the Debye temperature of Na

Reference	γ, $mJ \cdot K^{-2} \cdot mol^{-1}$	Θ_D/ K	Temp. range, K
Original Studies			
26SIM/ZEI	—	159	>17 K
55PAR/QUA	1.8 ± 0.2	158	1.5 - 4
57ROB	1.37 ± 0.04	158.2	2.4 - 4
60LIE/PHI	1.45	156	0.15 – 1
60GAU/HEE	1.32	158	0.4 - 2
61MAR	1.38 ± 0.02	156.5 ± 2	0.4 - 1.5
64BHA/STE	1.38	155.5 ± 2	(α-Na present)
64BHA/STE	1.40	154.0 ± 2	(β-Na only)
Review			
73HUL	1.38 ± 0.04	Based on 61MAR	
Adopted			
	1.36 ± 0.04	157 ± 2	Based on 57ROB, 60GAU/HEE, 60LIE/PHI, 61MAR

TABLE 3.2. Values of [63FIL/MAR] selected to derive heat capacity equation for β-Na

T/K	$C_p°$, $J \cdot K^{-1} \cdot mol^{-1}$	T/K	$C_p°$, $J \cdot K^{-1} \cdot mol^{-1}$
		14	1.539
4	0.038	16	2.194
5	0.072	18	2.950
6	0.125	20	3.767
7	0.198	22	4.657
8	0.300	24	5.581
9	0.429	26	6.485
10	0.586	28	7.443
12	1.000	30	8.330

TABLE 3.3. Values of [60MAR] selected to derive heat capacity equation for β-Na

T/K	$C_p°$, $J \cdot K^{-1} \cdot mol^{-1}$	T/K	$C_p°$, $J \cdot K^{-1} \cdot mol^{-1}$
30	8.33	140	24.39
35	10.52	150	24.74
40	12.43	160	25.03
45	14.28	170	25.28
50	16.13	180	25.55
55	16.74	190	25.79
60	17.67	200	26.00
65	18.62	210	26.23
70	19.40	220	26.45
75	20.12	230	26.60
80	20.74	240	26.82
85	21.28	250	27.04
90	21.74	260	27.26
95	22.13	270	27.50
100	22.46	280	27.77
110	23.02	290	28.02
120	23.53	300	28.16
130	23.98		

TABLE 3.4. Comparison of the heat capacity, enthalpy and entropy values for β-Na at 298.15 K

Reference	C_p°(298.15 K), J·K^{-1}·mol^{-1}	S°(298.15 K), J·K^{-1}·mol^{-1}	H°(298.15 K)-H°(0), J·mol^{-1}
73HUL	28.229	51.17 ± 0.08	6431
82GUR	28.230	51.30 ± 0.2	6460 ± 20
85JAN	28.154	51.455	6447
89COX/WAG	28.230	51.30 ± 0.2	6460 ± 20
Adopted:	28.16 ± 0.1	51.10 ± 0.3	6432 ± 30

TABLE 3.5. Characteristic temperatures of martensitic transformation of Na

Reference	Temperature, K				Comments
	M_s	A_s	A_f	M_d or T_{max}	
Original studies					
55BAR	31-36				Optical microscopy
56BAR	36	45	87	M_d=51	X-ray analysis
58MAR	45				C_p measurements
60DUG/GUG	30	40	70	M_d=45-51	Electrical resistivity
60MAR	35	40-45	60-80	T_{max}=45-55	C_p measurements
60HUL/ROS	31	65			X-ray analysis
64BHA/STE	35				Vibration measurement
76STE	35.7				Neutron scattering
84BLA/KRE	36				Neutron scattering
88SZE/TRI	35	50	75		Ultrasonic measurement
Reviews					
73HUL	40±5				Based on 60MAR
82GUR				M_d=51 ± 5	Based on 56BAR, 60MAR
85JAN				T_{max}=55	Based on 60MAR
Adopted					
	35±3	45±5	75±10		Based on 60DUG/GUG, 60MAR, 76STE, 84BLA/KRE, 88SZE/TRI

TABLE 3.6. Enthalpy of martensitic transformation of Na

Reference	$\Delta_{trs}H$, J·mol^{-1}	Comments
Original studies		
60MAR	42	Estimate from C_p measurements
88SAU/MIO	104	Estimate
Reviews		
73HUL	13 ± 3	Based on 60MAR
81MED	33 ± 8	Estimate from 60MAR
Adopted		
	42 ± 20	Estimate from 60MAR, 60DUG/GUG

TABLE 3.7. Temperature of fusion of Na

Reference	T_{fus}, K	Comments
Original Studies		
13REN, 14REN	371.03 ± 0.05	Enthalpy measurements
27EDM/EGE	370.83 ± 0.05	Thermal analysis
30LAD/THI	370.93 ± 0.1	Thermal analysis
35LOS	370.83 ± 0.1	Thermal analysis
50GIN/DOU	370.94 ± 0.03	Enthalpy measurements
56DOU	370.95 ± 0.02	Thermal analysis
56BRA/PEA	370.94 ± 0.04	Resistivity measurements
61PON	370.63 ± 1.5	Thermal analysis
67MAR	370.992 ± 0.005	Thermal analysis
69SCH/FRI	370.90 ± 0.01	Volume expansion
71OTT/GOA	371.03 ± 0.2	Thermal analysis
74ADL/FRI	370.96 ± 0.02	Lattice param. measurements
76MIR/KEN	370.73 ± 0.2	Thermal analysis
83KAM	370.93 ± 0.1	Sound velocity measurements
Reviews		
73HUL	371.0 ± 0.1	Based on 13REN, 30LAD/THI, 50GIN/DOU, 67MAR, 71OTT/GOA
82GUR	371.01 ± 0.03	Based on 67MAR
85JAN	370.98 ± 0.02	Based on 50GIN/DOU
85OHS/BAB	370.90 ± 0.10	Based on several studies
Adopted		
	370.95 ± 0.05	Based on 7 studies

TABLE 3.8. Enthalpy of fusion of Na

Reference	$\Delta_{fus}H$, J·mol^{-1}	Comments
Original Studies		
13REN, 14REN	2619	Enthalpy measurements
37BIN	2630	Calorimeter, estimation
50GIN/DOU	2602 ± 9	Enthalpy measurements
56SCH/HIL	2640 ± 40	Enthalpy measurements
67MAR	2598 ± 1	Adiabatic calorimeter
71MAL/GIG	2644 ± 40	Calvet calorimeter
Reviews		
73HUL	2598 ± 40	Based on 50GIN/DOU, 67MAR
82GUR	2598 ± 5	Based on 67MAR
85JAN	2602	Based on 50GIN/DOU
Adopted		
	2600 ± 25	Based on 50GIN/DOU, 67MAR

TABLE 3.9. Thermodynamic functions of Na below 298.15 K

T/K	C_p° $J \cdot K^{-1} \cdot mol^{-1}$	$H^\circ(T)$-$H^\circ(0)$ $J \cdot mol^{-1}$	$S^\circ(T)$ $J \cdot K^{-1} \cdot mol^{-1}$
5	0.0794	0.1014	0.0290
10	0.5866	1.4642	0.1987
15	1.8561	7.2658	0.6519
20	3.7721 (3.776)	21.105	1.4350
25	6.032	45.507	2.5147
30	8.351	81.504	3.8209
35	10.5030	128.733	5.2726
40	12.404	186.111	6.8022
45	14.031	252.314	8.3598
50	15.384 (15.385)	334.363	10.051
60	17.693	500.344	13.070
70	19.414	686.283	15.933
80	20.721	887.256	18.615
90	21.717	1099.671	21.116
100	22.479	1320.819	23.445
110	23.069	1548.678	25.616
120	23.543	1781.812	27.644
130	23.951	2019.312	29.545
140	24.343	2260.773	31.334
150	24.766 (24.728)	2506.269	33.028
160	25.038	2755.137	34.634
170	25.308	3006.891	36.160
180	25.551	3261.203	37.614
190	25.778	3517.861	39.001
200	25.995	3776.732	40.329
210	26.207	4037.744	41.603
220	26.418	4300.864	42.827
230	26.628	4566.090	44.006
240	26.842	4833.440	45.143
250	27.059	5102.943	46.243
260	27.281	5374.639	47.309
270	27.506	5648.568	48.343
280	27.735	5924.772	49.347
290	27.969	5924.772	50.325
298.15	28.161 (28.143)	6432.016	51.103

TABLE 3.10. Thermodynamic functions of Na above 298.15 K.

T/K	C_p° $J \cdot K^{-1} \cdot mol^{-1}$	$H^\circ(T)$-H°(298.15 K) $J \cdot mol^{-1}$	$S^\circ(T)$ $J \cdot K^{-1} \cdot mol^{-1}$
298.15	28.14	0.00	51.10
300.00	28.18	52.10	51.27
370.95 (sol)	31.62	2151.99	57.54
370.95 (liq)	31.83	4751.99	64.55
400.00	31.51	5671.86	66.94
500.00	30.55	8772.90	73.86
600.00	29.80	11788.75	79.37
700.00	29.27	14740.64	83.92
800.00	28.95	17649.85	87.80
900.00	28.84	20537.63	91.20
1000.00	28.95	23425.24	94.25
1100.00	29.26	26333.92	97.02
1200.00	29.79	29284.94	99.59
1300.00	30.54	32299.55	102.00
1400.00	31.49	35399.01	104.29
1500.00	32.66	38604.57	106.51
1600.00	34.04	41937.49	108.66

TABLE 3.11. SMOOTHED heat capacity of Na [14REN]

T/K	C_p°, J·K^{-1}·mol^{-1}	T/K	C_p°, J·K^{-1}·mol^{-1}
300	28.26	370.95 (sol)	31.44
320	29.16	370.95 (liq)	32.14
340	30.05	375	32.14
360	30.95		

TABLE 3.12. EXPERIMENTAL heat capacity of Na [18EAS/ROD]

T/K	C_p°, J·K^{-1}·mol^{-1}	T/K	C_p°, J·K^{-1}·mol^{-1}
64.6	18.91	159.0	25.06
67.9	19.50	181.7	25.73
71.1	19.96	183.8	25.82
74.2	20.12	234.7	26.90
84.6	21.25	292.1	28.37
94.8	22.17	293.5	28.41
156.8	25.19		

TABLE 3.13. EXPERIMENTAL heat capacity of Na [26SIM/ZEI]

T/K	C_p°, J·K^{-1}·mol^{-1}	T/K	C_p°, J·K^{-1}·mol
16.95	2.477	34.56	10.33
20.04	3.582	41.4	12.68
23.25	5.054	49.5	15.86
26.17	6.485	58.1	17.87
29.40	8.075	117.6	23.60

TABLE 3.14. EXPERIMENTAL heat capacity of Na [27DIX/ROD]

T/K	C_p°, J·K^{-1}·mol^{-1}	T/K	C_p°, J·K^{-1}·mol
394	31.50	451	30.75

TABLE 3.15. SMOOTHED heat capacity of Na [48PIC/SIM]

T/K	C_p°, J·K^{-1}·mol^{-1}	T/K	C_p°, J·K^{-1}·mol
2	0.023	10	0.586
3	0.033	12	1.046
4	0.0565	14	1.611
5	0.113	16	2.26
6	0.247	18	2.97
7	0.519	20	3.77
8	0.389	25	6.07
9	0.418		

TABLE 3.16. EXPERIMENTAL enthalpy values [$H°(T)$-$H°(273\ K)$] of Na [50GIN/DOU]

T/K	ΔH, J·mol^{-1}	T/K	ΔH, J·mol^{-1}
303.6	852	573	11688
332	1670	673	14642
350	2204	773	17565
367	2725	873	20460
373	5515	972.5	23323
423	7092	1069.8	26144
473	8641	1169.6	29087

TABLE 3.17. SMOOTHED heat capacity of Na [50GIN/DOU]

T/K	$C_p°$, J·K^{-1}·mol^{-1}	T/K	$C_p°$, J·K^{-1}·mol^{-1}
273	27.57	573	29.98
298	28.10	673	29.40
323	28.86	773	29.01
348	30.05	873	28.85
370.8 (sol)	31.35	973	28.90
370.8 (liq)	31.83	1073	29.16
373	31.807	1173	29.63
473	30.79		

TABLE 3.18. SMOOTHED heat capacity of Na [54DAU/MCD]

T/K	$C_p°$, J·K^{-1}·mol^{-1}	T/K	$C_p°$, J·K^{-1}·mol^{-1}
60	17.74	200	25.90
70	19.46	220	26.32
80	20.71	240	26.65
90	21.76	260	27.11
100	22.47	280	27.61
120	23.47	298.15	28.11
140	24.22	300	28.16
160	24.77	310	28.45
180	25.36	320	28.74

TABLE 3.19. SMOOTHED heat capacity of Na [55PAR/QUA]

T/K	$C_p°$, J·K^{-1}·mol^{-1}	T/K	$C_p°$, J·K^{-1}·mol^{-1}
1.5	0.00439	7.0	0.218
1.8	0.00607	8.0	0.326
2.0	0.00753	9.0	0.444
2.5	0.01213	10.0	0.594
3.0	0.01862	12.0	1.046
3.5	0.02803	14.0	1.611
4.0	0.04121	16.0	2.238
4.5	0.06067	18.0	2.971
5.0	0.0816	20.0	3.766
6.0	0.1444		

TABLE 3.20. EXPERIMENTAL enthalpy values [$H°(T)$-$H°(293\ K)$] of Na [56SCH/HIL]

T/K	ΔH, J·mol^{-1}	T/K	ΔH, J·mol^{-1}
Solid Na		Liquid Na	
345	1350	372	4925
351	1550	373	4925
356	1690	378	5000
361	1820	383	5200
364	2000	391	5465
366	2025	413	6170
370	2160	435	6950
		454	7690
		473	8200
		494	8840

TABLE 3.21. SMOOTHED heat capacity of Na [57ROB]

T/K	$C_p°$, J·K^{-1}·mol^{-1}	T/K	$C_p°$, J·K^{-1}·mol^{-1}
1.5	0.00372	8	0.280
2.0	0.00665	9	0.406
2.5	0.0107	10	0.548
3.0	0.0174	12	0.919
3.5	0.0258	14	1.452
4.0	0.0368	16	2.125
5.0	0.0686	18	2.841
6.0	0.1167	20	3.556
7.0	0.187		

TABLE 3.22. SMOOTHED heat capacity of Na [59NIK/KAL]

T/K	$C_p°$, J·K^{-1}·mol^{-1}	T/K	$C_p°$, J·K^{-1}·mol^{-1}
373	31.85	723	29.25
423	31.18	773	29.25
473	30.50	823	29.25
523	29.93	873	29.35
573	29.45	923	29.35
623	29.25	973	29.35
673	29.25		

TABLE 3.23. SMOOTHED heat capacity of Na [60GAU/HEE]

T/K	$C_p°$, mJ·K^{-1}·mol^{-1}	T/K	$C_p°$, mJ·K^{-1}·mol^{-1}
0.5	0.72	1.5	3.62
1.0	1.81	2.0	6.52

TABLE 3.24. SMOOTHED heat capacity of Na [60LIE/PHI]

T/K	$C_p°$, mJ·K^{-1}·mol^{-1}	T/K	$C_p°$, mJ·K^{-1}·mol^{-1}
0.2	0.29	1.0	1.96
0.5	0.79	1.4	3.43

TABLE 3.25. SMOOTHED heat capacity of Na [60MAR] for 'cast' sample

	Heat capacity after 5 different thermal treatments[a]				
	No. 1	No. 2	No. 3	No. 4	No. 5
T/K	C_p°, J·K^{-1}·mol^{-1}				
21	4.16	4.28	4.20	–	–
25	5.94	6.05	5.97	–	–
30	8.27	8.34	8.27	–	–
35	10.46	10.53	10.46	–	–
40	12.38	12.51	12.38	12.39	12.42
45	14.10	14.49	14.10	14.07	14.03
50	15.88	16.22	15.77	16.09	15.47
55	17.85	16.81	18.41	17.62	16.73
60	18.66	17.74	18.43	17.98	17.75
65	19.18	–	18.90	18.62	18.62
70	19.69	–	19.49	–	19.36
75	20.27	–	20.10	–	20.03
80	20.87	–	20.71	–	20.65
85	–	–	–	–	21.23
90	–	–	–	–	21.70
95	–	–	–	–	22.09
100	–	–	–	–	22.41
110	–	–	–	–	23.00
120	–	–	–	–	23.55
130	–	–	–	–	24.00
140	–	–	–	–	24.39
150	–	–	–	–	24.72
160	–	–	–	–	25.02
170	–	–	–	–	25.28
180	–	–	–	–	25.52
190	–	–	–	–	25.77
200	–	–	–	–	25.99
210	–	–	–	–	26.18
220	–	–	–	–	26.39
230	–	–	–	–	26.61
240	–	–	–	–	26.83
250	–	–	–	–	27.05
260	–	–	–	–	27.29
270	–	–	–	–	27.51
273.15	–	–	–	–	27.57
280	–	–	–	–	27.76
290	–	–	–	–	28.02
298.15	–	–	–	–	28.23
300	–	–	–	–	28.28

[a]Note: Treatment Scheme. Cooling from room temperature:
No. 1 to 2 K;
No. 2 to 20 K without annealing after experiment No. 1;
No. 3 to 20 K after annealing at 300 K;
No. 4 to 35 K;
No. 5 to 36 K; this treatment is shown in Fig. 3.3

TABLE 3.26. SMOOTHED heat capacity of Na [61MAR]

T/K	C_p° mJ·K^{-1}·mol^{-1}	T/K	C_p° mJ·K^{-1}·mol^{-1}
0.5	0.75	1.5	3.78
1.0	1.89		

TABLE 3.27. SMOOTHED heat capacity of Na [62ALA/PCH]

T/K	C_p°, J·K^{-1}·mol^{-1}	T/K	C_p°, J·K^{-1}·mol^{-1}
373	31.8	1073	28.9
473	30.7	1173	29.0
573	30.1	1273	29.1
673	29.6	1373	29.2
773	29.4	1473	29.4
873	29.2	1573	29.8
973	29.0		

TABLE 3.28. SMOOTHED heat capacity of Na [63FIL/MAR]

	Heat capacity after 7 different thermal treatments[a]						
	No.1	No.2	No.3	No.4	No.5	No.6	No.7
T/K			C_p°, J·K^{-1}·mol^{-1}				
3.0	0.018	—	—	—	—	—	–
3.5	0.026	0.027	0.028	—	—	—	0.027
4.0	0.038	0.039	0.040	—	—	—	0.038
5.0	0.070	0.072	0.072	0.075	—	—	0.072
6.0	0.101	0.124	0.091	0.138	—	—	0.125
7.0	0.182	0.198	0.190	0.208	—	—	0.198
8.0	0.284	0.298	0.307	0.315	—	—	0.300
9.0	0.410	0.428	0.436	0.451	—	—	0.429
10.0	0.574	0.588	0.610	0.620	—	—	0.586
12.0	0.979	1.003	1.036	1.051	—	—	1.000
14.0	1.518	1.543	1.594	1.602	—	—	1.539
16.0	2.181	2.192	2.264	—	—	—	2.194
18.0	2.936	—	3.011	—	—	—	2.950
20.0	3.749	—	3.831	—	—	—	3.767
22.0	4.619	—	4.711	—	4.669	4.728	4.657
24.0	5.540	—	5.631	—	5.606	5.694	5.581
26.0	6.447	—	6.535	—	6.522	6.602	6.485
28.0	7.364	—	7.464	—	7.435	7.519	7.443
30.0	8.318	—	8.406	—	8.297	8.435	8.347

[a]Note: Treatment Scheme:

No.1 = cooling from 293 K to 3 K;
No.2 = No.1 heating to 30 K, then cooling to 3 K;
No.3 = No.2 then heating to 90 K and cooling to 3 K;
No.4 = No.3 heating to 30 K, then cooling to 3K;
No.5 = No.4 then heating to 293 K and cooling to 20 K;
No.6 = No.5 then heating to 90 K and cooling to 20 K;
No.7 = No.6 then heating to 293 K and cooling to 3 K; this treatment is shown in Fig. 3−2.

TABLE 3.29. ESTIMATED heat capacity of α-Na and β-Na [63FIL/MAR]

T/K	β-Na C_p°, J·K^{-1}·mol^{-1}	α-Na
3.5	0.029	0.026
4.0	0.041	0.037
5.0	0.079	0.065
6.0	0.136	0.113
7.0	0.218	0.178
8.0	0.332	0.265
9.0	0.476	0.379
10.0	0.651	0.523
12.0	1.099	0.908
14.0	1.661	1.424
16.0	2.333	2.051
18.0	3.090	2.780
20.0	3.907	3.587
22.0	4.803	4.439
24.0	5.720	5.356
26.0	6.627	6.268
28.0	7.569	7.163
30.0	8.464	8.222

TABLE 3.30. EXPERIMENTAL heat capacity of Na [63EWI/STO]

T/K	C_p°, J·K^{-1}·mol^{-1}	T/K	C_p°, J·K^{-1}·mol^{-1}
589	30.2	428	31.3
873	29.0	528	30.3
997	28.0	625	30.0
1099	28.6	723	29.3
1194	30.1	828	28.6
1282	31.2	926	28.9
1283	31.3		

TABLE 3.31. EXPERIMENTAL enthalpy values [$H^\circ(T)$-H°(373 K)] of Na [65SHP/SOL]

T/K	ΔH, J·mol^{-1}	T/K	ΔH, J·mol^{-1}
573	6108	973	17785
573.5	6118	1073	20642
673.3	9186	1173	23499
773.3	12139	1223	24865
873.2	14938	1273.3	26250
923.8	16266	1273.2	26250

TABLE 3.32. SMOOTHED heat capacity of Na [65SHP/SOL]

T/K	C_p°, J·K^{-1}·mol^{-1}	T/K	C_p°, J·K^{-1}·mol^{-1}
600	29.95	1000	28.38
700	29.48	1100	28.12
800	29.05	1200	27.92
900	28.69	1300	27.77

TABLE 3.33. EXPERIMENTAL enthalpy values [$H°(T)$-$H°(298\ K)$] of Na [67ACH/FIS]

T/K	ΔH, J·mol^{-1}	T/K	ΔH, J·mol^{-1}
420	6100	1030	25600
475	8000	1060	26400
500	8900	1085	27100
590	10800	1110	26500
610	12200	1115	28900
645	11500	1140	29000
645	13800	1170	29700
670	14600	1200	31700
695	15400	1230	31000
730	16500	1250	32600
755	16400	1250	33400
780	18200	1260	30500
810	19000	1280	31200
840	18600	1280	32500
860	20500	1310	34500
895	20900	1340	34000
925	21600	1265	35700
950	23400	1390	35400
975	23900	1425	36000
1005	24200	1475	37000

TABLE 3.34. SMOOTHED heat capacity of Na [67MAR]

T/K	$C_p°$, J·K^{-1}·mol^{-1}	T/K	$C_p°$, J·K^{-1}·mol^{-1}
300	28.07	390	31.63
310	28.45	400	31.55
320	28.83	410	31.42
330	29.20	420	31.30
340	29.66	430	31.17
350	30.21	440	31.09
360	30.88	450	31.00
370	31.88	460	30.88
371.01 (sol)	32.01	470	30.79
371.01 (liq)	31.71	475	30.75
380	31.71		

TABLE 3.35. EXPERIMENTAL enthalpy values [$H°(T)$-$H°(273\ K)$] of Na [69NOV/GRU]

T/K	ΔH, J·mol^{-1}	T/K	ΔH, J·mol^{-1}
375.7	5616	793.4	18212
376.0	5573	797.3	18304
381.4	5779	839.0	19422
386.1	5923	842.1	19626
397.6	6279	858.5	20567
407.1	6567	865.4	20313
430.7	7595	906.2	21381
441.5	7665	928.9	22105
464.1	8435	941.2	22406
467.4	8485	948.6	22557
497.0	9456	971.5	23285
535.0	10657	976.7	23428
562.1	11467	1061.3	25927
591.8	12346	1084.0	26471
598.7	12368	1104.3	27137
604.6	12569	1110.7	27218
643.2	13781	1160.7	28858
654.1	14132	1195.8	29827
677.0	14850	1252.7	31455
713.1	15845	1316.1	33517
730.9	16399	1358.7	34794
770.7	17647	1359.3	34818
791.1	18144		

TABLE 3.36. SMOOTHED heat capacity of Na [69NOV/GRU]

T/K	$C_p°$, J·K^{-1}·mol^{-1}	T/K	$C_p°$, J·K^{-1}·mol^{-1}
373	31.85	973	28.72
473	30.51	1073	29.06
573	30.12	1173	29.54
673	29.40	1273	30.02
773	28.89	1373	30.79
873	28.71		

TABLE 3.37. EXPERIMENTAL enthalpy values [$H°(T)$-$H°(298\ K)$] of Na [74FRE/CHA]

T/K	ΔH, J·mol^{-1}	T/K	ΔH, J·mol^{-1}
553.7	10382	1136.0	27397
659.1	13603	1226.2	30100
752.8	16314	1226.3	30100
856.2	19324	1241.3	30528
856.3	19317	1275.1	31529
949.9	22017	1377.2	34549
1044.4	24189	1429.4	36198
1135.9	27421	1504.7	38560

TABLE 3.38. SMOOTHED heat capacity of Na [74FRE/CHA]

T/K	$C_p°$, J·K^{-1}·mol^{-1}	T/K	$C_p°$, J·K^{-1}·mol^{-1}
773	32.80	1373	29.16
873	30.46	1473	29.54
973	29.37	1573	30.00
1073	28.87	1673	30.50
1173	28.79	1773	31.05
1273	28.91	1873	31.63

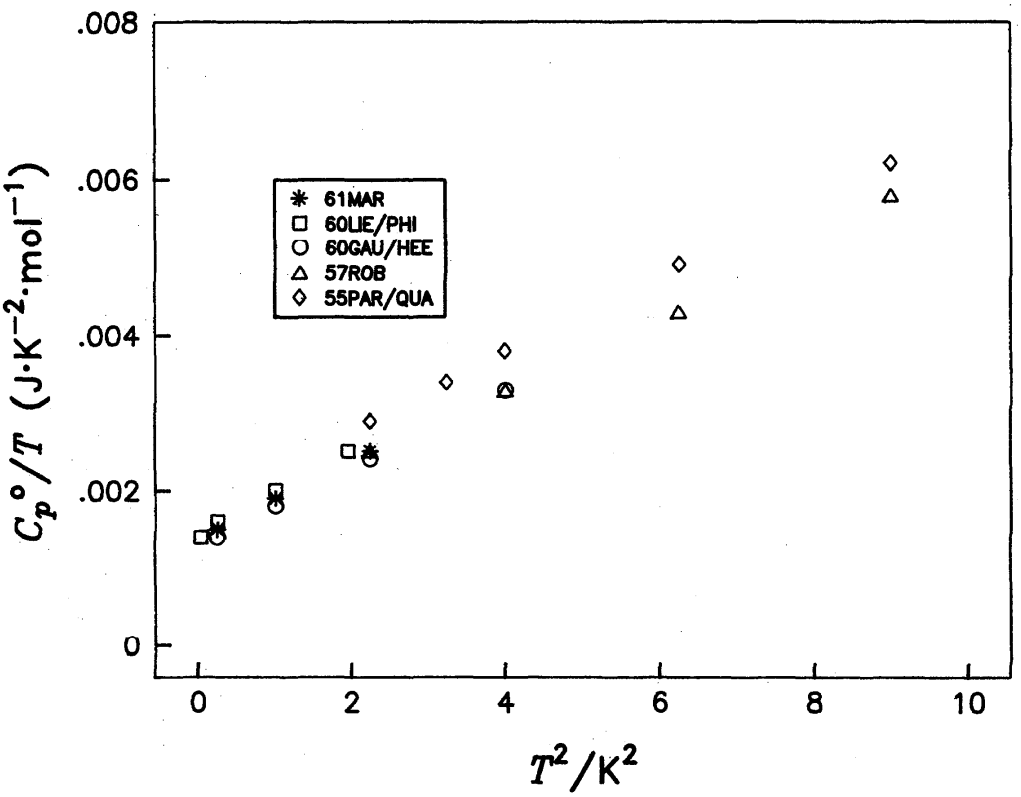

FIGURE 3.1. C_p/T versus T^2 for Na below 3 K

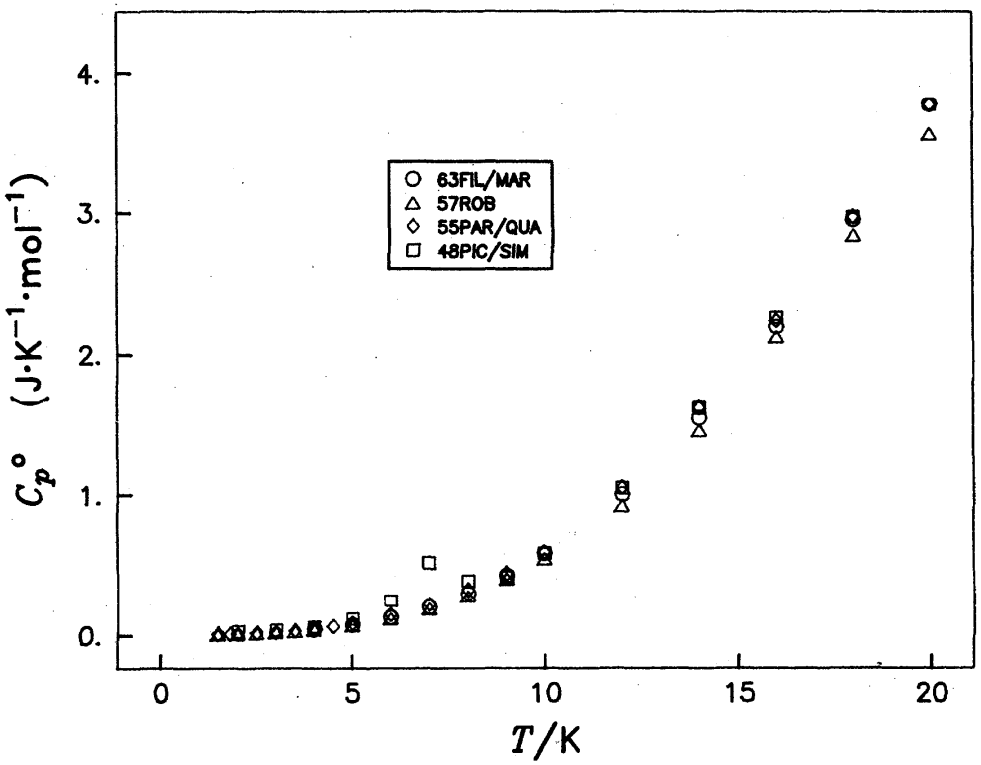

FIGURE 3.2. Heat Capacity of Na below 20 K

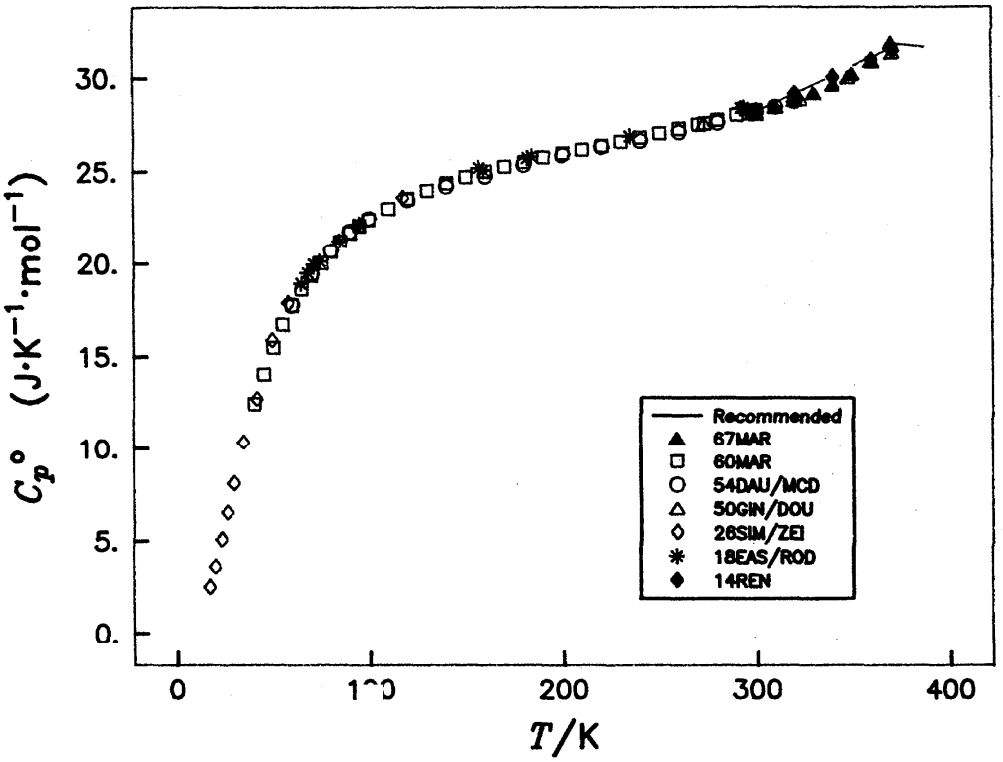

FIGURE 3.3. Heat Capacity of Solid Na

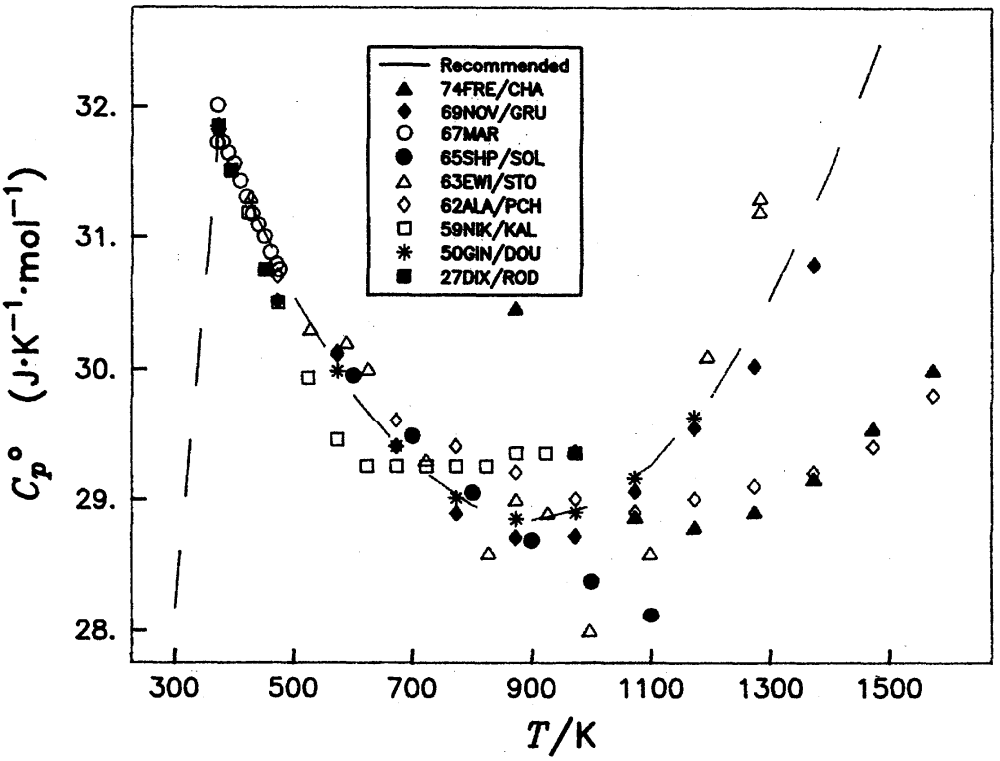

FIGURE 3.4. Heat Capacity of Liquid Na

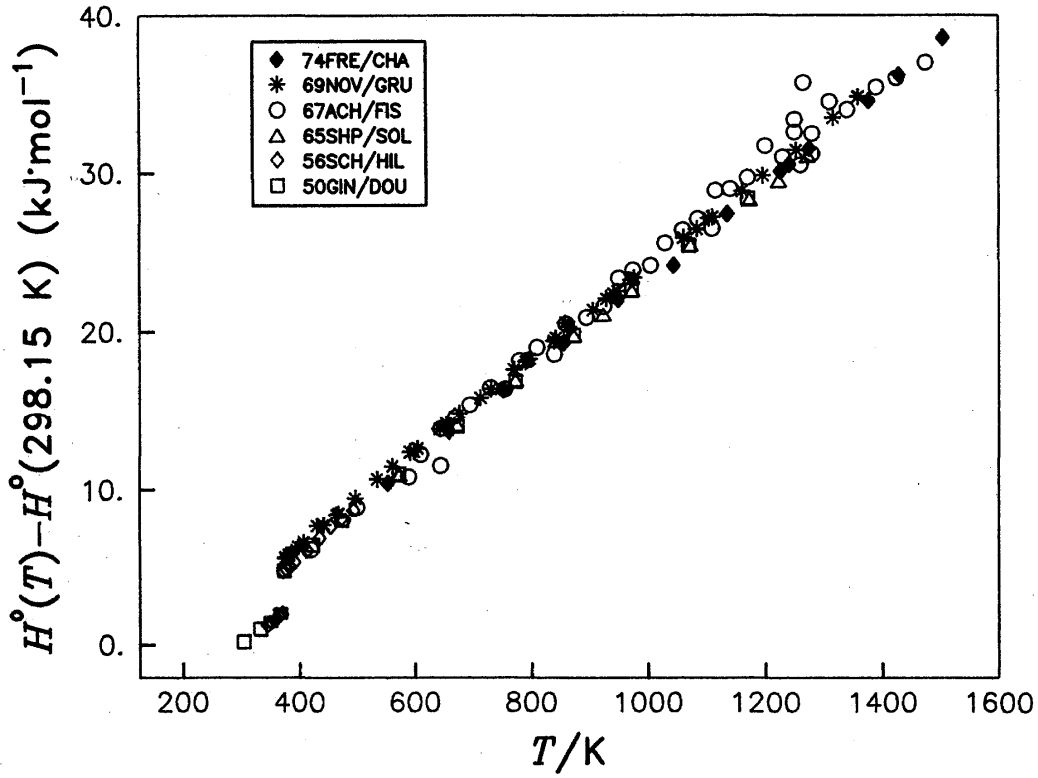

FIGURE 3.5. $H°(T)-H°(298.15\ K)$ of Na

4. Potassium

4.1. Introduction

At ambient pressure solid potassium has one (bcc) crystalline modification (Table 1.1). The thermodynamic properties of K are well established. The considerable discrepancies in the measured quantities above 1000 K require further investigation of liquid K with greater accuracy. The uncertainty in the melting point of K is greater than for other elements of the IA group; the original data are scattered.

4.2. Heat Capacity and Enthalpy Measurements

4.2.1. Temperature below 298.15 K

[18EAS/ROD]

Eastman and Rodebush measured the heat capacity of a commercial *Kahlbaum* potassium. Fourteen measured points between 68.6 and 286.7 K are given in Table 4.8 and shown in Fig. 4.3. The values are greater than those obtained by other investigators by about 3%. It should be remembered that Eastman and Rodebush obtained much better results for Na.

[26SIM/ZEI]

Simon and Zeidler measured the heat capacity of a commercial *Kahlbaum* potassium (<0.1% metallic impurities) from 15 to 276 K (22 points, Table 4.9, Fig. 4.2 and 4.3) in an adiabatic calorimeter. The Debye temperature was estimated as 99.5 K. The data are close to those obtained in more modern studies, and they are scattered within 1%. The authors tabulated heat capacities between 10 K and melting point.

[39CAR/STE]

Carpenter and Steward measured the heat capacity of a commercial *Kahlbaum* potassium, after an additional distillation, in a Nernst calorimeter at 203 to 610 K. The 84 measured points were reduced to 21 by the present authors. They are listed in Table 4.11 and shown in Fig. 4.3 and 4.4. The values are greater than those obtained in more recent investigations by 3% and have a random error of about 3%. A sharp premelting increase in heat capacity was explained by the presence of about 0.8 wt. % impurities in the samples. The melting point of K was determined as 336.56 K, and the enthalpy of fusion as $\Delta_{fus}H = 2377$ J·mol^{-1}.

[55DAU/MAR]

Dauphinee *et al.* measured the heat capacity of K from 30 to 330 K in an adiabatic calorimeter with continuous heating. The sample, prepared by Imperial Chemical Industries, contained <0.01 % Na (spectrographic analysis). Some irregularities were observed at 100–200 K; they were probably caused by a malfunction of the technique. The 73 measured points are given in a graphical form; the scatter was within 0.3 %. The 37 smoothed points were tabulated and reproduced in Table 4.14 and Fig. 4.3.

[57KRI/CRA]

Krier *et al.* measured the heat capacity of triply distilled K from 10 to 325 K in a directly-heated calorimeter. The 110 points were obtained in six series each with a different thermal treatment (Table 4.15). Smoothed results are reproduced in Table 4.16 and shown in Fig. 4.2 and 4.3. Thermal treatment did not influence the measured heat capacity. The average deviation of the individual points from a smoothed curve was 0.075 %, and only 10 % of all points deviate by greater than 0.15 %. The precision of the measurements was estimated as 0.1 %, and the study is considered very reliable.

[57ROB]

Roberts measured the heat capacity of K from 1.5 to 20 K. The sample, provided by the Atomic Energy Research Establishment, Harwell, had a purity of 99.995 % K. The 28 heat capacity values measured between 1.5 and 3.5 K were presented in a small-scale graph; the author's rounded values were tabulated between 1.5 and 20 K (Table 4.17, Fig. 4.1 and 4.2). Below 2.5 K the results deteriorated because of He desorption from the container walls; above 2 K a graph of C_p/T vs T^2 was not linear. Roberts introduced corrections and used points below 2 K to obtain $\gamma = 1.97$ mJ·K^{-2}·mol^{-1} and a Debye temperature $\Theta_D = 89$ K.

[60LIE/PHI], [64LIE/PHI]

Initially Lien and Phillips measured the heat capacity in an adiabatic calorimeter with a demagnetization cryostat from 0.17 to 1.1 K [60LIE/PHI]. A commercial material 99.99 wt.% K was used. Samples were cast into a calorimetric container under an inert atmosphere; after the experiment the analysis showed 0.2 % Na. About 45 data points are shown in a small-scale graph; the data were fitted to an equation corresponding to $\Theta_D = 89.9$ K and $\gamma = 2.2 \pm 0.1$ mJ·K^{-2}·mol^{-1}. The values calculated with these parameters are given in Table 4.19 and Fig. 4.1. Later Lien and Phillips [64LIE/PHI] remeasured the heat capacity using the same material and calorimeter from 0.2 to 1.2 K (46 points) and made additional measurements in a liquid-helium cryostat from 1.2 to 4.1 K (41 points). The data are reproduced in Table 4.23; several points are shown in Fig. 4.1; the two techniques produced a gap of 1.3 % at 1.2 K; those obtained at lower temperatures are greater and are considered to be less reliable. The uncertainty decreases from 1.5 % at 0.2 K to 0.3 % at 4 K. The data yielded $\Theta_D = 91.1 \pm 1$ K and $\gamma = 2.08 \pm 0.03$ mJ·K^{-2}·mol^{-1}.

[65FIL/MAR]

Filby and Martin measured the heat capacity of K in two calorimeters: a Nernst calorimeter with a ^{3}He cryostat was used from 0.4 to 1.5 K, and the temperature range 3 – 26 K was investigated in an adiabatic apparatus. Commercial samples (99.9+ % K) were obtained from MacKay (New York, U.S.A.) and Light (Colnbrook, England). The purity of the samples was checked by spectral analysis (only 0.01 % Na was detected) and by resistivity measurements (ratio $\rho_{293K}/\rho_{4.2K}$ varied from 450 to 650). The data are given in a graphic form below 15 K; smoothed values for the range 0.4 to 1.5 K and 3 to 26 K were tabulated; the data are reproduced in Table 4.25 and shown in Fig. 4.1, 4.2, and 4.3. The accuracy of the measurements was better than 1 %. The data below 0.7 K were used to yield $\gamma = 2.05 \pm 0.07$ mJ·K^{-2}·mol^{-1} and $\Theta_D = 90.3 \pm 0.7$ K.

[81AMA/KEE]

Amarasekara and Keesom measured the heat capacity of K (<10 ppm metallic impurities, Callery Chemical Co.) from 0.5 to 5 K. The results are in good agreement with [64LIE/PHI] above 1.2 K, and with [65FIL/MAR] between 0.9 and 1.5 K; however, below 0.9 K the values which were obtained are smaller than those of [64LIE/PHI] and [65FIL/MAR]. The authors suggested that their data are more reliable because they were obtained in one calorimeter with a germanium resistance thermometer which had been calibrated accurately. Indeed, the heat capacity data for Cu measured in the same study agree well with the best determinations by other authors. The heat capacity values were presented in a form of three-term equation

$$C_p^\circ = 1.83T + 2.66T^3 + 0.051T^5 \text{ mJ}\cdot\text{K}^{-1}\cdot\text{mol}^{-1}.$$

According to this equation $\gamma = 1.83$ mJ·K^{-2}·mol^{-1} and $\Theta_D = 90.1$ K. Table 4.29 and Fig. 4.1 show the values calculated by the above equation. The authors found a small anomaly centered at about 0.75 K and spread from 0.2 to 2 K; it was explained by a *phason contribution*. The magnitude of this anomaly corresponds to an increase in the enthalpy of about $\Delta H = 0.233$ mJ·mol^{-1} and entropy $\Delta S = 0.278$ mJ·K^{-1}·mol^{-1}. These small quantities could be ignored in calculation of the thermodynamic functions at 298.15 K.

4.2.2. Temperature above 298.15 K

[13REN], [14REN]

Rengade measured the enthalpy in a Bunsen ice calorimeter from 288 to 373 K. Potassium was prepared from KCl by Ca reduction and was doubly distilled in vacuum at 673 K. The measurements (8 points for solid K and 2 points for liquid K) were shown in a graph [14REN], and they were described for solid K by the equation:

$$C_p^\circ = 15.24 + 0.04777T \text{ J}\cdot\text{K}^{-1}\cdot\text{mol}^{-1},$$

and for liquid K, below 373 K:

$$C_p^\circ = -6.61 + 0.1093T \text{ J}\cdot\text{K}^{-1}\cdot\text{mol}^{-1}.$$

The heat capacity values obtained by these equations are given in Table 4.7 and Fig. 4.3. The heat capacities of liquid K are not accurate; they increase with temperature. The melting point was determined as $T_{fus} = 336.65$ K, and the enthalpy of fusion as $\Delta_{fus}H = 2393$ J·mol^{-1}. These two values agree well with modern data.

[27DIX/ROD]

Dixon and Rodebush measured the heat capacity of a commercial K purified by vacuum melting, filtering, and distillation. The method was based on measuring the adiabatic temperature-pressure coefficient; this gave rise to experimental difficulties due to the high thermal conductivity of potassium. The values obtained at 363, 409 and 454 K are listed in Table 4.10 and shown in Fig. 4.4.

[52DOU/BAL]

Douglas *et al.* measured the enthalpy of K between 298 and 1070 K in an ice drop calorimeter. Commercial potassium (Baker Chemical Co.) was purified by triple distillation and found to contain about 0.15 % metallic impurities by spectrographic analysis. The measured enthalpy is given in Table 4.12 and shown in Fig. 4.5; it is described for solid K by the equation

$$H^\circ(T,\text{cr}) - H^\circ(273\text{ K,cr}) = -4557 + 5.606T + 0.0406T^2 \text{ J}\cdot\text{mol}^{-1};$$

for liquid K below 1100 K:

$$H^\circ(T,\text{l}) - H^\circ(273\text{ K,cr}) = -7323.3 + 37.174T - 9.5577\times10^{-3}T^2 + 4.1054\times10^{-6}T^3, \text{ J}\cdot\text{mol}^{-1}.$$

Douglas *et al.* tabulated their smoothed heat capacity values (Table 4.13 and Fig. 4.3 and 4.4). The accuracy of these measurements was about 1.5 %. The triple point was determined as $T_{tr} = 336.35 \pm 0.1$ K; it differs from T_{fus} by 0.02 K. The enthalpy of fusion was estimated as $\Delta_{fus}H = 2334$ J·mol^{-1}.

[59NIK/KAL]

Nikol'skii *et al.* measured the heat capacity of liquid K by direct heating under isothermal conditions at 373 to 673 K. The published data are reproduced in Table 4.18 and shown in Fig. 4.4.

[62ALA/PCH]

Pchelkin *et al.* (quoted from [70SHP/YAK]) measured the heat capacity of liquid K (impurities: 1.5 % Na, 0.05 % Rb, 0.01 % Li) in an isothermal calorimeter at 373 to 1523 K. The smoothed results are listed in Table 4.20, and shown in Fig. 4.4; the original data have a scatter of about 8 %.

[63LEM/DEE]

Lemmon *et al.* measured the enthalpy of K in a drop calorimeter in the range 300 to 1420 K. Commercial potassium was distilled; it contained 35 – 50 ppm of oxygen and about 150 ppm of metallic impurities. The results were presented in a graphic form. The 21 data points were taken from the graph, reproduced in Table 4.21 and shown in Fig. 4.5. The authors fitted these data to two equations for solid K at 273–336 K:

$$H^\circ(T,\text{cr}) - H^\circ(273\text{ K,cr}) = -5060 + 9.18T + 68.54\times10^{-3}T^2, \text{ J}\cdot\text{mol}^{-1}.$$

and for liquid K at 336 – 1420 K;

$$H^\circ(T,\text{l}) - H^\circ(273\text{ K,cr}) = -7442 + 38.28T - 1.2524\text{X}10^{-2}T^2 + 6.2194\times10^{-6}T^3 \text{ J}\cdot\text{mol}^{-1}.$$

The C_p values calculated by these equations are listed in Table 4.22 and shown in Fig. 4.4. The accuracy was estimated as 2 % below 773 K and 5 % above 773 K. Extrapolation to the melting point yielded the enthalpy of fusion $\Delta_{fus}H = 2338$ J·mol^{-1}.

[65EWI/STO]

Ewing *et al.* measured the enthalpy of a commercial K (99.95%) which was additionally distilled; the impurities were determined by spectral analysis: 100 to 1000 ppm Rb, 10 to 100 ppm Na, and about 10 ppm of oxygen. The measurements were made in a copper drop calorimeter at three temperatures. The heat capacities calculated from these data are given in Table 4.24 and shown in Fig. 4.4. The accuracy of these data was estimated as about 3%.

[66TEP/ROE]

Tepper and Roehlich measured the enthalpy of K by drop calorimetry between 532 and 1444 K. The data are listed in Table 4.26 and shown in Fig. 4.5; they are taken from the review [85FIN/LEI].

[70SHP/KAG]

Shpil'rain and Kagan measured the enthalpy of liquid K from 411 to 1316 K in a boiling-point mixing calorimeter. The distilled sample contained 0.35 % Na and about 2 ppm of other alkali metals; after the experiment the amount of metallic impurities was about 200 ppm. The enthalpies adjusted to 273 K are given in Table 4.27 and shown in Fig. 4.5. A correction $H°(373\ K,l)-H°(273\ K,cr) = 5415\ J\cdot mol^{-1}$ was taken from [52DOU/BAL], and the data were fitted to the equation

$$H°(T,l)-H°(273\ K,cr) = -9863 + 49.643T - 0.02862T^2 + 1.30\times10^{-5}T^3,\ J\cdot mol^{-1}.$$

The derived heat capacity values are given in Table 4.28 and shown in Fig. 4.4. The experimental error was estimated as ± 4%.

4.3. Discussion of Heat Capacity and Enthalpy Data

4.3.1. K below 298.15 K

Measurements near 0 K. Below 2 K the heat capacity was measured in [57ROB], [60LIE/PHI], [64LIE/PHI], [65FIL/MAR], [81AMA/KEE]; the results are fitted to the two- or three-term equations shown in the C_p/T vs T^2 coordinates in Fig. 4.1. The values of γ and Θ_D derived from measured heat capacities are listed in Table 4.1. A third term of power of five with coefficient δ was introduced in [64LIE/PHI] and [81AMA/KEE] to describe the results; below 2 K the last term does not contribute more than 2 % to a total heat capacity value.

The data of [57ROB], [60LIE/PHI], [64LIE/PHI], [65FIL/MAR], [81AMA/KEE] (Fig. 4.1) have about the same slope, which corresponds to the Debye temperature $\Theta_D = 89 - 91$ K; the value 90 ± 1 K, taken from [81AMA/KEE], coincides with the average of all sources. The values of γ are varying from 1.83 to 2.08 $mJ\cdot K^{-2}\cdot mol^{-1}$. The values adopted, $\gamma = 1.83 \pm 0.15\ mJ\cdot K^{-2}\cdot mol^{-1}$, were taken from [81AMA/KEE] which was assumed to be a more accurate study than [57ROB], [60LIE/PHI], [64LIE/PHI], [65FIL/MAR]. A three-term equation proposed in [81AMA/KEE]

$$C_p° = 1.83T + 2.66T^3 + 0.051T^5\ mJ\cdot K^{-1}\cdot mol^{-1} \quad (1)$$

was used to calculate the thermodynamic functions below 2 K. The authors of [81AMA/KEE] showed that the heat capacity has an anomaly spread from 0.2 to 2 K, which corresponds to very small quantities, viz., $\Delta H = 0.233\ mJ\cdot mol^{-1}$ and $\Delta S = 0.278\ mJ\cdot K^{-1}\cdot mol^{-1}$. The anomaly needs to be proven, and the above quantities were ignored during calculation of $S°(298\ K)$ and $H°(298\ K)-H°(0)$.

Measurements between 2 and 20 K. The heat capacity measurements were made in [26SIM/ZEI] (above 15 K), [57KRI/CRA] (above 11 K), [57ROB] (1.5 − 20 K), [65FIL/MAR] (above 4 K). The data of [57KRI/CRA], [57ROB] and [65FIL/MAR] agree within 0.5 % (Fig. 4.2). The heat capacity values obtained in [65FIL/MAR] were selected as the most reliable, and they were fitted to the equation:

$$C_p° = 0.3143 - 0.2626T - 0.0196T^{-2} + 0.06483T^2 - 1.4\times10^{-3}T^3\ J\cdot K^{-1}mol^{-1}. \quad (2)$$

Measurements between 20 and 70 K. For this interval the measurements were made in [26SIM/ZEI], [55DAU/MAR] (above 30 K), [57KRI/CRA], [65FIL/MAR] (below 26 K). Below 26 K the data of [57KRI/CRA] and [65FIL/MAR] are in excellent agreement; above 30 K the data of [57KRI/CAR] and [55DAU/MAR] agree well. The smoothed data of [57KRI/CRA] were fitted to the equation

$$C_p° = -4.117 + 1.037T - 694.64T^{-2} - 0.01414T^2 + 7.022\times10^{-5}T^3\ J\cdot K^{-1}\cdot mol^{-1}. \quad (3)$$

Measurements between 70 and 300 K. For this interval the measurements were made in [18EAS/ROD], [26SIM/ZEI], [39CAR/STE], [55DAU/MAR], [57KRI/CRA], the data of [26SIM/ZEI], [55DAU/MAR] and [57KRI/CRA] being in good agreement. Study [57KRI/CRA] was considered to be better than [55DAU/MAR] which describes some irregularities at 100 − 200 K. The smoothed values of [57KRI/CRA] between 70 and 300 K (Table 4.16) were fitted to the equation

$$C_p° = 21.798 + 0.0528T - 7063.3T^{-2} - 2.1447\times10^{-4}T^2 + 4.184\times10^{-7}T^3\ J\cdot K^{-1}\cdot mol^{-1}. \quad (4)$$

Equations 1−4 were used to calculate $C_p°(298.15\ K)$, $H°(298.15\ K)-H°(0)$ and $S°(298.15\ K)$. The calculations are shown in Table 4.5. At the standard temperature the heat capacity, enthalpy and entropy were calculated as

$C_p°(298.15\ K) = 29.485\ J\cdot K^{-1}\cdot mol^{-1}$,
$S°(298.15\ K) = 64.628\ J\cdot K^{-1}\cdot mol^{-1}$,
$H°(298.15\ K)-H°(0) = 7079.94\ J\cdot mol^{-1}$.

These values can be compared with those recommended in previous reviews.

The calculated values are close to the previously recommended values listed above. The difference between this and the previous recommendations is small and mostly due to the use of a different treatment of the same information, particularly selection of [81AMA/KEE] for low temperatures.

4.3.2. Solid K above 298.15 K

Above 298.15 the enthalpy or heat capacity of solid potassium was measured in [13REN], [14REN] (C_p), [39CAR/STE] (C_p), [52DOU/BAL] (ΔH), [55DAU/MAR] (C_p below 330 K), [57KRI/CRA] (C_p below 320 K), [63LEM/DEE] (Fig. 4.3 and 4.5). The data of [39CAR/STE] are considerably higher than other data, and they were omitted from further consideration. The heat capacity data of [55DAU/MAR] and [57KRI/CRA] agree well; they differ <0.3% at 300 – 320 K. At 320 K the heat capacity values, derived from the enthalpy measurements of [52DOU/BAL] and [63LEM/DEE], are greater than the results of direct heat capacity measurements [55DAU/MAR] and [57KRI/KRA] by about 3% for [52DOU/BAL] and 1% for [63LEM/DEE]. The heat capacity values of [55DAU/MAR] and [57KRI/KRA] were fitted by [82GUR] to an equation:

$$C_p^\circ = 82.924 - 394.997\times10^{-3}T + 724.957\times10^{-6}T^2 \ \mathrm{J\cdot K^{-1}\cdot mol^{-1}}. \quad (5)$$

This equation describes well the experimental data for solid K and was adopted in this assessment.

[73HUL] and [85JAN] used the same information for the heat capacity values. The heat capacities recommended in [73HUL] deviate very little from [82GUR] at 298 K. However, a gap of 7 % exists between [85JAN] and [82GUR] near the melting point because of a different extrapolation of the data obtained at lower temperatures.

4.3.3. Liquid K

Enthalpy and heat capacity of liquid potassium were measured in [13REN], [14REN] (C_p, T<373 K), [27DIX/ROD] (C_p, 363–454 K), [39CAR/STE] (C_p, 338–610 K), [52DOU/BAL] (ΔH, 338–1070 K), [59NIK/KAL] (C_p, 373–673 K), [62ALA/PCH] (C_p, 373–1523 K), [63LEM/DEE] (ΔH, 370–1420 K), [65EWI/STO] (C_p, T = 1040, 1187, 1329 K), [66TEP/ROE] (ΔH, 532–1444 K), [70SHP/KAG] (ΔH, 411–1316 K); the data are shown in Fig. 4.4 and 4.5.

Figure 4.5 shows that below 1000 K the enthalpy data $H^\circ(T,\mathrm{l})-H^\circ(298.15\ \mathrm{K,\ cr})$ of [52DOU/BAL], [63LEM/DEE], [66TEP/ROE] and [70SHP/KAG] agree well, while above 1000 K the values of [66TEP/ROE] are greater than other data.

Below 600 K the C_p results of [27DIX/ROD] and [39CAR/STE] are much larger than other data, and so they were omitted from further consideration. Between the melting point and 1000 K, the directly measured heat capacity values [59NIK/KAL], [62ALA/PCH] and those derived from the enthalpy measurements [52DOU/BAL] and [63LEM/DEE] agree satisfactorily, while the heat capacity data derived from [70SHP/KAG] are smaller than others (Fig. 4.4). The quality of data below 1000 K was compared using the description of techniques, materials and procedures as criteria. Preference was given to [52DOU/BAL] whose results were confirmed in the less accurate studies [63LEM/DEE] and [70SHP/KAG] (Fig. 4.5). Several reviews also concluded that [52DOU/BAL] was the most reliable study below 1000 K. The heat capacity equation, proposed in [52DOU/BAL], was adopted here

$$C_p^\circ = 37.174 - 19.115\times10^{-3}T + 12.316\times10^{-6}T^2 \ \mathrm{J\cdot K^{-1}\cdot mol^{-1}}. \quad (6)$$

Above 1000 K the data diverge; for example, at 1300 K the difference between two Soviet studies [62ALA/PCH] and [70SHP/KAG] reaches 30 %; both of them are considered not very accurate. At 1000 – 1500 K the high heat capacity values were derived from [70SHP/KAG] and [63LEM/DEE]; the low heat capacity values were obtained in [62ALA/PCH]; data of [65EWI/STO] and those of [52DOU/BAL] occupy an intermediate position (Fig. 4.4).

Below 1000 K the recommendations of [70SHP/YAK], [73HUL] and [85JAN] are close and based on [52DOU/BAL]; however, above 1000 K different heat capacity values were proposed. For example, at 1500 K value of [70SHP/YAK] is greater than [85JAN] by 3.5%, and the latter is greater than [73HUL] again by about 3.5%; nevertheless all three recommendations appear to be reasonable.

The values recommended by [85FIN/LEI] and [82GUR] are much greater than those of [70SHP/YAK], [73HUL], [85JAN]. The recommendation of [85FIN/LEI] was based on the enthalpy measurements of [52DOU/BAL], [63LEM/DEE], [70SHP/KAG] which agree satisfactorily. However, the heat capacity values derived individually for each study are different. Small fluctuations in the enthalpy can result in considerable variations in the derived heat capacity values. An equal weight was given to all studies in [85FIN/LEI], and the less accurate data of [63LEM/DEE] and [70SHP/KAG] are weighted above the more careful data of [52DOU/BAL] and increase the mean value. The authors of [85FIN/LEI] proposed an equation:

$$C_p^\circ = 37.447 - 24.063\times10^{-3}T + 18.585\times10^{-6}T^2 \ \mathrm{J\cdot K^{-1}\cdot mol^{-1}}.$$

[82GUR] combined the results of [52DOU/BAL], [62ALA/PCH], [63LEM/DEE], [70SHP/KAG] and derived an equation:

$$C_p^\circ = 39.288 - 24.334\times10^{-3}T - 0.865\times10^{5}T^{-2} + 15.863\times10^{-6}T^2 \ \mathrm{J\cdot K^{-1}\cdot mol^{-1}}.$$

At 1400 K the heat capacity value calculated by the above equation is smaller than the heat capacity calculated in [85FIN/LEI] by 10%, but it is greater than C_p°(1400 K) of [70SHP/YAK] by 6%.

If Eq. 6 is extrapolated beyond 1100 K, the limit of the temperature measurements in [52DOU/BAL], it still describes most other available sources quite well up to 1600 K, giving values which lie between the data of [63LEM/DEE], [70SHP/KAG] and those of [62ALA/PCH] (Fig. 4.4). The temperature range covered by Eq. 6 can therefore be safely extended to 1600 K.

The values of $C_p^\circ(T)$, $S^\circ(T)$ and $H^\circ(T)-H^\circ(298.15\,K)$ were calculated using Eqs 5 and 6. They are listed in Table 4.6, and the heat capacity values are shown in Fig. 4.4.

4.4. Phase Equilibrium Data

The temperature of fusion of potassium was measured in [13REN], [14REN], [52DOU/BAL], [39CAR/STE] described in Sec. 4.2.; more information is given below.

[27EDM/EGE]

Edmondson and Egerton determined the melting point of a commercial sample of potassium, which was purified by distillation. According to thermal analysis, T_{fus} = 336.80 ± 0.05 K; this value is accurate considering time of measurements.

[35LOS]

Losana found by thermal analysis the melting point of potassium to be T_{fus} = 335.25 ± 0.1 K. A commercial *Kahlbaum* K was purified by distillation and contained <0.015 % Na. The obtained value is much smaller than other results; impurities in material can be suspected.

[66STO]

Stokes measured the density of K between 273 and 358 K. A commercially supplied material was doubly distilled; the initial freezing point, 336.66 K, was maintained to within ± 0.02 K until a half of the sample was frozen. The amount of impurities was roughly estimated as 2.5×10^{-3} at.%. The value obtained seems to be accurate.

[69BAS/VOL]

Basin *et al.* measured the density of potassium in the vicinity of the melting point. The samples had about 1.5 wt.% metallic impurities, the premelting zone was broad (~3.5 K), and the temperature obtained T_{fus} = 336.45 ± 0.2 K is not considered to be accurate.

[69OTT/GOA], [71GOA/OTT]

Ott, Goates *et al.* investigated potassium binary systems using a commercial material from MSA Research Corp. with 99.97+ % K, which was additionally distilled and contained <10 ppm Na. The melting point was determined by thermal analysis T_{fus} = 336.86 ± 0.1 K; the value appears to be high, but the technique used should be reliable judging by the results obtained by the same authors for other alkali metals.

The enthalpy of fusion was measured or estimated in [13REN], [14REN], [39CAR/STE], [52DOU/BAL], [63LEM/DEE], described in Sec. 4.2. Additional sources are given below.

[37BIN]

Binayendra determined the enthalpy of fusion calorimetrically 2.4 kJ·mol^{-1}, and assessed it from physical parameters as $\Delta_{fus}H$ = 1.89 kJ·mol^{-1}. No experimental details are given; it is difficult to estimate the accuracy of this study from the reported information.

[71MAL/GIG]

Malaspina *et al.* determined the enthalpy of fusion of K ('Fluka and Koch Light Lab', 99.9+ wt.% K) in a Calvet calorimeter. The calorimeter was slowly heated 0.6 − 1.1 K h^{-1} over the range 300 to 340 K. The average of six determinations was $\Delta_{fus}H$ = 2314 ± 21 J·mol^{-1}. Analyzing these and other data, the authors recommended $\Delta_{fus}H$ = 2343 ± 21 J·mol^{-1} which is higher than the measured value. This suggests that the uncertainty in the results should be greater, ± 40 J·mol^{-1}.

4.5. Discussion of Phase Equilibrium Data

The experimental temperatures of fusion listed in Table 4.3 were converted to ITS-90. The data are spread within more than 0.5 K, the quality of all studies is not uniformly high, and none of the experimental work can be used as a single source for recommendation. The rounded average of six studies [14REN], [27EDM/EGE], [39CAR/STE], [52DOU/BAL], [66STO], [69OTT/GOA], which are considered to be more reliable, was adopted as T_{fus} = 336.6 ± 0.2 K. This value is close to the recommendation of [85OHS/BAB], which is also an average of several studies listed in Table 4.3. The selected value differs from previous recommendations [73HUL], [82GUR], [85JAN] which are based on the results of a single study.

The experimental enthalpy of fusion is listed in Table 4.4. The adopted value $\Delta_{fus}H$ = 2335 J·mol^{-1} is based on [52DOU/BAL], the most accurate measurement among all considered. Studies [63LEM/DEE] and [71MAL/GIG] agree with this selection. The uncertainty is estimated as about ± 25 J·mol^{-1}. The selected value almost coincides with previous recommendations [73HUL], [82GUR] and [85JAN].

4.6. Adopted Values

Electronic contribution to C_p: γ = 0.00183 ± 0.00015 J·K^{-2}·mol^{-1}.
Debye temperature at 0 K: Θ_D = 90 ± 1 K.

Heat Capacity Equations
Solid K

Temperature range 0 − 2 K:
$C_p^\circ = 1.83\times10^{-3}T + 2.66\times10^{-3}T^3 + 5.1\times10^{-5}T^5$ J·K^{-1}·mol^{-1}.

Temperature range 2 − 20 K:
$C_p^\circ = 0.3143 - 0.2626T - 0.0196T^{-2} + 6.483\times10^{-2}T^2 - 1.4\times10^{-3}T^3$ J·K^{-1}·mol^{-1}.

Temperature range 20 − 70 K:
$C_p^\circ = -4.117 + 1.037T - 6.9464\times10^{2}T^{-2} - 1.414\times10^{-2}T^2 + 7.022\times10^{-5}T^3$ J·K^{-1}·mol^{-1}.

Temperature range 70 − 298.15 K:
$C_p^\circ = 21.798 + 0.0528T - 7.0633\times10^{3}T^{-2} - 2.1447\times10^{-4}T^2 + 4.184\times10^{7}T^3$ J·K^{-1}·mol^{-1}.

Temperature range 298.15 − 336.6 K:
$C_p^\circ = 82.924 - 394.997\times10^{-3}T + 724.957\times10^{-6}T^2$ J·K^{-1}·mol^{-1}.

Liquid K

Temperature range 336.6 − 1600 K
$C_p^\circ = 37.174 - 19.115\times10^{-3}T + 12.316\times10^{-6}T^2$ J·K^{-1}·mol^{-1}.

Values at 298.15 K

C_p°(298.15 K)= 29.49 ± 0.1 J·K^{-1}·mol^{-1};
S°(298.15 K)= 64.63 ± 0.2 J·K^{-1}·mol^{-1};
H°(298.15 K)−H°(0)= 7080 ± 20 J·mol^{-1}.

Phase Equilibrium Data

Temperature of fusion: T_{fus}= 336.6 ± 0.2 K.
Enthalpy of fusion: $\Delta_{fus}H$= 2335 ± 25 J·mol^{-1}.

4.7. Calculated Thermodynamic Functions of K

The thermodynamic functions presented in Tables 4.5 and 4.6 are calculated using the equations presented in the previous section. Values in brackets are calculated by using the equations for the next higher adjacent temperature intervals.

4.8. References for K

13REN E. Rengade, Compt. Rend. Acad. Sci. **156**, 1897–9 (1913); T_{fus}, $\Delta_{fus}H$, C_p (288–373 K).

14REN E. Rengade, Bull. Soc. Chim., France **76**, 130–47 (1914); T_{fus}, $\Delta_{fus}H$, C_p (288–373 K).

18EAS/ROD E. D. Eastman and W. H. Rodebush, J. Amer. Chem. Soc. **40**, 489–500 (1918); C_p (69–286 K).

26SIM/ZEI F. Simon and W. Zeidler, Z. Physik. Chem. **123**, 383–405 (1926); C_p (15–277 K).

27DIX/ROD A. L. Dixon and W. H. Rodebush, J. Am. Chem. Soc. **49**, 1162–74 (1927); C_p (363–454 K).

27EDM/EGE W. Edmondson and A. Egerton, Proc. Roy. Soc. **A113**, 520–533 (1927); T_{fus}.

35LOS L. Losana, Gazz. Chim. Ital. **65**, 851–64 (1935); T_{fus}.

37BIN N. S. Binayendra, Gazz. Chim. Ital. **67**, 714–5 (1937); $\Delta_{fus}H$.

39CAR/STE L. G. Carpenter and T. F. Steward, Phil. Mag. **27**, 551–64 (1939); T_{fus}, $\Delta_{fus}H$, C_p (203–610 K).

52DOU/BAL T. B. Douglas, A. F. Ball, D. C. Ginnings, and W. D. Davies, J. Amer. Chem. Soc. **74**, 2472–8 (1952); T_{fus}, $\Delta_{fus}H$, ΔH (298–1070 K).

55DAU/MAR T. M. Dauphinee, D. L. Martin, and H. Preston-Thomas, Proc. Roy. Soc., London **A233**, 214–27 (1955); C_p (30–330 K).

57KRI/CRA C. A. Krier, R. S. Craig, and W. E. Wallace, J. Phys. Chem. **61**, 522–9 (1957); C_p (12–320 K).

57ROB L. M. Roberts, Proc. Phys. Soc. **B70**, 744–52 (1957); C_p (1.5–20 K).

59NIK/KAL N. A. Nikol'skii, N. A. Kalakutskaya, I. M. Pchelkin, T. V. Klassen, and V. A. Vel'tischeva, "Problems of Heat Transfer," Akad. Nauk SSSR, 1–36 (1959); Translated and published as AEC-tr-4511 (1962); C_p (373–673 K).

60LIE/PHI W. H. Lien and N. E. Phillips, Phys. Rev. **118**, 958 (1960); C_p (0.17–1.1 K).

62ALA/PCH I. M. Pchelkin, (I. T. Aladyev, supervisor), Ph.D. Thesis, Moscow, ENIN (1962) (quoted from [70SHP/YAK] 78–79); C_p (373–1523 K).

63LEM/DEE A. W. Lemmon, Jr., H. W. Deem, E. A. Eldridge, E. H. Hall, J. Matolich, Jr., and J. F. Wallig, Battelle Memorial Institute, Report BATT-4673-Final (NASA CR-54017) 1–10 (1963); ΔH (273–1420 K).

64LIE/PHI W. H. Lien and N. E. Phillips, Phys. Rev. **A133**, 1370–7 (1964); C_p (0.26–4.1 K).

65EWI/STO C. T. Ewing, J. P. Stone, J. R. Span, E. W. Steinkuller, D. D. Williams, and R. R. Miller, U.S. Naval Res. Lab. Rpt. NRL-6233 (1965); C_p (1040, 1187, 1323 K).

65FIL/MAR J. D. Filby and D. L. Martin, Proc. Roy. Soc. (London) **A284**, 83–107 (1965); C_p (0.4–26 K).

66STO R. H. Stokes, J. Phys. Chem. Solids 27, 51–6 (1966); T_{fus}.

66TEP/ROE F. Tepper, and F. Roehlich, Air Force Materials, Lab. Rpt. AFML-TR-66-206 (1966) (quoted from [85FIN/LEI]); ΔH (532–1444 K).

69BAS/VOL A. S. Basin, S. P. Volchkova, and A. N. Soloviev, J. Appl. Mech. and Tech. Phys. **10**, 961–966 (1969); T_{fus}.

69OTT/GOA J. B. Ott, J. R. Goates, D. R. Anderson, and H. T. Hall, Trans. Faraday Soc. **65**, 2870–8 (1969); T_{fus}.

70SHP/KAG E. E. Spil'rain and D. N. Kagan, High Temp. **8**, 626–7 (1970); ΔH (519–1316 K).

70SHP/YAK E. E. Shpil'rain, K. A. Yakimovich, E. E. Totskyi, D. L. Timrot, and V. A. Fomin, "Thermophysical Properties. of Alkali Metals," Izd-vo Standartov, Moscow (1970); Review.

71GOA/OTT J. R. Goates, J. B. Ott, and E. Delawarde, Trans. Faraday Soc. **67**, 1612–6 (1971); T_{fus}.

71MAL/GIG L. Malaspina, R. Gigli, and V. Piacente, Gazz. Chim. Ital. **101**, 197–203 (1971); $\Delta_{fus}H$.

73HUL R. Hultgren, P. D. Desai, D. T. Hawkins, M. Gleiser, K. K. Kelley, and D. D. Wagman, "Selected Values of the Thermodynamic Properties of the Elements," Amer. Soc. Metals, Metals Park, OH, 263–9 (1973); Review.

81AMA/KEE C. D. Amarasekara and P. H. Keesom, Phys. Rev. Lett. **47** (18), 1311–3 (1981); C_p (0.5–5 K).

82GUR L. V. Gurvich, I. V. Veits, V. A. Medvedev, et al., V. P. Glushko, gen. ed., "Thermodynamic Properties of Individual Substances," Nauka, Moscow, **4** (1), 365–7 (1982); Review.

85FIN/LEI J. K. Fink and L. Leibowitz, "Handbook of Thermodynamic and Transport Properties of Alkali Metals," ed. R. W. Ohse, Blackwell Sci. Publ., Oxford, (1985) 411–434; liquid K, Review.

85JAN M. W. Chase, Jr., C. A. Davis, J. R. Downey, Jr., D. J. Frurip, R. A. McDonald, and A. N. Syverud, "JANAF Thermochemical Tables," J. Phys. Chem. Ref. Data 14, Supplement No. **1**, 1402–5 (1985); Review.

85OHS/BAB R. W. Ohse, J.-F. Babelot, J. Magill, and M. Tetenbaum, Pure Appl. Chem. **57**, 1407–26 (1985); Review of T_{fus}.

89COX/WAG J. D. Cox, D. D. Wagman, and V. A. Medvedev, "CODATA Key Values for Thermodynamics," Hemisphere Publ. Corp., New York, 257 (1989); Review.

4.9. Appendix – Experimental Results of K

Tables 4.7 to 4.29 present heat capacity or enthalpy data as they were presented in the original article. As a result, the numerical values listed in this Appendix are the actual exper-

imental values, tabular smoothed values, values calculated from equations, or values extracted from a graph. Where necessary, values are converted to joules (from calories). In all cases, the table heading indicates the type of data listed.

The enthalpy data for K are given mostly as $\Delta H = H°(T) - H°(T_{ref})$, where T_{ref} is usually equal to 273 or 298 K. When temperature $T > T_{fus}$, then the values of ΔH include the enthalpies of fusion (Tables 4.12, 21, 26, 27). The correction $H°(298.15\ K) - H°(273\ K)$ was estimated as 731 $J \cdot mol^{-1}$.

TABLE 4.1. Electronic contribution to the heat capacity and the Debye Temperature of K

Reference	γ,mJ·K^{-2}·mol^{-1}	Θ_D, K	Temp.range, K
Original studies			
26SIM/ZEI	—	99.5	> 15
57ROB	1.97	89	1.5– 2.5
60LIE/PHI	2.20	89.9	0.17– 1.1
64LIE/PHI	2.08	91.1	0.1– 1.2
65FIL/MAR	2.05	90.3	0.4– 1.5
81AMA/KEE	1.83	90.1	0.5– 5.0
Review			
73HUL	2.14 ± 0.2	Based on 60LIE/PHI, 64LIE/PHI, 65FIL/MAR	
Adopted			
	1.83 ± 0.15	90 ± 1	Based on 81AMA/KEE

TABLE 4.2. Comparison of the heat capacity, enthalpy and entropy values for K at 298.15 K

Reference	$C_p°$(298.15 K), J·K^{-1}·mol^{-1}	$S°$(298.15 K), J·K^{-1}·mol^{-1}	$H°$(298.15K)-$H°$(0), J·mol^{-1}
73HUL	29.547	64.68± 0.2	7084
82GUR	29.600	64.68± 0.2	7088± 20
85JAN	29.497	64.67	7082
89COX/WAG	29.600	64.68± 0.2	7088± 20
Adopted	29.49 ± 0.1	64.63± 0.2	7080± 20

TABLE 4.3. Temperature of fusion of K

Reference	T_{fus},K	Comments
Original studies		
13REN, 14REN	336.62± 0.05	Enthalpy measurements
27EDM/EGE	336.77± 0.05	Thermal analysis
39CAR/STE	336.53	Calorimeter
35LOS	335.22± 0.1	Thermal analysis
52DOU/BAL	336.32± 0.1	Enthalpy measurements
66STO	336.63± 0.02	Thermal analysis
69BAS/VOL	336.43± 0.2	Density measurements
69OTT/GOA	336.84± 0.1	Thermal analysis
Reviews		
73HUL	336.35± 0.5	Based on 52DOU/BAL
82GUR	336.86± 0.02	Based on 69OTT/GOA
85JAN	336.35	Based on 52DOU/BAL
85OHS/BAB	336.55± 0.2	Based on several studies
89COX/WAG	336.86	The same as 82GUR
Adopted		
	336.60± 0.2	Based on six studies

TABLE 4.4. Enthalpy of fusion of K

Reference	$\Delta_{fus}H$, J·mol^{-1}	Comments
Original studies		
13REN, 14REN	2393	Enthalpy measurements
39CAR/STE	2377	Calorimeter, estimate
37BIN	2400(1890)	Calorimeter (estimate)
52DOU/BAL	2334	Enthalpy measurements
63LEM/DEE	2338	Enthalpy measurements
71MAL/GIG	2314± 40	Calvet calorimeter
Reviews		
73HUL	2335± 80	Based on 52DOU/BAL
82GUR	2321± 20	Based on 52DOU/BAL
85JAN	2334	Based on 52DOU/BAL
89COX/WAG	2321± 20	The same as 82GUR
Adopted		
	2335± 25	Based on 52DOU/BAL

TABLE 4.5. Thermodynamic functions of K below 298.15 K

T/K	C_p° J·K^{-1}·mol^{-1}	$H°(T)-H°(0)$ J·mol^{-1}	$S°(T)$ J·K^{-1}·mol^{-1}
5	0.4463	0.510	0.1356
10	2.7711	7.860	1.0630
15	6.2370	30.123	2.8209
20	9.794 (9.792)	70.382	5.1126
25	12.956	127.622	7.6541
30	15.391	198.741	10.241
35	17.300	280.661	12.762
40	18.799	371.061	15.174
45	19.970	468.105	17.459
50	20.883	570.332	19.612
60	22.174	786.077	23.542
70	23.131 (23.145)	1012.69	27.034
80	23.760	1247.35	30.166
90	24.246	1487.47	32.994
100	24.645	1731.98	35.570
110	24.984	1980.17	37.935
120	25.278	2231.51	40.122
130	25.539	2485.62	42.156
140	25.774	2742.21	44.057
150	25.991	3001.04	45.843
160	26.193	3261.97	47.527
170	26.387	3524.88	49.120
180	26.575	3789.69	50.634
190	26.762	4056.38	52.076
200	26.950	4324.93	53.453
210	27.143	4595.39	54.773
220	27.343	4867.81	56.040
230	27.554	5142.28	57.260
240	27.778	5418.93	58.438
250	28.018	5697.89	59.576
260	28.277	5979.35	60.680
270	28.558	6263.51	61.753
280	28.862	6550.59	62.797
290	29.193	6840.84	63.815
298.15	29.485 (29.600)	7079.94	64.628

TABLE 4.6. Thermodynamic functions of K above 298.15 K

T/K	C_p° $J \cdot K^{-1} \cdot mol^{-1}$	$H^\circ(T)$-H° (298.15 K) $J \cdot mol^{-1}$	$S^\circ(T)$ $J \cdot K^{-1} \cdot mol^{-1}$
298.15	29,600	0.00	64.630
300.00	29.671	54.83	64.813
336.60 (sol)	32.105	1179.41	68.348
36.60 (liq)	32.135	3514.41	75.285
400.00	31.499	5531.08	80.776
500.00	30.696	8638.73	87.714
600.00	30.139	11678.39	93.257
700.00	29.828	14674.69	97.877
800.00	29.764	17652.27	101.853
900.00	29.946	20635.75	105.367
1000.00	30.375	23649.77	108.542
1100.00	31.050	26718.96	111.466
1200.00	31.971	29867.95	114.206
1300.00	33.139	33121.38	116.809
1400.00	34.552	36503.87	119.315
1500.00	36.213	40040.06	121.755
1600.00	38.119	43754.58	124.151

TABLE 4.7. SMOOTHED heat capacity of K [14REN]

T/K	C_p°, $J \cdot K^{-1} \cdot mol^{-1}$	T/K	C_p°, $J \cdot K^{-1} \cdot mol^{-1}$
290	29.09	336.6 (liq)	30.18
300	29.57	340	30.55
310	30.05	350	31.65
320	30.53	360	32.74
330	31.00	370	33.83
336.6 (sol)	31.32		

TABLE 4.8. EXPERIMENTAL heat capacity of K [18EAS/ROD]

T/K	C_p°, $J \cdot K^{-1} \cdot mol^{-1}$	T/K	C_p°, $J \cdot K^{-1} \cdot mol^{-1}$
68.6	24.10	116.7	25.94
72.3	24.02	119.3	26.07
76.0	24.18	152.2	26.78
79.8	24.52	199.5	27.95
87.0	24.94	203.5	28.12
94.1	25.44	285.1	29.50
101.8	25.36	286.7	29.71

TABLE 4.9. EXPERIMENTAL heat capacity of K [26SIM/ZEI]

T/K	C_p°, $J^{-1} \cdot mol^{-1}$	T/K	C_p°, $J \cdot K^{-1} \cdot mol^{-1}$
14.71	5.15	71.8	23.01
17.30	7.49	92.5	24.43
19.00	8.54	98.3	24.52
22.83	11.25	140.4	25.82
24.21	12.13	201.1	27.13
31.05	15.69	207.8	27.20
36.0	17.49	214.5	27.20
41.2	19.04	220.0	28.03
47.2	20.50	225.5	27.57
54.0	21.76	232.1	27.80
64.1	22.51	276.5	28.87

TABLE 4.10. EXPERIMENTAL heat capacity of K [27DIX/ROD]

T/K	C_p°, J·K^{-1}·mol^{-1}	T/K	C_p°, J·K^{-1}·mol^{-1}
363	32.64	454	32.17
409	32.13		

TABLE 4.11. EXPERIMENTAL AVERAGED heat capacity of K [39CAR/STE]

T/K	C_p°, J·K^{-1}·mol^{-1}	T/K	C_p°, J·K^{-1}·mol^{-1}
	Solid K		
204 (2 pts)	27.82	325 (8 pts)	32.65
276 (2 pts)	29.56	330 (5 pts)	33.47
288 (2 pts)	30.20	332 (9 pts)	33.05
305 (6 pts)	31.25	335 (6 pts)	33.51
315 (8 pts)	31.92		
	Liquid K		
338 (8 pts)	33.68	455 (2 pts)	32.97
355 (2 pts)	33.76	477 (2 pts)	32.68
377 (2 pts)	33.39	501 (2 pts)	33.01
397 (2 pts)	33.23	525 (2 pts)	32.13
418 (2 pts)	33.10	576 (3 pts)	32.55
437 (2 pts)	32.84	608 (2 pts)	33.72

TABLE 4.12. EXPERIMENTAL enthalpy values [H°(T)-H°(273 K)] of K [52DOU/BAL]

T/K	ΔH, J·mol^{-1}	T/K	ΔH, J·mol^{-1}
298.6	760	423	7002
304	890	473	8564
311	1112	573	11610
318	1335	673	14620
325	1553	773	17600
332	1776	873	20570
338	4308	973	23570
373	5419	1070	26540

TABLE 4.13. SMOOTHED heat capacity of K [52DOU/BAL]

T/K	C_p°, J·K^{-1}·mol^{-1}	T/K	C_p°, J·K^{-1}·mol^{-1}
273	27.78	673	29.88
298	29.80	773	29.75
323	31.80	873	29.86
348	32.00	973	30.22
373	31.75	1073	30.82
473	30.88		
573	30.26		

TABLE 4.14. SMOOTHED heat capacity of K [55DAU/MAR]

T/K	C_p°, $J \cdot K^{-1} \cdot mol^{-1}$	T/K	C_p°, $J \cdot K^{-1} \cdot mol^{-1}$
30	15.5	180	26.7
35	17.4	190	26.9
40	18.9	200	27.0
45	20.0	210	27.2
50	20.8	220	27.4
55	21.6	230	27.6
60	22.2	240	27.8
70	23.1	250	28.0
80	23.8	260	28.3
90	24.4	270	28.5
100	24.6	280	28.9
110	24.9	290	29.2
120	25.2	298.15	29.6
130	25.4	300	29.7
140	25.8	310	30.2
150	26.0	320	30.8
160	26.3	330	31.7
170	26.5		

TABLE 4.15. EXPERIMENTAL heat capacity of K [57KRI/CRA]

T/K	C_p°, J·K^{-1}·mol^{-1}	T/K	C_p°, J·K^{-1}·mol^{-1}
		Series I	
295.09	29.48	311.50	30.15
300.32	29.69	317.61	30.60
305.68	29.97		
		Series II	
279.94	28.86	306.08	29.93
284.92	29.00	311.69	30.20
290.08	29.19	317.33	30.52
295.34	29.44	322.80	30.98
300.63	29.58		
		Series III	
202.17	27.01	248.00	27.95
206.63	27.10	253.48	28.10
211.31	27.20	258.92	28.23
216.26	27.29	264.37	28.35
221.34	27.38	269.82	28.53
226.44	27.46	275.37	28.68
234.69	27.64	281.02	28.84
237.10	27.72	286.62	29.09
242.54	27.87		
		Series IV	
205.79	27.07	247.30	27.97
210.48	27.18	252.85	28.09
215.42	27.28	258.36	28.22
220.52	27.35	263.85	28.35
225.65	27.48	269.31	28.52
230.91	27.59	274.87	28.69
236.34	27.72	280.54	28.92
241.80	27.84	286.21	28.94
		Series V	
103.73	24.76	152.12	26.09
109.03	24.96	157.46	26.22
114.43	25.10	162.88	26.32
119.82	25.25	168.36	26.39
125.10	25.39	173.85	26.47
130.43	25.52	179.36	26.58
135.80	25.66	184.82	26.68
141.23	25.79	190.42	26.77
146.71	25.92	196.14	26.87
		Series VI	
11.12	3.389	106.35	24.85
12.62	4.611	112.46	25.05
14.64	6.050	118.43	25.20
16.99	7.745	124.27	25.37
19.51	9.456	129.99	25.52
22.16	11.23	135.81	25.66
25.03	12.94	141.74	25.80
28.10	14.53	147.57	25.96
31.36	15.97	153.52	26.07
34.76	17.28	159.61	26.18
38.29	18.34	165.63	26.32
41.98	19.31	171.77	26.43
45.82	20.08	178.02	26.70
49.80	20.83	184.20	26.65
54.14	21.48	190.37	26.77
59.06	22.08	196.38	26.87
64.32	22.66	202.20	27.00
69.67	23.06	207.39	27.10
75.32	23.45	212.07	27.19
81.26	23.86	217.01	27.28
87.32	24.20	222.09	27.41
93.62	24.42	227.15	27.48
100.05	24.64		

TABLE 4.16. SMOOTHED heat capacity of K [57KRI/CRA]

T/K	C_p°, J·K^{-1}·mol^{-1}	T/K	C_p°, J·K^{-1}·mol^{-1}
12	4.15	110	24.97
14	5.59	120	25.26
15	6.31	130	25.52
16	7.02	140	25.76
18	8.43	150	26.00
20	9.81	160	26.20
22	11.13	170	26.40
24	12.35	180	26.58
25	12.92	190	26.76
26	13.46	200	26.95
28	14.49	210	27.15
30	15.40	220	27.35
35	17.36	230	27.57
40	18.80	240	27.80
45	19.94	250	28.02
50	20.87	260	28.26
55	21.60	270	28.53
60	22.20	280	28.84
65	22.71	290	29.19
70	23.12	298.15	29.50
75	23.48	300	29.59
80	23.79	305	29.82
85	24.05	310	30.07
90	24.28	315	30.38
95	24.46	320	30.74
100		24.64	

TABLE 4.17. SMOOTHED heat capacity of K [57ROB]

T/K	C_p°, J·K^{-1}·mol^{-1}	T/K	C_p°, J·K^{-1}·mol^{-1}
1.5	0.0127	8	1.628
2.0	0.0264	9	2.176
2.5	0.0502	10	2.7616
3.0	0.0866	12	4.142
3.5	0.141	14	5.523
4.0	0.215	16	6.903
5.0	0.431	18	8.368
6.0	0.749	20	9.874
7.0	1.154		

TABLE 4.18. SMOOTHED heat capacity of K [59NIK/KAL]

T/K	C_p°, J·K^{-1}·mol^{-1}	T/K	C_p°, J·K^{-1}·mol^{-1}
373	31.90	573	30.26
423	31.41	623	30.10
473	30.92	673	29.94
523	30.59		

TABLE 4.19. SMOOTHED heat capacity of K [60LIE/PHI]

T/K	C_p°, mJ·K^{-1}·mol^{-1}	T/K	C_p°, mJ·K^{-1}·mol^{-1}
0.2	0.5	0.8	3.1
0.4	1.1	1.0	4.9
0.6	1.9	1.2	7.3

TABLE 4.20. SMOOTHED heat capacity of K [62ALA/PCH]

T/K	C_p°, J·K^{-1}·mol^{-1}	T/K	C_p°, J·K^{-1}·mol^{-1}
373	31.89	1073	29.60
473	31.23	1173	29.76
573	30.58	1273	30.25
673	30.09	1373	30.91
773	29.76	1473	31.72
873	29.60	1573	32.54
973	29.43		

TABLE 4.21. EXPERIMENTAL enthalpy values [H°(T)-H°(298 K)] of K [63LEM/DEE]

T/K	ΔH, J·mol^{-1}	T/K	ΔH, J·mol^{-1}
340	3340	1110	26900
370	4290	1150	28110
550	10120	1200	30240
590	11070	1200	30360
740	15470	1240	31660
890	19880	1300	34530
980	22500	1375	37130
1060	25120	1420	37850

TABLE 4.22. SMOOTHED heat capacity of K [63LEM/DEE]

T/K	C_p°, J·K^{-1}·mol^{-1}	T/K	C_p°, J·K^{-1}·mol^{-1}
273	27.88	773	30.07
298	29.60	873	30.61
323	31.31	973	31.53
348	31.79	1073	32.77
373	31.51	1173	34.39
473	30.61	1273	36.35
573	30.09	1373	38.69
673	29.91	1423	40.00

TABLE 4.23. EXPERIMENTAL heat capacity of K [64LIE/PHI]

T/K	C_p°, mJ·K^{-1}·mol^{-1}	T/K	C_p°, mJ·K^{-1}·mol^{-1}
	Adiabatic demagnetization thermostat		
0.2604	0.5852	0.5944	1.786
0.2781	0.6306	0.6414	2.027
0.2953	0.6786	0.6901	2.303
0.2501	0.5592	0.4805	1.292
0.2698	0.6066	0.5259	1.471
0.2894	0.6657	0.5661	1.659
0.3067	0.7104	0.6122	1.882
0.3270	0.7687	0.6614	2.143
0.3478	0.8362	0.7155	2.458
0.3734	0.9180	0.7697	2.798
0.3994	1.003	0.8296	3.242
0.4274	1.102	0.8922	3.765
0.4578	1.208	0.7236	2.511
0.2650	0.5969	0.7785	2.877
0.2885	0.6578	0.8332	3.310
0.3379	0.7962	0.8902	3.757
0.3644	0.8858	0.8710	3.617
0.3935	0.9732	0.9334	4.083
0.4231	1.021	1.013	4.899
0.4515	1.177	1.101	5.884
0.4835	1.302	1.180	6.874
0.4969	1.353	1.218	7.390
0.5435	1.551	1.238	7.696
	Liquid-helium thermostat		
1.1606	6.519	1.2033	7.115
1.2392	7.585	1.2834	8.269
1.3243	8.898	1.3918	10.07
1.4162	10.49	1.4897	11.97
1.5274	12.75	1.5884	14.12
1.6458	15.50	1.6968	16.80
1.7582	18.40	1.8162	20.15
1.8741	21.90	1.9358	24.00
1.9978	26.14	2.0585	28.47
2.1300	31.36	2.1932	34.11
2.2725	37.81	2.3415	41.30
2.4205	45.44	2.5007	50.26
2.5738	54.67	2.6600	60.48
2.7357	65.88	2.8279	73.27
2.9140	79.98	3.0084	88.62
3.1103	98.09	3.2078	108.6
3.3140	119.9	3.4143	132.1
3.5308	146.4	3.6325	160.6
3.7669	179.5	3.8819	198.1
4.0309	223.1	4.1012	236.2

TABLE 4.24. EXPERIMENTAL heat capacity of K [65EWI/STO]

T/K	C_p°, J·K^{-1}·mol^{-1}	T/K	C_p°, J·K^{-1}·mol^{-1}
1044	30.75	1329	33.37
1187	30.92		

TABLE 4.25. SMOOTHED heat capacity of K [65FIL/MAR]

T/K	C_p°, J·K^{-1}·mol^{-1}	T/K	C_p°, J·K^{-1}·mol^{-1}
	Temperature range 0.4– 1.5 K		
0.4	0.00109	1.0	0.00464
0.5	0.00144	1.1	0.00569
0.6	0.00188	1.2	0.00695
0.7	0.00240	1.3	0.00845
0.8	0.00303	1.4	0.01004
0.9	0.00378	1.5	0.01226
	Temperature range 3– 26 K		
3	0.088	12	4.10
4	0.213	14	5.51
5	0.44	16	6.98
6	0.76	18	8.43
7	1.16	20	9.83
8	1.64	22	11.12
9	2.19	24	12.36
10		2.79	26 13
.48			

TABLE 4.26. EXPERIMENTAL enthalpy values [$H°$(T)-$H°$(298 K)] of K [66TEP/ROE]

T/K	ΔH, J·mol^{-1}	T/K	ΔH, J·mol^{-1}
530	9760	940	22850
540	10240	990	24400
590	11780	1100	28580
610	11900	1130	30480
610	12130	1140	30710
660	13820	1180	30710
700	15360	1220	32860
760	15710	1270	35480
765	16420	1290	36540
790	18460	1320	36900
870	20240	1340	37780
920	21660	1380	39760
950	22720	1445	41900

TABLE 4.27. EXPERIMENTAL enthalpy values [$H°$(T)-$H°$(273 K)] of K [70SHP/KAG]

T/K	ΔH, J·mol^{-1}	T/K	ΔH, J·mol^{-1}
411.4	6966	914.6	21670
414.4	6732	1009.8	24720
519.3	9996	1061.6	26290
519.9	10010	1141.3	28500
551.5	10600	1313.7	35670
833.6	19230	1316.4	35560
834.4	19160		

TABLE 4.28. SMOOTHED heat capacity of K [70SHP/KAG]

T/K	C_p°, $J \cdot K^{-1} \cdot mol^{-1}$	T/K	C_p°, $J \cdot K^{-1} \cdot mol^{-1}$
400	32.99	900	29.72
500	30.77	1000	31.40
600	29.34	1100	33.87
700	28.69	1200	37.12
800	28.81	1300	41.14

TABLE 4.29. SMOOTHED heat capacity of K [81AMA/KEE]

T/K	C_p°, $mJ \cdot K^{-1} \cdot mol^{-1}$	T/K	C_p°, $mJ \cdot K^{-1} \cdot mol^{-1}$
0.5	1.24	3.0	88.9
1.0	4.51	3.5	146
1.5	12.0	4.0	228
2.0	26.3	4.5	342
2.5	50.7	5.0	497

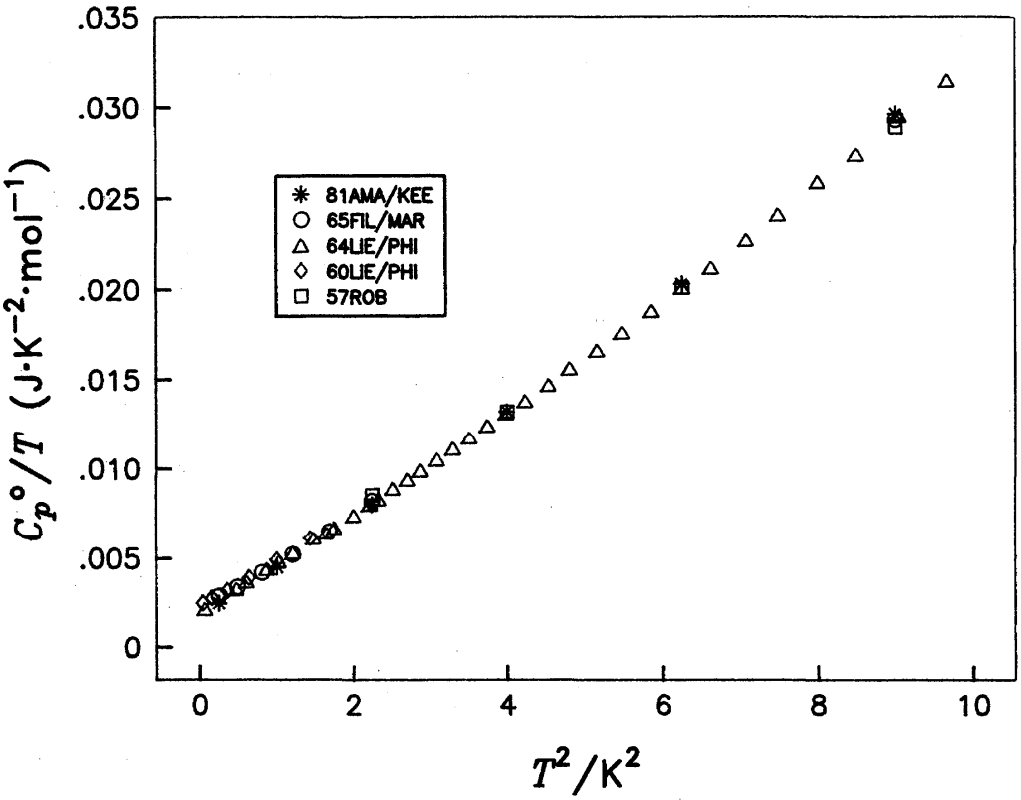

FIGURE 4.1. C_p/T versus T^2 for K below 3 K

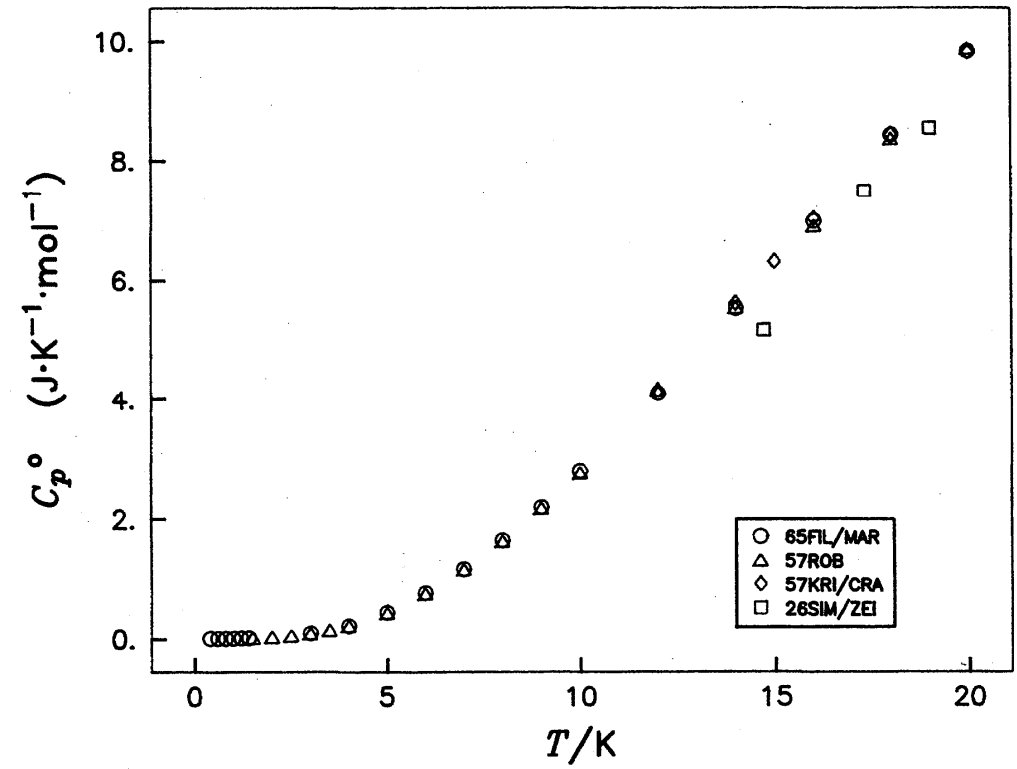

FIGURE 4.2. Heat Capacity of K below 20 K

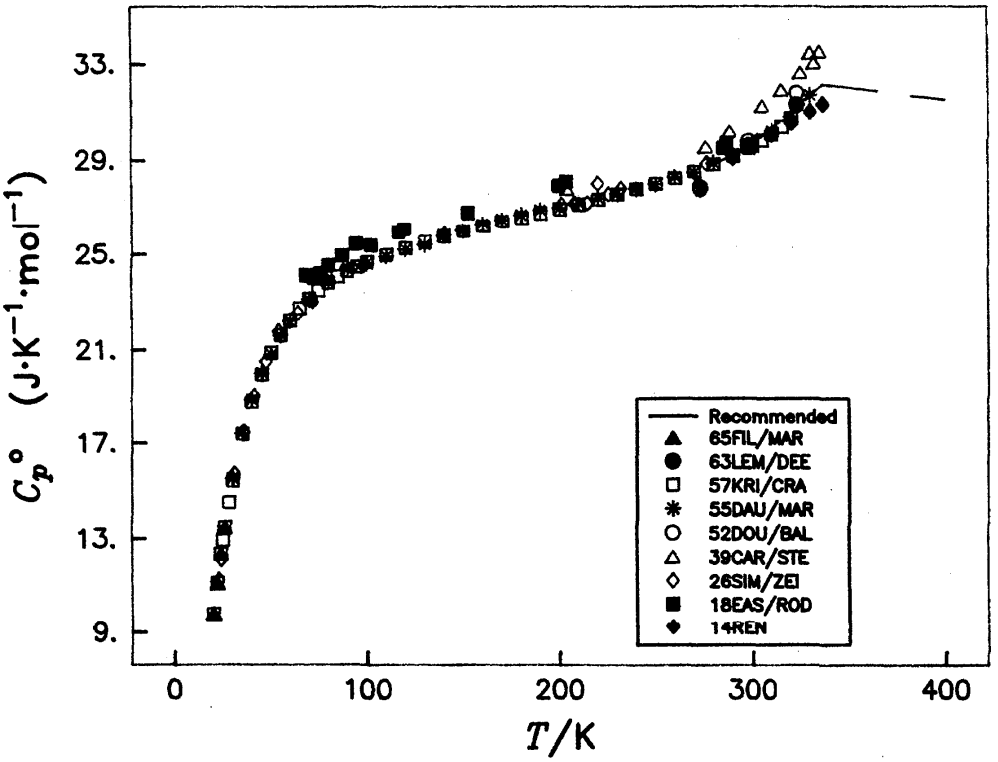

FIGURE 4.3. Heat Capacity of Solid K

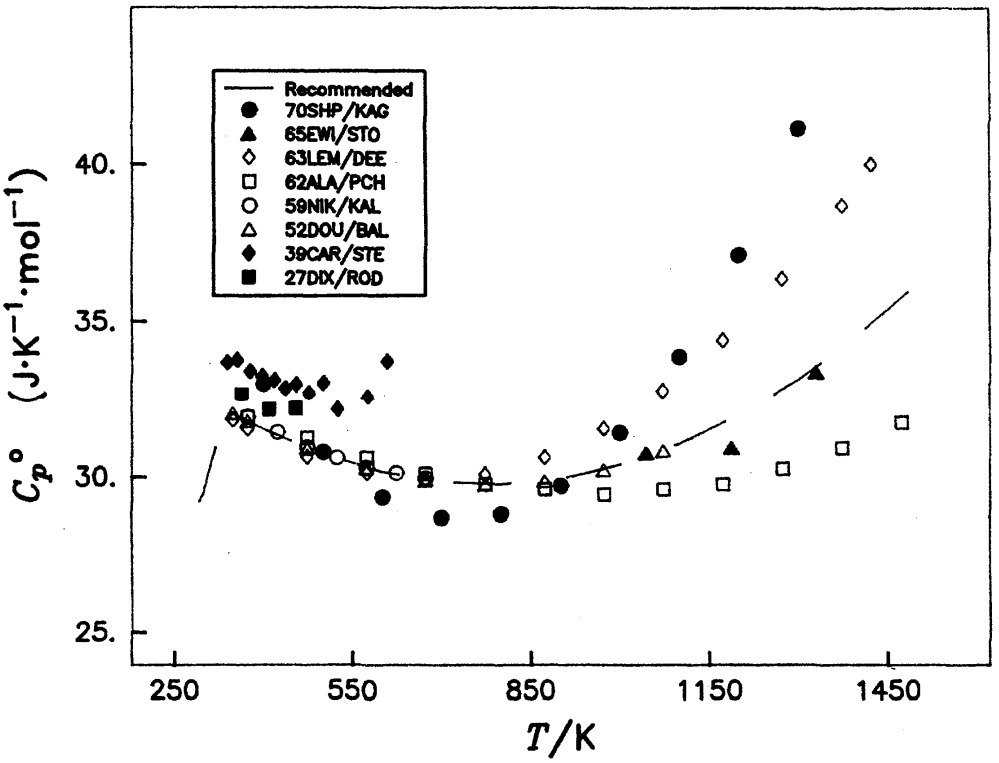

FIGURE 4.4. Heat Capacity of Liquid K

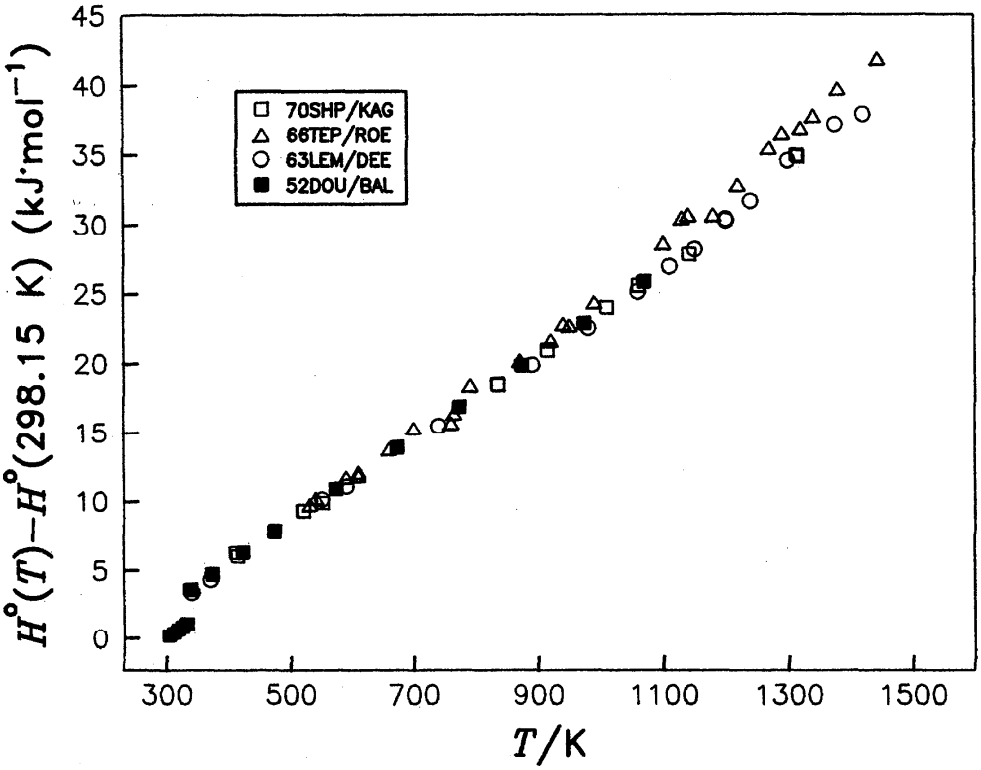

FIGURE 4.5. $H°(T)-H°(298.15\ K)$ of K

5. Rubidium

5.1. Introduction

At ambient pressure Rb has one crystalline modification (Table 1.1). The thermodynamic properties of solid Rb are fairly well established. However, the properties of liquid Rb are known poorly; the discrepancy between the heat capacity values measured in different studies requires further investigation.

5.2. Heat Capacity and Enthalpy Measurements

5.2.1. Temperature below 298.15 K

[55DAU/MAR]

Dauphinee *et al.* measured the heat capacity of Rb from 25 to 300 K in an adiabatic calorimeter. The sample (A.D. MacKay, New York) contained about 0.4% unsoluble impurities. Some irregularities were observed in the region 130 – 210 K. Later [65FIL/MAR] explained these anomalous effects in the experiment of [55DAU/MAR] in terms of the effects of strain on a copper thermometer which was used. The data are provided in the form of smoothed curves, and the 34 points taken from the graph were tabulated, reproduced in Table 5.8, and shown in Fig. 5.2 and 5.3. The authors also determined the approximate enthalpy of fusion $\Delta_{fus}H = 2260$ J·mol^{-1} and the melting point $T_{fus} = 311.90 \pm 0.5$ K.

[59MAN]

Manchester measured the heat capacity of Rb (A.D. MacKay, New York) from 1.2 to 4.2 K. The quality of the material was characterized by the ratio $\rho_{300K}/\rho_{4.2K} = 34$; Cs was mentioned as a main impurity. The percentage of impurities was not given, but it should be high, judging by the low magnitude of the resistivity ratio. The results (46 points) are presented in a graphical form. From this graph the smoothed values for heat capacity at six temperatures were taken and are reproduced in Table 5.9 and Fig. 5.1. Manchester determined the Debye temperature at 0 K as $\Theta_D = 52.6$ K.

[62MCC/SIL]

McCollum and Silsbee measured the heat capacity of Rb (A.D. Mackay, New York, no analysis was provided) in the temperature range 1.3 – 12 K in a Nernst calorimeter; for the temperature ranges below and above 4 K, two different calorimeters were used. The results (75 points) are given in a small-scale graph of the Debye temperature vs temperature. In calculations of the Debye temperature, the authors used $\beta = 2.45$ mJ·K^{-2}·mol^{-1} derived from a private communication of N.E. Phillips; a close value was reported in [64LIE/PHI]; see next paragraph. The graph Θ_D vs T has a complex shape with a minimum $\Theta_D = 50$ K at 3.3 K and a maximum $\Theta_D = 56$ K at about 9 K. The heat capacities estimated from the graph are given in Table 5.12 and Fig. 5.1 and 5.2. The data above 8 K are not accurate.

[64LIE/PHI]

Lien and Phillips measured the heat capacity of Rb from 0.2 to 1.2 K in an adiabatic demagnetization cryostat and from 1.2 to 4.0 K in a liquid-helium temperature cryostat. The purity claimed by the manufacturer was 99.8% Rb, but the analysis made by Lien and Phillips after completion of the experiment showed 3% K and 0.1% Cs in the specimen. The results (98 points) are reproduced in Table 5.16; some of the points are also shown in Fig. 5.1. The measurements at 0.2 – 0.9 K were fitted to a two-term equation which corresponds to $\Theta_D = 55.5 \pm 0.6$ K and $\gamma = 2.41 \pm 0.04$ mJ·K^{-2}·mol^{-1}. The data measured between 0.9 and 2.5 K were described by a three-term equation

$$C_p^\circ = (2.41 \pm 0.04)T + (11.4 \pm 0.1)T^3 + (0.636 \pm 0.05)T^5, \text{ mJ·K}^{-1}\text{·mol}^{-1}.$$

[64MAR/ZYC]

Martin *et al.* measured the heat capacity from 0.35 to 2 K in a Nernst calorimeter. A commercial material containing 99.9% Rb, 0.071% Cs, 0.068% K, <0.001% Li and Na was used. The results are given in a small-scale graph (95 points) of the heat capacity of sample plus container. The heat capacity of the container was estimated and subtracted from the measured values. The heat capacities for the Cs specimens were fitted to the equation

$$C_p^\circ = 4.075T + 9.599T^3 + 0.765T^5 + 0.0714T^7, \text{ mJ·K}^{-1}\text{·mol}^{-1}.$$

The above equation corresponds to $\gamma = 4.07$ mJ·K^{-2}·mol^{-1} and $\Theta_D = 58.7$ K; the heat capacity values calculated by this equation are given in Table 5.17 and shown in Fig. 5.1. The results have moderate accuracy.

[65FIL/MAR]

Filby and Martin measured the heat capacity of Rb in three devices: from 0.4 to 1.5 K a Nernst calorimeter with a helium-3 cryostat was used; the temperature range 3 – 26 K was covered with an adiabatic apparatus; the measurements from 20 to 320 K were made in an adiabatic calorimeter with continuous heating. A commercial material (Light, Colnbrook, England, 99.9% Rb) was analyzed spectrochemically, and found to contain Si and Sn 0.05 – 0.005% each; Fe, Si and Pb 0.01 – 0.001% each; Ca 0.005 – 0.0005%, Sr and Ba 0.001%; Mg and Ag 0.0005%; the analysis could not detect the presence of 0.1% Cs. From the depression of the melting point, the total amount of solid soluble impurities was estimated as 0.26 at.%. The level of impurities was also characterized by the ratio $\rho_{293K}/\rho_{4.2K} = 400$; this high ratio indicates that the total amount of impurities was probably underestimated by the authors. The data points are shown in two graphs from 0.4 and 1.5 K (80 points) and from 50 to 300 K (53 points). Smoothed values are listed in three tables for the ranges: from 0.4 to 1.5 K (12 points), from 3 to 26 K (16 points), and from 20 to 320 K (42 points); they are reproduced in Table 5.18 and shown in Fig. 5.1 to 5.4. The accuracy of the measurements was better than 1%. The data obtained below 0.7 K are not considered very accurate, and to determine the Debye temperature, the authors used a value $\beta = 2.41 \pm 0.3$ mJ·K^{-2}·mol^{-1} from [64LIE/PHI] and calculated $\Theta_D = 55.6 \pm 0.6$ K. A spontaneous heat evolution was observed between 3 and 26 K, although the effect was very

small. In the 100 − 200 K interval, the authors did not find the anomaly reported in [55DAU/MAR].

Filby and Martin estimated the temperature of fusion of Rb from partial melting over a range of temperatures; the experiment yielded a value of about 312.45 K. The authors assumed the presence of 0.26 atomic percent impurities and estimated T_{fus} = 312.65 ± 0.01 K. However, in more recent study [70MAR] Martin revised the impurity level suggested in [65FIL/MAR]. It was reassessed to be less than 0.01 atomic percent, and the temperature of fusion was reevaluated to be 312.485 K. The enthalpy of fusion was determined as $\Delta_{fus}H$ = 2194 ± 4 J·mol^{-1}.

[70MAR]

Martin improved the construction of the apparatus for heat capacity measurements between 0.4 and 3 K. A commercial material from Electronic Space Products, Los Angeles, had 99.9% Rb and about 100 ppm of metallic impurities. The samples were analyzed by the Analytical Chemistry Group of the National Research Council of Canada; they had 99.99% Rb; the resistivity ratio was $\rho_{293K}/\rho_{4.2K}$ = 310. The results of measurements were fitted to a five-term polynomial.

$$C_p^\circ = (2.613 \pm 0.013)T + (10.77 \pm 0.054)T^3 + (0.456 \pm 0.05)T^5 + (0.018 \pm 0.014)T^7 - (0.0035 \pm 0.001)T^9 \text{ mJ·K}^{-1}\text{·mol}^{-1}.$$

Several points calculated by this equation are listed in Table 5.21 and shown in Fig. 5.1. The equation corresponds to γ = 2.613 ± 0.027 mJ·K^{-2}·mol^{-1} and Θ_D = 56.5 ± 0.2 K. The melting point of Rb was measured as 312.46 K; this value was compared with the adjusted previous measurement [65FIL/MAR] 312.485 K, and the average of both studies T_{fus} = 312.47 ± 0.02 K has been recommended. The enthalpy of fusion had the same value as in [65FIL/MAR] $\Delta_{fus}H$ − 2194 ± 4 J·mol^{-1}.

5.2.2. Temperature above 298.15 K

[13REN], [14REN]

Rengade measured the enthalpy in a Bunsen ice calorimeter from 288 to 373 K. The rubidium sample was prepared by the reduction of RbCl with Ca; it was then doubly distilled in vacuum at 673 K. The measurements (7 points for solid Rb and 5 points for liquid Rb) are shown in a graph in [14REN]. The heat capacity values were described by linear equations for solid Rb:

$$C_p^\circ = -0.70 + 0.1076T \text{ J·K}^{-1}\text{·mol}^{-1};$$

for liquid Rb below 373 K:

$$C_p^\circ = 35.47 - 0.0093T \text{ J·K}^{-1}\text{·mol}^{-1}.$$

The accuracy of the results which were obtained is considered to be low. The calculated values are shown in Table 5.7 and Fig. 5.3 and 5.4. The melting point was determined as T_{fus} = 312.15 ± 0.1 K, and the enthalpy of fusion as $\Delta_{fus}H$ = 2195 J·mol^{-1}.

[62ALA/PCH]

Aladyev and Pchelkin (quoted from [70SHP/YAK]) measured the heat capacity of liquid commercial Rb (impurities: 3.8% K, 0.49 Cs, 0.006% Na) in an isothermal calorimeter in the temperature range 327 to 1038 K. The original and smoothed values are listed in Table 5.10 and 5.11, respectively. The smoothed corrected values are shown in Fig. 5.4. The originial values have an uncertainty of about 8%.

[63TEP/MUR]

Tepper *et al.* measured the enthalpy of Rb in a drop calorimeter from 504 to 1268 K. A distilled rubidium sample was purified by a Zr getter and contained 0.37% Cs; 0.21% K; 0.003% Na; 50 ppm O; 2 ppm N and 28 ppm C. The values which were obtained are listed in Table 5.13 and shown in Fig. 5.5. The measured values were described by a two-term equation with a standard deviation of about 2%:

$$H^\circ(T,\text{l}) - H^\circ(298 \text{ K,cr}) = -6795 + 31.505T \text{ J·mol}^{-1}.$$

According to this equation, the heat capacity of liquid Rb remains constant at 31.505 J·K^{-1}·mol^{-1} in the temperature range 500 − 1250 K. Using literature data the authors estimated the enthalpy of fusion as 2573 J·mol^{-1}.

[64ACH]

Achener measured the enthalpy of liquid Rb (99.5%) in a Bunsen calorimeter in the temperature range 337 − 1172 K. The material was purified at 700 K in the presence of a getter, which was a mixture of Zr and Ti chips, and was filtered through a stainless steel screen. The material contained 0.4% Cs, about 100 ppm of other metallic impurities and 10 ppm of oxygen. After the experiment was completed, the oxygen level had increased to 100 ppm, while the metallic impurities had decreased to nondetectable quantities and the Cs level fell to 0.33%. Achener obtained 36 points of which one third were discarded as poor. The results of these experiments are given in Table 5.14 and shown in Fig. 5.5. The data were fitted to the equation

$$H^\circ(T,\text{l})\text{-}H^\circ(273 \text{ K,cr}) = -7999 + 41.543T - 1.384\times10^{-2}T^2 + 5.016\times10^{-6}T^3, \text{ J·mol}^{-1}.$$

The relative error was estimated as 1.3%. The heat capacity calculated from the above equation showed a minimum at 920 K (Table 5.15 and Fig. 5.4). Achener estimated the enthalpy of fusion of Rb $\Delta_{fus}H$ = 2655 J·mol^{-1}, using his data for liquid alloys and Rengade's equation for solid Rb [14REN].

[69SHP/KAG]

Shpil'rain and Kagan measured the enthalpy of liquid Rb from 405 to 1334 K in a boiling-point drop calorimeter. The sample was prepared in the Institute of Rare Metals, Moscow, by Ca-reduction of RbCl and by distillation. The material contained 0.013% Na, 1.6 % K, <0.15% Cs and <0.003% Ca. The measured values are given in Table 5.19 and in Fig. 5.5, and the derived heat capacity values are shown in Table 5.20 and Fig. 5.4. The scatter of these experimental points was about 150 J·mol^{-1}. A correction for the difference

$$H°(373\ K,l)\text{-}H°(273\ K,cr) = 5360\ J\cdot mol^{-1}$$

was taken from [65FIL/MAR], and the data were fitted to the equation:

$$H°(T,l)\text{-}H°(273\ K,cr) = -6831 + 34.26T - 4.626\times10^{-3}T^2 + 1.96\times10^{-6}T^3,\ J\cdot mol^{-1}.$$

[76NOV/ROS]

Novikov *et al.* measured the enthalpy of Rb 99.93% (sample from the Institute of Rare Metals, Moscow) in a drop ice calorimeter from 327 to 1234 K. Twenty-two experimental points, given in Table 5.22 and Fig. 5.5, were described by the equation:

$$H°(T,l)\text{-}H°(273\ K,cr) = -6417 + 32.75T - 4.681\times10^{-3}T^2 + 2.914\times10^{-6}T^3,\ J\cdot mol^{-1}.$$

The heat capacity values calculated using this equation are listed in Table 5.23 and shown in Fig. 5.4. The accuracy of the data of [76NOV/ROS] was about 5%.

5.3. Discussion of Heat Capacity and Enthalpy Data

5.3.1. Rb below 298.15 K

Measurements below 3 K. Below 3 K the heat capacity was measured in [59MAN], [62MCC/SIL], [64LIE/PHI], [64MAR/ZYC], [65FIL/MAR], [70MAR]; the results are shown in the C_p/T vs T^2 coordinates (Fig. 5.1). In several studies the data are available only in form of the fitted equations, and the calculated values are shown in Fig. 5.1. The coefficient of the electronic contribution to the heat capacity and the Debye temperature derived from the measurements are listed below.

The data of [64LIE/PHI] for 0.2 – 0.9 K and [70MAR] for 0.4 – 3.0 K are close and seem to be the most reliable. As [64LIE/PHI] found 3% K in their samples, the results of [70MAR] were considered to be more accurate and were adopted in this assessment. The equation of [70MAR] was selected for the description of the data below 3 K. For simplicity the number of coefficients was reduced to three by combining the last three terms of the original equation in one. The adjusted equation is given below.

$$C_p° = 2.61T + 10.77T^3 + 0.333T^5\ mJ\cdot K^{-1}\cdot mol^{-1}. \quad (1)$$

The error introduced by Eq. 1 and caused by decreasing a number of terms in [70MAR] did not exceed 1% in the calculated values.

Measurements between 3 and 20 K. The heat capacity measurements were made in [59MAN] (below 4.2 K), [62MCC/SIL] (3 – 12 K), [64LIE/PHI] (below 4.2 K), and [65FIL/MAR] (3 – 20 K). The data of [65FIL/MAR] covering this range are probably the most reliable (Fig. 5.2). They were fitted to the equation:

$$C_p° = -3.707 + 0.76283T + 13.2365T^{-2} + 0.04519T^2 - 1.69\times10^{-3}T^3,\ J\cdot K^{-1}\cdot mol^{-1}. \quad (2)$$

Measurements between 20 and 100 K. For this interval the measurements were made in two studies [55DAU/MAR] (above 25 K) and [65FIL/MAR] (Fig. 5.2 and 5.3). The data are in good agreement. The data of [65FIL/MAR] were selected because they were obtained more recently in the same laboratory.

$$C_p° = 19.0595 + 0.1827T - 2.3348\times10^{3}T^{-2} - 1.8694\times10^{-3}T^2 + 7.1185\times10^{-6}T^3,\ J\cdot K^{-1}\cdot mol^{-1}. \quad (3)$$

Measurements between 100 and 260 K. For this range the measurements were made in [55DAU/MAR] and [65FIL/MAR] (Fig. 5.3); the data agree. The anomaly reported in [55DAU/MAR] at 100 – 200 K has not been confirmed in [65FIL/MAR]; the more accurate data of [65FIL/MAR] were fitted to the equation:

$$C_p° = 12.717 + 0.1675T + 2.12\times10^{4}T^{-2} - 7.32\times10^{-4}T^2 + 1.2476\times10^{-6}T^3,\ J\cdot K^{-1}\cdot mol^{-1}. \quad (4)$$

Measurements between 260 and melting point. As for other temperature ranges, the data of [65FIL/MAR] were used for fitting to the equation:

$$C_p° = 282.819 - 1348.62\times10^{-3}T - 27.979\times10^{5}T^{-2} + 2044.9\times10^{-6}T^2,\ J\cdot K^{-1}\cdot mol^{-1}. \quad (5)$$

Eqs. 1–5 were used to calculate $C_p°(T)$, $H°(T)\text{-}H°(0)$ and $S°(T)$. The calculations are shown in Table 5.5. At the standard temperature the heat capacity, enthalpy and entropy were calculated as

$C_p°(298.15\ K)$	$= 31.031\ J\cdot K^{-1}\cdot mol^{-1}$;
$S°(298.15\ K)$	$= 76.741\ J\cdot K^{-1}\cdot mol^{-1}$;
$H°(298.15\ K) - H°(0)$	$= 7488.84\ J\cdot mol^{-1}$.

These values are compared in Table 5.2 with those recommended in other reviews. The rounded calculated values are close to the previous recommendations listed above. They are all based on the same best studies [65FIL/MAR] and [70MAR].

5.3.2. Solid Rb above 298.15 K

Above 298.15 K the heat capacity of solid Rb was measured in [13REN], [14REN], [55DAU/MAR] and [65FIL/MAR] (Fig. 5.3). The data of [65FIL/MAR] are considered to be reliable, and they are described by Eq. 5 quoted above.

[82GUR] derived a two-term equation from 298 K to the melting point:

$$C_p° = 3.53 + 92.337\times10^{-3}T\ J\cdot K^{-1}\cdot mol^{-1}.$$

The equation gives heat capacity values which are close to those calculated by Eq. 5 (within 0.2%). Reviews [73HUL] and [85JAN] listed almost the same heat capacities.

5.3.3. Liquid Rb

The enthalpy and heat capacity of liquid Rb were measured in [13REN], [14REN] (C_p, T<373 K), [65FIL/MAR] (C_p, T = 312.5 and 320 K), [63TEP/MUR] (ΔH, 504–1268 K), [62ALA/PCH] (C_p, 327–1038 K), [64ACH] (ΔH, 337–1172 K), [69SHP/KAG] (ΔH, 405–1334 K), [76NOV/ROS] (ΔH, 327–1234 K). The results are shown in Fig. 5.4 and 5.5; the C_p data are scattered broadly at high temperatures. For example, at 1200 K the difference between the heat capacity values, derived from the data of [64ACH] and [76NOV/ROS], is about 13% (Fig. 5.4). Two points measured in [65FIL/MAR] near the melting point, the smoothed data of [62ALA/PCH] at 400–700 K and data of [65SHP/KAG] at 400 – 1000 K, appear to be more reliable than others.

[73HUL] used values from [64ACH] without any adjustment. It is not reasonable to select a single study because all of these sources have low accuracy, exceeding 5%, and show poor agreement. Reviewers usually combine several studies to derive a common equation; such a procedure was used in [82GUR] and [85FIN/LEI]. [82GUR] combined studies [63TEP/MUR], [62ALA/PCH], [69SHP/KAG], [76NOV/ROS] and the three enthalpy values at 1400, 1600 and 1800 K, estimated from the data for K and Cs (Cs is not as well-known as Rb) and derived an equation:

$$C_p^\circ = 23.082 + 20.33\times10^{-3}T + 4.198\times10^{5}T^{-2} - 23.180\times10^{-6}T^{2} + 10.824\times10^{-9}T^{3},\ \mathrm{J\cdot K^{-1}\cdot mol^{-1}}.$$

This equation yields acceptable values above 700 K, but below this temperature the values appear to be underestimated.

The equation proposed in [85FIN/LEI] from the analysis of all data seems to be more appropriate:

$$C_p^\circ = 35.494 - 12.864\times10^{-3}T + 8.541\times10^{-6}T^{2},\ \mathrm{J\cdot K^{-1}\cdot mol^{-1}}. \quad (6)$$

The heat capacity values calculated by this equation are close to those of [69SHP/KAG], [62ALA/PCH] and are consistent with the values of [65FIL/MAR]. Eq. 6 was adopted here as a good approximation to the experimental results. The difference in the heat capacity values calculated using equation derived by [82GUR] and Eq. 6 does not exceed 3%; [85JAN] also used Eq. 6. It should be pointed out that there is need for accurate measurements on liquid Rb to resolve the present discrepancy between different investigators.

The values of C_p°s (T), $S^\circ(T)$ and $H^\circ(T)$-H°(298.15 K) below 1600 K were calculated using Eqs 5 and 6; they are listed in Table 5.6.

5.4. Phase Equilibrium Data

The temperature of fusion of rubidium was described in Sec. 5.2. in [13REN], [14REN], [55DAU/MAR], [65FIL/MAR], [70MAR]. Several more studies are discussed below.

[35LOS]

Losana used thermal analysis to determine the melting point of rubidium T_{fus} = 311.95 ± 0.1 K. The material was prepared by reduction of RbCl by Ca and purified by distillation; Li, K and Cs were not detected.

[63WEA]

Weatherford (quoted by [85OHS/BAB]) measured the melting point of Rb by thermal analysis T_{fus} = 312.54 K.

[69BAS/VOL]

Basin *et al.* measured the density of rubidium below and above the melting point. The material contained 99.93% Rb and 0.02% metallic impurities. The premelting zone was about 0.05 K, the melting point being determined as 312.31 ± 0.05 K, but the suggested accuracy was probably underestimated. The value which was obtained is smaller than those obtained in more recent investigations.

[71GOA/OTT]

Goates *et al.* investigated rubidium binary systems using a commercial material from Kawecki Chemical Company. According to the batch analysis the material had 99.8+ wt. percent Rb and contained metallic impurities in atomic percent: Cs – 0.034, K – 0.017, Na – 0.018, Si – 0.015. The melting point was determined by thermal analysis as T_{fus} = 312.45 ± 0.1 K.

[73SIM]

Simon investigated the Rb-O system by thermal and X-ray analysis. Rb was prepared by the reduction of RbCl with Ca, followed by double distillation in vacuum; the analysis of Rb was not given. The temperature of fusion was determined as 312.52 ± 0.01 K.

The enthalpy of fusion was measured or estimated in [13REN], [14REN], [55DAU/MAR], [65FIL/MAR], [70MAR], [63TEP/MUR], [64ACH], discussed in Sec. 5.2; two more studies are given below.

[37BIN]

Binayendra determined the enthalpy of fusion in a calorimeter, 2.18 $\mathrm{kJ\cdot mol^{-1}}$, for which no experimental details are given. The author derived $\Delta_{fus}H$ = 1.8 $\mathrm{kJ\cdot mol^{-1}}$ from physical parameters. It is difficult to assess the accuracy of this study from the reported information.

[71MAL/GIG]

Malaspina *et al.* determined the enthalpy of fusion of Rb in a Calvet calorimeter. The material was *Fluka and Koch Light Lab*, 99.9 wt.% Rb. Four measurements yielded the values 2238, 2243, 2167, and 2213 $\mathrm{J\cdot mol^{-1}}$, and the average was reported as $\Delta_{fus}H$ = 2218 ± 29 $\mathrm{J\cdot mol^{-1}}$. The authors of [71MAL/GIG] recommended the value $\Delta_{fus}H$ = 2222 ± 41 $\mathrm{J\cdot mol^{-1}}$, using the literature and their own data.

5.5. Discussion of Phase Equilibrium Data

The measured temperatures of fusion were converted to ITS-90 (Table 5.3). The most accurate and reliable results are 312.475 K [65FIL/MAR], corrected in [70MAR], 312.46 K [70MAR], and 312.44 K [71GOA/OTT]; their rounded average, T_{fus} = 312.45 K, is recommended. The uncertainty in the

amount of impurities in the specimens of [65FIL/MAR] and [70MAR] can result in a systematic error of about 0.05 K, and so the total uncertainty in the melting point of Rb was estimated as ± 0.1 K. Almost the same selection was made in [82GUR] who adopted the value 312.47 K from [70MAR]. The selections made in [73HUL], [85OHS/BAB] and [85JAN] are based on the value 312.65 K initially recommended in [65FIL/MAR]. This recommendation was later revised in [70MAR]. However, the revised value was not used in [85OHS/BAB] and [85JAN].

The adopted enthalpy of fusion 2190 $J \cdot mol^{-1}$ is based on the most accurate measurements of [65FIL/MAR] and [70MAR] (Table 5.4). The uncertainty was estimated as ± 25 $J \cdot mol^{-1}$. The selected value agrees, within the uncertainty limit, with the results of less accurate studies [13REN], [14REN] and [37BIN] and with [71MAL/GIG]. The adopted value almost coincides with all previous reviews.

5.6. Adopted Values

Electronic contribution to C_p: $\gamma = 2.61 \pm 0.05$ $mJ \cdot K^{-2} \cdot mol^{-1}$.
Debye temperature at 0 K: $\Theta_D = 56.5 \pm 1.0$ K.

Heat Capacity Equations

Solid Rb
Temperature range 0 − 3 K:
$C_p^\circ = 2.61\times10^{-3}T + 1.077\times10^{-2}T^3 + 3.33\times10^{-4}T^5$ $J \cdot K^{-1} \cdot mol^{-1}$.
Temperature range 3 − 20 K:
$C_p^\circ = -3.707 + 0.76283T + 13.2365T^{-2} + 4.519\times10^{-2}T^2 - 1.69\times10^{-3}T^3$ $J \cdot K^{-1} \cdot mol^{-1}$.
Temperature range 20 − 100 K:
$C_p^\circ = 19.0595 + 0.1827T - 2.3348\times10^{3}T^{-2} - 1.8694\times10^{-3}T^2 + 7.1185\times10^{-6}T^3$ $J \cdot K^{-1} \cdot mol^{-1}$.
Temperature range 100 − 260 K:
$C_p^\circ = 12.717 + 0.1675T + 2.12\times10^{4}T^{-2} - 7.32\times10^{-4}T^2 + 1.2476\times10^{-6}T^3$ $J \cdot K^{-1} \cdot mol^{-1}$.
Temperature range 260 − 312.45 K:
$C_p^\circ = 282.819 - 1348.62\times10^{-3}T - 27.979\times10^{5}T^{-2} + 2044.9\times10^{-6}T^2$ $J \cdot K^{-1} \cdot mol^{-1}$.

Liquid Rb
Temperature range 312.45 − 1600 K.
$C_p^\circ = 35.494 - 12.864\times10^{-3}T + 8.541\times10^{-6}T^2$ $J \cdot K^{-1} \cdot mol^{-1}$.

Values at 298.15 K

C_p°(298.15 K)	= 31.03 ± 0.1 $J \cdot K^{-1} \cdot mol^{-1}$;
S°(298.15 K)	= 76.74 ± 0.3 $J \cdot K^{-1} \cdot mol^{-1}$;
H°(298.15 K)-H°(0)	= 7489 ± 20 $J \cdot mol^{-1}$.

Phase Equilibrium Data

Temperature of fusion T_{fus}	= 312.45 ± 0.1 K.
Enthalpy of fusion $\Delta_{fus}H$	= 2190 ± 25 $J \cdot mol^{-1}$.

5.7. Calculated Thermodynamic Functions of Rb

The thermodynamics functions presented in Tables 5.5 and 5.6 are calculated using the equations presented in the previous section. Values in brackets are calculated by using the equations for the next higher adjacent temperature intervals.

5.8. References for Rb

13REN E. Rengade, Compt. Rend. **156**, 1897–9 (1913); T_{fus}, $\Delta_{fus}H$, C_p (288–373 K).

14REN E. Rengade, Bull. Soc. Chim. France **15**, 130–147 (1914); T_{fus}, $\Delta_{fus}H$, C_p (288–373 K).

35LOS L. Losana, Gazz. Chim. Ital. **65**, 851–864 (1935); T_{fus}.

37BIN N. S. Binayendra, Gazz. Chim. Ital. **67**, 714–5 (1937); $\Delta_{fus}H$.

55DAU/MAR T. M. Dauphinee, D. L. Martin, and H. Preston-Thomas, Proc. Roy. Soc. (London) **A233**, 214–22 (1955); T_{fus}, $\Delta_{fus}H$, C_p (25–300 K).

59MAN F. D. Manchester, Can. J. Phys. **37**, 525–7 (1959); C_p (1.2–4.2 K).

62ALA/PCH I. M. Pchelkin, Ph.D. Thesis, I. T. Aladyev, supervisor, ENIN, Moscow (1962) (quoted from [70SHP/YAK], 92–93); C_p (327–1038 K) .

62MCC/SIL D. C. McCollum, Jr. and H. B. Silsbee, Phys. Rev. **127**, 119–20 (1962); C_p (1.3–12 K).

63TEP/MUR F. Tepper, A. Murchison, J. Zelenak, and F. Roehlich, "Thermophysical Properties of Rubidium and Cesium," Air Force Materials Lab., Repts. RTD-TDR-63–133, RTD-TDR-63–4018, I, MSA Research Corp., Callery, PA, (1963); ΔH (504–1268 K).

63WEA W. A. Weatherford, Jr., R. K. Johnston, et al., Aeronautical Systems Division, Wright-Patterson Air Force Base, Report ASD-TR-63, 413 (1963); T_{fus}.

64ACH P. Y. Achener, "The Determination of the Latent Heat of Vaporization, Vapor Pressure, Enthalpy, Specific Heat, and Density of Liquid Rubidium and Cesium up to 1800 F," USAEC Rept. AGN-8090, Aerojet-General Nucleonic, (Jan. 1964); ΔH (337–1172 K).

64LIE/PHI W. H. Lien and N. E. Phillips, Phys. Rev. **A133**, 1370–7 (1964); C_p (0.19–4.1 K).

64MAR/ZYC B. D. Martin, D. A. Zych, and C. V. Heer, Phys. Rev. **A135**, 671–9 (1964); C_p (0.35–2 K).

65FIL/MAR J. D. Filby and D. L. Martin, Proc. Roy. Soc. (London) **A284**, 83–107 (1965); C_p (0.4–320 K), T_{fus}, $\Delta_{fus}H$.

69BAS/VOL A. S. Basin, S. P. Volchkova, and A. N. Soloviev, J. Appl. Mech. and Tech. Phys. **10**, 961–6 (1969); T_{fus}.

69SHP/KAG E. E. Shpil'rain and D. N. Kagan, High Temp. **7**, 328–30, (1969); ΔH (405–1334 K).

70GOA/OTT J. R. Goates, J. B. Ott, and C. C. Hsu, Trans. Faraday Soc. **66**, 25–9 (1970); T_{fus}.

70MAR D. L. Martin, Can. J. Phys. 48, 1327–39 (1970); C_p (0.4–3 K), T_{fus}, $\Delta_{fus}H$.

70SHP/YAK E. E. Shpil'rain, K. A. Yakimovich, E. E. Totskii, D. L. Timrot, and V. A. Fomin, "Thermophysical Properties of Alkali Metals," V.A. Kirillin, ed., Izd. Standartov, Moscow (1970); Review.

71GOA/OTT J. R. Goates, J. B. Ott, and E. Delawarde, E., Trans. Faraday Soc. **67**, 1612–6 (1971); T_{fus}.

71MAL/GIG L. Malapsina, R. Gigli, and V. Placente, Gazz. Chim. Ital. **101**, 197–203 (1971); $\Delta_{fus}H$.

73HUL R. Hultgren, P. D. Desai, D. T. Hawkins, M. Gleiser, K. K. Kelley, and D. D. Wagman, "Selected Values of the Thermodynamic Properties of the Elements," Amer. Soc. Metals, Metals Park, OH, 410–15 (1973); Review.

73SIM A. Simon, Z. Anorg. Allg. Chem. **395**, 301–319 (1973); T_{fus}.

76NOV/ROS I. I. Novikov, V. V. Roschupkin, and L. K. Fordeeva, High Temp. **14**, 66–68 (1976); C_p (327–1234 K).

82GUR L. V. Gurvich, I. V. Veits, V. A. Medvedev, et al., V. P. Glushko, gen. ed., "Thermodynamic Properties of Individual Substances," Nauka, Moscow, **4** (1), 422–5 (1982); Review.

85FIN/LEI J. K. Fink and L. Leibowitz, "Handbook of Thermodynamic and Transport Properties of Alkali Metals," ed. R. W. Ohse, Blackwell Sci. Publ., Oxford, (1985) 411–434; liquid Rb, Review.

85JAN M. W. Chase, Jr., C. A. Davis, J. R. Downey, Jr., D. J. Frurip, R. A. McDonald, and A. N. Syverud, "JANAF Thermochemical Tables," J. Phys. Chem. Ref. Data 14, Suppl. **1**, 1764–7 (1985); Review.

85OHS/BAB R. W. Ohse, J.-F. Babelot, J. Magill, and M. Tetenbaum, Pure Appl. Chem. **57**, 1407–26 (1985); T_{fus}, Review.

89COX/WAG J. D. Cox, D. D. Wagman, and V. A. Medvedev, "CODATA Key Values for Thermodynamics," Hemisphere Publ. Corp., NY, 260 (1989); Review.

5.9. Appendix – Experimental Data of Rb

Tables 5.7 to 5.23 present heat capacity or enthalpy data as they were presented in the original article. As a result, the numerical values listed in this Appendix are the actual experimental values, tabular smoothed values, values calculated from equations, or values extracted from a graph. Where necessary, values are converted to joules (from calories). In all cases, the table heading indicates the type of data listed.

The enthalpy data for Rb are given mostly as $\Delta H = H°(T) - H°(T_{ref})$, where T_{ref} is usually equal to 273 or 298 K. When temperature $T > T_{fus}$, then the values of ΔH include the enthalpies of fusion (Tables 5.13, 14, 19, 22). The correction term $H°(298.15\ K) - H°(273\ K)$ was determined as 759 $J \cdot mol^{-1}$.

TABLE 5.1. Electronic Contribution to the heat capacity and the Debye temperature of Rb

Reference	γ, $mJ \cdot K^{-2} \cdot mol^{-1}$	Θ_D, K	Temp. range, K
Original studies			
59MAN	–	52.6	1.2 – 4.2
64LIE/PHI	2.41 ± 0.04	55.5 ± 0.6	0.2 – 0.9
64MAR/ZYC	4.07	58.7	0.4 – 2.0
65FIL/MAR	–	55.6 ± 0.6	0.4 – 1.5
70MAR	2.61 ± 0.03	56.5 ± 0.2	0.4 – 3.0
Review			
73HUL	2.41 ± 0.02	Based on 64LIE/PHI	
Adopted			
	2.61 ± 0.05	56.5 ± 1.0	Based on 70MAR

TABLE 5.2. Comparison of the heat capacity, enthalpy and entropy values for Rb at 298.15 K

Reference	C_p°(298.15 K) $J \cdot K^{-1} \cdot mol^{-1}$	S°(298.15 K) $J \cdot K^{-1} \cdot mol^{-1}$	H°(298.15 K)-H°(0), $J \cdot mol^{-1}$
73HUL	31.062	76.78 ± 0.3	7489
82GUR	31.060	76.780 ± 0.3	7490
85JAN	31.062	76.778 ± 0.3	7490
89COX/WAG	31.060	76.780 ± 0.3	7489 ± 20
Adopted:	31.03 ± 0.1	76.74 ± 0.3	7489 ± 20

TABLE 5.3. Temperature of fusion of Rb

Reference	Temperature, K	Comments
Original studies		
13REN, 14REN	312.15 ± 0.05	Enthalpy measurements
35LOS	311.93 ± 0.1	Thermal analysis
55DAU/MAR	311.88 ± 0.5	Thermal analysis
63WEA	312.52	Cooling curve method
65FIL/MAR	312.44	Thermal analysis (measured)
65FIL/MAR	312.475 ± 0.01	Corrected value
69BAS/VOL	312.30 ± 0.05	Density measurements
70MAR	312.45	Thermal analysis (measured)
70MAR	312.46 ± 0.02	Corrected value
71GOA/OTT	312.44 ± 0.1	Thermal analysis
73SIM	312.51 ± 0.01	Thermal analysis
Reviews		
73HUL	312.64 ± 0.05	Based on 65FIL/MAR
82GUR	312.47 ± 0.03	Based on 70MAR
85JAN	312.65 ± 0.1	Based on 85OHS/BAB
85OHS/BAB	312.65 ± 0.1	Based on 65FIL/MAR
Adopted		
	312.45 ± 0.1	Based on 65FIL/MAR, 70MAR, 71GOA/OTT

TABLE 5.4. Enthalpy of fusion of Rb

Reference	$\Delta_{fus}H$, J·mol^{-1}	Comments
Original studies		
13REN, 14REN	2195	Enthalpy measurements
37BIN	2180 (1800)	Calorimeter (estimate)
55DAU/MAR	2260	Enthalpy measurements
63TEP/MUR	2573	Estimate
64ACH	2655	Estimate
65FIL/MAR	2194 ± 4	Adiabatic calorimeter
70MAR	2194 ± 4	Adiabatic calorimeter
71MAL/GIG	2218 ± 29	Calvet calorimeter
Reviews		
73HUL	2192 ± 80	Based on 65FIL/MAR and 14REN
82GUR	2192 ± 5	Based on 65FIL/MAR, 70MAR
85JAN	2190 ± 90	Based on 14REN, 65FIL/MAR, 70MAR
Adopted		
	2190 ± 25	Based on 65FIL/MAR, 70MAR

TABLE 5.5. Thermodynamic functions of Rb below 298.15 K

T/K	C_p° J·K^{-1}·mol^{-1}	$H^\circ(T)$-$H^\circ(0)$ J·mol^{-1}	$S^\circ(T)$ J·K^{-1}·mol^{-1}
5	1.555	1.970	0.5299
10	6.883	22.584	3.1748
15	12.258	70.779	7.0091
20	16.139 (16.186)	142.669	11.118
25	18.834	230.831	15.042
30	20.465	329.343	18.630
35	21.563	434.548	21.871
40	22.373	544.485	24.806
45	22.991	657.960	27.478
50	23.477	774.176	29.927
60	24.181	1012.71	34.274
70	24.654	1257.03	38.039
80	24.991	1505.33	41.354
90	25.261	1756.63	44.314
100	25.521 (25.515)	2010.53	46.988
110	25.697	2266.56	49.429
120	25.904	2524.55	51.673
130	26.117	2784.66	53.755
140	26.325	3046.87	55.698
150	26.525	3311.13	57.521
160	26.716	3577.34	59.239
170	26.900	3845.43	60.865
180	27.081	4115.33	62.407
190	27.261	4387.04	63.876
200	27.448	4660.58	65.279
210	27.646	4936.03	66.623
220	27.861	5213.55	67.914
230	28.100	5493.32	69.16
240	28.369	5775.64	70.359
250	28.675	6060.82	71.523
260	29.025 (29.024)	6349.28	72.655
270	29.385	6641.27	73.757
280	29.838	6937.29	74.833
290	30.427	7238.48	75.890
298.15	31.031	7488.84	76.741

TABLE 5.6. Thermodynamic functions of Rb above 298.15 K

T/K	C_p° J·K^{-1}·mol^{-1}	$H^\circ(T)$-H° 298.15 K J·mol^{-1}	$S^\circ(T)$ J·K^{-1}·mol^{-1}
298.15	31.031	0.00	76.740
300.00	31.186	57.55	76.932
312.45 (sol)	32.416	453.13	78.224
312.45 (liq)	32.308	2643.13	85.233
400.00	31.715	5444.80	93.141
500.00	31.197	8588.98	100.159
600.00	30.850	11689.94	105.814
700.00	30.674	14764.75	110.554
800.00	30.669	17830.49	114.648
900.00	30.835	20904.25	118.268
1000.00	31.171	24003.11	121.533
1100.00	31.678	27144.15	124.526
1200.00	32.356	30344.44	127.310
1300.00	33.205	33621.09	129.932
1400.00	34.225	36991.16	132.429
1500.00	35.415	40471.73	134.830
1600.00	36.777	44079.90	137.158

Table 5.7. SMOOTHED heat capacity of Rb [14REN]

T/K	C_p°, J·K^{-1}·mol^{-1}	T/K	C_p°, J·K^{-1}·mol^{-1}
290	30.50	320	32.49
300	31.58	330	32.40
310	32.66	340	32.31
312.45 (sol)	32.92	350	32.12
312.45 (liq)	32.56	360	32.03

TABLE 5.8. SMOOTHED heat capacity of Rb [55DAU/MAR]

T/K	C_p°, J·K^{-1}·mol^{-1}	T/K	C_p°, J·K^{-1}·mol^{-1}
25	18.8	160	26.8
30	20.5	170	26.9
35	21.5	180	27.1
40	22.4	190	27.3
45	22.9	200	27.5
50	23.3	210	27.7
55	23.8	220	27.8
60	24.1	230	28.1
70	24.6	240	28.4
80	25.0	250	28.7
90	25.35	260	29.0
100	25.5	270	29.4
110	25.7	273.15	29.5
120	25.9	280	29.9
130	26.1	290	30.4
140	26.4	300	31.05
150	26.6		

TABLE 5.9. EXPERIMENTAL heat capacity of Rb [59MAN]

T/K	C_p°, mJ·K^{-1}·mol^{-1}	T/K	C_p°, mJ·K^{-1}·mol^{-1}
1.5	46	3.0	391
2.0	107	3.5	625
2.5	220	4.0	898

TABLE 5.10. EXPERIMENTAL heat capacity of Rb [62ALA/PCH]

T/K	C_p°, J·K^{-1}·mol^{-1}	T/K	C_p°, J·K^{-1}·mol^{-1}
326.5	33.3	773.8	31.4
370	31.8	765.7	32.9
404	32.9	818	30.4
420	32.9	876	31.1
489	31.8	923.8	31.4
512.7	31.8	971	31.1
573.8	32.2	1001	32.9
628.5	32.5	1038	31.1
676.5	32.2		

TABLE 5.11. SMOOTHED heat capacity of Rb [62ALA/PCH]

T/K	C_p°, J·K^{-1}·mol^{-1}		T/K	C_p°, J·K^{-1}·mol^{-1}	
		(corrected)			(corrected)
323	33.25		773	31.41	(30.04)
373	32.89	(31.47)	873	31.41	(30.04)
473	32.54	(31.11)	973	31.83	(30.40)
573	32.18	(30.75)	1073	32.54	(31.11)
673	31.83	(30.40)			

TABLE 5.12. SMOOTHED heat capacity of Rb [62MCC/SIL]

T/K	C_p°, J·K^{-1}·mol^{-1}	T/K	C_p°, J·K^{-1}·mol^{-1}
2.0	0.12	8.0	5.84
4.0	1.00	10.0	11.09
6.0	2.68	12.0	21.96

TABLE 5.13. EXPERIMENTAL enthalpy values [$H°(T)$-$H°(298\ K)$] of Rb [63TEP/MUR]

T/K	ΔH, J·mol^{-1}	T/K	ΔH, J·mol^{-1}
504.4	9318	991.5	24907
622.5	12749	1017.5	25953
737.6	16853	1172.0	30066
853.6	19355	1205.0	31497
946.7	21920	1268.0	33003

TABLE 5.14. EXPERIMENTAL enthalpy values [$H°(T)$-$H°(273\ K)$] of Rb [64ACH]

T/K	ΔH, J·mol^{-1}	T/K	ΔH, J·mol^{-1}
337	4715	642	14224
342	4664	671	14892
369	5578	704	16274
370	5968	733	17090
397	6737	758	17965
427	7385	816	19578
452	8159	874	21076
478	9421	931	22168
506	10260	979	24047
536	11232	1033	25768
564	11693	1088	27788
596	12918	1172	29561
621	12793		

TABLE 5.15. SMOOTHED heat capacity of Rb [64ACH]

T/K	$C_p°$, J·K^{-1}·mol^{-1}	T/K	$C_p°$, J·K^{-1}·mol^{-1}
400	32.88	900	28.82
500	31.47	1000	28.91
600	30.35	1100	29.30
700	29.54	1200	30.00
800	29.03		

TABLE 5.16. EXPERIMENTAL heat capacity of Rb [64LIE/PHI]

T/K	C_p, mJ·K^{-1}·mol^{-1}	T/K	C_p, mJ·K^{-1}·mol^{-1}
	Adiabatic demagnetizing cryostat		
0.2002	0.5701	0.5686	3.555
0.2191	0.6439	0.6151	4.229
0.2391	0.7282	0.6573	4.931
0.2616	0.8336	0.7245	6.264
0.2936	0.9953	0.7969	7.952
0.1954	0.5537	0.8708	10.02
0.2143	0.6223	0.4168	1.862
0.2321	0.6968	0.4596	2.255
0.2548	0.8001	0.5002	2.681
0.2819	0.9344	0.5395	3.121
0.3140	1.113	0.5867	3.810
0.3456	1.309	0.6418	4.724
0.3816	1.569	0.7053	5.924
0.4185	1.868	0.7736	7.457
0.4615	2.260	0.8497	9.489
0.5015	2.693	0.9289	11.87
0.5549	3.358	1.011	14.93
0.1859	0.5189	1.098	18.85
0.2087	0.6064	0.6381	4.617
0.2326	0.7025	0.7084	5.947
0.2548	0.8022	0.7862	7.735
0.2798	0.9257	0.8634	9.845
0.3048	1.063	0.9455	12.49
0.3285	1.201	1.041	16.26
0.3511	1.350	1.135	20.71
0.3830	1.582	1.237	26.43
0.4177	1.863	1.214	25.13
0.4527	2.172	1.167	22.46
0.4882	2.538	1.245	26.88
0.5252	2.979		
	Liquid-helium temperature cryostat		
1.1991	24.07	2.1287	142.6
1.3249	32.22	2.3342	191.4
1.4630	43.46	2.5471	251.8
1.6163	59.22	2.7886	336.9
1.7867	81.31	3.0530	445.1
1.9718	111.4	3.3361	581.1
2.1610	149.7	3.6579	757.4
2.3660	200.3	4.0081	969.1
2.5961	269.1	1.5881	55.89
2.8521	361.7	1.7361	73.97
3.1428	486.5	1.9055	99.58
3.4535	644.5	2.0910	143.4
3.7762	827.6	2.2887	179.3
4.0713	1009.0	2.5015	238.5
1.1952	23.83	2.7254	313.0
1.3076	30.99	2.9798	412.5
1.4365	41.12	3.2642	543.7
1.5882	56.00	3.5784	711.6
1.7523	76.35	3.9231	914.7
1.9314	104.3		

TABLE 5.17. SMOOTHED heat capacity of Rb [64MAR/ZYC]

T/K	C_p°, mJ·K^{-1}mol^{-1}	T/K	C_p°, mJ·K^{-1}·mol^{-1}
0.5	3.3	1.5	45.5
1.0	14.5	2.0	118.6

TABLE 5.18. SMOOTHED heat capacity of Rb [65FIL/MAR]

T/K	C_p°, J·K^{-1}·mol^{-1}	T/K	C_p°, J·K^{-1}·mol^{-1}
	Temperature range 0.4– 1.5 K		
0 .4	0.00185	1.0	0.0137
0 .5	0.00271	1.1	0.0179
0 .6	0.00410	1.2	0.0228
0 .7	0.00565	1.3	0.0289
0 .8	0.00778	1.4	0.0365
0 .9	0.0104	1.5	0.0469
	Temperature range 3– 26 K		
3	0.38	12	9.19
4	0.87	14	11.30
5	1.57	16	13.17
6	2.46	18	14.76
7	3.48	20	16.15
8	4.60	22	17.23
9	5.74	24	18.21
10	6.91	26	19.06
	Temperature range 20– 320 K		
20	16.19	160	26.72
25	18.74	170	26.91
30	20.43	180	27.09
35	21.59	190	27.27
40	22.41	200	27.45
45	23.01	210	27.64
50	23.48	220	27.85
55	23.85	230	28.10
60	24.16	240	28.38
65	24.42	250	28.69
70	24.64	260	29.02
75	24.83	270	29.39
80	25.00	273.15	29.53
85	25.15	280	29.84
90	25.28	290	30.41
95	25.40	298.15	31.06
100	25.51	300	31.19
110	25.71	310	32.17
120	25.91	312.64 (sol)	32.40
130	26.11	312.64 (liq)	32.40
140	26.32	320	32.26
150	26.52		

TABLE 5.19. EXPERIMENTAL enthalpy values [$H^\circ(T)$-H°(273 K)] of Rb [69SHP/KAG]

Temp., K	ΔH, J·mol^{-1}	Temp.,K	ΔH, J·mol^{-1}
404.9	6335	988.1	23950
507.7	9803	1086.2	27710
628.8	13470	1204.5	31420
770.8	17660	1333.9	35120
887.8	21270		

TABLE 5.20. SMOOTHED heat capacity of Rb [69SHP/KAG]

T/K	C_p°, J·K^{-1}·mol^{-1}	T/K	C_p°, J·K^{-1}·mol^{-1}
400	31.50	900	30.70
500	31.10	1000	30.89
600	30.83	1100	31.20
700	30.67	1200	31.63
800	30.62	1300	32.17

TABLE 5.21. SMOOTHED heat capacity of Rb [70MAR]

T/K	C_p°, mJ·K^{-1}·mol^{-1}	T/K	C_p°, mJ·K^{-1}·mol^{-1}
0.5	3	2.0	107
1.0	14	2.5	217
1.5	44	3.0	380

TABLE 5.22. EXPERIMENTAL enthalpy values [$H^\circ(T)$-H°(273 K)] of Rb [76NOV/ROS]

T/K	ΔH, J·mol^{-1}	T/K	ΔH, J·mol^{-1}
326.8	3880	605.4	12360
353.3	4680	631.8	12980
375.6	5430	650.3	13620
378.3	5440	674.8	14390
395.5	6050	764.8	17120
401.0	6170	836.6	19490
431.2	7070	939.6	22110
446.2	7560	1017.5	25780
471.0	8360	1109.5	28670
505.9	9350	1220.9	31320
561.8	11000	1233.8	32390

TABLE 5.23. SMOOTHED heat capacity of Rb [76NOV/ROS]

T/K	Cp°, J·K^{-1}·mol^{-1}	T/K	C_p°, J·K^{-1}·mol^{-1}
400	30.42	900	31.47
500	30.28	1000	32.21
600	30.31	1100	33.13
700	30.52	1200	34.22
800	30.91		

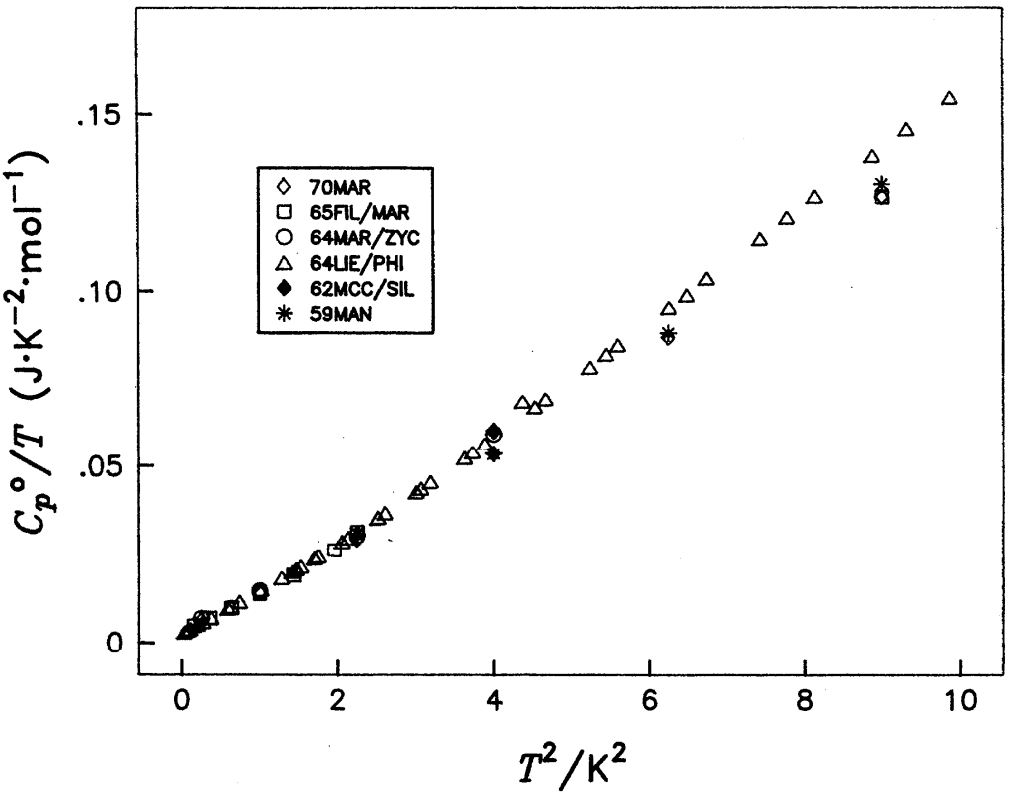

FIGURE 5.1. C_p/T versus T^2 for Rb below 3 K

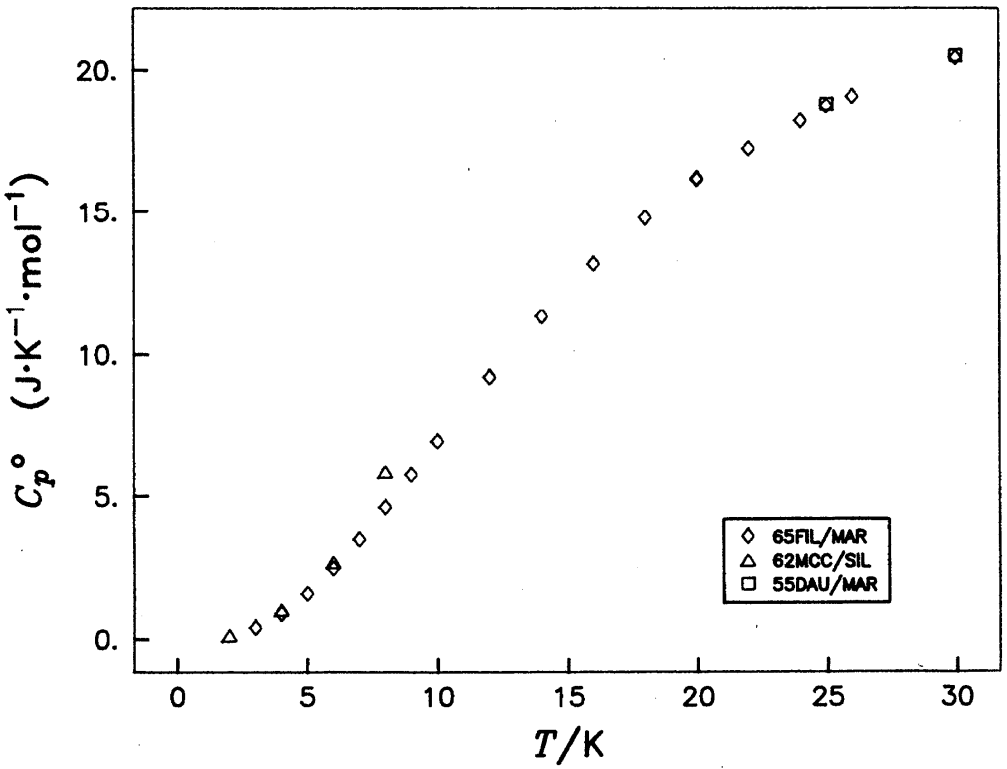

FIGURE 5.2. Heat Capacity of Rb below 30 K

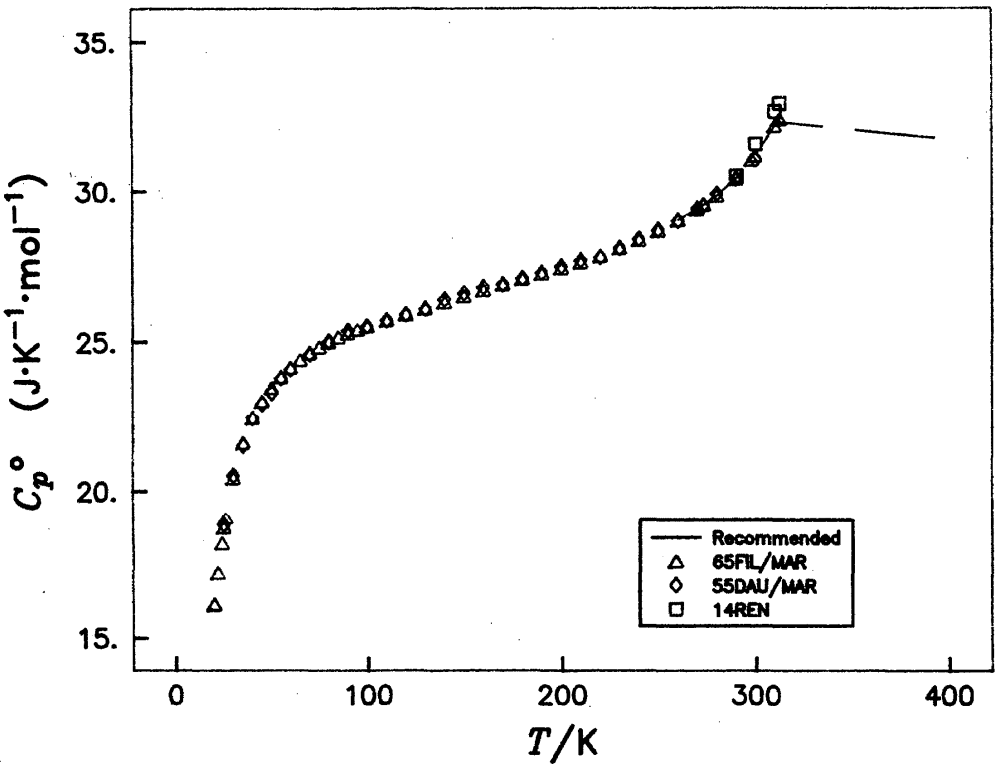

FIGURE 5.3. Heat Capacity of Solid Rb

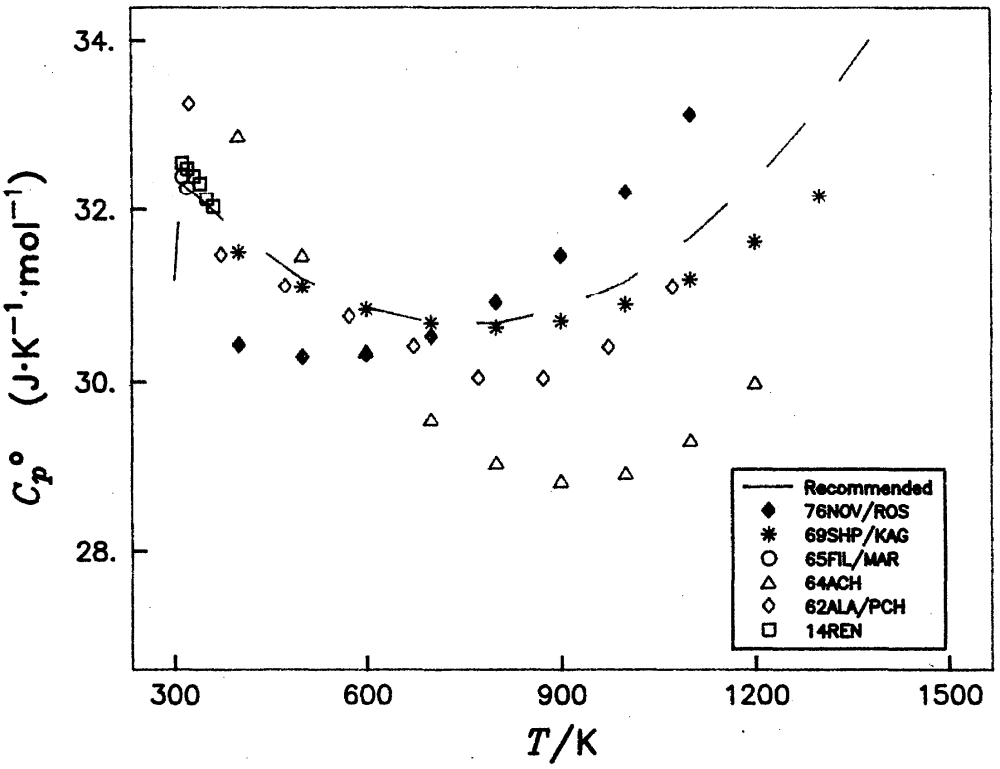

FIGURE 5.4. Heat Capacity of Liquid Rb

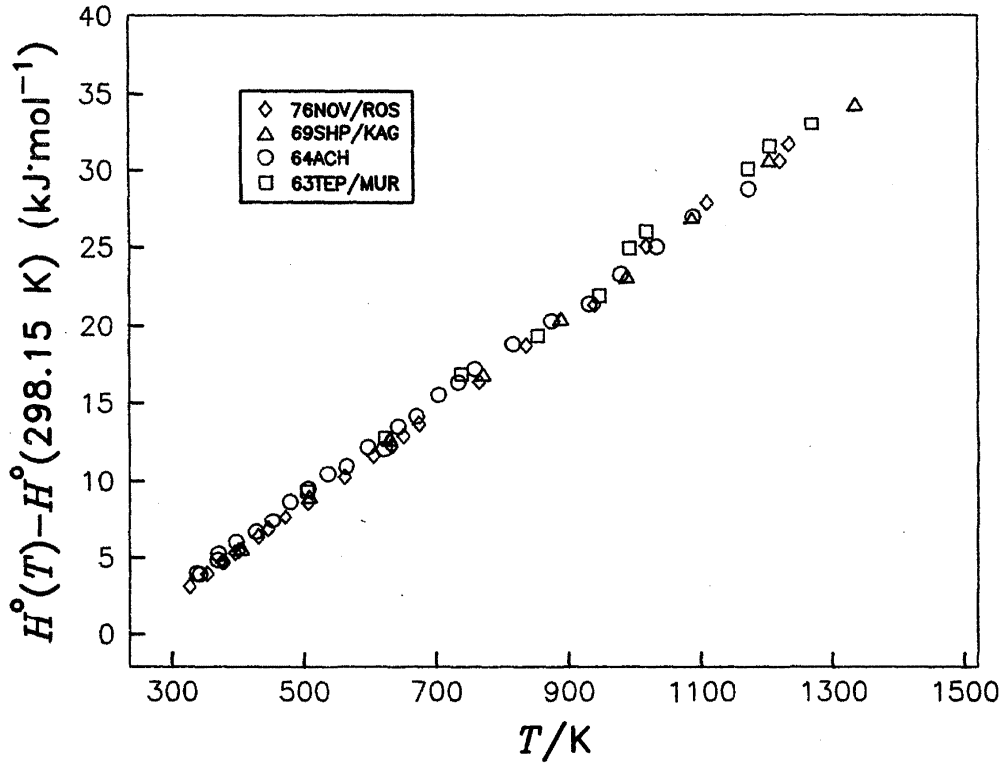

FIGURE 5.5. $H°(T)-H°(298.15\ K)$ of Rb

6. Cesium

6.1. Introduction

Cesium has only one crystalline modification, at ambient pressure (Table 1.1). The heat capacity of solid Cs has not been determined accurately above 270 K due to premelting phenomena. The discrepancy between results of different investigations of the heat capacity of liquid Cs is considerable.

The temperature and enthalpy of fusion and the heat capacity below 270 K are known fairly well. However, measurements at the lowest temperatures should be repeated with purer samples.

6.2. Heat Capacity and Enthalpy Measurements

6.2.1. Temperature below 298.15 K

[55DAU/MAR]

Dauphinee *et al.* measured the heat capacity of Cs from 20 to 320 K in an adiabatic calorimeter. The authors assumed that the commercial samples used (A.D. MacKay, New York, no analysis was given) contained about 0.3 atomic percentage of oxygen according to the depression of the melting point. Some irregularities of the heat capacity values (of about 2%) were observed at 100 − 200 K; a hysteresis was registered within the anomaly. The anomaly was explained later [65FIL/MAR] by annealing in a copper thermometer which was strained on cooling. Another anomaly, a steep peak in the heat capacity values, was observed at about 270 K and was explained by the eutectic reaction in the Cs-O system. Another steep increase in the heat capacity values was registered prior to melting. The measured data were presented in the form of a smoothed graph without showing the individual points. Smoothed data (34 points) taken from the curve were tabulated in the paper and are reproduced in Table 6.8 and Fig. 6.3. Eutectic and premelting anomalies indicate high level of impurities and the low accuracy of the results; for example, the result at 290 K is erroneous.

[62MCC/SIL]

McCollum and Silsbee measured the heat capacity of Cs (A.D. MacKay, New York, no analysis provided) at 1.3−12 K in a Nernst calorimeter; two different devices were used below and above 4 K. The results (75 data points) are given in a small-scale graph as a dependence of Θ_D vs. T. When calculating Θ_D, the authors used $\gamma = 3.47$ mJ·K^{-2}·mol^{-1} from an unpublished work of N.E. Phillips (a close value was given in [64LIE/PHI], see below). The Debye temperature showed a minimum 36 K at 2.0 K and a maximum 45 K at about 9 K. The heat capacities were estimated from the graph shown by the authors; they are given in Table 6.11 and shown in Fig. 6.1 and 6.2 below 8 K. Comparing these results with other data it is evident that below 6 K these data are reasonable, but above 6 K they become extremely high, and the study was rated as inaccurate.

[64LIE/PHI]

Lien and Phillips measured the heat capacity of Cs from 0.2 to 1.2 K in an adiabatic demagnetizing cryostat (58 points) and from 1.2 to 4.1 K in a liquid-helium cryostat (37 points). The purity of a commercial material was certified as 99.8% Cs; the spectral analysis performed on request of Lien and Phillips showed more impurities than the supplier stated: 0.2% Na, 0.2% K and 0.4% Rb. The tabulated results are reproduced in Table 6.16 and shown partially in Fig. 6.1. The data for 0.2 − 0.7 K were fitted to a two-term equation which corresponds to $\Theta_D = 39.5 \pm 0.3$ K and $\gamma = 3.20 \pm 0.07$ mJ·K^{-2}·mol^{-1}. The data measured between 0.9 and 1.5 K were described by a three-term equation

$$C_p^\circ = (3.20 \pm 0.07)T + (31.4 \pm 0.2)T^3 + (2.78 \pm 0.2)T^5 \text{ mJ·K}^{-1}\text{·mol}^{-1}.$$

Despite the high levels of metallic impurities, these heat capacity values appear to be reliable.

[64MAR/ZYC]

Martin *et al.* measured the heat capacity of Cs from 0.35 to 1.6 K in a Nernst calorimeter. The commercial sample contained, by assay, 99.98% Cs, 0.002% Rb, <0.001% K, Li and Na. The experimental data of heat capacity of sample plus container were given in graphical (65 points) and tabulated (25 points) forms. The heat capacity values for Cs were determined by subtracting values of the heat capacity of the container which were estimated. The resulting heat capacity values of Cs were fitted to a four-term polynomial

$$C_p^\circ = 6.291T + 28.97T^3 + 1.48T^5 + 0.945T^7 \text{ mJ·K}^{-1}\text{·mol}^{-1}.$$

The above equation corresponds to $\gamma = 6.29$ mJ·K^{-2}·mol^{-1} and $\Theta_D = 40.6$ K, and the calculated heat capacity values are shown in Table 6.17 and Fig. 6.1. The results have moderate accuracy because the heat capacity of the container was only known approximately.

[65FIL/MAR]

Filby and Martin measured the heat capacity of Cs in three different calorimeters: at 0.4 − 1.5 K, 3 − 26 K and 20 − 320 K. Commercial materials (L. Light, Colnbrook, England, and A.D. MacKay, New York) contained 99.9% Cs by assay. Filby and Martin analyzed the MacKay material by spectral analysis; it contained Fe, Cu and Cr 0.05 − 0.005 wt. %; Si, Ag and Na 0.1 − 0.01 wt. %; B, Pb, Sn, Ni, and Ca 0.01 − 0.001 wt. %; Mn 0.001 − 0.0001 wt. %; Mg 0.0005 − 0.00005 wt. %. The level of impurities for different MacKay samples was also characterized by the ratios $\rho_{293K}/\rho_{4.2K} = 500$ and 120 which are not high and indicate impurities. The Light samples had about 0.07 atomic percentage of solid insoluble impurities, estimated from the depression of the melting point. The level of impurities for the Light samples was characterized by the ratio $\rho_{293K}/\rho_{4.2K} = 220$. A special procedure was introduced to prevent contamination of the samples during their handling.

The C_p/T vs T^2 data are shown by the authors in a graph between 0.4 and 1.5 K (60 points). Another graph of calculated Θ_D values was given between 3 and 25 K (130 points). Smoothed heat capacity values were tabulated for three ranges 0.4 − 1.5 K, 3 − 26 K and 20 − 320 K; these data are reproduced in Table 6.18 and shown in Fig. 6.1 to 6.4. Filby

and Martin suggested that their data below 0.7 K are not accurate. To determine the Debye temperature, they used γ = 3.20 mJ·K^{-2}·mol^{-1} from [64LIE/PHI] and calculated Θ_D = 38.4 ± 0.6 K. In the range of 3–26 K a spontaneous heat evolution of about 0.02 mJ·mol^{-1} s^{-1} was observed, which could have been caused by an experimental error. In the interval 100–200 K the authors did not find the anomaly, mentioned in [55DAU/MAR]. The authors estimated the accuracy of measurements to be about 1%. However, this value could be underestimated. Above 290 K the measured heat capacity values increased steeply probably due to the presence of impurities in the sample, and so these data were rejected. Instead Filby and Martin extrapolated data below 260 K to higher temperatures and assumed that at the melting point the heat capacity of liquid and solid Cs are equal. The use of estimates above 260 K reduces the accuracy of these data.

The authors also assessed the melting point of Cs from partial melting data over a range of temperatures. They made an allowance of 0.24 K for the presence of 0.07% atomic impurities and recommended T_{fus} = 301.55 ± 0.01 K. The enthalpy of melting was determined as $\Delta_{fus}H$ = 2087 ± 2 J·mol^{-1}.

[70MAR]

Martin improved the construction of the apparatus for heat capacity measurements between 0.4 and 3 K and revised the data of [65FIL/MAR]. The material (Electronic Space Products, Los Angeles) was certified as 99.99% Cs, <70 ppm of metallic impurities and <15 ppm oxygen. Spectral analysis performed on request of the author showed 60–600 ppm Na, 3–30 ppm each of Cu, Ag, Al, Si and Mg, and less than 10 ppm oxygen. From the depression of the melting point, the purity was estimated as 99.5 ± 0.4% assuming soluble impurities, and as 99.97 ± 0.01% assuming insoluble impurities. The results of two sets of measurements were fitted to a five-term polynomial

$$C_p^\circ = (4.050 \pm 0.040)T + (28.72 \pm 0.188)T^3 + (6.071 \pm 0.197)T^5 - (0.967 \pm 0.059)T^7 + (0.05 \pm 0.005)T^9 \text{ mJ·K}^{-1}\text{·mol}^{-1}.$$

Smoothed values calculated by this equation in steps of 0.5 K are given in Table 6.22 and shown in Fig. 6.1. The deviations of the 130 experimental data points from the calculated values are shown in a graph; the deviations do not exceed 1%. The electronic specific heat and the Debye temperature were estimated as γ = 3.97 ± 0.08 mJ·K^{-2}·mol^{-1} and Θ_D = 40.5 ± 0.3 K. These data appear to be reliable and have a small systematic error.

The thermal analysis was performed with the same material, the melting point was measured six times. Martin combined these results and those obtained earlier in [65FIL/MAR], and recommended T_{fus} = 301.67 ± 0.13 K. The enthalpy of melting was determined as $\Delta_{fus}H$ = 2096 ± 4 J·mol^{-1} which is close to the values of [65FIL/MAR], but is probably more accurate because the sample in [70MAR] contained less oxygen.

6.2.2. Temperature above 298.15 K

[13REN], [14REN]

Rengade measured the enthalpy of Cs in a Bunsen ice calorimeter from 288 to 373 K. Cesium was prepared by a reduction of CsCl with Ca and by double distillation in vacuum. The measurements (7 points for solid Cs and 5 points for liquid Cs) are shown in a graph in [14REN]. The heat capacity values were described by linear equations

for solid Cs (288<T<301.6):

$$C_p^\circ = -12.58 + 0.1524T \text{ J·K}^{-1}\text{·mol}^{-1};$$

for liquid Cs (301.6<T<373):

$$C_p^\circ = 38.75 - 0.0189T \text{ J·K}^{-1}\text{·mol}^{-1}.$$

The values calculated by these equations are reproduced in Table 6.7 and shown in Fig. 6.3 and 6.4. The accuracy of the heat capacity data is not high. The melting point was determined as 301.6 ± 0.1 K; the enthalpy of fusion as 2091 J·mol^{-1}; the values of T_{fus} and $\Delta_{fus}H$ agree well with modern measurements.

[62ALA/PCH]

Aladyev and Pchelkin (quoted from [70SHP/YAK]) measured the heat capacity of a commercial Cs (certified impurities: 0.02% K, 0.078% Rb, 0.015% Na) in an isothermal calorimeter at 307 to 955 K. The experimental and smoothed data are listed in Tables 6.9 and 6.10, respectively, and the smoothed data are shown in Fig. 6.4. The accuracy of the study is not high; the original data are scattered within 10%.

[63TEP/MUR]

Tepper *et al.* measured the enthalpy of Cs in a drop calorimeter from 351 to 1238 K. Cesium contained in ppm: Rb − 70; K − 15; Na − 10; O − 14; N < 2 and C − 30. The experimental enthalpy values are listed in Table 6.12 and shown in Fig. 6.5. Above 600 K the measured values were described by a two-term equation with a standard deivation of about 1.5%:

$$H^\circ(T,\text{l}) - H^\circ(298\text{ K,cr}) = -6300 + 30.33T \text{ J·mol}^{-1}.$$

According to the equation, the heat capacity of liquid Cs is constant. Tepper *et al.* noticed a reproducible anomaly below 600 K, which was not confirmed in more recent studies. Above 600 K the uncertainty of this study is about 4%.

[64ACH]

Achener measured the enthalpy of liquid Cs (about 99.5% Cs) in a Bunsen calorimeter at 340–1175 K. The material contained about 60 ppm of metallic impurities and 260 ppm of oxygen. After the experiment the amount of metallic impurities increased to 800 ppm; this fact indicates a reaction between a specimen and a container. The 23 data points below 1175 K (Table 6.13, Fig. 6.5) were fitted to an equation

$$H^\circ(T,\text{l}) - H^\circ(273\text{ K,cr}) = -15026 + 79.1232T - 7.565\times10^{-2}T^2 + 35.966\times10^{-6}T^3 \text{ J·mol}^{-1}.$$

The derived heat capacity has a minimum at 700 K (Table 6.14, Fig. 6.4). The uncertainty in the derived heat capacity data was high, greater than 10%. Achener estimated the enthalpy of melting of Cs, $\Delta_{fus}H = 2096$ J·mol^{-1}, using his own data for liquid alloys and Rengade's equation for solid Cs [14REN].

[64LEM/DEE]

Lemmon *et al.* measured the enthalpy of a commercial sample of Cs in a Bunsen ice calorimeter from 295 to 1435 K (Table 6.15, Fig. 6.5). According to the supplier's analysis, the material has 150 ppm metallic impurities; Lemmon *et al.* found that the sample contains less than 100 ppm impurities. The data for solid Cs correspond to a constant $C_p^\circ = 31.08$ J·K^{-1}·mol^{-1}; at 600 to 1000 K the experimental heat capacity increased. Lemmon *et al.* explained this increase as being due to inaccuracy and assumed that heat capacity of liquid Cs below 371 K and above 573 K is constant and equal to 30.8 and 33.36 J·K^{-1}·mol^{-1}, respectively. The enthalpy of liquid Cs at 301.67 − 373 K was expressed as

$$H^\circ(T,\text{l})-H^\circ(273\text{ K,cr}) = -6436 + 30.80T\text{ J·mol}^{-1},$$

and at 564 − 1435 K as

$$H^\circ(T,\text{l})-H^\circ(273\text{ K,cr}) = -8830 + 33.36T\text{ J·mol}^{-1}.$$

The uncertainty in these results is high (>5%). The average melting point of 6 samples was determined as $T_{fus} = 301.67$ K. The enthalpy of fusion was determined as $\Delta_{fus}H = 1969$ J·mol^{-1}.

[66ACH/FIS]

Achener and Fisher measured the enthalpy using a material containing 300 ppm Na, 50 ppm of other metallic impurities and <150 ppm oxygen. Twenty-four data points were obtained at 922–1339 K. The data (Table 6.19) were widely scattered and have low accuracy (Fig. 6.5); they were combined with previous results of [64ACH] in an equation proposed for the temperature range 920–1280 K.

$$H^\circ(T,\text{l})-H^\circ(298\text{ K,cr}) = -6190 + 30.6T\text{ J·mol}^{-1}.$$

The uncertainty of this result is high (>5%) because the heat capacity should increase with temperature as indicated by other studies in this temperature range.

[69SHP/KAG]

Shpil'rain and Kagan measured the enthalpy of liquid Cs from 430 to 1330 K in a drop calorimeter with evaporating water. The sample was prepared in the Moscow State Institute of Rare Metals by Ca-reduction of CsCl and by distillation; the material contained 0.01% Li, 0.02% Na, 0.05% K, 0.05% Rb. The enthalpy is given in Table 6.20 and in Fig. 6.5; the derived heat capacity values are given in Table 6.21 and shown in Fig. 6.4. A correction for the difference H°(37 K,l)-H°(273 K,cr) = 5297 J·mol^{-1} was made using the data of [65FIL/MAR]. The data were fitted to the equations:

$$H^\circ(T,\text{l})-H^\circ(273\text{ K,cr}) = -7965 + 40.583T - 1.5395\times10^{-2}T^2 + 6.9375\times10^{-6}T^3,\text{ J·mol}^{-1}.$$

Shpil'rain and Kagan estimated that the average scatter of experimental points from the above equation was about 120 J·mol^{-1}. However, the results contain an essential systematic error, and the uncertainty in the derived heat capacity values is greater than 5%.

[83BLA/FIL]

Blagonravov *et al.* determined the heat capacity per unit of volume for liquid Cs at high pressure 4.5 to 13.6 MPa at 1200–1900 K. The measurements were made by a method based on a periodic heating of samples by electric current; the quality of samples was not described. The method was crude, according to the authors; the random error in the heat capacity was about 10% and the systematic error 11–14%. Using the equation proposed by Blagonravov *et al.* and density tabulated by [70SHP/YAK], the present authors estimated the heat capacity at ambient pressure at 1200 to 1500 K (Table 6.23). The value determined for 1200 and 1300 K does not contradict other data (Fig. 6.4); however, the method used could be classified as semiquantitative, the heat capacity values increase sharply above 1300 K, and they were excluded from further discussion.

6.3. Discussion of Heat Capacity and Enthalpy Data

6.3.1. Cs below 298.15 K

Measurements below 3 K. Below 3 K the heat capacity was measured in [62MCC/SIL], [64LIE/PHI], [64MAR/ZYC], [65FIL/MAR], [70MAR]. Some of the tabulated results are shown in the C_p/T vs T^2 graph (Fig. 6.1). The coefficient of electronic contribution to the heat capacity and the Debye temperature derived from the measurements are listed below in Table 6.1.

The γ and Θ_D values of [64LIE/PHI] and [70MAR] are very close and seem to be the most reliable. The average values of these two studies were adopted in this assessment. However, it should be mentioned that the material in both studies was not very pure, and further investigations are desirable.

For the heat capacity below 3 K, several expressions were proposed; among them are a three-term equation of [64LIE/PHI] and a five-term equation of [70MAR] quoted above. A new three-term equation was derived here on the basis of the measurements of [70MAR], [64LIE/PHI] and the adopted values of γ and Θ_D.

$$C_p^\circ = 3.60T + 30.37T^3 + 1.08T^5\text{ mJ·K}^{-1}\text{·mol}^{-1}. \quad (1)$$

The accuracy of the representation of the data by this equation is about 3%.

Measurements between 3 and 20 K. The heat capacity measurements were made in [62MCC/SIL] (3–12 K), [64LIE/PHI] (below 4.2 K), and [65FIL/MAR] (3–20 K) (Fig. 6.2). The data of [65FIL/MAR] cover this temperature range and are more reliable than those of [62MCC/SIL]. They were fitted to the equation:

$$C_p^\circ = -8.539 + 2.5044T + 24.2717T^{-2} - 0.060446T^2 + 2.5435\times10^{-4}T^3 \text{ J·K}^{-1}\text{·mol}^{-1}. \quad (2)$$

Measurements between 20 and 80 K. For this interval the measurements were reported in [55DAU/MAR] (above 25 K) and in [65FIL/MAR]; both studies came from the same laboratory and are in good agreement (Fig. 6.3). The data of [65FIL/MAR] were selected as they were made more recently and more carefully.

$$C_p^\circ = 19.976 + 0.21825T - 1.482\times10^{3}T^{-2} - 3.2614\times10^{-3}T^2 + 1.7947\times10^{-5}T^3 \text{ J·K}^{-1}\text{·mol}^{-1}. \quad (3)$$

Measurements between 80 and 180 K. Anomalies were reported in this temperature range in [55DAU/MAR] which have not been confirmed in a more recent and better study [65FIL/MAR] (Fig. 6.3). The data of [65FIL/MAR] were fitted to equation

$$C_p^\circ = 40.19 - 0.2794T - 1.7322\times10^{4}T^{-2} + 1.9775\times10^{-3}T^2 - 4.4801\times10^{-6}T^3 \text{ J·K}^{-1}\text{·mol}^{-1}. \quad (4)$$

Measurements between 180 and 260 K. The measurements made in [55DAU/MAR] and [65FIL/MAR] are in satisfactory agreement (Fig. 6.3). Again preference was given to the data of [65FIL/MAR] which were fitted to equation.

$$C_p^\circ = -517.377 + 5.2517T + 2.287\times10^{6}T^{-2} - 18.9017\times10^{-3}T^2 + 2.4216\times10^{-5}T^3 \text{ J·K}^{-1}\text{·mol}^{-1}. \quad (5)$$

Measurements between 260 K and melting point. The measurements were made in [13REN], [14REN] (above 273 K), [55DAU/MAR] and [65FIL/MAR] (Fig. 6.3). The premelting phenomena were registered in all studies, the measured data were corrected in [65FIL/MAR], and the latter values were fitted to equation:

$$C_p^\circ = 9.299 - 82.261\times10^{-3}T + 9.239\times10^{5}T^{-2} + 416.603\times10^{-6}T^2 \text{ J·K}^{-1}\text{·mol}^{-1}. \quad (6)$$

The heat capacity values calculated with the above equation have a higher uncertainty than at lower temperatures. This temperature interval requires further investigation with purer materials.

Equations 1–6 were used to calculate $C_p^\circ(T)$, $H^\circ(T)$-$H^\circ(0)$ and $S^\circ(T)$. The calculations are shown in Table 6.5. At the standard temperature the heat capacity, enthalpy, and entropy were calculated as

C_p°(298.15 K)= 32.199 J·K^{-1}·mol^{-1}
S°(298.15 K)= 85.095 J·K^{-1}·mol^{-1}
H°(298.15 K)-H°(0)= 7716.59 J·mol^{-1}.

These values can be compared with those recommended in previous reviews (Table 6.2).

The calculated values are close to the previous recommendations; they are based on the same information [65FIL/MAR] and [70MAR]. The results of calculations are closer to [85JAN] than to [73HUL] and [82GUR]. The less accurate C_p values are localized at the lowest temperatures and in the vicinity of the melting point. The uncertainty in the enthalpy at 298.15 K was increased to 25 J·mol^{-1} because the C_p values above 280 K are not accurate [65FIL/MAR].

6.3.2. Solid Cs above 298.15 K

Cs melts at 301.6 K, and the region of stability of solid Cs between 298.15 K and the melting point is very short. The experimental data and Eq. 6, which are valid up to the melting point, were discussed above. [82GUR] gave a two-term equation for the interval 298.15–301.55 K.

$$C_p^\circ = 4.922 + 91.525\times10^{-3}T \text{ J·K}^{-1}\text{·mol}^{-1}.$$

This equation gives almost the same values as Eq. 6. [73HUL] and [85JAN] also list almost the same heat capacity values.

6.3.3. Liquid Cs

The enthalpy and heat capacity of liquid cesium were measured in [13REN], [14REN] (C_p, T<373 K), [55DAU/MAR] (C_p, T<320 K), [62ALA/PCH] (C_p, 307–955 K), [63TEP/MUR] (ΔH, 351–1238 K), [64ACH] (ΔH, 340–1175 K), [64LEM/DEE] (ΔH, 295–1435 K), [65FIL/MAR] (C_p, T<320 K), [66ACH/FIS] (ΔH, 922–1359 K), [69SHP/KAG], (ΔH, 430–1330 K) (Fig. 6.4 and 6.5).

Fig. 6.5 shows that the $H^\circ(T,l)$-H°(298 K,cr) values of [63TEP/MUR] above 600 K, [64ACH], [64LEM/DEE], [69SHP/KAG] agree well while those of [63TEP/MUR] below 600 K and [66ACH/FIS] are scattered.

The heat capacity results shown in Fig. 6.4 are scattered within 20%. It is difficult to select a reliable study among those mentioned. A minimum formed by the heat capacity values of [64ACH] is much sharper than those adopted for Na, K and Rb. At a temperature of 800 K, which is close to the heat capacity minimum, a considerable scatter among the data is observed (Fig. 6.4): C_p = 30.6 J·K^{-1}·mol^{-1} [62ALA/PCH], 27.1 J·K^{-1}·mol^{-1} [64ACH], 30.3 J·K^{-1}mol^{-1} [63TEP/MUR], 29.27 J·K^{-1}·mol^{-1} [69SHP/KAG]. Of these data the higher values of [62ALA/PCH] and [63TEP/MUR] seem to be more reasonable than those of [64ACH]. Points obtained in [65FIL/MAR] appear to be very reliable.

[73HUL] adopted values of [64ACH] which are of low accuracy. Other reviews derived their recommendations from combination of several sources. [82GUR] combined results of [69SHP/KAG] and the semiquantitative measurements at high pressure [83BLA/FIL] and derived the equation:

$$C_p^\circ = 46.727 - 40.865\times10^{-3}T - 3.630\times10^{5}T^{-2} + 24.449\times10^{-6}T^2 \text{ J·K}^{-1}\text{·mol}^{-1}.$$

This equation corresponds to a minimum 29.1 J·K^{-1}·mol^{-1} at 800 K, and a steep increase in heat capacity above 800 K.

[85JAN] derived the values using [63TEP/MUR], [64ACH], [64LEM/DEE]. The values below 800 K are reasonable, but

above 800 K the changes are small and not consistent with the increase observed for Na, K and Rb.

[85FIN/LEI] used the enthalpy data of [64ACH], [64LEM/DEE], [69SHP/KAG] and obtained the equation

$$C_p^\circ = 36.519 - 21.139\times10^{-3}T + 15.891\times10^{-6}T^2, \text{ J}\cdot\text{K}^{-1}\cdot\text{mol}^{-1}.$$

This equation gives a relatively low value at the melting point and high at 1200 K, 31.6 and 34 $\text{J}\cdot\text{K}^{-1}\cdot\text{mol}^{-1}$, respectively.

Considering the data presented in Fig. 6.4 , it was suggested that the C_p curve should approach 32.3 $\text{J}\cdot\text{K}^{-1}\cdot\text{mol}^{-1}$ near the melting point [65FIL/MAR] and 30.5 $\text{J}\cdot\text{mol}^{-1}\,\text{K}^{-1}$ at 800 K· The last value was obtained from a linear approximation of the enthalpy data from 600 to 1000 K (Fig. 6.5). The suggested values 32.3 $\text{J}\cdot\text{K}^{-1}\cdot\text{mol}^{-1}$ at T_{fus} and 30.5 $\text{J}\cdot\text{K}^{-1}\cdot\text{mol}^{-1}$ at 800 K were compared with those calculated using two equations from [85FIN/LEI] recommended for Rb and Cs. They were closer to the curve recommended for Rb than for Cs.

The C_p vs T dependences for solid Rb and Cs are very close (compare Fig 5.3 and 6.3; above 100 K the heat capacity values of solid Cs are greater than those of Rb by 1–1.5%). It is suggested that the values for liquid Rb and Cs should also be close. In agreement with Fig. 6.4, the equation recommended for the description of liquid Rb in [85FIN/LEI] (Eq. 7 below) was adopted in this assessment and also for the heat capacity of liquid Cs.

$$C_p^\circ = 35.494 - 12.864\times10^{-3}T + 8.541\times10^{-6}T^2 \text{ J}\cdot\text{K}^{-1}\cdot\text{mol}^{-1} \quad (7)$$

The values of $C_p^\circ(T)$, $S^\circ(T)$ and $H^\circ(T)$-$H^\circ(298.15\text{ K})$ from 298.15 to 1600 K were calculated using Eqs. 6 and 7. They are listed in Table 6.6, and heat capacity values are shown in Fig. 6.4.

6.4. Phase Equilibrium Data

The temperature of fusion of cesium was measured in [13REN], [14REN], [64LEM/DEE], [65FIL/MAR], [70MAR] and has already been described in the preceding Sec. 6.2.; additional information is given below.

[30DEB/BRO]

De Boer *et al.* measured the melting point of Cs by thermal analysis; T_{fus} = 301.75 K.

[34RIN]

Rinck investigated the Na-Cs system by thermal analysis and determined the melting point of cesium T_{fus} = 301.45 K. The material was prepared by the reduction of CsCl by Ca; no analysis was provided.

[35LOS]

Losana used thermal analysis to determine the melting point of cesium T_{fus} = 301.95 ± 0.1 K. The material was prepared by the reduction of CsCl by Ca and purified by distillation; the presence of 0.03% Rb was detected.

[37TAY/LAN]

Taylor and Langmuir measured the vapor pressure of cesium, purified by many-stage fractional distillation; the melting point was determined as 301.75 K.

[54CLU/STE]

Clusius and Stern measured the enthalpy of melting of Cs in a Nernst calorimeter $\Delta_{fus}H$ = 2176 ± 4 $\text{J}\cdot\text{mol}^{-1}$; the melting point of Cs was determined as 301.79 ± 0.17 K. The sample was prepared by decomposition in vacuum of Cs azide; the analysis of the material was not given.

[62KEN/JAY]

Kennedy *et al.* investigated the pressure dependence of the melting point of Cs. According to thermal analysis at 100 kPa, Cs melted at 302.15 K, the temperature increased to 470 K at 2.25 MPa. Three different solid phases and two triple points were found at higher pressures up to 5 MPa.

[69BAS/VOL]

Basin *et al.* measured the density of cesium below and above the melting point. The material contained less than 0.01% of metallic impurities. The melting point 301.65 K was determined with the accuracy of ± 0.2 K; the premelting zone was about 3 degrees.

[71OTT/GOA]

Goates *et al.* investigated the Cs-Rb binary systems using a commercial cesium of Kawecki Chemical Company containing 99.9 wt. % Cs and impurities in atomic percent: Rb − 0.049, K − 0.01, Na − 0.025. The melting point was determined T_{fus} = 301.59 ± 0.1 K.

[73MAK/IVA]

Makarenko *et al.* measured the melting point of Cs as a function or pressure. The melting temperature increased from 301.52 K at ambient pressure to 471.2 K at 2.23 GPa. The enthalpy of melting was estimated as $\Delta_{fus}H$ = 2124 $\text{J}\cdot\text{mol}^{-1}$ from the temperature vs. pressure and volume vs. pressure data.

[73SIM]

Simon studied the Cs-O system by thermal and X-ray analysis. The Cs sample was prepared by double vacuum distillation of a material obtained by reduction of CsCl with Ca. The temperature of fusion was determined accurately as T_{fus} = 301.67 ± 0.01 K.

The enthalpy of melting was measured or estimated in studies [13REN], [14REN], [64ACH], [64LEM/DEE], [65FIL/MAR], [70MAR] described in Sec. 6.2.; some additional information is given below.

[37BIN]

Binayendra determined a value for the enthalpy of fusion in a calorimeter, 2.09 $\text{kJ}\cdot\text{mol}^{-1}$; no experimental details are given. Binayendra estimated $\Delta_{fus}H$ = 1.66 $\text{kJ}\cdot\text{mol}^{-1}$ from physical parameters.

[71MAL/GIG]

Malaspina *et al.* determined the enthalpy of fusion of Cs in a Calvet calorimeter. The material was *Fluka and Koch Light Lab*, 99.9+ wt.% Cs. The enthalpy of melting was determined from the area under the thermogram. Four measurements yielded an average value of $\Delta_{fus}H$ = 2134 ± 30 J·mol^{-1}.

6.5. Discussion of Phase Equilibrium Data

Table 6.3 lists temperatures of fusion of Cs converted to ITS-90. Similar to [85OHS/BAB], the results of studies [65FIL/MAR], [70MAR], [71OTT/GOA] and [73SIM] were selected as more reliable. The uncertainty in the value was increased to 0.1 K to correct for the influence of impurities in samples. Values adopted in [73HUL], [82GUR] and [85JAN] are close to the selected one within the error limits.

Table 6.4 lists experimental enthalpies of fusion. The adopted value of $\Delta_{fus}H$ = 2090 J·mol^{-1} is based on the accurate measurements of [65FIL/MAR] and [70MAR]. Less accurate studies [14REN] and [37BIN] agree with the selection very well. The uncertainty was increased to ± 25 J·mol^{-1}; the allowance was made for probable chemical reactions of the impurities. Previous recommendations are based on the same information and give almost the same value.

6.6. Adopted Values

Electronic contribution to C_p: γ = 3.6 ± 0.1 mJ·K^{-2}·mol^{-1}.
Debye temperature at 0 K: Θ_D = 40.0 ± 1.0 K.

Heat Capacity Equations

Solid Cs

Temperature range 0 − 3 K:

$$C_p = 3.6\times10^{-3}T + 3.037\times10^{-2}T^3 + 1.08\times10^{-3}T^5 \text{ J·K}^{-1}\text{·mol}^{-1}.$$

Temperature range 3 − 20 K:

$$C_p = -8.539 + 2.5044T + 24.2717T^{-2} - 6.0446\times10^{-2}T^2 + 2.5435\times10^{-4}T^3 \text{ J·K}^{-1}\text{·mol}^{-1}.$$

Temperature range 20 − 80 K:

$$C_p = 19.976 + 0.21825T - 1.482\times10^{3}T^{-2} - 3.2614\times10^{-3}T^2 + 1.7947\times10^{-5}T^3 \text{ J·K}^{-1}\text{·mol}^{-1}.$$

Temperature range 80 − 180 K:

$$C_p = 40.19 - 0.2794T - 1.7322\times10^{4}T^{-2} + 1.9775\times10^{-3}T^2 - 4.4801\times10^{-6}T^3 \text{ J·K}^{-1}\text{·mol}^{-1}.$$

Temperature range 180 − 260 K:

$$C_p = -517.377 + 5.2517T + 2.287\times10^{6}T^{-2} - 1.89017\times10^{-2}T^2 + 2.4216\times10^{-5}T^3 \text{ J·K}^{-1}\text{·mol}^{-1}.$$

Temperature range 260 − 301.6 K:

$$C_p = 9.299 - 82.261\times10^{-3}T + 9.239\times10^{5}T^{-2} + 416.603\times10^{-6}T^2 \text{ J·K}^{-1}\text{·mol}^{-1}.$$

Liquid Cs

Temperature range 301.6 − 1600 K:

$$C_p = 35.494 - 12.864\times10^{-3}T + 8.541\times10^{-6}T^2 \text{ J·K}^{-1}\text{·mol}^{-1}.$$

Values at 298.15 K

C_p°(298.15 K)= 32.20 ± 0.1 J·K^{-1}·mol^{-1}
S°(298.515 K)= 85.10 ± 0.3 J·K^{-1}·mol^{-1}
H°(298.15 K)-H°(0)= 7717 ± 25 J·mol^{-1}

Phase Equilibrium Data

Temperature of fusion − 301.6 ± 0.1 K.
Enthalpy of fusion − 2090 ± 25 J·mol^{-1}

6.7. Calculated Thermodynamic Functions of Cs

The thermodynamic functions presented in Tables 6.5 and 6.6 are calculated using the equations presented in the previous section. Values in brackets are calculated by using the equations for the next higher adjacent temperature intervals.

6.8. References for Cs

13REN E. Rengade, Compt. Rend. 156, 1897–9 (1913); T_{fus}, $\Delta_{fus}H$, C_p (288–373 K).

14REN E. Rengade, Bull. Soc. Chim. **15**, 130–47 (1914); T_{fus}, $\Delta_{fus}H$, C_p (288–373 K).

30DEB/BRO J. H. De Boer, J. Broos, and H. Emmens, Z. Anorg. Chem. **191**, 113–121, (1930); T_{fus}.

34RIN E. Rinck, Compt. Rend. **199**, 1217–1219 (1934); T_{fus}.

35LOS L. Losana, Gazz. Chim. Ital. **65**, 851–64 (1935); T_{fus}.

37BIN N. S. Binayendra, Gazz. Chim. Ital. **67**, 714–5 (1937); $\Delta_{fus}H$.

37TAY/LAN J. B. Taylor and I. Langmuir, Phys. Rev. **51**, 753–60 (1937); T_{fus}.

54CLU/STE K. Clusius and H. Stern, Z. Angew. Physik **6**, 194–6 (1954); T_{fus}.

55DAU/MAR T. M. Dauphinee, D. L. Martin, and H. Preston-Thomas, Proc. Roy. Soc. London **A233**, 214–22 (1955); C_p (20–320 K).

62ALA/PCH I. M. Pchelkin, Ph.D. Thesis, I. T. Aladyev, supervisor, ENIN (Moscow Power Institute), Moscow (1962) (quoted from [70SHP/YAK], 102–3); C_p (307–955 K).

62KEN/JAY G. C. Kennedy, A. Jayaraman, and R. C. Newton, Phys. Rev. **126**, 1363–6 (1962); T_{fus}.

62MCC/SIL D. C. McCollum, Jr., and H. B. Silsbee, Phys. Rev. **127**, 119–20 (1962); C_p (1.3–12 K).

63TEP/MUR F. Tepper, A. Murchison, J. Zelenak, and F. Roehlich, "Thermophysical Properties of Rubidium and Cesium," *RT*D-TDR-63-4018, Part I, MSA Research Corp., Callery, PA, (Nov. 1963); ΔH (351–1238 K).

64ACH P. Y. Achener, "The Determination of the Latent Heat of Vaporization, Vapor Pressure, Enthalpy, Specific Heat, and Density of Liquid Rubidium and Cesium up to 1800 F," AGN-8090, Aerojet-General Nucleonics (Jan. 1964); ΔH (340–1175 K).

64LEM/DEE A. W. Lemmon, Jr., H. W. Deem, E. A. Eldridge, E. H. Hall, J. Matolich, Jr., and J. F. Walling, "The Specific Heat, Thermal Conductivity, and Viscosity of Liquid Cesium," Battelle Memorial Institute, Rept. BATT-4673-T7 (Feb. 1964); T_{fus}, $\Delta_{fus}H$, ΔH (295–1435 K).

64LIE/PHI W. H. Lien and N. E. Phillips, Phys. Rev. **A133**, 1370–7 (1964); C_p (0.2–4.1 K).

64MAR/ZYC D. L. Martin, D.A. Zych, and C.V. Heer, Phys. Rev. **A135**, 671–9 (1964); C_p (0.35–2 K).

65FIL/MAR J. D. Filby and D. L. Martin, Proc. Roy. Soc. (London) **A284**, 83–107 (1965); C_p (0.4–320 K), T_{fus}, $\Delta_{fus}H$.

66ACH/FIS P. Y. Achener and D. L. Fisher, "The Specific Heat of Liquid Cesium," USAEC Rept. AGN-8192, **5**, Aerojet-General Nucleonics, San Ramon, CA (1966); ΔH (922–1339 K).

69BAS/VOL A. S. Basin, S. P. Volchkova, and A. N. Soloviev, J. Appl. Mech. and Tech. Phys. **10**, 961–966 (1969); T_{fus}.

69SHP/KAG E. E. Spil'rain and D. N. Kagan, High Temp. **7**, 328–30 (1969); ΔH (430–1330 K).

70GOA/OTT J. R. Goates, J.B. Ott, and E. Delawarde, Trans. Farad. Soc. **66**, 1612–6 (1970); T_{fus}.

70MAR D. L. Martin, Can. J. Phys. **48**, 1327–39 (1970); C_p (0.4–3 K), T_{fus}, $\Delta_{fus}H$.

70SHP/YAK E. E. Shpil'rain, K. A. Yakimovich, E. E. Totskii, D. L. Timrot, and V. A. Fomin, "Thermophysical Properties of Alkali Metals," V.A. Kirillin, ed., Izd. Standartov. Moscow (1970); Review.

71MAL/GIG L. Malapsina, R. Gigli, and V. Placente, Gazz. Chim. Ital. **101**, 197–203 (1971); $\Delta_{fus}H$.

71OTT/GOA J. B. Ott, J. R. Goates, and D. E. Oyler, Trans. Farad. Soc. **67**, 31–4 (1971); T_{fus}.

73HUL R. Hultgren, P. D. Desai, D.T. Hawkins, M. Gleiser, K. K. Kelley, and D. D. Wagman, "Selected Values of the Thermodynamic Properties of the Elements," Amer. Soc. Metals, Metals Park, Ohio, 142–8 (1973); Review.

73MAK/IVA I. N. Makarenko, V. A. Ivanov, and S. M. Stishov, Soviet Physics, Letters to the Editor. **18**, 187–9 (1973); T_{fus}, $\Delta_{fus}H$.

73SIM A. Simon, Z. Anorg. Allg. Chem. **395**, 301–19 (1973); T_{fus}.

82GUR L. V. Gurvich, I. V. Veits, V. A. Medvedev, et al., V. P. Glushko, gen. ed., "Thermodynamic Properties of Individual Substances," Nauka, Moscow, **4** (1), 463–6 (1982); Review.

83BLA/FIL L. A. Blagonravov, L. P. Filippov, V. A. Alekseev, and V. N. Shnerko, J. Eng. Phys. **44**, 304–308 (1983); C_p (1200–1900 K), High Pressure.

85FIN/LEI J. K. Fink and L. Leibowitz, "Handbook of Thermodynamic and Transport Properties of Alkali Metals," ed. R. W. Ohse, Blackwell Sci. Publ., Oxford, (1985) 411–434; Liquid Cs, Review.

85JAN M. W. Chase, Jr., C. A. Davis, J. R. Downey, Jr., D. J. Frurip, R. A. McDonald, and A. N. Syverud, "JANAF Thermochemical Tables," J. Phys. Chem. Ref. Data 14, Suppl. 1, 943–6 (1985); Review.

85OHS/BAB R. W. Ohse, J.-F. Babelot, J. Magill, and M. Tetenbaum, M., Pure Appl. Chem. **57**, 1407–26 (1985); T_{fus}, Review.

89COX/WAG J. D. Cox, D. D. Wagman, and V. A. Medvedev, "CODATA Key Values for Thermodynamics," Hemisphere Publ. Corp., New York, 263 (1989); Review.

6.9. Appendix – Experimental Results of Cs

Tables 6.7 to 6.23 present heat capacity or enthalpy data as they were presented in the original article. As a result, the numerical values listed in this Appendix are the actual experimental values, tabular smoothed values, values calculated from equations, or values extracted from a graph. Where necessary, values are converted to joules (from calories). In all cases, the table heading indicates the type of data listed.

The enthalpy data for Cs are given mostly as $\Delta H = H°(T)-H°(T_{ref})$, where T_{ref} is usually equal to 273 or 298 K. When temperature $T>T_{fus}$, then the values of ΔH include the enthalpies of fusion (Tables 6.12, 13, 15, 19, 20). The correction term $H°(298.15\ K) - H°(273\ K)$ was determined as 784 $J \cdot mol^{-1}$.

TABLE 6.1. Electronic contribution to heat capacity and the Debye temperature of Cs.

Reference	γ, mJ·K^{-2}·mol^{-1}	Θ_D, K	T/K
Original studies			
64LIE/PHI	3.20 ± 0.07	39.5 ± 0.3	0.2–0.7
64MAR/ZYC	6.29	40.6	0.4–2.0
65FIL/MAR	–	38.4 ± 0.6	0.4–1.5
70MAR	3.97 ± 0.08	40.5 ± 0.3	0.4–3.0
Review			
73HUL	3.38	Based on 64LIE/PHI	
Adopted			
Based on 64LIE/PHI, 70MAR		3.60 ± 0.10	40.0 ±1.0

TABLE 6.2. Comparison of the heat capacity, enthalpy and entropy values for Cs at 298.15 K

Reference	C_p°(298.15 K), J·K^{-1}·mol^{-1}	S°(298.15 K), J·K^{-1}·mol^{-1}	H°(298.15 K)-H°(0) J·mol^{-1}
73HUL	32.175	85.06 ± 0.4	7711
82GUR	32.210	85.23 ± 0.4	7711 ± 20
85JAN	32.195	85.147 ± 0.21	7717
89COX/WAG	32.210	85.23 ± 0.4	7711 ± 20
Adopted:	32.20 ± 0.1	85.10 ± 0.3	7717 ± 25

TABLE 6.3. Temperature of fusion of Cs

References	T_{fus}, K	Comments
Original studies		
13REN, 14REN	301.6 ± 0.1	Enthalpy measurements
30DEB/BRO	301.73	Thermal analysis
34RIN	301.43	Thermal analysis
35LOS	301.93 ± 0.1	Thermal analysis
37TAY/LAN	301.73	Thermal analysis
54CLU/STE	301.77 ± 0.17	Enthalpy measurements
62KEN/JAY	302.13	Thermal analysis
64LEM/DEE	301.65	Thermal analysis
65FIL/MAR	301.53 ± 0.01	Partial melting
69BAS/VOL	301.64 ± 0.2	Density measurements
70MAR	301.66 ± 0.13	Partial melting
71OTT/GOA	301.58 ± 0.1	Thermal analysis
73MAK/IVA	301.51	Thermal analysis
73SIM	301.66 ± 0.01	Thermal analysis
Reviews		
73HUL	301.55 ± 0.05	Based on 65FIL/MAR
82GUR	301.59 ± 0.02	Based on 71OTT/GOA
85JAN	301.55 ± 0.01	Based on 65FIL/MAR
85OHS/BAB	301.60 ± 0.05	Based on 65FIL/MAR, 70MAR, 71OTT/GOA
Adopted		
	301.6 ± 0.1	Based on 65FIL/MAR, 70MAR, 71OTT/GOA, 73SIM

TABLE 6.4. Enthalpy of fusion of Cs

References	$\Delta_{fus}H$, J·mol^{-1}	Comments
Original studies		
13REN, 14REN	2091	Enthalpy measurements
37BIN	2090 (1660)	Calorimeter (estimate)
54CLU/STE	2176 ± 4	Enthalpy measurements
64LEM/DEE	1969	Enthalpy measurements
64ACH	2096	Estimate
65FIL/MAR	2087 ± 2	Adiabatic calorimeter
70MAR	2096 ± 4	Adiabatic calorimeter
71MAL/GIG	2134 ± 30	Calvet calorimeter
73MAK/IVA	2124	High pressure (estimate)
Reviews		
73HUL	2092 ± 20	Based on 65FIL/MAR, 14REN
82GUR	2096 ± 5	Based on 65FIL/MAR, 70MAR
85JAN	2087 ± 4	Based on 65FIL/MAR
Adopted		
	2090 ± 25	Based on 65FIL/MAR, 70MAR

TABLE 6.5. Thermodynamic functions of Cs below 298.15 K

Temp., K	$C_p^\circ(T)$, J·K^{-1}·mol^{-1}	$H^\circ(T)$-$H^\circ(0)$, J·mol^{-1}	$S^\circ(T)$, J·K^{-1}·mol^{-1}
5	3.475	5.016	1.3712
10	10.958	41.629	6.1460
15	16.393	110.998	11.6971
20	19.466 (19.475)	201.610	16.889
30	22.426	413.493	25.440
40	23.710	644.919	32.089
50	24.386	885.722	37.460
60	24.795	1131.76	41.944
70	25.126	1381.36	45.791
80	25.520 (25.494)	1634.49	49.171
90	25.657	1890.27	52.183
100	25.813	2147.61	54.894
110	25.989	2406.60	57.363
120	26.193	2667.49	59.632
130	26.420	2930.54	61.738
140	26.656	3195.92	63.704
150	26.884	3463.63	65.551
160	27.083	3733.50	67.293
170	27.232	4005.12	68.940
180	27.306 (27.328)	4277.88	70.499
190	27.544	4552.12	71.982
200	27.798	4828.82	73.401
210	28.039	5108.03	74.763
220	28.259	5389.53	76.073
230	28.483	5673.21	77.334
240	28.760	5959.36	78.552
250	29.159	6248.81	79.552
260	29.762 (29.741)	6543.21	80.888
270	30.132	6842.41	82.017
280	30.712	7146.48	83.123
290	31.465	7457.23	84.213
298.15	32.199	7716.59	85.095

TABLE 6.6. Thermodynamic functions of Cs above 298.15 K

T/K	$C_p^\circ(T)$ J·K^{-1}·mol^{-1}	$H^\circ(T)$-H°(298.15 K) J·mol^{-1}	$S^\circ(T)$ J·K^{-1}·mol^{-1}
298.15	32.20	0.00	85.10
300.00	32.38	59.74	85.30
301.60 (sol)	32.54	111.67	85.47
301.60 (liq)	32.39	2201.67	92.40
400.00	31.72	5354.34	101.45
500.00	31.20	8498.52	108.47
600.00	30.85	11599.48	114.13
700.00	30.67	14674.29	118.87
800.00	30.67	17740.03	122.96
900.00	30.83	20813.79	126.58
1000.00	31.17	23912.65	129.84
1100.00	31.68	27053.68	132.84
1200.00	32.36	30253.98	135.62
1300.00	33.20	33530.63	138.24
1400.00	34.22	36900.70	140.74
1500.00	35.41	40381.27	143.14
1600.00	36.78	43989.44	145.47

TABLE 6.7. SMOOTHED heat capacity of Cs [14REN]

T/K	C_p°, J·K^{-1}·mol^{-1}	T/K	C_p°, J·K^{-1}·mol^{-1}
290	31.62	310	32.89
295	32.38	330	32.51
301.6 (sol)	33.39	350	32.14
301.6 (liq)	33.05	370	31.76

TABLE 6.8. SMOOTHED heat capacity of Cs [55DAU/MAR]

T/K	C_p°, J·K^{-1}·mol^{-1}	T/K	C_p°, J·K^{-1}·mol^{-1}
20	19.75	160	26.95
25	21.25	170	27.00
30	22.40	180	27.15
35	23.25	190	27.30
40	23.75	200	27.40
45	24.05	210	27.60
50	24.30	220	27.80
55	24.40	230	28.10
60	24.65	240	28.50
70	25.00	250	28.90
80	25.30	260	29.40
90	25.55	270	—
100	25.80	273.15	31.20
110	26.00	280	32.60
120	26.20	290	41.00
130	26.50	310	31.90
140	26.70	320	31.90
150	26.80		

TABLE 6.9. EXPERIMENTAL heat capacity of Cs [62ALA/PCH]

T/K	C_p°, J·K^{-1}·mol^{-1}	T/K	C_p°, J·K^{-1}·mol^{-1}
307	35.0	674	30.6
325	32.3	708	30.0
379	33.3	734	31.1
423	31.7	785	30.0
475	30.6	819	31.1
486	31.6	832	31.7
515	31.1	866	30.6
557	30.6	914	30.6
587	28.4	952	32.3
616	32.3	955	32.3

TABLE 6.10. SMOOTHED heat capacity of Cs [62ALA/PCH]

T/K	C_p°, J·K^{-1}·mol^{-1}	T/K	C_p°, J·K^{-1}·mol^{-1}
323	33.9	673	30.6
373	32.8	773	30.6
473	31.7	873	31.1
573	31.1	973	31.7

TABLE 6.11. SMOOTHED heat capacity of Cs [62MCC/SIL]

T/K	C_p°, mJ·K^{-1}·mol^{-1}	T/K	C_p°, mJ·K^{-1}·mol^{-1}
2.0	0.34	8.0	10.95
4.0	2.11	10.0	21.36
6.0	5.30	12.0	42.28

TABLE 6.12. EXPERIMENTAL enthalpy values [$H^\circ(T)$-H°(298 K)] of Cs [63TEP/MUR]

T/K	ΔH, J·mol^{-1}	T/K	ΔH, J·mol^{-1}
351.1	4665	691.1	15260
376.5	5970	721.5	16670
389.7	6477	737.1	16440
399.9	6811	855.0	20905
420.8	8050	879.7	21520
454.2	10255	916.8	22065
506.1	11924	970.0	23730
513.1	11598	1027.0	25630
533.0	12260	1116.0	28315
534.8	12297	1190.0	30430
545.0	12050	1238.0	32015
689.6	14455		

TABLE 6.13. EXPERIMENTAL enthalpy values [$H°(T)$-$H°$(273 K)] of Cs [64ACH]

T/K	ΔH, J·mol^{-1}	T/K	ΔH, J·mol^{-1}
339.8	4420	640.4	14070
367.6	5830	675.4	14960
396.5	6730	698.8	15560
422.5	7390	752.1	16920
451.0	8190	812.6	18600
473.8	9460	865.4	19890
477.6	9590	921.0	21780
506.6	10440	978.2	23840
533.2	11240	1033.2	25200
562.6	12000	1086.5	28440
589.9	12390	1175.4	31620
617.6	13740		

TABLE 6.14. SMOOTHED heat capacity of Cs [64ACH]

T/K	$C_p°$, J·K^{-1}·mol^{-1}	T/K	$C_p°$, J·K^{-1}·mol^{-1}
400	35.87	800	27.14
500	30.45	900	30.35
600	27.19	1000	35.72
700	26.08	1100	43.25

TABLE 6.15. EXPERIMENTAL enthalpy values [$H°(T)$-$H°$(273 K)] of Cs [64LEM/DEE]

T/K	ΔH, J·mol^{-1}	T/K	ΔH, J·mol^{-1}
295.5	700	725	15070
299	784	890	20800
300	845	897	20300
303	2897	1065	26915
367	4782	1178	31140
372	5100	1251	32975
469	8565	1357	36090
474	8620	1435	39200
564	10340		

TABLE 6.16. EXPERIMENTAL heat capacity of Cs [64LIE/PHI]

T/K	C_p°, mJ·K^{-1}·mol^{-1}	T/K	C_p°, mJ·K^{-1}·mol^{-1}
	Adiabatic demagnetization cryostat		
0.1874	0.8048	0.3339	2.247
0.2073	0.9445	0.3598	2.629
0.2351	1.159	0.3916	3.158
0.2568	1.357	0.4190	3.695
0.2832	1.624	0.4539	4.433
0.3143	1.988	0.4963	5.490
0.1923	0.8402	0.5480	7.035
0.2141	1.003	0.5952	8.728
0.2416	1.226	0.6461	0.87
0.2629	1.428	0.6951	13.31
0.2883	1.691	0.7468	16.19
0.3166	2.031	0.8072	20.20
0.3434	2.390	0.8801	25.82
0.3719	2.833	0.9524	32.96
0.4056	3.431	1.034	41.98
0.4370	4.051	1.118	53.35
0.4755	4.964	1.217	69.85
0.5214	6.210	1.146	57.92
0.5612	7.474	1.099	50.97
0.6059	9.156	1.200	66.98
0.6550	11.29	1.022	38.42
0.7130	14.24	0.5293	6.451
0.2080	0.9499	0.5800	8.147
0.2225	1.061	0.6321	10.26
0.2361	1.177	0.6884	12.93
0.2519	1.313	0.7503	16.43
0.2739	1.524	0.8136	20.64
0.2984	1.786	0.8457	23.10
0.3155	1.996	0.9181	29.45
	Liquid-helium temperature cryostat		
1.2031	65.61	1.2459	73.14
1.2932	82.03	1.3371	91.29
1.3883	102.8	1.4373	114.7
1.4897	128.8	1.5444	144.1
1.6006	161.6	1.6575	180.2
1.7185	202.8	1.7799	226.0
1.8435	253.2	1.9111	282.1
1.9803	317.3	2.0522	351.8
2.1302	397.5	2.2053	439.2
2.2875	492.0	2.3645	541.2
2.4529	605.4	2.5355	662.7
2.6285	735.7	2.7183	805.4
2.8182	892.4	2.9183	978.2
3.0238	1077	3.1364	1185
3.2512	1299	3.3691	1421
3.5012	1566	3.6290	1702
3.7667	1861	3.8761	1978
4.0437	2180	4.0880	2217
1.1779	61.56		

TABLE 6.17. SMOOTHED heat capacity of Cs [64MAR/ZYC]

T/K	C_p°, mJ·K^{-1}·mol^{-1}	T/K	C_p°, mJ·K^{-1}·mol^{-1}
0.5	6.82	1.5	135
1.0	37.7		

TABLE 6.18. SMOOTHED heat capacity of Cs [65FIL/MAR]

T/K	C_p°, J·K^{-1}·mol^{-1}	T/K	C_p°, J·K^{-1}·mol^{-1}
	Temperature range 0.4–1.5 K		
0.4	0.00380	1.0	0.0379
0.5	0.00648	1.1	0.0506
0.6	0.00975	1.2	0.0665
0.7	0.0140	1.3	0.0858
0.8	0.0199	1.4	0.1092
0.9	0.0278	1.5	0.1385
	Temperature range 3–26 K		
3	1.11	12	13.49
4	2.16	14	15.48
5	3.49	16	17.16
6	4.99	18	18.48
7	6.52	20	19.49
8	8.10	22	20.31
9	9.61	24	21.02
10	11.03	26	21.62
	Temperature range 20–320 K		
20	19.51	160	27.06
25	21.23	170	27.18
30	22.43	180	27.33
35	23.24	190	27.53
40	23.75	200	27.79
45	24.09	210	28.05
50	24.35	220	28.27
55	24.56	230	28.46
60	24.77	240	28.72
65	24.98	250	29.20
70	25.17	260	29.74
75	25.34	270	30.13
80	25.48	273.15	30.30
85	25.59	280	30.71
90	25.68	290	31.46
95	25.75	298.15	32.21
100	25.82	300	32.38
110	25.96	301.55 (sol)	32.53
120	26.16	301.55 (liq)	32.41
130	26.42	310	32.30
140	26.69	320	32.13
150	26.91		

TABLE 6.19. EXPERIMENTAL enthalpy values [$H°(T)$-$H°$(273 K)] of Cs [66ACH/FIS]

T/K	ΔH, J·mol^{-1}	T/K	ΔH, J·mol^{-1}
922	21900	1144.5	27150
977.5	21150	1145	28650
978	30750	1144.5	30300
1033	18750	1176	29100
1033	30750	1172.5	27000
1033	30150	1174	33000
1033	24450	1200	32250
922	22350	1228	31050
980.5	25500	1214	33450
1033	25200	1255.5	24450
1033	29850	1284	32250
1091	28650	1311	26400
1016.5	25050	1339	20850
1016.5	32550	1255	32400
1016	29250		

TABLE 6.20. EXPERIMENTAL enthalpy values $[H°(T)-H°(273\ K)]$ of Cs [69SHP/KAG]

T/K	ΔH, J·mol^{-1}	T/K	ΔH, J·mol^{-1}
429.8	7310	754.5	16820
471.5	8550	800.7	17840
486.5	8750	833.4	19170
518.3	9810	905.8	21250
580.1	12010	997.8	24070
609.1	12580	1181.0	30200
703.9	15720	1330.2	34980

TABLE 6.21. SMOOTHED heat capacity of Cs [69SHP/KAG]

T/K	$C_p°$, J·K^{-1}·mol^{-1}	T/K	$C_p°$, J·K^{-1}·mol^{-1}
400	31.60	900	29.73
500	30.39	1000	30.61
600	29.60	1100	31.90
700	29.23	1200	33.61
800	29.27	1300	35.73

TABLE 6.22. SMOOTHED heat capacity of Cs [70MAR]

T/K	$C_p°$, mJ·K^{-1}·mol^{-1}	T/K	$C_p°$, mJ·K^{-1}·mol^{-1}
0.5	6	2.0	334
1.0	38	2.5	652
1.5	135	3.0	1129

TABLE 6.23. SMOOTHED heat capacity of Cs [83BLA/FIL]

T/K	$C_p°$, J·K^{-1}·mol^{-1}	T/K	$C_p°$, J·K^{-1}·mol^{-1}
1200	33.1	1400	36.3
1300	34.2	1500	40.5

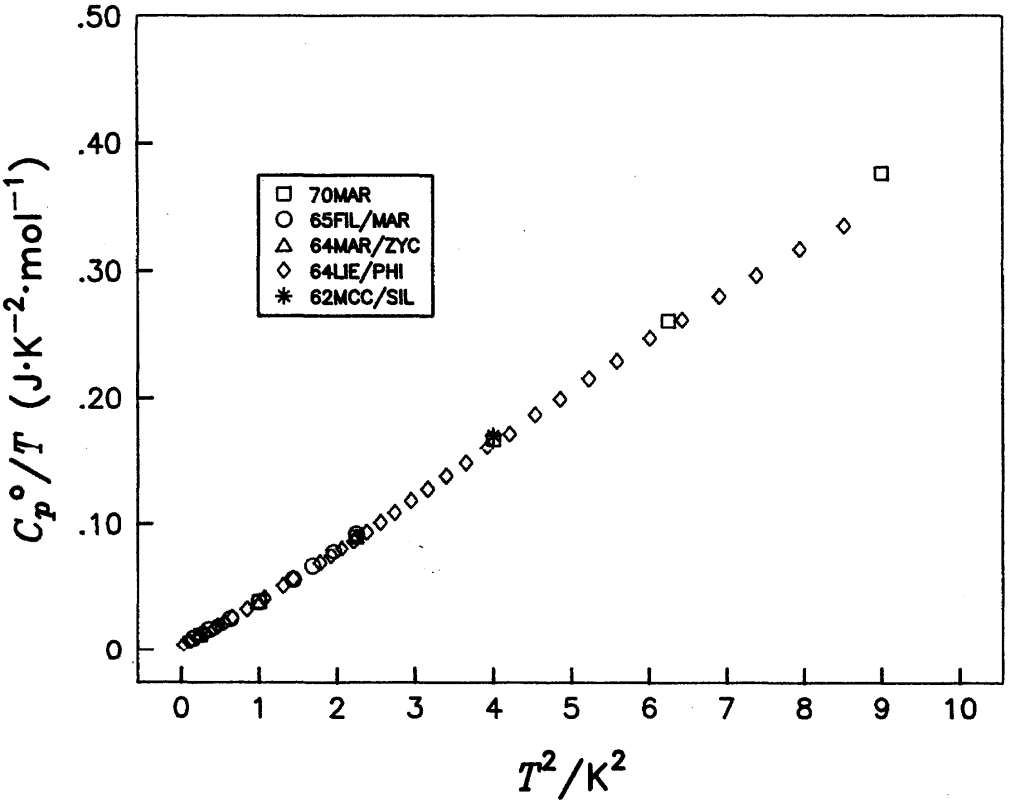

FIGURE 6.1. C_p/T versus T^2 for Cs below 3 K

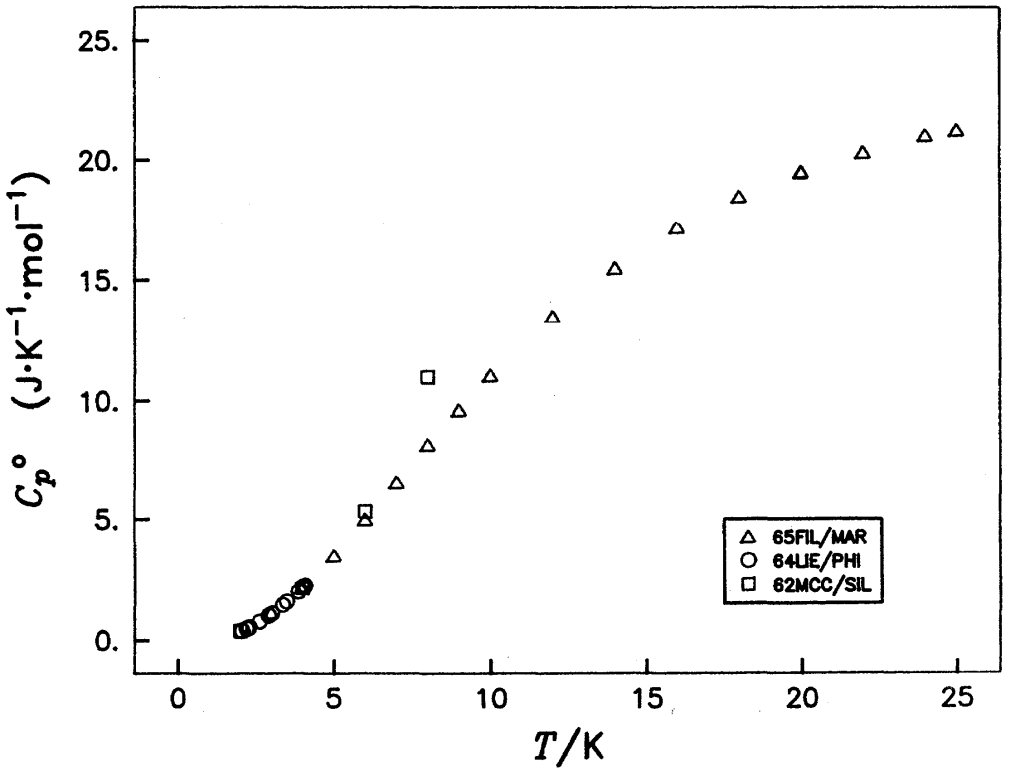

FIGURE 6.2. Heat Capacity of Cs below 30 K

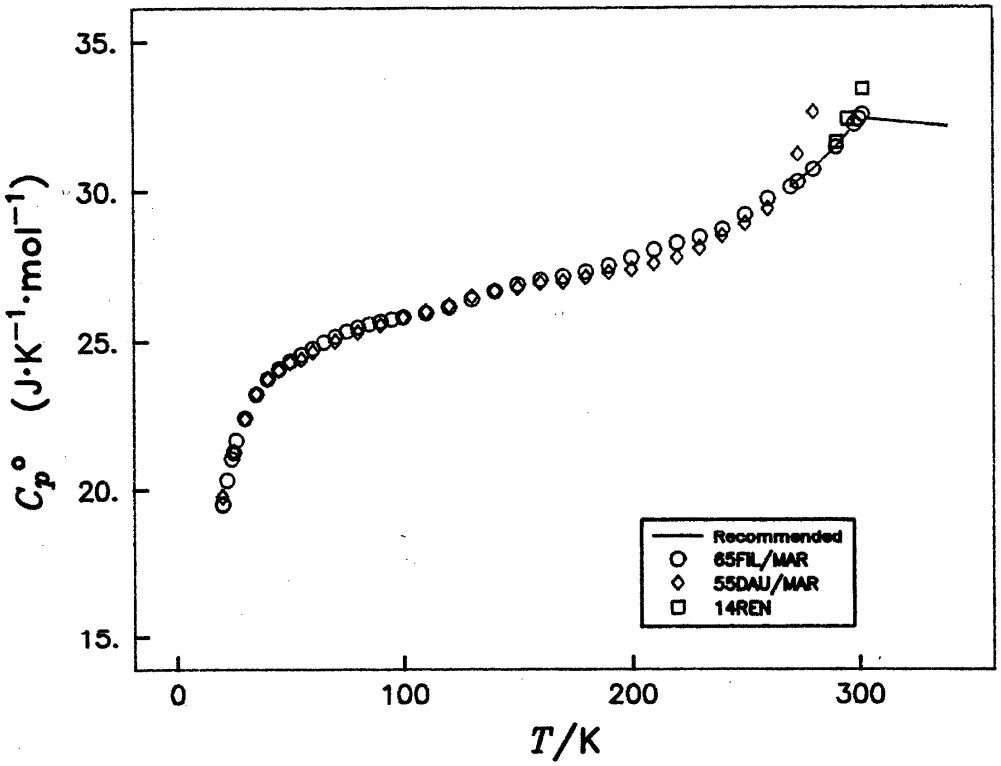

FIGURE 6.3. Heat Capacity of Solid Cs

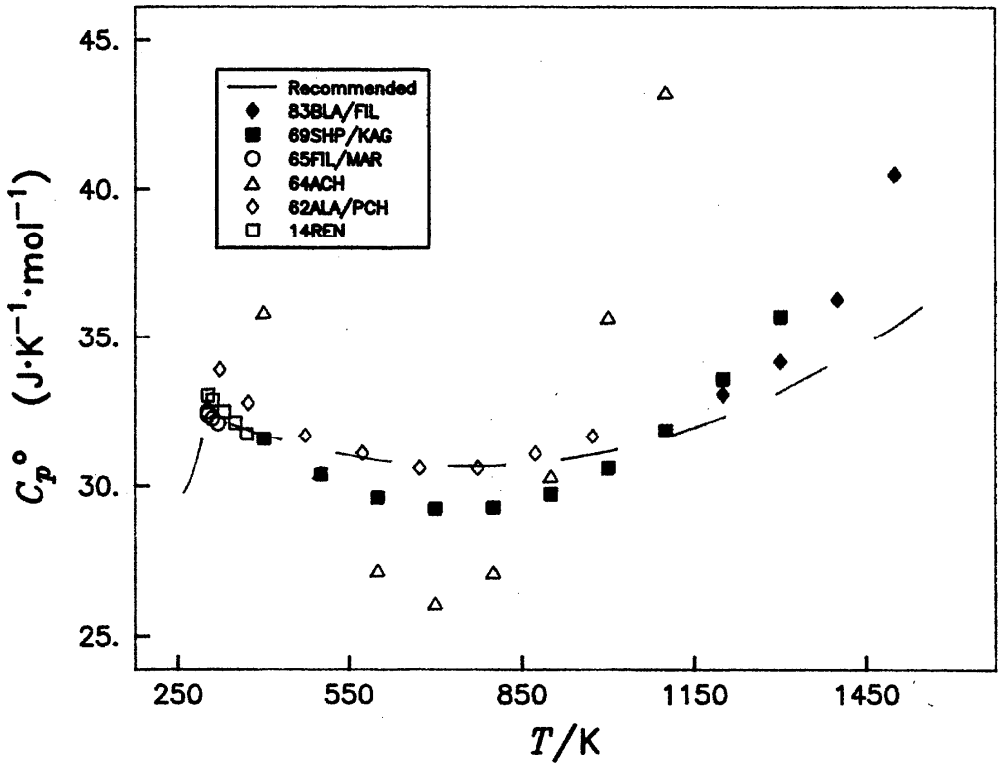

FIGURE 6.4. Heat Capacity of Liquid Cs

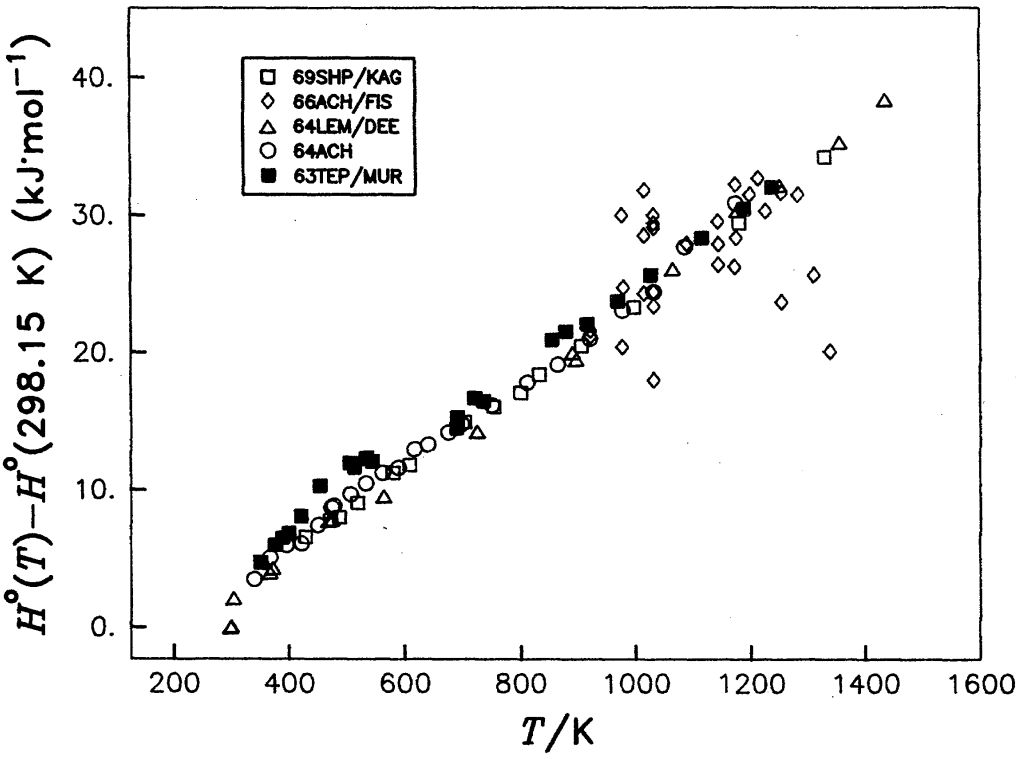

FIGURE 6.5. $H°(T)-H°(298.15\ K)$ of Cs

7. Conclusion

7.1. Comparison of Properties of the IA Group

The thermodynamic properties of the elements of the IA group which have been adopted are combined in Tables 7.1 to 7.4 and Figures 7.1, 7.2. Table 7.1 gives the Debye temperature [Θ_D] and electronic heat capacity coefficient [γ] at 0 K. The value of Θ_D differs considerably from element to element, the general tendency being a decrease with increasing atomic number, which is to be expected. The values of γ do not change in a consistent manner. The relatively low accuracy of the heat capacity measurements could lead to deviations in the values of γ, but the main reason for the discrepancy is probably the martensitic transformation in Li and Na. Near $T/K = 0$, samples of Li and Na contain two phases: β (bcc) and α(hcp). The percentage of individual phases in two-phase samples is known poorly, and the heat capacity measurements have not been complemented with structural measurements. As the predominant phase in a two-phase mixture is usually β(bcc), the experimental heat capacity data were assigned to this phase. These data should be treated as *apparent*, and a correcting term is needed to convert the *apparent* into a *true* heat capacity of the β phase. The Θ_D and γ values of the β-phase derived from the low-temperature heat capacity data for Li and Na cannot be accurate. Below 3 K, the C_p/T vs T^2 dependences for K, Rb, Cs are not linear. The deviation from linearity requires further investigation.

The martensitic β(bcc)$\rightarrow\alpha$(hcp) transformation is described by several parameters which are given in Table 7.2. Below the martensitic start temperature, M_s, Li and Na consist of two phases. The amount of the hcp phase (α-Li and α-Na) increases and the amount of the bcc phase (β-Li and β-Na) decreases with decreasing temperature. Table 7.2 omits one major component, degree of transformation (% of β in a mixture of α and β) which depends on temperature. The degree of transformation is known only very roughly and therefore the measured thermal effects only could be converted to the enthalpy of transformation per·mol with a high uncertainty. Further investigations are clearly needed.

Figure 7.1 shows the heat capacities below 298.15 K. The results assigned to the β phase are consistent with the relative positions of the elements in the Periodic Table; Li has the lowest heat capacity while Cs the highest. It should be remembered that the results for Li and Na below M_s are distorted by the martensitic transformation. The data for α-Li and α-Na are not available. Above 100 K the difference in the heat capacity of K and Rb is about 3%, and the difference between Rb and Cs is even smaller (about 1.5%). Table 7.3 shows that the values of heat capacity, entropy and enthalpy increment at 298.15 K change consistently with the position of the elements in the Periodic Table.

Figure 7.2 shows heat capacities above 298 K. At 30 to 40 K below the melting point of Na, K, Rb and Cs, the heat capacity values start to increase with temperature at a greater rate than at lower temperatures. This tendency is more pronounced in the heavier elements. This increase could be a natural property of these elements, but a possibility exists that the phenomenon could be partially induced by the presence of impurities or caused by inaccurate data acquisition. Additional accurate measurements near the melting point should better determine the scope of the premelting phenomena. Figure 7.2 shows also that at the melting point the heat capacities of liquid and solid phases of Na, K, Rb and Cs are very close. The heat capacity of solid Li is noticeably smaller (by about 1 $J \cdot K^{-1} \cdot mol^{-1}$) than for liquid Li. This observation needs confirmation by additional accurate measurements.

Table 7.4 shows that the temperature and the enthalpy of fusion in the IA group decrease in a regular manner with an increase of the atomic number. The absence of a recognizable sequence in the entropy of fusion of Na, K, Rb and Cs is probably due to fluctuations in the data for the enthalpy of fusion about an average value $\sim$0.84 R. The entropy of fusion of Li is definitely smaller than other elements.

Heat capacities for the liquid alkali metals are known only approximately (Fig. 7.2). Despite the low accuracy of the data, they are compatible with the position of the elements in the Periodic Table. All elements except Li show a minimum in the heat capacity values at about 700 − 900 K. A similar but less pronounced minimum may exist in Li. Description of the data for liquid Cs by the equation adopted for Rb is a temporary solution. The uncertainties in data for these two elements are suggested to be much greater than the difference in their heat capacities; this could lead to the values for Cs being underestimated by 1–3%. Accurate measurements for the liquid state are required for all of these elements.

7.2. Recommendations for Future Measurements

The data for the properties listed below are considered to be inaccurate. They are placed in a sequence depending on the uncertainty, the first property in a column being the least certain.

Lithium and Sodium

1) Heat capacity of liquid Li and Na.
2) Simultaneous calorimetric and structural measurements of Li and Na at low temperatures may yield:
   a better estimate of heat capacity for α-Li and α-Na, and consequently
   a better estimate of heat capacity for β-Li and β-Na, and a better estimate of the enthalpy of the $\beta \rightleftharpoons \alpha$ transformation.
3) Accurate heat capacity measurements below the melting point.

Potassium, Rubidium and Cesium

1) Heat capacity of liquid K, Rb and Cs.
2) Accurate heat capacity measurements below the melting point.
3) Heat capacity below 5 K.

TABLE 7.1 Debye temperature and electronic heat capacity coefficient for the elements of group IA

Element	Θ_D/K	γ/mJ·K^{-2}·mol^{-1}
Li	344 ± 2.5	1.63 ± 0.04
Na	157 ± 2.0	1.36 ± 0.04
K	90 ± 1.0	1.83 ± 0.15
Rb	56.5 ± 1.0	2.61 ± 0.05
Cs	40.0 ± 1.0	3.60 ± 0.10

TABLE 7.2 Martensitic transformation in Li and Na

	Li	Na
Start of the direct transformation, M_s/K	70 ± 5	35 ± 3
End of the direct transformation, M_f/K	not achieved	
Start of the reverse transformation, A_s/K	95 ± 5	45 ± 5
End of the reverse transformation, A_f/K	165 ± 10	75 ± 10
Enthalpy of transformation, $\Delta_{trs}H$/J·mol^{-1}	54 ± 25	42 ± 20
Entropy of transformation, $\Delta_{trs}S$/J·K^{-1}·mol^{-1}	0.43 ± 0.2	0.70 ± 0.35

TABLE 7.3 Heat capacity, enthalpy and entropy values for the elements of group IA at 298.15 K

Element	C_p°(298.15 K) J·K^{-1}·mol^{-1}	S°(298.15 K) J·K^{-1}·mol^{-1}	H°(298.15 K)-$H^\circ(0)$ J·mol^{-1}
Li	24.78 ± 0.1	28.99 ± 0.3	4617 ± 30
Na	28.16 ± 0.1	51.10 ± 0.3	6432 ± 30
K	29.49 ± 0.1	64.63 ± 0.2	7080 ± 20
Rb	31.03 ± 0.1	76.74 ± 0.3	7489 ± 20
Cs	32.20 ± 0.2	85.10 ± 0.3	7717 ± 25

TABLE 7.4 Fusion of the elements of group IA

Element	T_{fus}/K	$\Delta_{fus}H$ J·mol^{-1}	$\Delta_{fus}S$ J·K^{-1}·mol^{-1}
Li	453.65 ± 0.05	3000 ± 30	6.613
Na	370.95 ± 0.05	2600 ± 25	7.009
K	336.6 ± 0.20	2335 ± 25	6.937
Rb	312.45 ± 0.10	2190 ± 25	7.009
Cs	301.6 ± 0.10	2090 ± 25	6.930

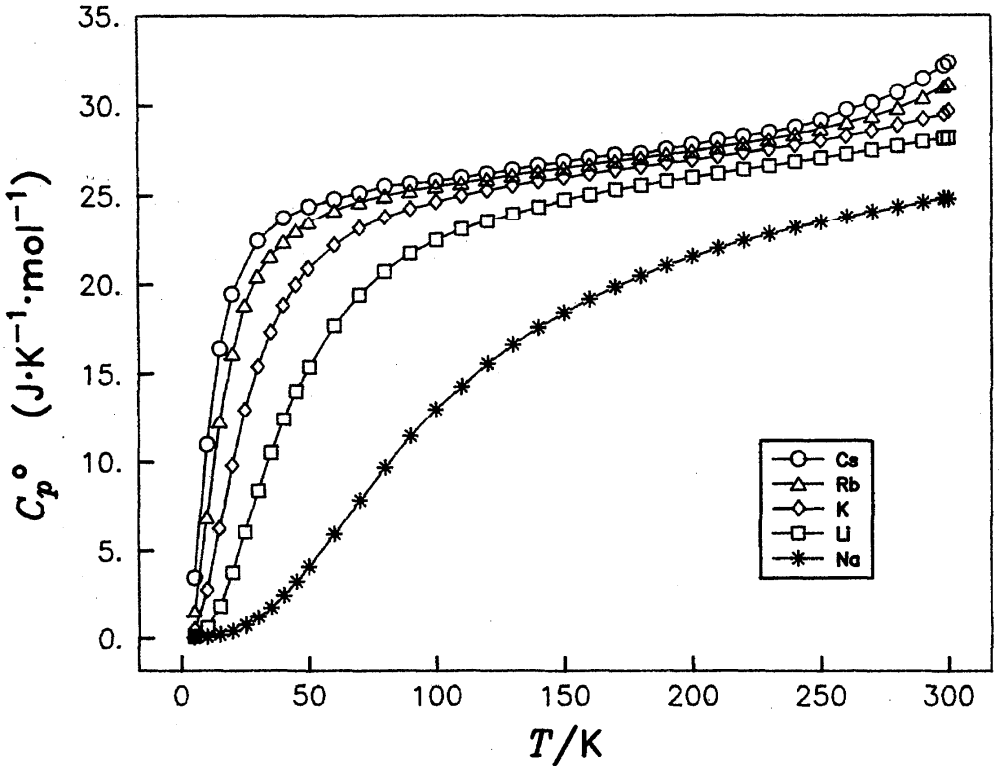

FIGURE 7.1. Heat Capacity of the Elements of Group IA below 300 K

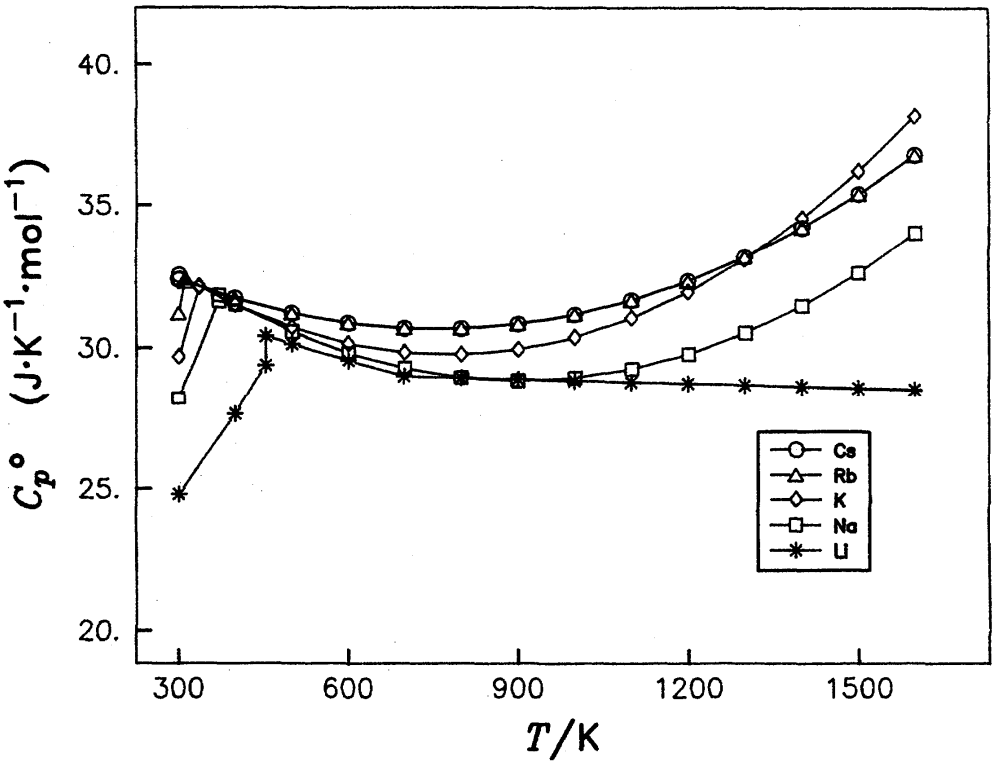

FIGURE 7.2. Heat Capacity of the Elements of Group IA above 300 K